# Design, synthesis and characterization of benign semifluorinated polymers for the delivery of hydrophobic pharmaceuticals

By

Michelle Fleetwood

A dissertation submitted in partial fulfilment of the requirements for the degree of

Doctor of Philosophy

(Chemistry)

At the

University of Wisconsin-Madison

2018

Date of final oral examination: April 9, 2018
The dissertation is approved by the following members of the final oral committee:
      Sandro Mecozzi, Associate Professor, Department of Chemistry and School of Pharmacy
      Helen Blackwell, Professor, Department of Chemistry
      Glen Kwon, Professor, School of Pharmacy
      Richard Hsung, Professor, School of Pharmacy

# Design, synthesis and characterization of benign semifluorinated polymers for delivery of hydrophobic pharmaceuticals

Michelle Catherine Fleetwood

Under the supervision of Professor Sandro Mecozzi

At the University of Wisconsin-Madison

## ABSTRACT

Polymeric nanoparticles have been studied extensively for their use in drug delivery systems due to the observed increase in biocompatibility, high drug loading capacity and tunable drug release profiles. The incorporation of a perfluorinated block within a water soluble polymer can increase the nanoparticles *in vivo* stability and thus its circulating half-life, as well as providing a means to solubilize fluorous pharmaceuticals.

However, recent environmental concerns of perfluorinated molecules, specifically C7 and higher, have caused a re-evaluation in industry and academic labs in terms of which perfluorinated compounds are benign. The search for degradable, non-bioaccumulable and nontoxic fluorinated compounds has increased in the industrial setting in the past decade due to these concerns.

The synthesis of two classes of semifluorinated polymers was designed and executed to prepare environmentally benign amphiphiles for use in the delivery of hydrophobic chemotherapeutics and fluorous anesthetics. The emphasis on creating degradable and nontoxic fluorinated segments was studied, by introducing small fluorinated segments throughout a lipophilic block or using biodegradable, linear fluorinated oligoether blocks. The formulation of fluorous anesthetic nanoemulsions, was studied to evaluate the stabilization efficacy and relative

fluorophilicity of the polymers containing alternative fluorinated blocks compared to traditional straight chain fluorocarbons. The toxicity profile of these synthesized polymers was verified through *in vivo* testing with a wild type zebrafish model.

The stability of polymeric nanoparticles is dictated greatly by dilution upon administration and interactions with blood serum proteins. To test these events *in vitro*, fluorescence studies have been created to estimate the kinetic stability of micellar systems. Current experiments require the encapsulation of two large hydrophobic dyes, which is not possible for all polymers due to small hydrophobic cores in some systems. An aggregation-induced emission fluorophore was investigated to develop a comparative stability test for micelle systems, which only requires the encapsulation of one small dye.

# ACKNOWLEDGEMENTS

I would like to thank my advisor, Professor Sandro Mecozzi, for his kind guidance and encouragement throughout my time in his research group. Thank you for fostering my development into a curious scientist and allowing me to explore my own hypotheses and interests.  I would also like to extend my sincere thanks to my thesis committee for their time and support over the years: Professors Helen Blackwell, Glen Kwon, and Richard Hsung.

The University of Wisconsin's Chemistry Department and School of Pharmacy are full of brilliant people who have helped my work tremendously. I am thankful to Dr. Martha Vestling for help in interpreting very complicated mass spectra. I would especially like to thank the Analytical Instrumentation Center at the School of Pharmacy, specifically Dr. Cameron Scarlett, Dr. Thomas Stringfellow and Gary Girdaukas for all of their help throughout my graduate career. Thank you to Professor Michael Taylor (UW School of Pharmacy) for your insight and collaboration in zebrafish testing of our compounds.

Thank you to the Mecozzi group members throughout the years who I have been privileged to know and work beside. You all have provided helpful conversations, a fun work environment and massive amounts of support during my time at UW-Madison. I would like to give a special thank you to Dr. Aaron McCoy and Dr. William Tucker for helping me establish myself in the lab and within these research projects. Thank you to Moira Esson for her help in polymer characterization and for always agreeing to get food with me. I am thankful for the opportunity to complete an internship at HP Inc. in San Diego, CA and be able to work for Dr. Gregg Lane and his ink chemistry team. I appreciated their easygoing, collaborative culture and thoughtful insights as mentors.

Thank you to my friends outside of Madison–Victoria, Katie, and Lisa–for being constant sources of support and humor. To all of my friends in Madison, thank you for commiserating our graduate school woes, while also showing me more fun than I thought possible.

Finally, thank you to my family–none of this would have been possible without your continued confidence and love. Luckily, Madison was only a short drive away from home, allowing me to spend cherished quality time with all of you. While at UW-Madison, I was fortunate to meet Joe, who has been the greatest supporter and partner. You inspire me daily to reach further and be my best self–thank you.

**TABLE OF CONTENTS**

# LIST OF FIGURES AND TABLES

## LIST OF FIGURES

**Chapter 3: Perfluorooligoethers vs. Long-Alkyl Chain Fluorocarbons. Physicochemical Differences and Toxicity Issues**

**Chapter 4: Aggregation Induced Emission to Elucidate Micelle Kinetic Stability**

**Appendix 1: Synthesis of poly(2-oxazoline)s as triphilic polymers for drug delivery applications**

## LIST OF TABLES

**Chapter 1: Biomedical applications of perfluorinated molecules and their environmental implications**

**Chapter 2: Synthesis and characterization of environmentally benign, semifluorinated polymers and their applications in drug delivery**

**Chapter 3: Perfluorooligoethers vs. Long-Alkyl Chain Fluorocarbons. Physicochemical Differences and Toxicity Issues**

**Chapter 4: Aggregation Induced Emission to Elucidate Micelle Kinetic Stability**

# LIST OF ABBREVIATIONS

This manuscript is written mostly in American Chemical Society (ACS) style, however other abbreviations are adopted and listed below.

ABC          accelerated blood clearance

ACN          acetonitrile

ACQ          aggregation-caused quenching

AIE          aggregation-induced emission

CMC          critical micelle concentration

DCM          dichloromethane

DiI          1,1'-dioctadecyl-3,3,3',3'-tetramethylindocarbocyanine perchlorate

DiO          3,3'-dioctadecyloxacarbocyanine perchlorate

DLS          dynamic light scattering

EPA          United States Environmental Protection Agency

EPR          enhanced permeation and retention

FDA          United States Food and Drug Administration

FRET         Förster resonance energy transfer

GPC          gel permeation chromatography

HPLC         high performance liquid chromatography

IV           intravenous

MALDI        matrix-assisted laser desorption/ionization

mPEG         monomethoxy poly(ethylene glycol)

MOPS         3-($N$-morpholino)propanesulfonic acid

MRI          magnetic resonance imaging

NMR          nuclear magnetic resonance

| | |
|---|---|
| P3P | 1,3-bis-(1-pyrenyl)propane |
| PBS | phosphate buffered saline |
| PEG | poly(ethylene glycol) |
| PFC | perfluorocarbon |
| PFCE | perfluoro-15-crown-5-ether |
| PFE | perfluorooligoether |
| PFOA | perfluorooctanoic acid |
| PFOB | perfluorooctyl bromide |
| PFOS | perfluorooctane sulfonic acid |
| PFPE | perfluoropolyether |
| PPT | parts per trillion |
| PTX | paclitaxel |
| TCD | tetraphenylcyclopentadieneone |
| THF | tetrahydrofuran |
| TPE | tetraphenylethylene |
| USP | United States Pharmacopeia |
| v/v | volume/volume |
| wt. | weight |

# Chapter 1: Biomedical applications of perfluorinated molecules and their environmental implications

**Chapter 1: Biomedical applications of perfluorinated molecules and their environmental implications**

**1.1 Perfluorinated Molecules**

*1.1.1 Unique Properties of Perfluorocarbons*

The addition of fluorine to organic molecules can drastically alter their thermal and mechanical properties as well as the hydrogen bonding properties and metabolism. Perfluorocarbons (PFCs), as such, are regarded for their unmatched range of unique properties, which find applications in the agrochemical,[1] fire-fighting,[2] electrical,[3] and medical industries,[4] to name a few.

In regards to PFC biomedical uses and potential, the chemical and biological inertness constitutes the most important characteristics. The unreactive quality of PFCs is related to the strength of the C–F bond, which is due to the high Coulombic force resulting from fluorine's high electronegativity.[5, 6, 7] To quantify this property, the bond dissociation energy (BDE) of a C–F bond in fluoromethane ($CH_3F$) is 115 kcal/mol, while the BDE is 104.9 kcal/mol for a C–H bond is methane ($CH_4$).[8] In addition, as the fluorine content increases, so does the BDE–evident as this value increases to 130.5 kcal/mol for tetrafluoromethane ($CF_4$).[9]

Other important qualities of the fluorine atom lead to interesting behaviors of perfluorocarbons that are not seen in hydrocarbons. Compared to aliphatic hydrogen, fluorine is more electronegative (3.98 (fluorine) vs. 2.20 (hydrogen) on the Pauling scale),[10] has a larger mean van der Waals radius (1.47 Å vs. 1.20 Å)[11], and has a lower polarizability (0.557 Å$^3$ vs. 0.667 Å$^3$).[12] Due to the steric repulsion of highly electronegative neighboring fluorine atoms, PFCs exhibit a rigid, helical structure compared to hydrocarbons, which are flexible and have antiperiplanar conformations. This rigidity results in higher melting points than for the corresponding hydrocarbons, and a narrower liquid phase domain.[13] The low polarizability of

fluorine leads to low van der Waals interactions between PFC chains, which leads to physical properties such as low surface tension, low water solubility of liquids, and low intermolecular cohesion.[14]

Perfluorocarbons, in turn, are also extremely hydrophobic due to low polarizability, low van der Waals interactions and their neutral electrostatic surface potential.[14, 15] The van der Waals interactions of PFCs are so low that they also become lipophobic, which causes these molecules to segregate among themselves, leading to a new phase–termed the "fluorous phase", shown in Figure 1.1.[16] Molecules that segregate into this third phase are termed fluorophilic,[17] and have been empirically found to have the following qualities: a minimum of 60 wt.% fluorine content, the presence of at least one perfluoroalkyl moiety, limited polar groups and little to no hydrogen bonding capabilities.[18] The dual hydrophobicity and lipophobicity of PFCs prohibits them from interacting with many physiological materials, further adding to the biological inertness of these molecules.[19]
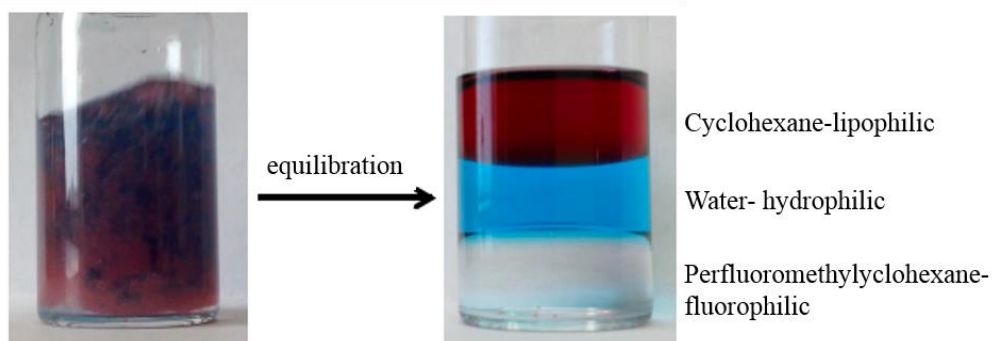


**Figure 1.1: Phase separation of lipophilic, hydrophilic and fluorophilic molecules.** The separation shows three distinct phases after equilibration: cyclohexane (dyed red with tetraphenylcyclopentadienone), water (dyed blue with copper sulfate) and perfluoromethylcyclohexane (colorless).

The outstanding inertness of perfluorocarbons is evidenced by the Federal Drug Administration's (FDA) approval of the administration of perfluorooctyl bromide ($C_8F_{17}Br$) in liter-size doses as a contrast agent in magnetic resonance imaging (MRI).[19, 20] In addition, many

fluoropolymers are used in everyday medical devices, such as tubing and membranes.[21] The use of perfluorocarbons has extended into other fields such as biomedical imaging and drug delivery, which will be described in Section 1.3.

*1.1.2 Semifluorinated Polymers*

The detailed properties of perfluorocarbons above lead to high thermal stability, low chemical reactivity, low friction, high specific gravity and oil and water repellency.[22] Fluoropolymers, or polymers which have a high fluorine content throughout, also possess these unique qualities, which can be advantageous for many industrial applications. The global fluoropolymer market was valued at $7.39 billion in 2016 and is expected to rise to $10.49 billion in 2021.[23] Interestingly, the start of the fluoropolymer market began with the fortuitous finding of polytetrafluoroethylene (PTFE) by Roy J. Plunkett of DuPont.[24] The polymer was initially used in WWII in artillery shell fuses and after in the production of nuclear material for the Manhattan Project. Later, DuPont trademarked the polymer as Teflon, and commercialized it for use in home products and engineering markets.[25] Numerous fluoropolymers are used in many different applications, evidenced in Table 1.1.

**Table 1.1:** Common fluoropolymers and applications. Adapted from references 22, 26, and 27.

| Fluoropolymer | Structural Repeating Unit | Application |
|---|---|---|
| PTFE |  | Non-stick cookware, electrical wiring, microporous membranes, catheters, vascular implants |
| PVDF |  | Microporous membranes, coatings, solar panels |

| Name | Structure | Application |
|---|---|---|
| FEP | | Plastic labware, electrical wiring |
| PFA | | Resistant tubing, containment vessels |
| Nafion | | Batteries, fuel cells |
| Fluoroacrylates | R=H, Me, CF₃<br>R_f=fluoroalkyl (1-24 fluorines) | Soft contact lenses |
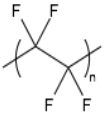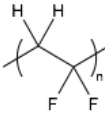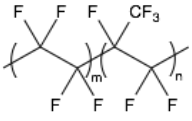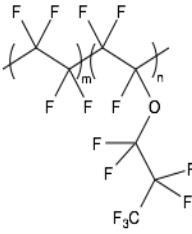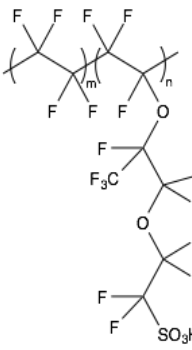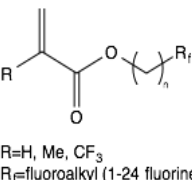
### 1.1.3 Amphiphilic PFCs/Fluorosurfactants

Perfluorocarbons can also be employed in amphiphilic molecules that contain both hydrophobic and hydrophilic segments. As described above, PFCs have strong hydrophobic and lipophobic effects, which constitutes powerful driving forces for segregation and self-organization of fluorinated amphiphiles.[15] The larger than usual hydrophobic effect leads to large interfacial effects. For example, fluorinated surfactants are more effective than comparable hydrogenated surfactants at reducing the surface tension of water. Fluorous surfactants reduce water's normal 72 mN/m to 15-20 mN/m whereas hydrogenated analogs reduce the surface tension to a range of 24-50 mN/m.[28] In the same regard, the critical micelle concentration (CMC) of fluorous surfactants is one to two orders of magnitude lower than their non-fluorinated

counterparts.[19] Fluorosurfactants in turn favorably self-assemble into a multitude of nanostructures, such as micelles,[29] inverse micelles,[30] bilayers,[31, 32] and vesicles[33]—all of which are based on the architecture of the hydrophobic and hydrophilic portions.[34]

**1.2 Environmental Persistence of PFCs**

The unreactive quality of C–F bonds leads to increased thermal and chemical resistance in PFCs, which have been utilized in many applications detailed above. However, this strong organic bond also makes these compounds resistant to degradation by metabolic,[35] osmotic,[36] or photolytic pathways.[37] Because of this, PFCs have become environmentally persistent–showing up in blood samples of the general U.S. population and even in remote areas such as the Arctic and Antarctica.[38-40] At high concentrations, certain PFCs have been linked to adverse health effects in laboratory animals that may indicate connections between exposure to these chemicals and some human health issues such as low birth weight,[41] delayed puberty onset,[42] reduced immunologic responses to vaccination,[43] and elevated cholesterol levels.[44]

*1.2.1 PFOA and PFOS*

The long-range use of perfluorocarbons in industry has been scrutinized due to the environmental persistence and toxicity of certain PFCs heavily produced as waste in their production. In particular, perfluorooctanoic acid (PFOA) and perfluorooctane sulfonic acid (PFOS) have been extensively studied for their biological accumulation and toxicity (Figure 1.2). PFOA was commonly used as a surfactant in emulsion polymerizations, such as with Teflon,[45] while PFOS was a key ingredient in many stain repellents, most notably 3M's Scotchgard.[46] Both PFOA and PFOS are also main degradation products of other commonly used fluorinated molecules.[45] Sources of PFOA and PFOS in water include aqueous fire-fighting foam, discharge from industrial facilities where it is made or used, effluent from wastewater treatment plants, and

landfill leachate.[47, 48] In addition, PFOA has been established as a dangerous chemical, which may have toxic effects on the liver, immune and endocrine systems.[49, 50] PFOA and PFOS do not degrade in the environment and cannot be metabolized in the body, leading to human half-lives of 3.6 and 5.4 years, respectively.[51]
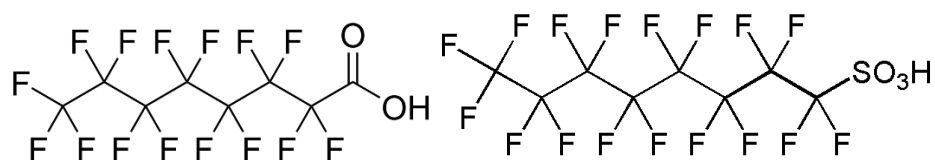


**Figure 1.2: Chemical structures of perfluorooctanoic acid (PFOA) and perfluorooctane sulfonic acid (PFOS)**.

The United States Environmental Protection Agency (EPA) constructed the 2010/2015 PFOA Stewardship Program to reduce emissions with eight industry partners. By the program's first deadline in 2010, 95% of residual content and emissions of PFOA and similar long-chain PFCs were to be cut, while the 2015 deadline called for complete elimination.[52] All eight industrial partners have successfully followed these guidelines. With the use of PFCs for biomedical applications, the use of nontoxic and non-bioaccumulative molecules is of the utmost importance.

*1.2.2 Long-chain PFCs*

The environmental persistence and bioaccumulation of PFCs have been correlated to the chain length.[53, 54] It has been found that the unwanted environmental longevity of PFCs is observed for perfluoroheptyl moieties (C7) and above, whereas C6 and below are rapidly excreted.[55] To date, no adverse effects in the general human population have been documented; however unfavorable results have been seen in laboratory animals as well as wildlife, as mentioned above. The long half-lives (on the year range) for many of these long-chain chemicals leads to increased exposure and ultimate toxic effects.

*1.2.3 Industrial Alternatives*

Although most perfluorocarbons are not toxic, the search for alternatives that possess the same desirable qualities of long-chain PFCs is essential. Industry leaders that partnered with the EPA and its 2010/2015 PFOA Stewardship Program have shown initiative in using alternative fluoropolymers that pose a lesser threat to the environment and wildlife. It was found that levels of PFOS in U.S. adult blood donors dropped 60% between 2000 and 2006, while PFOA levels dropped 25%, in the same timeframe.[56]

One strategy to increase potential for degradation is to introduce points of degradation with the use of weak bonds. This typically involves the replacement of a C–F bond with a C–H bond. A PFC alternative that uses this strategy is 3M's fluorosurfactant, ADONA, that replaces one C–F bond at the β position in relation to the carboxylate.[57-59] Similar to this surfactant, oligo(vinylidene fluoride), consisting of alternating $CH_2$ and $CF_2$ groups is being used as an alternative to PFCs. These C–H bonds are much more susceptible to degradation than the inert C–F bonds.[58, 60]

*1.2.4 Perfluoroethers*

Another strategy adopted in industry replaces PFCs with perfluorooligoethers and perfluoropolyethers (PFPE). Perfluoropolyethers have emerged as an interesting alternative to polymeric PFCs, as long chains and high molecular weights can still be used. These perfluoroethers contain oxygen atoms throughout the chain, causing a disruption in the perfluorocarbon's rigid helical structure. With this increased rotational freedom about the fluorous chain, it is hypothesized these molecules can degrade in the environment.[61, 62] Three such PFPEs are 3M's ADONA, DuPont's Krytox® and Solvay's Solvera®, which have similar properties to Teflon.[60, 63]

**Table 1.2:** Alternative fluorinated molecules used in industry. Adapted from references 57-60, 63, 64, 66-69.

| Surfactant structure | Company | Trade Name |
|---|---|---|
|  | 3M | ADONA™ |
|  | DuPont | Krytox® |
|  | Solvay | Solvera® |
|  | 3M | Novec™ |
|  | DuPont | Capstone™/ Forafac® |
|  | Merck | Tivida® |
|  | OMNOVA | Polyfox® |
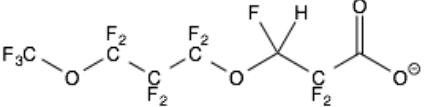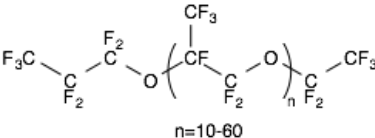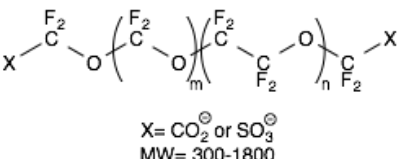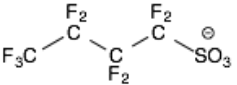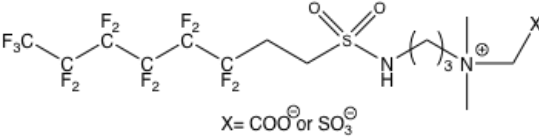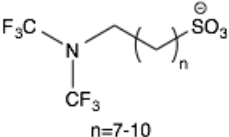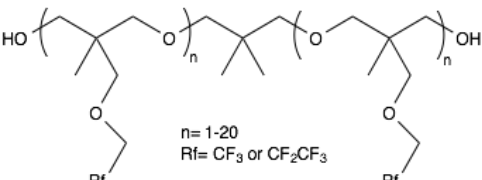
*1.2.5 Short Chain PFCs*

Bioaccumulation from PFCs are primarily seen with long chain molecules–specifically C7 and above. Short chain PFCs (C6 and below) have shown to be excreted rapidly in multiple organisms and thus have been explored for their use as alternatives in the fluoropolymer and

fluorosurfactant industry.[55] In 2003, 3M switched their Scotchgard recipe and replaced PFOS with a perfluorobutane sulfonate-based surfactant, Novec™ FC-4434, which has a half-life in humans of about one month.[64, 65] In lieu of these changes, the reported presence of perfluorobutane sulfonic acid has increased in environmental water, no doubt partially due to the conversion to shorter chain PFCs.[65] DuPont has also brought short chain fluorosurfactants to the market, with multiple options from the Capstone™/Forafac® lines.[66] These sulfonic and carboxylic acid surfactants utilize a perfluorohexyl group to afford the unique surface properties of PFCs. Many other companies have switched to short chain PFCs, including Merck's Tivida® line of surfactants and OMNOVA's Polyfox® line of polymers.[67-69]

Although the bioaccumulation of short-chain PFCs is much less than longer analogues, the toxicity profile may be comparable to longer chain analogues. For example, DuPont's Forafac® 1157 induced stress and immunosuppression in juvenile turbot, but its overall toxicity profile was much less harmful than PFOS.[70] In general, little work has been done to study the toxicological profile of these alternative fluorinated molecules.

*1.2.6 Fluorous Anesthetics*

Over the past decade, the atmospheric concentrations of fluorinated anesthetics sevoflurane, isoflurane and desflurane have increased globally by 0.13 parts per trillion (ppt), 0.097 ppt and 0.30 ppt, respectively.[71] Emissions of these anesthetics is worrisome due to their contribution to the greenhouse effect, and potential destruction of the ozone layer due to their long atmospheric lifetimes. Halogenated inhalational anesthetics undergo little metabolism during clinical application; 5%, 0.2 %, and <0.02 %, for sevoflurane, isoflurane, and desflurane, respectively.[72] For the protection of hospital and clinic personnel, the exhaled drug is vented to the outside without any current means of waste capture. Although the emitted amounts seem

small in contrast to carbon dioxide ($CO_2$, ~400 ppm), these anesthetics have a much higher

global warming potential. For example, every 1 kilogram of desflurane is equal to 2500

kilograms of $CO_2$.[71] In one study, the bottom-up estimates show the annual emission of the three

fluorous anesthetics were equivalent to ~4.4 million tons $CO_2$.[73] The increasing atmospheric

concentrations of these greenhouse gases have some scientists looking for ways to capture and

recycle the drug during clinical use.

**1.3 Biomedical Applications**

Perfluorocarbons have been studied over the last few decades for biomedical applications

due to their high chemical and thermal stability, high gas solubilization, and spectroscopic

properties. Below are some areas of biomedical research in which perfluorocarbons have been

utilized.

*1.3.1 Oxygen Delivery to Tissues*

Blood substitutes, also known as artificial blood, have been the focus of relentless

research, due to many areas of the world with blood shortages as well as the poorly understood

risk of allogeneic (donor) blood transfusions on host defenses.[74] Since the demonstration by

Clark and Gollan in 1966 that mice and cats could live while breathing an oxygen-saturated

liquid PFC, the utilization of these molecules as blood substitutes has been investigated.[75] PFCs

and gases show similar low intermolecular cohesion, as expressed by similar Hildebrandt

coefficients, which allows large concentrations of gases, such as oxygen, to dissolve in them.[76, 77]

Unlike other oxygen delivery systems, such as peroxides and cross-linked hemoglobin that

chemically interact with the gas and which can be toxic, PFCs carry physically entrapped oxygen

that can be easily released.[78] However, PFCs are hydrophobic and cannot be administered

directly into the body. To successfully mix them with hydrophilic fluids, many PFCs must be

emulsified with amphiphilic surfactants, and subsequently introduced into blood or other biological fluids.[79] Once these PFC emulsions are flushed with oxygen and injected into tissues, physically caged oxygen is released via diffusion.[78] Perfluorocarbon-oxygen emulsions have been successful in animal models and have shown promise in humans, without severe side effects.

Perfluorooctyl bromide (PFOB) has been tested experimentally for liquid breathing. It was found that partial liquid ventilation lead to clinical improvement and survival in some human infants with severe respiratory distress syndrome that were not expected to survive.[80]

*1.3.2 Contrast Agents*

Liquid PFCs have been studied as contrast agents–substances used to increase the contrast of structures or fluids within the body for ultrasonography and magnetic resonance imaging (MRI) since the late 1970s.[81] In 1977, Liu and Long reported the use of PFOB as an orally-administered diagnostic contrast agent medium for gastroenterography. Due to the hydro- and lipophobicity of PFOB, oil-in-water emulsions were formulated to better deliver the fluorophilic agent.[82] This PFC has also been studied as an MRI contrast agent for cell tracking applications.[83]

Additionally, perfluoro-15-crown-5 ether (PFCE) has been investigated as a $^{19}$F-MRI contrast agent.[84] The fluorine present in the body is mostly in the form of solid fluoride in bones and teeth. Since this endogenous fluorine is immobilized, it exhibits a very short spin–spin relaxation time ($T2$) that is not visible to conventional MRI methods. Thus, the absence of naturally occurring fluorine in the body allows for two advantages using PFCs in imaging: 1) very small amounts of fluorous imaging agent are needed to produce a signal and 2) the derived signal is from one compound, making it much less complex than a comparable proton image

where there are multiple components adding to the signal.[85] Additionally, PFCE contains 20 equivalent $^{19}F$ spins, equating to a single resonance in the MRI.[84] In practice, dendritic cells used to treat cancers and immunological disorders have been labeled with PFCE for theranostic applications.[86] In another study, PFCE-labelled macrophages were used to study the invasive and evasive phase of the macrophage in adoptive transfer experimental allergic encephalomyelitis by $^{19}F$-MRI in rats.[87]

*1.3.3 Anesthetic Emulsion Delivery*

Early anesthetics, namely diethyl ether and cyclopropane, were highly flammable and explosive.[88] Chloroform, also previously used to induce anesthesia, suffered from cardiac and hepatic toxicity.[89] Modern anesthetics are fluorous in nature and do not suffer from chemical flammability, explosiveness or extreme toxicity.[90] Some common anesthetics in use today are the fluorous molecules sevoflurane, isoflurane, and desflurane, shown in Figure 1.3.



| Sevoflurane | Isoflurane | Desflurane |
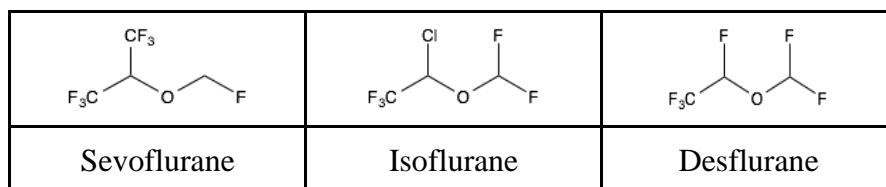
**Figure 1.3: Structure of fluorous anesthetics.**

These anesthetics are commonly used to induce and maintain general anesthesia through a vaporizer. However, the induction and recovery times using this machinery are slow and can lead to pain experienced by patients. This had led to the development of anesthetic emulsions, which eliminates the need for equilibration with the lungs.[91] Oil-in-water (o/w) nanoemulsions are appealing delivery systems for hydrophobic pharmaceuticals, such as anesthetics, because of their high-loading capability.[92, 93]

Nanoemulsions are non-equilibrium, metastable delivery systems. For an o/w mixture, a separated phase is thermodynamically most stable.[94] Therefore, energy must be input into the system to emulsify a dispersed oil-in-water phase (Figure 1.4). Nanoemulsions used in biomedical applications are formed through high-shear stirring,[95] ultrasonic emulsification,[96] homogenization,[97] or microfluidization,[98] which disrupt the oil and water phases to produce o/w nanodroplets. To be clinically relevant, the United States Pharmacopeia (USP) requires nanoemulsions to maintain an average particle size less than 500 nm, with a twelve month shelf life recommended by the US Food & Drug Administration (FDA).[99]
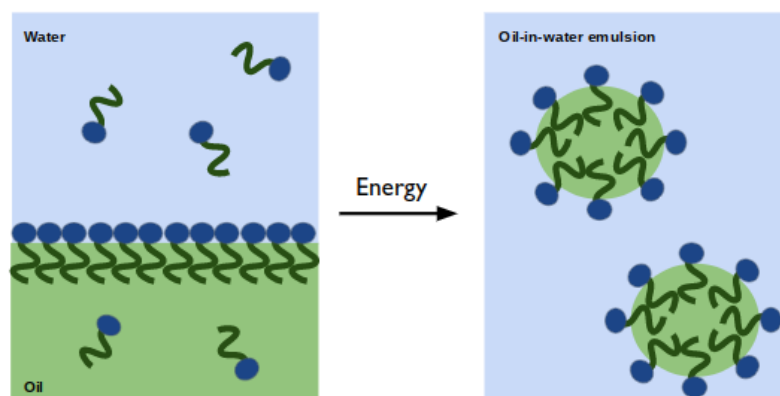


**Figure 1.4: Schematic representation of the formation of an emulsion**. An oil-in-water mixture spontaneously phase-separates, so that energy must be input into the system to disrupt the two phases, resulting in nanodroplets, which are stabilized by a surfactant.

Nanoemulsions are thermodynamically unstable systems, and their long-term stability is the main problem in formulation. Given the heterogeneity in particle sizes, emulsion nanodroplets have different chemical potential velocities. Flocculation is the trapping of smaller particles by larger particles, forming particle aggregates. Due to their higher curvature, smaller droplets have greater chemical potential than do larger droplets. To reduce the chemical potential of the system, average particle size will increase through either droplet combination (coalescence) or the diffusion of the oil phase from smaller to larger droplets (Ostwald

ripening).[92, 93] Once large enough particles or particle aggregates are formed, creaming, or

sedimentation, will occur. Due to the small size of nanoemulsions, Brownian motion is able to

overcome flocculation and limit creaming. Coalescence can also be prevented through

electrostatic or steric repulsion, by choice of surfactant. Therefore, Ostwald ripening is the only

observed mechanism for nanoemulsions to coarsen and decompose (Figure 1.5).[93]
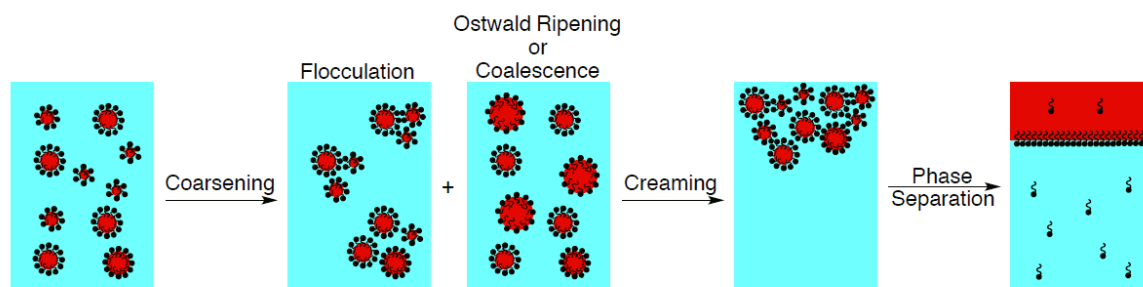


**Figure 1.5: Nanoemulsion destabilization process.** Nanoemulsion particles can grow in size through flocculation, coalescence or Ostwald ripening. This leads to sedimentation or creaming, with eventual phase separation.

Nanoemulsions have been explored for the delivery of fluorous anesthetics, due to the

ability of administration through intravenous (IV) injection. This allows for the rapid onset and

recovery of anesthesia, when compared to the slow induction associated with inhalation

methods.[91] Work in the Mecozzi lab has shown successes in utilizing novel, synthesized

fluorosurfactants, with the fluorous additive PFOB, to stabilize fluorous droplets of sevoflurane

(up to 30 vol. %).[100-102] Likewise, these polymers were studied to emulsify the same

concentration of isoflurane, a slightly more lipophilic molecule than sevoflurane, but were

unsuccessful. For traditional biphilic (hydrophilic/lipophilic) systems as well as triphilic

(hydrophilic, lipophilic, fluorophilic) amphiphiles, 15 vol. % isoflurane emulsions have been the

limit in nanoemulsion formulations. The problem seems to arise from the dual lipo- and

fluorophilicity of isoflurane, with the increased lipophilicity coming from the solo chloride

substituent. The development of a stable 20 vol. % isoflurane emulsion has recently been achieved by using a polymer that utilizes pendant fluorophilic chains off of a lipophilic backbone, and will be discussed further in Chapter 2.[103]

*1.3.4 Chemotherapeutic Delivery*

A persistent challenge confronted by the pharmaceutical industry is the low solubility of promising drug candidates. One study estimated that 40% of currently marketed drugs and 70% of those in the pipeline are poorly water-soluble.[104] These hydrophobic agents suffer from low and variable adsorption upon oral administration, thus leading to poor bioavailability.[105] Additionally, administration of these poorly water-soluble drugs through parenteral routes can lead to localized precipitation, hemolysis, pain and toxicity upon injection.[104] Unfortunately, the development of water-soluble formulations remains a challenge for these extremely hydrophobic therapeutic agents, which results in few candidates making it to the clinic.

One strategy to mitigate these solubility issues is using polymeric micelles as a delivery vehicle. Within these colloidal nanoparticles, the cytotoxic agent is protected within a hydrophobic core while a hydrophilic corona allows for water solubility,[106] increased circulation times,[107-108] and controlled release of the active agent.[109] Recently, amphiphilic polymers containing fluorous moieties have been studied for the delivery of small molecules and proteins by forming micellar delivery systems. When dissolved in water, these polymers spontaneously self-assemble into micelles, due to the hydrophobic effect (Figure 1.6).[15, 19] In these systems, a lipophilic segment of the polymer affords drug encapsulation while a fluorophilic block contributes to micelle stability and drug release kinetics.[110] Due to the increased hydrophobicity the fluorous block offers, nanoparticles that contain this fluorophilic segment have been shown to dissociate slower than those without one.[111]
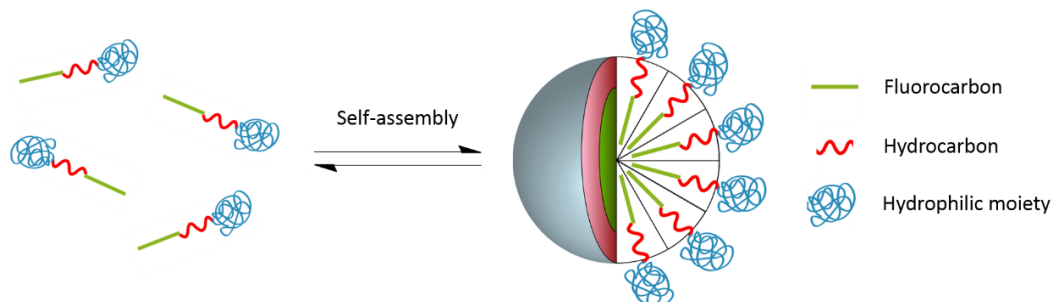
**Figure 1.6: Polymer unimer-micelle equilibrium.** Schematic representation of the equilibrium that exists between unimer and micelle in solution. Polymer contains a fluorophilic core (green), a lipophilic shell (red) and hydrophilic corona (blue).

The leading targets for nanoparticle drug delivery are solid, cancerous tumors. For the delivery of chemotherapeutics, micelle sizes range from 5-100 nm, as to take advantage of the enhanced permeation and retention (EPR) effect, i.e. passive targeting. Within this phenomenon, as tumors develop, new vasculature is formed that is characterized as porous and lacking an effective lymphatic system. Due to the large spaces between endothelial cells in the tumor vasculature, small nanoparticles can permeate into the tumor tissue and then accumulate in concentrated amounts, due to poor lymphatic drainage (Figure 1.7).[112, 113]
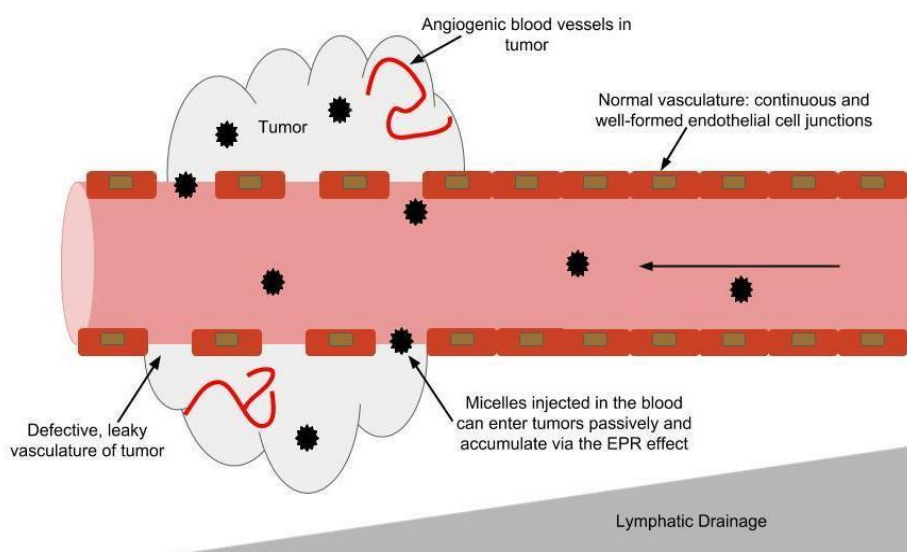


**Figure 1.7**: **Schematic representation of the EPR effect**. Tumor angiogenesis leads to the growth of new, leaky vasculature that allows for the permeation of nanoparticles that are too large to pass through endothelial junctions of healthy blood vessels. The lack of effective an effective lymphatic system allows for retention of nanoparticles. Adapted from reference 113.

Piccionello et al. studied polyaspartamides partially functionalized with a side chain containing a fluorocarbon. These polymeric micelles encapsulated flutamide, a chemotherapeutic, and successfully delivered the active drug to cells *in vitro*.[114] Again, the fluorocarbon block of these polymers was not added to encapsulate the anticancer drug, but instead led to stabilization of the aggregate by utilizing the fluorophilic effect.

In one study, Nystrom and others synthesized eight semifluorinated linear and star-shaped polymeric nanoparticles for the encapsulation and delivery of cancer agent, doxorubicin. However, in this study the fluorinated segment was incorporated in the hydrophilic corona to afford $^{19}$F-MRI imaging potential instead of increasing the colloidal stability.[115]

Another study presents a versatile carrier, low molecular weight fluorodendrimers, for the co-delivery of fluorinated drugs and therapeutic genes for combination cancer therapy. These carrier systems displayed both high drug loading efficacy and high gene transfection efficacy. It was found that the co-delivery of fluorinated anticancer drugs (sorafenib or 5-Fluorouracil) and TNF-related apoptosis-inducing ligand (TRAIL) causes a synergistic effect on ablating breast cancer cells.[116]

In addition, the Mecozzi group has utilized polymeric micelles containing a fluorophilic block to successfully encapsulate the anticancer drug, paclitaxel. These triphilic polymers are designed with a hydrophilic block, typically polyethylene glycol (PEG), to afford water solubility and biocompatibility, a hydrocarbon block to encapsulate the hydrophobic pharmaceutical and finally a fluorocarbon to stabilize the assembly. One such system, containing a perfluoro-tert-butyl block, showed improved *in vitro* release kinetics for paclitaxel over the comparable non-fluorinated polymer.[111] This system could also be used as a $^{19}$F-MRI contrast agent, as all the $CF_3$ groups accounted for one signal. In a recent study, triphilic nanoemulsions

with the lipophilic oil, medium chain triglyceride, have been able to solubilize massive amounts of paclitaxel (up to 4 mg/mL), with remarkable release kinetics, when compared to traditional micellar delivery. Addition of the contrast agent PFCE to these nanoemulsions further improves these drug release kinetics by sealing the fluorous shell, as well as adding a diagnostic component to the system.[117]

## 1.4 Outlook on PFCs

The rising fluoropolymer market and widespread industrial applications of fluorous chemicals are indicative of the need for materials that possess the unique chemical and physical properties of PFCs. Due to their successes in biomedical applications, the need to further characterize the environmental impact and toxicological profile of these PFCs is of the utmost importance. Even though the use of long chain PFCs has diminished substantially after regulations imposed by the U.S. EPA, in-depth studies on the environmental fate of short-chain perfluorocarbons have yet to be initiated. In addition, the capture and recycle of fluorinated anesthetics is becoming rising problem due to their alarming greenhouse effect.

## 1.5 Thesis Objectives

This thesis serves to investigate new short-chain and biodegradable alternative PFCs as viable fluorous segments for polymers in drug delivery. The scope of this work includes the design, synthesis, and physicochemical study of semifluorinated polymers utilizing environmentally benign PFC blocks. To study the polymer's lipophilic and fluorophilic characteristics, fluorous oil-in-water emulsions were formulated and particle size observed over time (Chapter 2 & 3). The toxicity of the polymers containing alternative fluorinated blocks was also investigated using a zebrafish model (Chapters 2 & 3). In addition, the measurement of kinetic stability for our amphiphilic polymers has been a constant problem for the group, due to

irreproducible results gained from the standard experimental method. Thus, Chapter 4 details the

study of aggregation-induced emission dyes as probes to study polymeric nanoparticle stability.

## 1.6 References

(1) Jeschke, P. The Unique Role of Fluorine in the Design of Active Ingredients for Modern Crop Protection. *ChemBioChem* **2004**, *5*(5), 570-589.

(2) Military Specification, "Fire Extinguishing Agent, Aqueous Film-Forming Foam (AFFF) Liquid Concentrate, for Fresh and Seawater," MIL-F-24385F, 7 January 1992.

(3) Hawkinson, T. E., & Korpela, D. B. (1998). Chemical hazards in semiconductor operations. In R. A. Bolmen, Semiconductor safety handbook (pp. 163). Westweed (USA): NOYES.

(4) Purser, S.; Moore, P. R.; Swallow, S.; Gouverneur, V. V. Fluorine in Medicinal Chemistry. *Chem. Soc. Rev.* **2008**, *37*(2), 320-330.

(5) Champagne, P. A.; Desroches, J.; Hamel, J. D.; Vandamme, M.; Paquin, J.F. Monofluorination of Organic Compounds: 10 Years of Innovation. *Chem. Rev.* **2015**, *115*(17), 9073-9174.

(6) Smart, B. E. Fluorocarbons. In The chemistry of functional groups, supplement D: The chemistry of halides, pseudo-halides and azides. Part 1; Patai, S., Rappoport, Z., Eds.; John Wiley & Sons Ltd.: New York, 1983; pp 603-656.

(7) Hansen, N. M. L.; Jankova, K.; Hvilsted, S.; Fluoropolymer materials and architectures prepared by controlled radical polymerizations. *Eur. Polym. J*. **2007**, *43*(2), 255-293.

(8) Blanksby, S. J.; Ellison, G. B. Bond Dissociation Energies of Organic Molecules. *Acc. Chem. Res*. **2003**, *36*(4), 255–263.

(9) Lemal, D. M. Perspective on Fluorocarbon Chemistry. *J. Org. Chem.* **2004**, *69*(1), 1-11.

(10) Nagle, J. K. Atomic Polarizability and Electronegativity. *J. Am. Chem. Soc.* **1990**, *112*(12), 4741-4747.

(11) Bondi, A. Van Der Waals Volumes and Radii. *J. Phys. Chem.* **1964**, *68*(3), 441–451.

(12) Miller, T. Atomic and Molecular Polarizabilities. In *Handbook of Chemistry and Physics*; Haynes, W. M., Bruno, T. J., Lide, D., Eds.; CRC Press: Boca Raton, FL; pp 10/187-10/196.

(13) Zhang, G.; Maaloum, M.; Muller, P.; Benoit, N.; Krafft, M. P. Surface Micelles of Semifluorinated Alkanes in Langmuir-Blodgett Monolayers. *Phys. Chem. Chem. Phys.* **2004**, *6*(7), 1566-1569.

(14) Janjic, J.; Ahrens, E. Fluorine Containing Nanoemulsions for MRI Cell Tracking. *Wiley Interdiscip. Rev. Nanomedicine Nanobiotechnolog*y **2009**, *1*, 492-501.

(15) Krafft, M. P. Fluorocarbons and Fluorinated Amphiphiles in Drug Delivery and Biomedical Research. *Adv. Drug Deliv. Rev.* **2001**, *47*(2-3), 209–228.

(16) Horvath, I. T. Fluorous Biphase Chemistry. *Acc. Chem. Res*. **1998**, *31*(10), 641-650.

(17) Kiss, L. E.; Kövesdi, I.; Rábai, J. An Improved Design of Fluorophilic Molecules: Prediction of the ln P Fluorous Partition Coefficient, Fluorophilicity, Using 3D QSAR Descriptors and Neural Networks. *J. Fluor. Chem.* **2001**, *108*(1), 95-109.

(18) Huque, F. T. T.; Jones, K.; Saunders, R. A.; Platts, J. A. Statistical and Theoretical Studies of Fluorophilicity. *J. Fluor. Chem.* **2002**, *115*(2), 119-128.

(19) Krafft, M. P.; Riess, J. G. Perfluorocarbons: Life Sciences and Biomedical Uses. *J. Polym. Sci. Part A: Polym. Chem.* **2007**, *45,* 1185-1198.

(20) FDA Approved Drug Products. https://www.accessdata.fda.gov/scripts/cder/daf/index.cfm?event=overview.process&ApplNo=0 20091. (Accessed 02/01/2018)

(21) Bigonzi-Jaker, A. M.; Jaker, M. L. (Rtc, Inc., USA) Membranes suitable for medical use. US Patent 6,240,968 B1, June 5, 2001.

(22) Teng, H. Overview of the Development of the Fluoropolymer Industry. *Applied Sciences* **2012**, 2, 496–512.

(23) Fluoropolymer Market by Types (PTFE, PVDF, FEP, and Fluoroelastomers), for Automotive & Transportation, Electrical & Electronics, Chemical Processing, and Industrial Equipment Applications – Global Industry Perspective, Comprehensive Analysis and Forecast 2016 - 2022. https://www.prnewswire.com/news-releases/fluoropolymer-market-ptfe-pvdf-fep-and-fluoroelastomers-report---global-trends-and-forecasts-to-2019-498347681.html (Accessed 02/01/2018).

(24) Plunkett, R. J. (Kinetic Chemicals, USA). Tetrafluoroethylene Polymers. US Patent 2,230,654, July 1, 1939.

(25) Roy J. Plunkett. https://www.chemheritage.org/historical-profile/roy-j-plunkett. (Accessed 01/31/2018).

(26) Gardiner, J. Fluoropolymers: Origin, Production, and Industrial and Commercial Applications. *Aust. J. Chem.* **2015**, *68*(1), 13-22.

(27) Salamone, J.C. Fluorine containing soft contact lens hydrogels. US Patent 5,684,059 A, November 4, 1997.

(28) Krafft, M. P. Basic Principles and Recent Advances in Fluorinated Self-Assemblies and Colloidal Systems. In *Handbook of fluorous chemistry*, Gladysz, J. A.; Curran, D. P.; Horvath, I. T. Eds. Wiley-VCH: Weinheim, 2004, 478-490.

(29) Stahler, K.; Selb, J.; Candau. F. Multicompartment polymeric micelles based on hydrocarbon and fluorocarbon polymerizable surfactants, *Langmuir* **1999**, *15*(22),7565-7576.

(30) Courrier, H. M,.; Pons, F.; Lessinger, J. M.; Frossard, N.; Krafft, M.P.; Vandamme, T. F. IN vivo evaluation of a reverse water-in-fluorocarbon emulsion stabilized with a semifluorinated amphiphile as a drug delivery system through the pulmonary route. *Int. J. Pharm.* **2004**, *282*(1-2), 131-140.

(31) Rojas, O. J.; Macakova, L.; Blomberg, E.; Emmer, A.; Claesson, P. M. Fluorosurfactant Self-Assembly at Solid/Liquid Interfaces. *Langmuir* **2002**, *18*, 8085-8095.

(32) Wang, K.; Karlsson, G.; Almgren, M. Aggregation Behavior of Cationic Fluorosurfactants in Water and Salt Solutions. A CryoTEM Survey. *J. Phys. Chem. B* **1999**, *103*, 9237-9246.

(33) Burkitt, S. J.; Ottewill, R. H.; Hayter, J. B.; Ingram, B. T. Small angle neutron scattering studies on micellar systems part 1. Ammonium octanoate, ammonium decanoate and ammonium perfluoroocatanoate. *Colloid Polym. Sci.* **1987**, *265*, 619-627.

(34) Israelachvili, J. N.; Mitchell, D. J.; Ninham, B. W. Theory of Self-Assembly of Hydrocarbon Amphiphiles into Micelles and Bilayers. *J. Chem. Soc. Faraday Trans. 2* **1976**, *72*, 1525-1568.

(35) Vanden Heuvel, J. P.; Kuslikis, B. I.; Van Ragelghem, M. L.; Peterson, R. E. Tissue distribution, metabolism and elimination of perfluorooctanoic acid in male and female rats. *J. Biochem. Toxicol*. **1991**, *6*, 83-92.

(36) 3M Company (2000): Voluntary use and exposure information profile for perfluorooctanoic acid and salts. Submission to USEPA, June 8.

(37) Hatfield, T. (2001): Screening studies on the aqueous photolytic degradation of perfluorooctanoic acid (PFOA). 3M Environmental Laboratory. Lab request number E-00-2192. St. Paul, MN.

(38) Calafat, A.M.; Kuklenyik, Z.; Reidy, J.A.; Caudill, S. P.; Tully, J. S.; Needham, L. L. Serum concentrations of 11 polyfluoroalkyl compounds in the U.S. population: Data from the National Health and Nutrition Examination Survey (NHANES). *Environ. Sci. Technol*. **2007**, *41*, 2237-2242.

(39) Martin, J. W.; Smithwick, M. M.; Braune, B. M.; Hoekstra, P. F.; Muir, D. C. G.; Mabury, S. A. Identification of long-chain perfluorinated acids in biota from the Canadian Arctic. *Environ. Sci. Technol.* **2004**, *38*, 373-380.

(40) Muhle, J.; Ganesan, A. L.; Miller, B. R.; Salameh, P. K.; Harth, C. M.; Greally, B. R.; Rigby, M.; Porter, L. W.; Steele, L. P.; Trudinger, C. M.; Krummel, P. B.; O'Doherty, S.; Fraser, P. J.; Simmonds, P. G.; Prinn, R. G.; Weiss, R. F. Perfluorocarbons in the global atmosphere: tetrafluoromethane, hexafluoroethane, and octafluoropropane. *Atmos. Chem. Phys.* **2010**, *10*, 5145-5164.

(41) Bach, C. C.; Bech, B. H.; Brix, N.; Nohr, E. A.; Bonde, J. P. E.; Henriksen, T. B. Perfluoroalkyl and polyfluoroalkyl substances and human fetal growth: A systematic review. *Crit. Rev. Toxicol.* **2015**, *45*, 53-67.

(42) Lopez-Espinosa, M. J.; Fletcher, T.; Armstrong, B.; Genser, B.; Dhatariya, K.; Mondal, D.; Ducatman, A.; Leonardi, G. Association of Perfluorooctanoic Acid (PFOA) and Perfluorooctane Sulfonate (PFOS) with age of puberty among children living near a chemical plant. *Environ. Sci. Technol*. **2011**, *45*, 8160-8166.

(43) Granum, B.; Haug, L. S.; Namork, E.; Stolevik, S. B.; Thomsen, C.; Aaberge, I. S.; van Loveren, H.; Lovik, M.; Nygaard, U. C. Pre-natal exposure to perfluoroalkyl substances may be associated with altered vaccine antibody levels and immune-related health outcomes in early childhood. *J. Immunotoxicol.* **2013**, *10*, 373-379.

(44) Zeng, X. W.; Qian, Z.; Emo, B.; Vaughn, M.; Bao, J.; Qin, X.D.; Zhu, Y.; Li, J.; Lee, Y. L.; Dong, G. H. Association of polyfluoroalkyl chemical exposure with serum lipids in children. *Sci. Total Environ.* **2015**, 512-513.

(45) Tyrell, J. A. Fluoropolymers. In *Fundamentals of Industrial Chemistry: Pharmaceuticals, Polymers, and Business;* John Wiley & Sons: Inc. Hoboken, NJ, 2014, pp 127-128.

(46) Saikat, S.; Kreis, I.; Davies, B.; Bridgmanb, S.; Kamanyirea, R.The impact of PFOS on health in the general population: a review. *Environ. Sci.: Processes Impacts* **2013**, *15*, 329-335.

(47) Hansen, K. J.; Johnson, H. O.; Eldridge, J. S.; Butenhoff, J. L.; Dick, L. A.Quantitative characterization of trace levels of PFOS and PFOA in the Tennessee River. *Environ. Sci. Technol*. **2002**, *36*(8), 1681-1685.

(48) Chen, H.; Zhang, C.; Han, J.; Yu, Y.; Zhang, P. PFOS and PFOA in influents, effluents, and biosolids of Chinese wastewater treatment plants and effluent-receiving marine environments. *Environmental Pollut*. **2012**, *170*, 26-31.

(49) White, S.S.; Fenton, S.E.; Hines, E.P.; Endocrine disrupting properties of perfluorooctanoic acid. *J. Steroid Biochem. Mol. Bio*l. **2011**, *127*, 16–26.

(50) Post, G.; Cohn, P. D.; Cooper, K. R. Perfluorooctanoic acid (PFOA), an emerging drinking water contaminant: A critical review of recent literature. *Environ. Res.* **2012**, *116*, 93-117.

(51) Olsen, G. W.; Burris, J. M.; Ehresman, D. J.; Froehlich, J. W.; Seacat, A. M.; Butenhoff, J. L.; Zobel, L. R. Half-life of serum elimination of perfluorooctanesulfonate, perfluorohexane-sulfonate, and perfluorooctanoate in retired fluorochemical workers. *Environ. Health Perspect.* **2007**, *115*, 1298-1305.

(52) Risk Management for Per- and Polyfluoroalkyl Substances (PFASs) under TSCA. https://www.epa.gov/assessing-and-managing-chemicals-under-tsca/risk-management-and-polyfluoroalkyl-substances-pfass#tab-3 (Accessed 02/02/2018).

(53) Frömel, T.; Knepper, T. P. Biodegradation of fluorinated alkyl substances. *Rev. Environ. Contam. Toxicol.* **2010**, *208*, 161-77.

(54) Conder, J. M.; Hoke, R. A.; De Wolf, W.; Russell, M. H.; Buck, R. C. Are PFCAs bioaccumulative? A critical review and comparison with regulatory criteria and persistent lipophilic compounds. *Environ. Sci. Tech*. **2008**, *42*(4), 995-1003.

(55) Dinglasan, M. J. A.; Ye, Y.; Edwards, E. A.; Mabury, S. A., Fluorotelomer alcohol biodegradation yields poly- and perfluorinated acids. *Environ. Sci. Technol*. **2004**, *38*(10), 2857-2864.

(56) Olsen, G. W.; Mair, D. C.; Church, T. R.; Ellefson, M. E.; Reagen, W. K.; Boyd, T. M.; Herron, R. M.; Medhdizadehkashi, Z.; Nobiletti, J. B.; Rios, J. A.; Butenhoff, J. L.; Zobel, L. R. Decline in Perfluorooctanesulfonate and Other Polyfluoroalkyl Chemicals in American Red Cross Adult Blood Donors, 2000−2006. *Environ. Sci. Technol.* **2008**, *42* (13), 4989–4995.

(57) Kostov, G.; Boschet, F.; Buller, J.; Badache, L.; Brandsadter, S.; Ameduri, B., First Amphiphilic Poly(vinylidene fluoride-co-3,3,3-trifluoropropene)-b-oligo(vinyl alcohol) Block Copolymers as Potential Nonpersistent Fluorosurfactants from Radical Polymerization Controlled by Xanthate. *Macromolecules* **2011**, *44*(7), 1841-1855.

(58) Kostov, G.; Boschet, F.; Ameduri, B., Original fluorinated surfactants potentially non-bioaccumulable. *J. Fluorine Chem.* **2009**, *130*(12), 1192-1199.

(59) Gordon, S. C. Toxicological evaluation of ammonium 4,8-dioxa-3H-perfluorononanoate, a new emulsifier to replace ammonium perfluorooctanoate in fluoropolymer manufacturing. *Regul. Toxicol. Pharmacol.* **2011**, *59*(1), 64-80.

(60) Zaggia, A.; Ameduri, B. Recent advances on synthesis of potentially non-bioaccumulable fluorinated surfactants. *Curr. Opin. Colloid Interface Sci.* **2012**, *17*(4), 188-195.

(61) Ameduri, B.; Sawada, H. *Fluorinated Polymers,* 2nd ed.; The Royal Society of Chemistry: Cambridge, 2017; p 120.

(62) Hamada, T. Rotational isomeric state study of molecular dimensions and elasticity of perfluoropolyethers: Differences between Demnum-, Fomblin-, and Krytox type main chains. *Phys. Chem. Chem. Phys.* **2000**, *2*, 115-122.

(63) Ojakaar, L.; Schnell, R. W.; Russell, W.; Senior, K. A.(du Pont de Nemours, E.I., and Co., U.S.A.) Perfluoroelastomer compositions containing perfluoropolyethers with improved low-temperature properties. US Patent 5,268,405, December 5, 1993.

(64) 3M™ Novec™ Fluorosurfactant https://solutions.3m.com/3MContentRetrievalAPI/BlobServlet?lmd=1413809788000&locale=en_EU&assetType=MMM_Image&assetId=1258560709372&blobAttribute=ImageFile (Accessed 02/02/2018).

(65) Lassen, C.; Brinch, A.Norwegian Environment Agency. Investigation of sources to PFBS in the environment. May 5, 2017. http://www.miljodirektoratet.no/Documents/publikasjoner/M759/M759.pdf (Accessed 02/02/2018).

(66) DuPont™ Capstone® Fluorosurfactants: High value-in-use applications that require maximum performance http://www2.dupont.com/Capstone/en_US/assets/downloads/DuPont(TM)_Capstone(R)_Fluorosurfactants_Brochure_K-24287.pdf (Accessed 02/02/2018).

(67) Peschka, M.; Fichtner, N.; Hierse, W.; Kirsch, P.; Montenegro, E.; Seidel, M.; Wilken, R. D.; Knepper, T. P., Synthesis and analytical follow-up of the mineralization of a new fluorosurfactant prototype. *Chemosphere* **2008**, *72*(10), 1534-1540.

(68) Kausch, C. M.; Leising, J. E.; Medsker, R. E.; Russell, V. M.; Thomas, R. R. Synthesis, characterization, and unusual surface activity of a series of novel architecture, water-dispersible poly(fluorooxetane)s. *Langmuir* **2002**, *18*(15), 5933-5938.

(69) Malik, A. A.; Park, Cameron; A.; Thomas, G. (Aerojet General Co., USA). Polymers and prepolymers from mono-substituted fluorinated oxetane monomers. US Patent 5,807,977, September 15, 1998.

(70) Hagenaars, A.; Meyer, I.J.; Herzke, D.; Pardo, B.G.; Martinez, P.; Pabon, M.; De Coen, W.; Knapen, D. The search for alternative aqueous film forming foams (AFFF) with a low environmental impact: Physiological and transcriptomic effects of two Forafac® fluorosurfactants in turbot. *Aquat. Toxicol*. **2011**, *104*, 168-176.

(71) Vollmer, M.K.; Rhee, T.S.; Rigby, M.; Hofstetter, D.; Hill, M.; Schoenenberger, F.; Reimann, S. Modern inhalation anesthetics: Potent greenhouse gases in the global atmosphere. *Geophys. Res. Lett*. **2015**, *42*, 1606-1611.

(72) Halpern, D. F. Recent developments in fluorine substituted volatile anesthetics. In *Organofluorine Compounds in Medicinal Chemistry and Biomedical Applications*. Filler, R.; Y.

Kobayashi, Y.; Yagupolskii, L. M. Eds; Studies in Organic Chemistry, Elsevier, Amsterdam, Netherlands, 1993: pp 101-133.

(73) Sulbaek Andersen, M. P.; Sander, S. P.; Nielsen, O. J.; Wagner, D. S.; Sandford Jr., T. J.; Wallington, T. J. Inhalation anesthetics and climate change, *Br. J. Anaesth.* **2010**, *105*(6), 760-766.

(74) Spahn, D. R. Blood substitutes Artificial oxygen carriers: perfluorocarbon emulsions. *Crit. Care*. **1999**, *3(*5), 93-97.

(75) Clark, L.C.; Gollan, F. Survival of Mammals Breathing Organic Liquids Equilibrated with Oxygen at Atmospheric Pressure. *Science* **1966**, *152*, 1755-1766.

(76) Freire, M. G.; Gomes, L.; Santos, L. M. N. B. F.; Marrucho, I. M.; Coutinho, J. A. P. Water Solubility in Linear Fluoroalkanes Used in Blood Substitute Formulations. *J. Phys. Chem. B* **2006**, *110*(45), 22923-22929.

(77) Riess, J.G.; Fluorous Materials for Biomedical Uses. In *Handbook of fluorous chemistry*, Gladysz, J. A.; Curran, D. P.; Horvath, I.T. Eds. Wiley-VCH: Weinheim, 2004: pp 521-573.

(78) Farris, A. L.; Rindone, A. N.; Grayson, W. L. Oxygen Delivering Biomaterials for Tissue Engineering. *J. Mater. Chem. B Mater. Biol. Med*. **2016**, *4*(20), 3422–3432.

(79) Riess, J. G.; Highly Fluorinated Systems for Oxygen-Transport, Diagnosis And Drug-delivery. *Colloids Surf. A* **1994**, *84*(1), 33-48.

(80) Leach, C. L.; Greenspan, J. S.; Rubenstein, S. D.; Shaffer, T. H.; Wolfson, M. R.; Jackson, J. C.; Delemos, R.; Fuhrman, B. P. Partial Liquid Ventilation with Perflubron in Premature Infants with Severe Respiratory Distress Syndrome. *N. Engl. J. Med.* **1996**, *335*(11), 761-767.

(81) Diaz-Lopez, R.; Tsapix, N.; Fattal, E. Liquid Perfluorocarbons as Contrast Agents for Ultrasonography and F-19-MRI. *Pharm. Res.* **2010**, *27*(1), 1-16.

(82) Liu, M. S.; Long, D. M. Perfluoroctylbromide as a Diagnostic Contrast-Medium in Gastroenterography. *Radiology* **1977**, *122*(1), 71-76.

(83) Giraudeau, C.; Flament, J.; Marty, B.  A new paradigm for high-sensitivity 19F magnetic resonance imaging of perfluorooctylbromide. *Magn. Reson. Med.* **2010**, *63*(4), 1119–1124.

(84) Schweighardt, F. K.; Rubertone, J. A. (Air Products and Chemicals, Inc., USA) Perfluoro-crown ethers in fluorine magnetic resonance imaging. US Patent 4,838,274 A, June 13, 1989.

(85) Tirotta, I.; Valentina Dichiarante, V.; Pigliacelli, C.; Cavallo, G.; Terraneo, G.; Bombelli, F. B.; Metrangolo, P.; Resnati, G.[19]F Magnetic Resonance Imaging (MRI): From Design of Materials to Clinical Applications. *Chem. Rev*. **2015**, *115*(2), 1106-1129.

(86) Zhang, H. Perfluoro-15-crown-5 ether-labeled dendritic cells. 2008 Aug 1, Updated 2008 Sep 3]. In: Molecular Imaging and Contrast Agent Database (MICAD). Bethesda (MD): National Center for Biotechnology Information (US); 2004-2013. https://www.ncbi.nlm.nih.gov/books/NBK23192/ (Accessed 02/02/2018).

(87) Nöth, U.; Morrissey, S. P.; Deichmann, R.; Jung, S.; Adolf, H.; Haase, A.; Lutz, J. Perfluoro-15-crown-5-ether labelled macrophages in adoptive transfer experimental allergic encephalomyelitis. *Artif. Cells Blood Substit. Immobil. Biotechnol.* **1997**, *25*(3), 243-54.

(88) Hudson, E.; Hemmings, H. C. Pharmacokinetics of Inhaled Anesthetics. In *Pharmacology and Physiology for Anesthesia*. Elsevier Health Sciences, Philadelphia, PA, 2012, pp 43-45.

(89) Safari, S. Motavaf, M.; Siamdoust, S. A. S.; Alavian, S. M. Hepatotoxicity of Halogenated Inhalational Anesthetics. *Iran Red Crescent Med. J.* **2014**, *16*(9), e20153.

(90) Eger, E. I. New Inhaled Anesthetics. *Anesthesiology* **1994**, *80*, 906-922.

(91) Musser, J. B.; Fontana, J. L.; Mongan, P. D. The Anesthetic and Physiologic Effects of an Intravenous Administration of a Halothane Lipid Emulsion (5% vol/vol). *Anesth. Analg.* **1999**, *88*(3), 671-675.

(92) Shah, P.; Bhalodia, D.; Shelat, P. Nanoemulsion: A Pharmaceutical Review. *Syst. Rev. Pharm.* **2010**, *1*(1), 24-32.

(93) Gupta, A.; Eral, H. B.; Hatton. T. A.; Doyle, P. S. Nanoemulsions: formation, properties and applications. *Soft Matter* **2016**, *12*, 2826-2841.

(94) Tucker, W. B.; Mecozzi, S. Nanoemulsions in Medicine. In *Handbook of Nanobiomedical Research, Volume 1*; Torchilin, V. P., Ed.; World Scientific Publishing, 2014; pp 141-167.

(95) Bałdyga, J.; Orciuch, W.; Makowski, Ł.; Malski-Brodzicki, M.; Malik, K. Break up of Nano-Particle Clusters in High-Shear Devices. *Chem. Eng. Process. Process Intensif.* **2007**, *46*(9 SPEC. ISS.), 851-861.

(96) Leong, T. S. H.; Wooster, T. J.; Kentish, S. E.; Ashokkumar, M. Minimising Oil Droplet Size Using Ultrasonic Emulsification. *Ultrason. Sonochem.* **2009**, *16*(6), 721-727.

(97) Schultz, S.; Wagner, G.; Urban, K.; Ulrich, J. High-Pressure Homogenization as a Process for Emulsion Formation. *Chem. Eng. Technol.* **2004**, *27*(4), 361-368.

(98) Okushima, S.; Nisisako, T.; Torii, T.; Higuchi, T. Controlled Production of Monodisperse Double Emulsions by Two-Step Droplet Breakup in Microfluidic Devices. *Langmuir* **2004**, *20*(23), 9905-9908.

(99) Globule Size Distribution in Lipid Injectable Emulsions. In *United States Pharmacopeia and National Formulary (USP 36 - NF 31)*; United States Pharmacopeia Convention: Rockville, MD, 2012; pp 321-323.

(100) Fast, J. P.; Perkins, M. G.; Pearce, R. A.; Mecozzi, S. Fluoropolymer-based Emulsions for the Intravenous Delivery of Sevoflurane. *Anesthesiology* **2008**, *10*(109), 651-656.

(101) Jee, J-P.; Parlato, M. C.; Perkins, M. G.; Mecozzi, S.; Pearce, R. A. Exceptionally Stable Fluorous Emulsions for the Intravenous Delivery of Volatile General Anesthetics. Anesthesiology **2012**, *116*(3), 580-585.

(102) Decato S.; Bemis T.; Madsen E.; Mecozzi S. Synthesis and characterization of perfluoro-tert-butyl semifluorinated amphiphilic polymers and their potential application in hydrophobic drug delivery. *Polym. Chem*. **2014**, *5*, 6461-6471.

(103) Fleetwood M. C.; McCoy A. M.; Mecozzi S. Synthesis and characterization of environmentally benign, semifluorinated polymers and their applications in drug delivery. *J. Fluorine Chem*. **2016,** *190*, 75-80.

(104) Williams, H. D.; Trevaskis, N. L.; Charman, S. A.; Shanker, R. M.; Charman, W. N.; Pouton, C. W.; Porter, C. J. H. Strategies to Address Low Drug Solubility in Discovery and Development. *Pharmacol. Rev*. **2013**, *65*(1), 315-499.

(105) Pouton, C. W. Formulation of Poorly Water-Soluble Drugs for Oral Administration: Physicochemical and Physiological Issues and the Lipid Formulation Classification System. *Eur. J. Pharm. Sci*. **2006**, *29*(3-4 SPEC. ISS.), 278-287.

(106) Kwon, G. S. Polymeric Micelles for Delivery of Poorly Water-Soluble Compounds. *Crit. Rev. Ther. Drug Carrier Syst*. **2003**, *20*(5), 357-403.

(107) Lukyanov, A. N.; Gao, Z.; Torchilin, V. P. Micelles from Polyethylene Glycol/phosphatidylethanolamine Conjugates for Tumor Drug Delivery. *J. Control. Release* **2003**, *91*(1-2), 97-102.

(108) Weissig, V.; Whiteman, K. R.; Torchilin, V. P. Accumulation of Protein-Loaded Long-Circulating Micelles and Liposomes in Subcutaneous Lewis Lung Carcinoma in Mice. *Pharm. Res*. **1998**, *15*(10), 1552-1556.

(109) Aw, M. S.; Kurian, M.; Losic, D. Polymeric Micelles for Multidrug Delivery and Combination Therapy. *Chem. Eur. J*. **2013**, *19*(38), 12586-12601.

(110) Jee, J. P.; McCoy, A.; Mecozzi, S. Encapsulation and Release of Amphotericin B from an ABC Triblock Fluorous Copolymer. *Pharm. Res*. **2012***, 29*(1), 69-82.

(111) Decato, S. E. Semifluorinated theranostic nanoparticles: development of stabilized colloidal drug delivery vehicles. Ph.D. Thesis. University of Wisconsin-Madison, Madison, WI, 2015.

(112) Maeda, H.; Greish, K.; Fang, J. The EPR Effect and Polymeric Drugs: A Paradigm Shift for Cancer Chemotherapy in the 21st Century. *Adv. Polym. Sci.* **2006**, *193*(1), 103-121.

(113) Jhaveri, A. M.; Torchilin, V. P. Multifunctional Polymeric Micelles for Delivery of Drugs and siRNA. *Front. Pharmacol.* **2014,** *5*, 1-26.

(114) Piccionello, A. P.; Pitarresi, G.; Pace, A.; Triolo, D.; Pasquale Picone, P.; Buscemi, S.; Giammona, G. Fluorinated and pegylated polyaspartamide derivatives to increase solubility and efficacy of Flutamide. *J. Drug Target*. **2012**, *20*(5), 433-444.

(115) Porsch, C.; Zhang, Y.; Östlund, A.; Damberg, P.; Ducani. C.; Malmström, E.; Nyström, A.M. In Vitro Evaluation of Non-Protein Adsorbing Breast Cancer Theranostics Based on ^{19}F-Polymer Containing Nanoparticles. *Part. Part. Syst. Charact.* **2013**, *30*, 381-390.

(116) Wang, H.; Hu, J.; Cai, X.; Xiao, J.; Cheng, Y. Self-assembled fluorodendrimers in the co-delivery of fluorinated drugs and therapeutic genes. *Polym. Chem.* **2016**, *7*, 2319-2322.

(117) Barres A. R.; Wimmer M. R.; Mecozzi S. Multicompartment Theranostic Nanoemulsions Stabilized by a Triphilic Semifluorinated Block Copolymer. *Mol Pharm*. **2017**, *14*, 3916-3926.

# Chapter 2: Synthesis and characterization of environmentally benign, semifluorinated polymers and their applications in drug delivery

**\*This chapter is published in part under the same title-Reference:** Fleetwood M. C.; McCoy A. M.; Mecozzi S. Synthesis and characterization of environmentally benign, semifluorinated polymers and their applications in drug delivery. *J. Fluor. Chem.* **2016**, *190*, 75–80.

**Synthesis and characterization of environmentally benign, semifluorinated polymers and their applications in drug delivery**

**Abstract**

Herein, we describe the synthesis, physicochemical studies and pharmaceutical assessment of a class of PEGylated semifluorinated amphiphilic block-polymers based on short pendant fluorinated side chains attached to moderately hydrophobic units. These polymers allowed us to investigate how the balance between hydrophobicity and fluorophilicity in the polymer can be tuned to match that of small molecules to be used in drug delivery. Remarkably, we found that using short perfluoroethyl groups in the polymer allows the preferential stabilization of nanoemulsions based on isoflurane, a fluorinated anesthetic made partly hydrophobic by the presence of a chlorine atom. In comparison, nanoemulsions of sevoflurane, a purely fluorophilic anesthetic, were not as stable. The lipophilicity of the polymers was also investigated in regards to solvation of hydrophobic molecules. Surface properties such as critical micelle concentration (CMC) and surface tension demonstrated the uniqueness of these fluorinated amphiphiles. Finally, the use of short perfluoroethyl chains makes these polymers environmentally benign in terms of bioaccumulation and toxicity.

**2.1 Introduction**

Perfluorinated compounds are heavily utilized in fire-fighting applications, cosmetics, paints, lubricants and pharmaceutical formulations.[1, 2] However, longer chain fluorocarbons have been replaced for general use in the US with short-chain perfluoroethers. This was done out of concern for bioaccumulation and general toxicity.[3] Specifically, perfluorooctanoic acid (PFOA) and perfluorooctanesulfonic acid (PFOS), which were used as surfactants during the synthesis of perfluorinated polymers, have received the most attention after their detection in places ranging

from remote areas in the Arctic to blood samples of the general U.S. population.[4, 5]

Perfluorocarbon bioaccumulation and toxicity tend to increase with longer chain length, with

groups composed of six perfluorinated carbons (perfluorohexyl) or less being considered safe for

humans.[2-4]

Short fluorocarbons are used in a variety of industrial materials. For instance, the

OMNOVA Polyfox© line lists polymers in which short perfluoroethers are used for the purpose

of achieving optimal properties in paints and coatings. The Polyfox© surfactants are synthesized

commercially by polymerization of fluorinated oxetane monomers, using a Lewis acid catalyst

and nucleophilic initiator.[5, 6] The most common fluorocarbon used is a perfluoroethyl, a fluorous

group significantly shorter than longer fluorocarbons that have shown toxicity and

bioaccumulation.[6, 7] These use of multiple perfluoroethyl groups throughout their polymer leads

to similar properties seen when using a longer chain analogue. The Polyfox© line has undergone

all required environmental and health related studies and has been granted full regulatory

approval by The United States EPA, allowing for the manufacture and sale of these

environmentally-benign products.[8]

Pharmaceutical applications of perfluorocarbon derivatives are based on the unique

physicochemical properties of fluorous compounds, including thermal and chemical stability,

biological inertness, high surface tension, and the ability of dissolving large amounts of oxygen.

Previous studies have shown that highly fluorinated amphiphilic diblock copolymers can

successfully be used for emulsifying fluorous anesthetics in drug delivery applications.[9-11] With

the inclusion of perfluorooctyl bromide (PFOB), an FDA-approved additive, these polymers

were shown to stably emulsify sevoflurane (Fig. 2.4) at concentrations up to 20–30% v/v, a

significant increase over the 3.5% v/v concentration of sevoflurane that can be achieved with a

classical hydrophobic emulsion as Intralipid.[11] In contrast, the same polymers were not able to

properly stabilize emulsions of isoflurane , likely due to the increased lipophilicity of this

compound as opposed to sevoflurane. As a result of a chloride substitution for one

trifluoromethyl group, isoflurane has a lower fluorine content than sevoflurane (51% w/w *vs.*

67% w/w), making the molecule more lipophilic. To date, the best formulations to emulsify

isoflurane are based on classical surfactants and provide a concentration of anesthetic between 8

and 15% v/v.[12, 13] We reasoned that in order to stably emulsify this anesthetic, a surfactant must

include a balance between fluorophilicity and lipophilicity that would be close or match that of

isoflurane. The new diblock copolymer described below is composed of a very short

hydrophobic backbone to which a pendant perfluoroethyl is attached, similarly to the

composition of some of the OMNOVA Polyfox© polymers. PEGylation of this small oligomer

leads to the formation of an amphiphilic polymer, which is highly water-soluble and can be used

to efficiently emulsify isoflurane when using a specific size of the hydrophobic/fluorophilic

perfluoroether moiety.
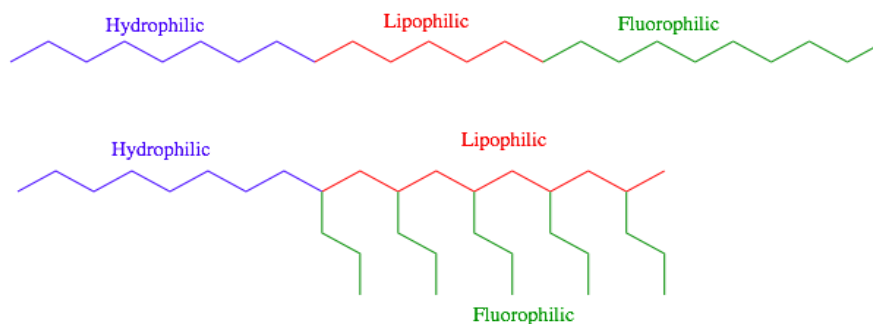


**Figure 2.1: Schematic representation of redesigned semifluorinated polymers.** These triphilic polymers include a hydrophilic block (blue), usually poly(ethylene glycol), attached to a lipophilic hydrocarbon (red), which can then be attached directly to a fluorocarbon (green) in the traditional design, or have pendant fluorous groups off the lipophilic backbone in the redesigned architecture.

## 2.2 Results and Discussion

### 2.2.1 Synthesis of semifluorinated polymers

The synthesis of these block copolymers was adapted from patents,[14, 15] and earlier work done in our group (Figure 2.1).[16] In glacial acetic acid, the triol, 1,1,1-tris(hydroxymethyl)ethane (**2-1**), was treated with sulfuric acid and sodium bromide to generate hydrogen bromide *in situ* to give the dibrominated product, 3-bromo-2-bromomethyl-2-methylpropyl acetate (**2-2**), as the major substitution product. Under biphasic conditions, the acetate was cleaved with sodium hydroxide allowing for *in situ* cyclization to give 3-(bromomethyl)-3-methyloxetane (**2-3**). This was then functionalized with 1H,1H-pentafluoropropan-1-ol. This reaction was found to work best under phase transfer conditions. Both oxetane monomers (**2-3** and **2-4)** were purified by distillation, but yields were lower than expected due to the high volatility of these molecules. PEGylation was achieved by using the terminal alcohol of methoxy polyethylene glycol (mPEG) as a macroinitiator in the presence of boron trifluoride diethyl etherate to carry out a ring-opening polymerization of the fluorous oxetane. Two methoxy polyethylene glycol molecular weights of 1000 and 5000 g/mol were used to synthesize different diblock copolymers (**2-5** and **2-6**) and explore their ability at emulsifying and encapsulating lipophilic and fluorophilic molecules.
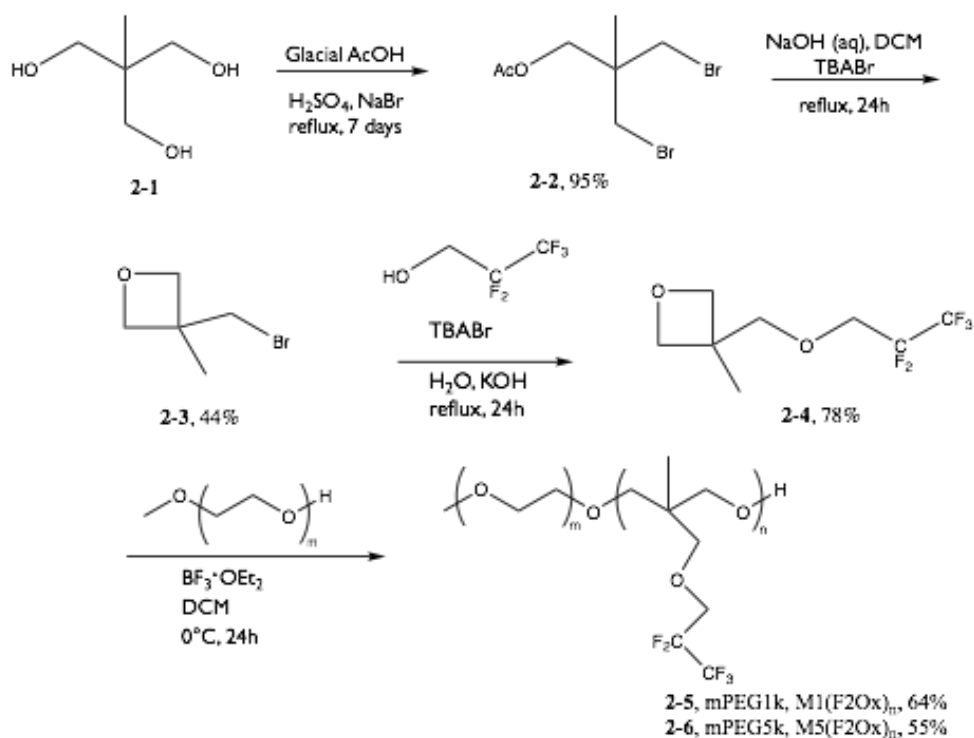
**Figure 2.2: Synthesis of Mx(F2Ox)n.** Note on nomenclature: M corresponds to mPEG, with the following number being the average molecular weight (1=1 kDa, 5=5 kDa). (F2Ox) indicates the opened oxetane monomer with a perfluoroethyl side chain, and n denotes the number of oxetane units added.

Resulting polymers were purified by an automated CombiFlash® system. Polymerization yielded products with 3–10 oxetane monomers added. Using this system, different fractions of polymer, composed of a mixture of perfluoroether telomers added were isolated. The mPEG-1000 polymers contain mostly 3–4 and 4–5 unit fractions, while the mPEG-5000 contains fractions composing mostly of 3–5 and 7–9 units added. This polydispersity agrees with similar behavior reported in the literature.[17, 18]

It can be seen from the above synthetic scheme (Figure 2.1), that polymerization yields were not as high as expected, with the CombiFlash separation showing significant amounts of unreacted polyethylene glycol eluting just before the reaction product. Efforts were made to increase yield and selectivity of the polymerization by changing reaction conditions such as temperature, reaction time, solvent, and Lewis acid. Selected experiments are shown in Table

2.1. Note: pre-reaction time signifies the period of mixing between mPEG and Lewis acid,

before the addition of oxetane monomer, which showed to be inconsequential in terms of

monomers added or yield.

**Table 2.1: Selected oxetane polymerizations with varying experimental parameters.**

| Solvent | Temp. (°C) | Lewis Acid | Time | % Yield (purified) |
|---------|-----------|------------|------|-------------------|
| DCM | 0 | $BF_3 \cdot OEt_2$ | 30 min pre-react, 24 h total | 25 |
| DCM | -20 | $BF_3 \cdot OEt_2$ | 20 min pre-react, 1 h total | 31 |
| DCM | -78 | $BF_3 \cdot OEt_2$ | 30 min pre-react, 2 h total | 22 |
| DCM | -78 | $BF_3 \cdot OEt_2$ | 30 min pre-react, syringe pump added oxetane over 12 h | 20 |
| DCM | -78 | $BF_3 \cdot OEt_2$ | 1 h pre-react, 2 h total | 64 |
| DCM | -78 | $BF_3 \cdot OEt_2$ | 1 h pre-react, 5 h total | 25 |
| DCM | -78 | $BF_3 \cdot OEt_2$ | 1 h pre-react, 24 h total | 51 |
| THF | 0 | $BF_3 \cdot OEt_2$ | 2 h pre-react, 24 h total | 56 |
| DCM | 0 | $TiCl_4$ | 1 h pre-react, 24 h total | No reaction |
| DCM | 0 | LiCl | 1 h pre-react, 24 h total | No reaction |

After studying these variables, it was seen that yields were not consistent and fluctuated

between 20 and 70 percent. Reaction time and temperature appeared to be unimportant in yield

as well as selectivity–always producing polymers with 3-10 oxetane united added. The fluorous

oxetane was added via syringe pump for one experiment to see if the selectivity could be

controlled. It was presumed that if added slowly, each polymer would react with the oxetane at

equal rates and produce a monodisperse polymer with a predetermined amount of oxetane added,

however this trial was not successful in affecting the dispersity. Although the varying of these

conditions did not produce better yields, it was concluded that boron trifluoride diethyl etherate

was the most successful Lewis acid used, as the others yield no product. These results suggest the kinetics of polymerization do not depend on the size of the polymer and it is fast enough to only produce a polydisperse product. The necessity of using boron trifluoride diethyl etherate did not allow us to explore slower reaction kinetics.

Another possible hindrance to the success of the reaction is the use of mPEG. This hydrophilic polymer can easily absorb water and cause low reactivity to oxetane polymerization. To explore this, 1-decanol, which is not hygroscopic, was employed instead as the macroinitiator, shown in Figure 2.3. After purification, it was seen that yields were comparable to the previous polymerization using mPEG as the macroinitiator, suggesting that the quality of mPEG used was not an issue. Selectivity was also similar in this reaction, as it was seen that 2-8 oxetane units were added to the lipophilic alcohol.
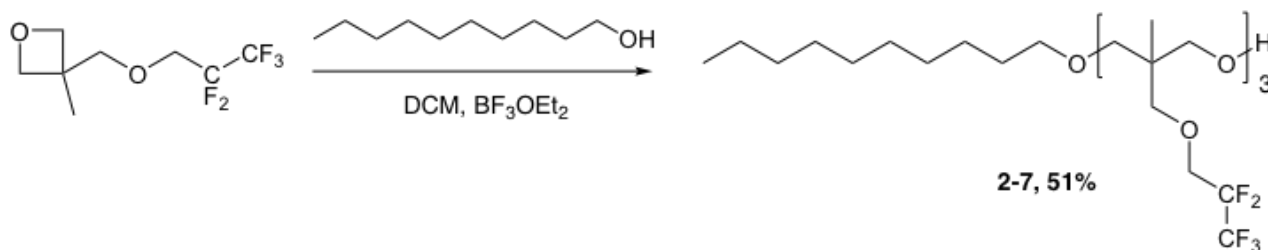


**Figure 2.3: Synthesis of H10(F2Ox)$_n$, starting from fluorous oxetane and 1-decanol**.

*2.2.2 Physicochemical characterization*

Dynamic light scattering (DLS) was applied to measure the average hydrodynamic size of the amphiphilic aggregates in solution. The particle size data are summarized in Table 2.2. As expected, as the length of hydrophobic chain increases, so does the aggregate size. Most of the polymer sizes are consistent with known micelle-forming fluorocarbon polymers according to PEG size, besides M1(F2Ox)$_{3-4}$ and M5(F2Ox)$_{3-5}$.[9] The small size of these aggregates suggest the DLS measurement was probably the size of the monomer. This hypothesis is corroborated for M1(F2Ox)$_{3-4}$, as the polymer does not form micelles to encapsulate the P3P probe for

microviscosity experiments. In contrast, M5(F2Ox)$_{3-5}$, which also has a small hydrodynamic size, does in fact encapsulate P3P, suggesting the polymer does form micelles. This difference in encapsulation may be due to the slight increase in oxetane units added to this polymer (3-4 versus 3-5). Interestingly, a CMC value could be calculated for M1(F2Ox)$_{3-4}$, even though it may not be forming micelles, leading to a disagreement in data. It should be noted that cryogenic transmission electron microscopy (cryo-TEM) is commonly used to validate the aggregate shape. However, these amphiphiles contain a relatively small hydrophobic core compared to a large mPEG chain, which is highly solvated and indistinguishable from vitrified water.[19]

**Table 2.2: Physicochemical data of selected Mx(F2Ox)$_n$ polymers.** [a]Particle sizes of fluoropolymer-based aggregates. Data are given with the standard deviation (n = 3). Each measurement was repeated in triplicate. [b]Critical micelle concentration determined by surface tension. Each measurement repeated four times. CMCs of M1(F2OX)$_{7-9}$, M5(F2OX)$_{6-7}$, and M5(F2OX)$_{8-10}$ were not determined due to insufficient yields of these polymer fractions. Values commonly reported as pCMC (-log(M))  [c]Microviscosity determined by P3P excimer fluorescence, repeated in triplicate.

| Polymer | Particle Size (nm)[a] | CMC (log (M)±SD)[b] | Microviscosity (Im/Ie)[c] |
|---|---|---|---|
| **M1(F2Ox)$_{3-4}$** | 4.35 ± 1.00 | -5.01 ± 0.03 | No P3P encapsulation |
| **M1(F2Ox)$_{4-5}$** | 15.74± 0.63 | -4.77 ± 0.03 | 2.4 ± 0.11 |
| **M1(F2Ox)$_{7-9}$** | 16.27 ± 0.39 | N/A | 7.30 ± 0.51 |
| **M5(F2Ox)$_{3-5}$** | 4.51 ± 0.75 | -4.99 ± 0.08 | 3.40 ± 0.40 |
| **M5(F2Ox)$_{6-7}$** | 15.61 ± 0.32 | N/A | 5.43 ± 0.19 |
| **M5(F2Ox)$_{8-10}$** | 43.25 ± 0.95 | N/A | 18.08 ± 0.12 |

The critical micelle concentrations (CMC) of these polymers were estimated by measuring the surface tension of polymer solutions at various concentrations in water. Increasing the concentration of the polymer under the CMC leads to a linear decrease in the surface tension. At the CMC, micelle formation begins and any additional surfactant will aggregate and not affect the surface tension any longer (Figure 2.4). It has been shown that substitution of fluorine atoms

for hydrogen decreases an amphiphile's surface activity for aqueous solutions, which promotes

micellization at lower concentrations.[20] For these polymers, the CMC was unaffected by the

length of hydrophilic segment (PEG), but had a slight increase as more hydrophobic monomers

were added.
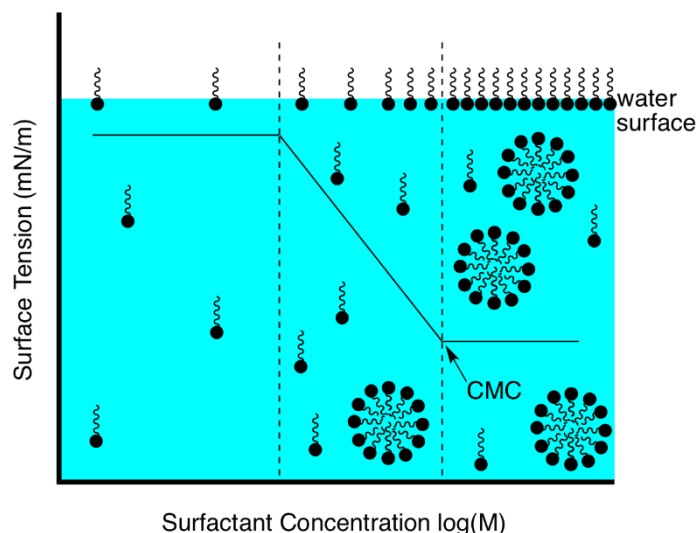


**Figure 2.4: Schematic relating concentration, surface tension of water, and the critical micelle concentration (CMC).** Region A corresponds to low adsorbed surfactant where surface tension is close to that of pure water. B is where surface tension drops as adsorbed surfactant concentration increases, beginning to form nanoparticles. Region C is where surface tension plateaus at surface saturation.

The micelle core microviscosity, which is related to micelle stability, was then measured.

Typically, increases in microviscosity are correlated with more crystalline micelles, which is a

result of tighter packing of unimers or chain entanglement. A more viscous core is thought to

dissociate more slowly, allowing for longer circulation times of the drug-loaded micelle. This

property is investigated through the encapsulation of 1,3-(1,1'-Dipyrenyl)-propane (P3P), which

is a small, hydrophobic fluorescent probe that segregates into the hydrophobic core of the

micelle. P3P forms intramolecular pyrene excimers due to free rotation of the carbon bond

between the pyrene fragments when excited. As P3P is encapsulated in the micellar core, this

conformational change is restricted by core friction proportional to the viscosity of its

environment. A higher monomer to excimer fluorescence intensity ratio ($I_M/I_E$) is indicative of a microenvironment viscosity.[21] Table 2.2 shows that as fluorophilic character increases, so does the microviscosity. As M1(F2Ox)$_3$ did not encapsulate P3P, along with the small particle size, it can be suggested that this specific polymer did not form micelles, and the DLS was measuring size of monomer. Additionally, as the fluorous block become longer, 7-9 monomers added, the viscosity was much larger, owing to a more viscous and stable core.
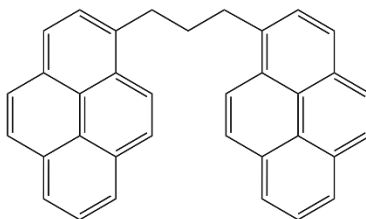


**Figure 2.5: Chemical structure of 1,3-bis(1'-pyrenyl)propane (P3P).**

To further evaluate the lipophilicity of the aggregate's core, and its potential for drug delivery applications, attempts at solubilizing a highly hydrophobic molecule were undertaken. The anticancer agent paclitaxel was used as a model lipophilic small molecule to encapsulate within the nanoparticle core. PTX-loaded micelles were prepared by the solvent evaporation method (SEM) and the amount quantified using HPLC directly after preparation and then after 24 hours (Table 2.3).
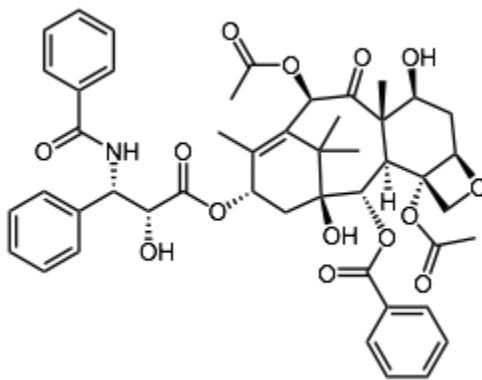


**Figure 2.6: Chemical structure of paclitaxel.**

It was found that the presence of short fluorocarbons in the micelle core prevents the binding and encapsulation of purely hydrophobic molecules (Table 2.3). This result suggests that the micellar core is not adequately lipophilic for drug encapsulation, which makes sense, as there are pendant fluorous chains throughout which repel molecules that are not fluorophilic.

**Table 2.3: Encapsulation of paclitaxel in polymeric micelles at 0 and 24h.** Results are expressed as Mean ± S.D. (n=3).

| Polymer | Initial solubility (µg/mL) | Drug Loading Efficiency (%) | Drug solubility 24 h (µg/mL) | % Retained at 24 h |
|---|---|---|---|---|
| M1(F2Ox)$_3$ | 68 ± 7.1 | 2.1 ± 0.2 | 5.6 ± 2.9 | 8.1 ± 3.3 |
| M1(F2Ox)$_5$ | 94 ± 10.0 | 2.3 ± 0.2 | 2.3 ± 0.3 | 2.4 ± 0.5 |

Upon addition to dissociative media, such as blood serum proteins, micelles display different rates of dissociation.[22] Attempts were made to evaluate this rate, also termed the *in vitro* kinetic stability, of M1(F2Ox)$_5$ using two FRET probes. In this experiment, the minimal fluorescence and eventual absence of fluorescence, after 15 minutes, indicated the FRET pair DiI and DiO were not encapsulated well within the hydrophobic core of the micelle. The results seen here are common problems with using FRET fluorophores as a way to measure kinetic stability of micelles, which will be further discussed in Chapter 4.
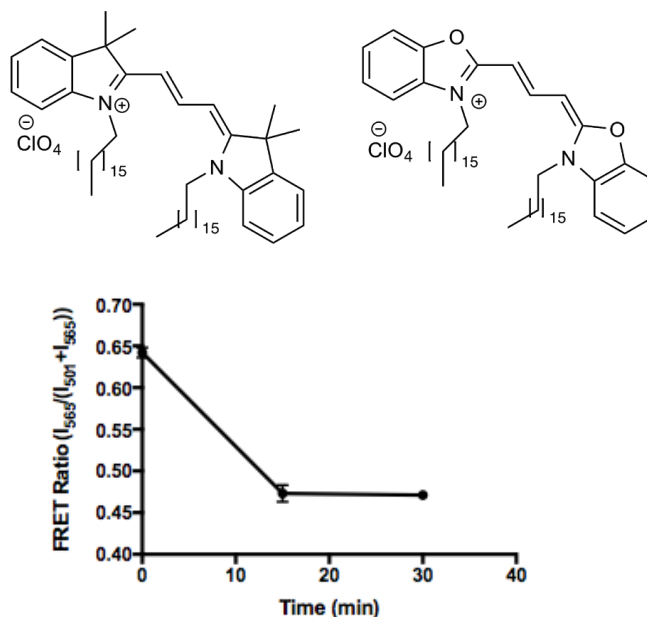
**Figure 2.7: DiI/DiO chemical structures and the FRET ratio of M1(F2Ox)₅ micelles measured over time in human serum at 22°C.**

*2.2.3 Fluorous anesthetic emulsions*

The results on the poor loading of lipophilic molecules within the micellar core suggest that the polyoxetane block is more fluorophilic than lipophilic. To test this conclusion, the emulsification of fluorinated anesthetics was studied, specifically looking at possible differences between the fluorophilic sevoflurane and the more lipophilic isoflurane (Figure 2.5). Both of these anesthetics are liquid at room temperature and typically administered through inhalation techniques. However, the administration of these through IV in a nanoemulsion formulation has some advantages: i) eliminates the need for equilibration with the lungs, therefore induction of anesthesia is quicker and ii) IV administration leads to near 100% bioavailability, allowing for smaller doses.[23]
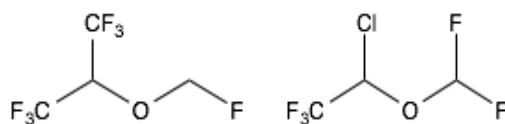


**Figure 2.8: Chemical structures of the fluorous anesthetics sevoflurane (left) and isoflurane (right).**

Previous studies have shown that PEG-based copolymers with a fluorocarbon core can form stable emulsions with sevoflurane. The polymers used in those studies typically contained a purely fluorophilic chain with more than eight carbon atoms.[9, 10] In contrast, use of polymers with perfluoroethyl groups attached as side chains of hydrophobic monomers led to a significant difference in stability between sevoflurane and isoflurane emulsions, the latter being remarkably more stable. The main mechanism of destabilization of fluorocarbon-based emulsions is molecular diffusion, better known as Ostwald ripening.[24] In this mechanism, individual molecules of fluorous anesthetic diffuse out of smaller particles, due to the higher curvature of these particles and therefore higher chemical potential, to join larger growing droplets. The rate of increase of the droplets' volume over time is a linear function of the interfacial tension, the solubility and diffusion of the dispersed perfluorocarbon in the aqueous phase, and the particle radius.[24] Plotting particle size *vs.* time gives a fair representation of emulsion stability (Figure 2.9). For practical use, IV injectable emulsions must maintain a mean diameter ≤500 nm within an 11-month period when stored at 5°C.[10]
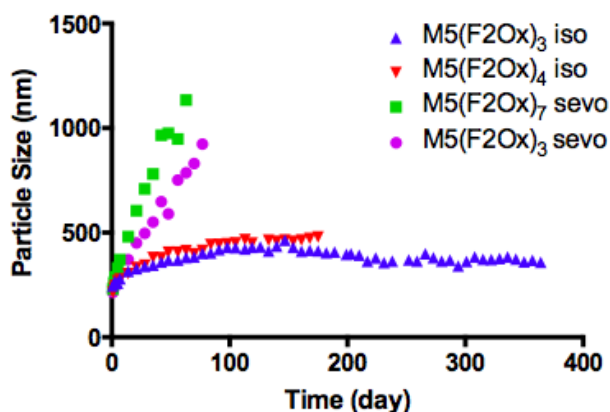


**Figure 2.9: Change in particle sizes of fluoropolymer-based emulsions with time**: (green) M5(F2Ox)7 with sevoflurane; (purple) M5(F2Ox)3 with sevoflurane; (blue) M5(F2Ox)3 with isoflurane, (red) M5(F2Ox)4 with isoflurane. All emulsions contained 20% of respective fluorous anesthetic and 10% perfluorooctyl bromide (a stabilizing additive) and were prepared in saline (0.9% w/w NaCl). Note standard error bars are removed for clarity.

Fig. 2.7 shows the ripening behavior with time of emulsions of sevoflurane and isoflurane made with the polymer containing either and average of 3, 4, or 7 units of the perfluoroether telomer. While the sevoflurane emulsion showed a quick increase in particle size and eventual phase-separation, isoflurane led to a much more stable formulation containing 20% v/v of anesthetic, with particle size staying around 400 nm for over a year. Polymers with longer fractions of polyoxetane were poorly water-soluble and thus unable to make sevoflurane or isoflurane emulsions. Possibly the use of a larger PEG and/or a different hydrophilic block could provide adequate water solubility for these amphiphiles to be used in various applications.

The variation of particle size between the emulsions of polymer M5(F2Ox)$_3$ can be explained when considering the chemical structure of both polymer and fluorous anesthetic. Sevoflurane has a greater fluorine content than isoflurane and will be solubilized better by a fully fluorophilic chain. The hydrophobic chain used in these polymers contains a short perfluoroethyl group, as well as a polyether backbone, giving the polymer both lipophilic and fluorophilic properties. Therefore, we ascribe the difference in stability between the two emulsions to a better match between the hydrophobicity/fluorophilicity balance of the polymer with that of isoflurane.

**2.3 Conclusions**

In summary, we have synthesized amphiphilic block polymers where a methoxy-PEG is attached to a short hydrophobic block with a lipophilic backbone and perfluoroethyl side chains. The size of the hydrophobic/fluorophilic moiety affected surface properties such as critical micelle concentration, hydrophobic drug encapsulation and nanoemulsion stability. It was found that the short pendant perfluoroethyl side chain induced a balance of hydrophobicity and fluorophilicity optimal for emulsification of isoflurane. In contrast, the more fluorophilic sevoflurane formed unstable emulsions and the encapsulation of purely hydrophobic molecules

was not possible at therapeutic concentrations, confirming the mixed lipophilic/fluorophilic environment provided by the perfluoro telomer block.

Highly concentrated, 20% v/v emulsions of isoflurane were possible with the polymer containing up to three or four units of perfluoroether telomer. The emulsions were found to be stable over a period of 12 months. These results indicate that fluorophilic behavior can be induced using short, perfluoroethyl groups. Potential metabolism products of such short fluorocarbons do not bioaccumulate and therefore toxicity considerations will not be a limiting factor for their application.[3, 4]

## 2.4 Experimental Section

### 2.4.1 Materials

Paclitaxel was purchased from LC Laboratories. Isoflurane was purchased from Piramel Healthcare. Sevoflurane was purchased from Abbott Labs and normal saline (AirLife sterile 0.9% NaCl for irrigation USP) from Braun Medical Inc. Pooled normal human serum was purchased from Innovative Research, Inc. Fluorous alcohols and perfluorooctyl bromide were purchased from SynQuest. All other reagents and solvents were of ACS grade or higher, were purchased from Sigma-Aldrich, and were used as received, unless otherwise specified.

### 2.4.2 Instrumentation and Methods

$^1$H, $^{13}$C and $^{19}$F NMR experiments were conducted on a Varian *UNITY INOVA*-400 NMR spectrometer at 25°C using deuterochloroform (CDCl$_3$) as the solvent with TMS as an internal reference.

Small molecules were purified with using regular phase chromatography, using Silicycle 60 Å silica. Surfactants were purified by automated flash chromatography using a CombiFlash® Rf 4x system equipped with ELSD for compound visualization and a REDI-Sep Rf Gold C-18

silica high-performance aqueous reverse phase cartridge. Products were eluted with a 10–100% methanol in water (0.1% formic acid) gradient.

*2.4.3 Synthesis of 3-bromo-2-bromomethyl-2-methylpropyl acetate (2-2)*

1,1,1-Tris(hydroxymethyl)ethane (TME) (25.58 g, 212.9 mmol) was weighed into a 500 mL round bottom flask and glacial acetic acid (100 mL) was added, stirring vigorously for 2 h to partially dissolve TME. Sodium bromide (65.75 g, 638.97 mmol) was added and reaction fitted with addition funnel and flushed with argon. Sulfuric acid (25 mL, 511 mmol) was added dropwise over 1 h, and the flask fitted with condenser and heated to 110°C. After 7d, heat was turned off and reaction came to room temperature. The reaction was then diluted with 250 mL $H_2O$ and layers separated. Organic layer was washed with $H_2O$ (100 mL), 0.5 M NaOH (2 x 200 mL), and aq. NaCl (200 mL). The reaction was then dried over anhydrous magnesium sulfate and filtered. Crude oil was purified by flash column, packing with hexane and eluting with 5% ethyl acetate/hexane to collect first product only. Oil was isolated by rotary evaporation to give 58.42 g (95% yield). $^1$H NMR (400 MHz, CDCl$_3$): δ 4.06 (s, 2 H), 3.45 (dd, $J$ = 12.8, 10.4 Hz, 4 H), 2.08 (s, 3 H), 1.17 (s, 3 H). $^{13}$C NMR (100 MHz, CDCl$_3$): δ 170.6, 67.3, 39.2, 38.5, 34.7, 31.8, 25.5, 22.9, 21.0, 20.4, 14.3.

*2.4.4 Synthesis of 3-(bromomethyl)-3-methyloxetane (2-3)*

3-Bromo-2-bromomethyl-2-methylpropyl acetate (20.13 g, 69.92 mmol) was dissolved in $CH_2Cl_2$ (100 mL) and aq. NaOH (3 M, 100 mL). Tetrabutylammonium bromide (1.32 g, 4.09 mmol) was added and reaction stirred vigorously under argon and heated to reflux. After 24h, reaction was stopped and layers were separated. Excess $CH_2Cl_2$ was gently removed under reduced pressure. Oil was purified by vacuum distillation, collecting fraction at 50 C to give 5.07

g (43.9%). $^1$H NMR (400 MHz, CDCl$_3$): δ 4.38 (d, $J$ = 6.4 Hz, 2 H), 4.33 (d, $J$ = 6.4 Hz, 2 H), 3.59 (s, 2 H), 1.37 (s, 3 H). $^{13}$C NMR (100 MHz, CDCl$_3$): δ 80.74, 41.63, 40.79, 22.62.

*2.4.5 Synthesis of 3-(1H,1H-perfluoropropan-1-oxymethyl)-3- methyloxetane (2-4)*

3-(Bromomethyl)-3-methyloxetane (5.07 g, 30.76 mmol), pentafluoropropan-1-ol (4.73 g, 31.49 mmol), tetrabutylammonium bromide (246.3 mg, 0.76 mmol) and water (4.5 mL) were added to a 100 mL round-bottom flask with stir bar, flask flushed with argon and heated to 95 C. Potassium hydroxide (4.36 g, 40% solution in water) was added over 10 min to the stirring reaction at 95 C. Reaction was left overnight under argon. Mixture was then allowed to cool to room temperature and CH$_2$Cl$_2$ (12 mL) was added and layers separated. The aqueous layer was extracted with dichloromethane (20 mL). Combined organic layers were dried over anhydrous magnesium sulfate and the solvent gently removed by rotary evaporation. The remaining oil was purified by vacuum distillation, collection fractions at 20°C to yield 1.05 g (57% yield). $^1$H NMR (400 MHz, CDCl$_3$): δ 4.49 (d, J = 6 Hz, 2 H), 4.37 (d, $J$ = 6 Hz, 2 H), 3.96 (tq, J = 12, 1.2 Hz, 2 H), 3.69 (s, 2 H) 1.32 (s, 3 H). $^{13}$C NMR (100 MHz, CDCl$_3$): δ 79.83, 78.32, 68.24 (t, $J$ = 26.8 Hz), 40.15, 21.11. Carbons containing F's were not visible with the used acquisition scans. $^{19}$F NMR (376 MHz, CDCl$_3$): δ 84.01 (s, 3 F), 123.59 (t, $J$ = 12.4 Hz, 2 F).

*2.4.6 Synthesis of M1(F2Ox)$_n$ (2-5)*

Monomethoxy polyethylene glycol (430 mg, average molecular weight = 880 g/mol) was dissolved in 7 mL anhyd. CH$_2$Cl$_2$. Boron trifluoride–diethyl ether complex (75 mL) was added under argon and the mixture was allowed to stir for 30 min. Solution was then cooled in an ice bath and fluorous oxetane, 3-(1H,1H-perfluoropropan-1-oxymethyl)-3- methyloxetane, (1.00 g) dissolved in CH$_2$Cl$_2$ was added dropwise over the course of 30 min. The reaction was stirred under argon overnight and brought to room temperature. Reaction was then quenched with water

and diluted with $H_2O$ (5 mL) and aq. NaCl (5 mL) to break up emulsion. Layers were separated

and the aqueous layer was extracted with $CH_2Cl_2$ (2 x 5 mL). Organic layers were combined and

dried over anhyd. magnesium sulfate and filtered. The solvent was removed under low pressure

and the residue was purified by reverse-phase flash chromatography to yield 563 mg (64%

yield). ^{1}H NMR (400 MHz, CDCl$_3$): δ 3.84 (t, $J$ = 12.8 Hz, 34 H), 3.65 (m, 80 H), 3.43 (m, 20

H), 3.37 (m, 11 H), 3.18 (m, 5 H), 0.90 (m, 46 H). ^{19}F NMR (376 MHz, CDCl$_3$): δ 84.07 (m, 3

F), 123.84 (m, 2 F).

*2.4.7 Synthesis of M5(F2Ox)$_n$ (2-6)*

Monomethoxy polyethylene glycol (2.24 g, average molecular weight = 4200 g/mol) was

dissolved in 7 mL anhyd. $CH_2Cl_2$. Boron trifluoride–diethyl ether complex (55mL) was added

under argon and the mixture was allowed to stir for 30 min. Solution was then cooled in an ice

bath and fluorous oxetane, 3-(1H,1H-perfluoropropan-1-oxymethyl)-3- methyloxetane, (1.05 g)

in dichloromethane solution was added dropwise over the course of 30 min. The reaction was

stirred under argon overnight and brought to room temperature. Reaction was then quenched

with water, diluted with $H_2O$ (5 mL) and aq. NaCl (5 mL) to break up emulsion. Layers were

separated and the aqueous layer was extracted with $CH_2Cl_2$ (2 x 5 mL). Organic layers were

combined and dried over anhyd. magnesium sulfate and filtered. The solvent was removed under

low pressure. Polymer was purified by reverse-phase flash chromatography to yield 1.408 g

(55% yield). ^{1}H NMR (400 MHz, CDCl$_3$): δ 3.84 (t, $J$ = 12.8 Hz, 79 H), 3.65 (m, 480 H), 3.43

(m, 41 H), 3.37 (m, 30 H), 3.18 (m, 124 H), 0.90 (m, 108 H). ^{19}F NMR (376 MHz, CDCl$_3$): δ

84.07 (m, 3 F), 123.84 (m, 2 F).

*2.4.8 Synthesis of H10(F2Ox)$_n$ (2-7)*

Decanol (60.1 mg, 0.37 mmol) was added to a dry 50 mL round bottom flask, followed by 20 mL $CH_2Cl_2$. $BF_3OEt_2$ (60 μL, 0.48 mmol) was added and the reaction was stirred under argon for 30 minutes. The fluorous oxetane, 3-(1H,1H-perfluoropropan-1-oxymethyl)-3-methyloxetane, (797.7 mg, 3.41 mmol) in a solution of $CH_2Cl_2$ was added dropwise and allowed to react for 3 hours. The reaction was quenched with water, layers separated, and the aqueous solution extracted with $CH_2Cl_2$ (2 x 50 mL). The combined organic layers dried over anhyd. $MgSO_4$, rotovapped gently to remove solvent until a clear oil remained. MALDI distribution centered at $[M+Na]^+=883$, with peaks corresponding to 2-8 units of oxetane added.

*2.4.9 Micelle preparation—solvent evaporation method (SEM)*

The polymer is dissolved in methanol or acetonitrile to a desired concentration. Polymer solution and additive (e.g., paclitaxel in acetonitrile) are added to a 25 mL round bottom flask and rotated for 5 min at 60°C on a rotary evaporator, no vacuum, and then the solvent was removed in vacuo with rotation for 15 min. The film was then dispersed with Millipore water heated to 60°C and filtered with a 0.45-mm nylon filter.

*2.4.10 Preparation of fluorous anesthetic nanoemulsions*

Polymer solution in normal saline solution (10 mM, 11.9 mL) was prepared freshly. Normal saline was made with 0.9% (w/w) of sodium chloride. Sevoflurane or isoflurane (3.4 mL) and perfluorooctyl bromide (1.7 mL) were added to the polymer solution, for a total volume of 17 mL. The homogenizer and microfluidizer were previously cleaned with 70% and 100% ethanol, followed by 70% and 100% methanol, and finally with three rinses of Millipore water to remove any solvents from previous washes. Once prepared the mixture is then homogenized (Power Gen 500, Fisher Scientific, Hampton, NH) for 1 min at 21000 rpm at room temperature.

The crude emulsion made with the high speed homogenizer was further homogenized with a Microfluidizer (model 110 S, Microfluidics Corp., Newton, MA) for 1 min under 5000 psi with the cooling bath kept at 15°C. The final emulsion was then filtered with a 0.45mm nylon filter and stored in plastic centrifuge tubes (Corning Inc., Corning, NY) at 4°C.

*2.4.11 Particle size determination by dynamic light scattering (DLS)*

Particle sizes of polymeric micelles were analyzed by dynamic light scattering (Zetasizer Nano-ZS, Malvern Instruments, Worcestershire, UK). The polymer solution was measured directly without dilution and analyzed. Each particle size analysis was run at room temperature and repeated in triplicate with the number of scans of each run determined automatically by the instrument according to the concentration of the solution. The data was analyzed using Malvern software analysis and reported as volume weighted average diameters. Particle sizes of emulsions were analyzed by dynamic light scattering (NICOMP 380ZLS, Particle Sizing Systems, Santa Barbara, CA). The emulsions were diluted at the intensity factor of 300 by adding 60mL of the emulsion to 2.940 mL of Millipore water. Each particle size analyzing was run for 5 min at room temperature and repeated three times. The data was analyzed using Gaussian analysis and reported as volume weighted average diameters.

*2.4.12 Critical micelle concentration (CMC) determination—surface tensiometry*

Polymer was dissolved in Millipore water to a concentration of 1 mM and concentrations down to 1 nm were prepared by serial dilution and transferred to 20 mL disposable scintillation vials. After solutions were made, the samples were vortexed and sonicated and then heated in a water bath at 40°C for 2–3 h. Solutions were then allowed to equilibrate for 24 hours. Surface tensions were measured on a KSV sigma 701 tensiometer (KSV Instruments, Helsinki, Finland) equipped with a Julabo F12-MC circulator for constant temperature control. Custom round rod

made of platinum with a diameter of 1.034 nm with wetted length of 3.248 mm was used. First, the rod was submerged into absolute alcohol and flame dried with a Bunsen burner for 4 s, then repeated after 4 min and hung on instrument and allowed to cool to room temperature without touching any surface. Before running the experimental samples, the surface tension of Millipore water was measured as control to confirm vial and rod were fully cleaned and surface tension was within 1 of 78.2 mN/m. The surface tension measurements began with the least concentrated solution and proceed to successively more concentrated solutions. The surface tension at each concentration was measured in quadruplet and average recorded. The critical micelle concentration value was determined from crossover point of two lines: the baseline of minimal surface tension and the slope where surface tension showed linear decline; error determined by weighted least squares analysis.

*2.4.13 Measurement of Core Microviscosity-P3P encapsulation*

The relative microviscosity of the micelle core was estimated from the intensity ratio ($I_M/I_E$) of monomer and excimer emission of 1,3-(1,1$^{'}$-Dipyrenyl)-propane (P3P) at 376 and 480 nm, respectively, in response to excitation at 333 nm. P3P was dissolved in chloroform in an amber vial to achieve a final concentration of $2 \times 10^{-7}$ M and 0.4 mM polymer solutions were prepared in ACN. Micelle solutions were prepared in triplicate via the solvent evaporation method. The samples were then redispersed with 60°C PBS (2 mL), shaken vigorously and filtered through a 0.45 μm filter and stored in amber vials. The fluorescence analysis was carried out on an AMINCO-Bowman Series 2 spectrometer with excitation at 333 nm, emission at 378 nm and a spectral window of 350-500 nm. (Thermo Fisher, Madison, WI).

*2.4.14 Paclitaxel Encapsulation*

Micelles were prepared in triplicate by the thin film evaporation method. Paclitaxel stock solution was generated by dissolving PTX in ACN, aided by sonication, at a concentration of 1 mg/mL. Polymer was dissolved in ACN to give a final concentration of 2.4 mM. Micelle solutions were prepared by adding polymer solution (1 mL) to a round bottom flask, followed by PTX solution (230 μL). The thin film was rehydrated with 60°C PBS (1 mL) with gentle agitation. The sample was then centrifuged at 12,000 rpm for 5 minutes and filtered through 0.45 μm nylon syringe filter to remove any insoluble precipitate. The content of paclitaxel loaded in the micelle was quantified by reverse phase HPLC. The HPLC system used for quantifying was a Shimadzu prominence HPLC system (Shimadzu, Japan), consisting of a LC-20AT pump, SIL-20 AC HT autosampler, CTO-20 AC column oven and an SPD-M20A diode array detector. A 100-μL aliquot of micelle solution was mixed with 900 μL of methanol, and 20 μL of the mixture was injected into a C18 column (Agilent XDB-C8, 4.6 Å x 150 mm), eluting with an isocratic mixture of 25% water in acetonitrile. The run time was 3 min, the flow rate was 1.0 mL/min and the detection was at 227 nm.

*2.4.15 In vitro micelle kinetic stability-FRET method*

Polymer was dissolved in MeOH to give a concentration of 1 mg mL$^{-1}$. DiO and DiI were then separately prepared in MeOH to give concentrations of 0.1 mg mL$^{-1}$.  Four micelle solutions were prepared by the solvent evaporation method: 1 solution contained only polymer solution (1 mL), and was redispersed with 60°C PBS (1 mL) and filtered through a 0.45 μm nylon filter. Three solutions contained polymer solution (1 mL), DiI (46 μL) and DiO (44 μL) solutions. These were then redispersed with 60°C PBS (1 mL). The FRET experiment was performed by using AMINCO-Bowman Series 2 Luminescence Spectrometer (Thermo Fisher, Madison, WI).

The detector high voltage was adjusted for 50% of a maximum output signal. The sample was excited at 484 nm and emission spectra were measured from 495-600 nm. 150 μL of the micelle solution was mixed with 2.85 mL human serum. Fluorescence emission was measured every 20 minutes for 2 hours. To remove baseline noise due to human serum, fluorescence of empty micelles in the presence of human serum was also measured and subtracted from the spectra. The stability change of FRET proves loaded micelles was monitored by calculating the FRET ratio: $I_R/(I_G+I_R)$, where $I_R$ and $I_G$ are the peak fluorescence intensities of DiI and DiO at 565 and 501 nm, respectively, at t minutes in response to excitation at 484 nm. FRET ratio at each time point was then normalized to the initial FRET ratio.

## 2.5 References

(1) Zaggia, A.; Ameduri, B. Recent advances on synthesis of potentially nonbioaccumulable fluorinated surfactants. *Curr. Opin. Colloid Interface Sci*. **2012**, *17*, 188–195.

(2) Conder, J. M.; Hoke, R. A.; De Wolf, W.; Russell, M. H.; Buck, R. C.; Are PFCAs bioaccumulative? A critical review and comparison with regulatory criteria and persistent lipophilic compounds. *Environ. Sci. Technol*. **2007**, *42*(4), 995–1003.

(3) Dinglasan, M. J.; Ye, Y.; Edwards, E. A.; Mabury, S. A.; Fluorotelomer alcohol biodegradation yields poly- and perfluorinated acids. *Environ. Sci. Technol*. **2004**, *38*, 2857–2864.

(4) Wilson, C. J.; Wilson, D. A.; Feiring, A. E.;  Percec, V. Disassembly via an environmentally friendly and efficient fluorous phase constructed with dendritic architectures. *J. Polym. Sci. Part A Polym. Chem.* **2010**, *48*(11), 2498–2508.

(5) Kausch, C. M.; Leising, J. E.; Medsker, R. E.; Russell, V. M.; Thomas, R. R.; Synthesis, characterization and unusual surface activity of a series of novel architecture, water-dispersible poly(fluorooxetane)s. *Langmuir* **2002**, *18*(15), 5933–5938.

(6) Fujiwara, T.; Makal, U.; Wynne, K. J. Synthesis and characterization of novel amphiphilic telechelic polyoxetanes. *Macromolecules* **2003**, *36*, 9383–9389.

(7) Moody, C. A.; Field, J. A.; Perfluorinated surfactants and the environmental implications of their use in fire-Fighting foams. *Environ. Sci. Technol*. 2000, 34(18), 3864-3870.

(8) PolyFox, A Novel Fluorochemical, (2015) http://www.omnova.com/products/chemicals/PolyFox.aspx (accessed 12/14/15).

(9) Fast, J. P.; Perkins, M. G.; Pearce, R. A.; Mecozzi, S.; Fluoropolymer-based emulsions for the intravenous delivery of sevoflurane. *Anesthesiology* **2008**, *109*(4), 651–656.

(10) Jee, J. P.; Parlato, M. C.; Perkins, M. G.; Mecozzi, S.; Pearce, R. A. Exceptionally stable fluorous emulsions for the intravenous delivery of volatile general anesthetics. *Anesthesiology* **2012**, *116*(3), 580–585.

(11) Parlato, M. C.; Jee, J. P.; Teshite, M.; Mecozzi, S. Synthesis, characterization, and applications of hemifluorinated dibranched amphiphiles, *J. Org. Chem.* **2011**, *76*, 6584–6591.

(12) Yang, X. L.; Ma, H. X.; Yang, Z. B.; Liu, A. J.;  Luo, N. F.; Zhang, W. S.;  Wang, L.; Jiang, X. H.; Li, J.; Liu, J. Comparison of minimum alveolar concentration between intravenous isoflurane lipid emulsion and inhaled isoflurane in dogs. *Anesthesiology* **2006**, *104*(3), 482-7.

(13) Krahn, C. L.; Raffin, R. P.; Santos, G. S.; Queiroga, L. B.; Ruben, L.; Serpa, P.; Dallegrave, E.; Mayorga, P. E.; Pohlmann, A. R.; Natalini, C. C.; Guterres, S. S.; Limberger, R. P.; Weltin, H. Isoflurane-loaded nanoemulsion prepared by high pressure homogenization: investigation of stability and dose reduction in general anesthesia, *J. Biomed. Nanotechnol.* **2012**, *8*, 849–858.

(14) Malik, A. A.; Park, C.; Archibald, T. G. (Aerojet General Co., USA). Polymers and prepolymers from mono-substituted fluorinated oxetane monomers, US Patent 5,807,977, September 15, 1998.

(15) R.J. Weinert, M. Fay, G.C. Garcia, J.E. Robbins, OMNOVA Solutions, Inc., USA. Two stage thermoformable fluorinated polyoxetane-polyester copolymers, US Patent App 2002/0127420 A1 September 12 (2002).

(16) A.M. McCoy, Synthesis and Physicochemical Characterization of Highly Fluorinated Polymeric Amphiphiles for Intravenous Drug Delivery Applications. Ph.D. Thesis. University of Wisconsin-Madison, Madison, WI, 2014.

(17) Makal, U.; Uilk, J.; Kurt, P.; Cooke, R. S.; Wynne, K. J.; Ring opening polymerization of 3-semifluoro- and 3-bromomethyloxetanes to poly(2,2-substituted-1,3- propylene oxide) telechelics for soft blocks in polyurethanes. *Polymer* **2005**, *46*, 2522–2530.

(18) Kausch, C. M.; Leising, J. E.; Mesker, R. E.; Russell, V. M.; Thomas, R. R. Synthesis, characterization, and unusual surface activity of a series of novel architecture, water-dispersible poly(fluorooxetane)s. *Langmuir* **2002**, *18*, 5933–5938.

(19) Johansson, E.; Lundquist, A.; Zuo, S.; Edwards, K. Nanosized bilayer disks: attractive model membranes for drug partition studies. *Biochim. Biophys. Act,a* **2007**, *1768*, 1518–1525.

(20) Myers, D. Association colloids: micelles, vesicles, and membranes, In *Surfaces, Interfaces, and Colloids: Principles and Applications*; John Wiley & Sons, New York, NY; 1999, pp 358–396.

(21) Zana, R. Microviscosity of Aqueous Surfactant Micelles: Effect of Various Parameters. *J. Phys. Chem.* **1999**, *103*(43), 9117–9125.

(22) Yang, C.; Ebrahim Attia, A. B.; Tan, J. P. K.; Ke, X.; Gao, S.; Hedrick, J. L.; Yang, Y. Y. The Role of Non-Covalent Interactions in Anticancer Drug Loading and Kinetic Stability of Polymeric Micelles. *Biomaterials* **2012**, *33*(10), 2971–2979.

(23) Raphael, J.; Lynch, C. Intravenous administration of halogenated inhaled anesthetics-research tool or real application? *Can. J. Anaesth.* **2009**, *56*(2), 91-95.

(24) Taylor, P. Ostwald ripening in emulsions: estimation of solution thermodynamics of the disperse phase, *Adv. Colloid Interface* **2003**, *106*, 261–285.

# Chapter 3: Perfluorooligoethers vs. Long-Alkyl Chain Fluorocarbons. Physicochemical Differences and Toxicity Issues

**Perfluorooligoethers vs. Long-Alkyl Chain Fluorocarbons. Physicochemical Differences and Toxicity Issues**

**Abstract**

Long-alkyl chain fluorocarbon acids are inert to environmental degradation and highly bioaccumulative, resulting in a potential danger to aquatic life and those exposed to contaminated water. Perfluorooligoethers (PFE) and short perfluoroalkyl chain-containing polymers have been proposed as a benign alternative to perfluorocarbons (PFC) due to their quick metabolic degradation *in vivo*, thus eliminating bioaccumulation. Here we report how PFEs behave in terms of physicochemical properties and as alternatives to the use of pure PFCs in PEGylated diblock copolymers. The fluorophilicity of PFEs was analyzed both computationally through the calculation of electrostatic potential surfaces and experimentally through the effect that PEGylated PFEs (PEG-PFE) have on the stability of fluorous emulsions as compared to standard PEGylated perfluorocarbons (PEG-PFC). An attenuated fluorophilicity in PFE was identified. Furthermore, the toxicity of PFE acids and their corresponding PEGylated derivatives was tested on a Zebrafish model. These toxicity tests were used to compare the toxicity of standard perfluorinated surfactants such as perfluorooctanoic acid with that of PFE acids as well as PEG-PFCs and PEG-PFEs. Toxicity results showed that both PEG-PFCs and PEG-PFEs are nontoxic up to a 1 mM concentration, while all perfluorinated acids, including the PFE acids, showed increased mortality and morphological toxicity at much lower concentrations.

**3.1 Introduction**

Perfluorinated compounds have garnered increased attention in the past two decades for their reported bioaccumulation and toxicity.[1,2] Perfluorinated polymers and surfactants used in industry typically degrade into shorter chain perfluorinated carboxylic (PFCA) and sulfonic

(PFSA) acids.[3] However, these acids are not degraded by abiotic mechanism such as hydrolysis or photolysis in water to any significant degree. In particular, perfluorooctanoic acid (PFOA) and perfluorooctanesulfonic acid (PFOS) have been shown to be toxic to aquatic life and persistent in the environment. These industrial surfactants have also been detected in municipal water treatment plants, with average concentrations in human serum at 3.4 and 14.5 ng/mL concentrations, respectively.[4] Specifically, extreme levels of PFOS and PFOA in human serum were detected in blood samples of workers in the fluorochemical manufacturing industry, ranging from 12.8 to 114 mg/mL, respectively.[5]

Government regulations have been implemented due to the observed perfluoroalkyl environmental persistence of these chemicals. For example, the Environmental Protection Agency (EPA) 2010/15 PFOA Stewardship Program called for all long-chain PFCAs and their precursors from various industrial companies to be eliminated from products and emissions.[6] However, not all perfluorinated molecules are toxic, with most being physiologically inactive.[7] Interestingly, the most toxic fluorous chemicals are perfluorinated acids, where the acid functionality is directly linked to the strongly electron-withdrawing perfluorocarbon, leading to very acidic species. The pKa of octanoic acid is 4.9,[8] whereas its fluorinated partner, perfluorooctanoic acid, has a calculated pKa of -0.5.[9] Also, the toxicity and bioaccumulation become more prevalent with longer perfluorocarbon chain length, particularly with those of six fluorinated carbons or more.[10] In addition, sulfonic acids tend to be more toxic than the corresponding carboxylic acids.[11]

Due to these issues, attempts to alleviate environmental persistence of PFCs are underway. Alternative perfluorinated substances have been investigated in hopes to replace those that are toxic while maintaining advantageous properties. One common effort seen in Solvay

Solexis products,[12] is introducing heteroatoms, usually oxygen, in between perfluoroalkyl

segments. It is expected that these ether linkages will promote degradation to small, nontoxic

perfluorinated derivatives, such as perfluoroethanol due to the increased reactivity of ether

linkages between fluorine-bearing carbon atoms.[2, 13, 14]

Despite their environmental pervasiveness, PFCs have admirable qualities such as low

surface tension, high heat and chemical resistance and oil and water repellence. PFCs have been

used in lubricants, fire-fighting applications, paints, polishes, adhesives and more.[15, 16] These

chemicals have also been utilized as polymeric blocks within water-soluble polymers in used in

drug delivery. Although not water-soluble themselves, PFCs can be covalently attached through

ether linkages to longer, hydrophilic chains to create amphiphilic systems, capable of

encapsulating important pharmaceuticals. It has been shown that polymers incorporating a

perfluorinated segment are capable of emulsifying volatile, fluorous anesthetics for intravenous

delivery.[17, 18] This mode of delivery is advantageous over inhalation techniques due to quick

equilibration, no need for expensive equipment and fast recovery times from anesthesia. The

water-soluble and biocompatible block of these polymers is usually a poly(ethylene glycol),

which is commonly used in drug delivery polymers. PEGylation has been used in the past to

improve water solubility and lessen the toxicity of certain molecules.[19] We hypothesize this

modification of PFCs consistently leads to decreased toxicity.

Perfluoroethers (PFE) represent a class of fluorous molecules that has been chosen to

replace perfluoroalkanes in industrial products. In the case of semifluorinated polymers for drug

delivery, the use of PFEs must create equally stable nanoparticles as their PFC predecessors.

Specifically, PFE PEGylated polymers must stably emulsify sevoflurane emulsions in a similar

manner than their perfluroalkyl counterpart. Previous work has shown the polymer M1F13

(Table 3.1), can form a stable nanoemulsions of the fluorinated volatile anesthetic sevoflurane. We used the ability of PFE polymers to stabilize sevoflurane emulsions as a tool for experimentally comparing perfluorooligoethers to perfluoroalkyl chains. The stability of each formulation is assessed by measuring the particle size and growth kinetics by dynamic light scattering (DLS). Furthermore, we have used electrostatic potential surface calculations as a mean of comparing the polarity and fluorophilicity of PFCs and PFEs.

Zebrafish toxicity studies have emerged as the premier way of efficiently looking at the toxicity of chemicals and nanoparticles.[19-21] Wide recognition of zebrafish as a popular animal model is due to the excellent set of characteristics these studies possess. For example, the embryos and hatched fish are transparent allowing for observations at every cell stage. Zebrafish also produce large numbers of offspring that develop rapidly, allowing for a quick (5 day) study with a large sample population.[20, 21] These features allow for rapid toxicity screenings of multiple chemicals while also being able to easily observe developmental malformations to young zebrafish. This model was used to screen the toxicity of perfluorinated acids and synthesized PEGylated perfluoroethers (PEG-PFEs) (Table 3.1).

**Table 3.1. Fluorous acids and polymers evaluated in zebrafish toxicity studies**. n=average repeating units of 23, x=average repeating unit 110, y=average repeating unit of 7.

| | |
|---|---|
| PFOA | |
| PFTDA | |
| FE2-COOH | |
| FE3-COOH | |
| bFE4-COOH | |
| M1F13 | |
| M1FE2 | |
| M1FE3 | |
| M1bFE4 | |
| M5(F2Ox) | |

### 3.2 Results and Discussion

*3.2.1 Synthesis and physicochemical characterization of PEGylated perfluorooligoethers*

Perfluorinated compounds are useful in many industrial applications, but have received increased examination due to environmental persistence. Recent modifications to perfluoroalkyl chains, such as introducing regularly spaced heteroatoms have reduced potential for bioaccumulation. This study examines the performance of PEGylated-perfluoroethers compared to traditionally used PEGylated-perfluoroalkanes in respect to fluorous emulsion stability. The synthesis of PEGylated perfluorooligoethers is rather straightforward, allowing us to investigate three different polymers, with varying lengths and side groups. Figure 3.1 shows the synthesis, which begins with converting the hydroxy-terminated end of hydrophilic poly(ethylene glycol) to a mesylate. This can then undergo a Williamson ether synthesis with the perfluoroether alcohol of choice to form the diblock polymer.
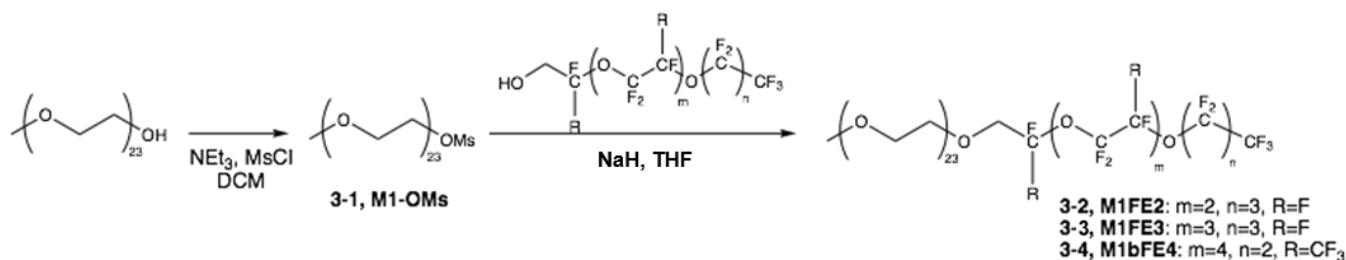


**Figure 3.2: Synthesis of PEGylated perfluorooligoethers (M1FE2, M1FE3 and M1bFE4).**

Dynamic light scattering (DLS) was used to measure the average hydrodynamic size of the amphiphilic aggregates in solution. The particle size data are summarized in Table 3.2. As expected, as the length of hydrophobic chain increases, so does the aggregate size. The polymer sizes are consistent with known micelle-forming fluorocarbon polymers according to PEG size.

To determine the critical micelle concentration (CMC), the concentration above which aggregates begin to form, surface tension analysis was used. Surfactant solutions were prepared

in deionized water at concentrations from 1 mM to 1 nM. The CMC was then determined as the

crossover of two lines and the error was determined by weighted, least-squares analysis. These

values are consistent with other semifluorinated polymers, in that they have a reduced CMC

compared to those without a fluorocarbon.

| Polymer | Particle Size (nm)[a] | CMC (log (M)±SD)[b] |
|---|---|---|
| M1FE2 | 8.99 ± 2.24 | -4.34 ± 0.07 |
| M1FE3 | 9.69 ± 2.0 | -6.03 ± 0.13 |
| M1bFE4 | 12.55 ± 3.36 | -4.35 ± 0.14 |

**Table 3.2: Physicochemical data for PEGylated perfluorooligoethers (M1FE2, M1FE3 and M1bFE4).** [a]Particle sizes of fluoropolymer-based aggregates. Data are given with the standard deviation (n = 3). Each measurement was repeated in triplicate. [b]Critical micelle concentrations determined by surface tension. Each measurement repeated four times.

*3.2.2 Fluorous anesthetic emulsions*

As a means of evaluating the fluorophilicity and potential for drug delivery of these PEG-

PFEs, the fluorous anesthetic sevoflurane was emulsified and the particle size was measured over

time. Previous studies in the group show the PEGylated perfluoroalkyl polymer, M1F13, can

stably emulsify 20% sevoflurane/10% perfluorooctyl bromide (PFOB) for around 3 months

while maintaining an average particle size below 500 nm.[22] The PEGylated perfluorooligoethers

were also tested in their abilities to emulsify sevoflurane. Interestingly, these formulations

exhibited an increased rate of particle growth, with eventual phase separation at week three

(Figure 3.2).
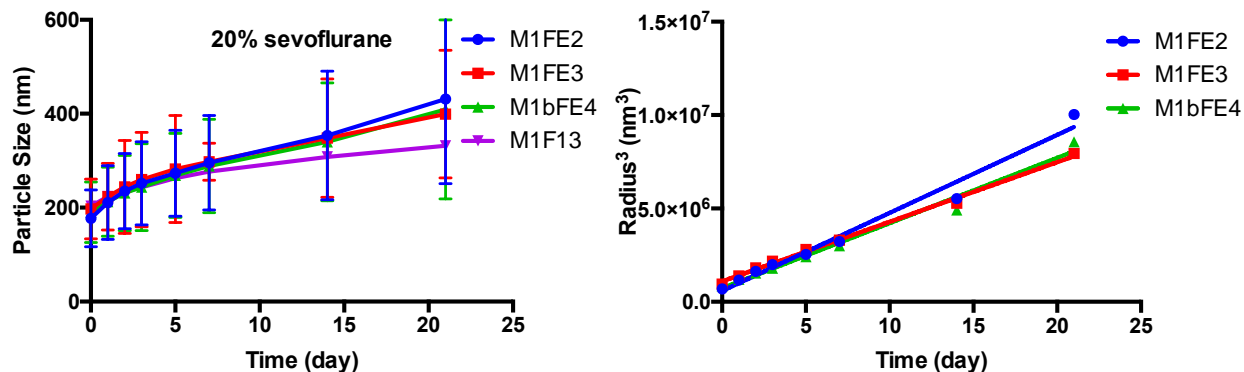
**Figure 3.2: Particle size growth for 20% sevoflurane emulsions stabilized by PEG-PFEs (left) and the cube of the radius (right).**

The Ostwald ripening rate of each polymer is displayed in Table 3.3. M1F13, which contains a rigid perfluoroalkyl chain that can effectively stabilize a fluorous droplet for emulsion stabilization. However, M1FE2, M1FE3 and M1bFE4, which contain perfluorooligoether chains, cannot stabilize the fluorous droplet. This behavior can be explained as due to a combination of decreased fluorophilicity as well as decreased rigidity [23-25] of the semifluorinated block.

| Polymer | Ostwald ripening rate ($nm^3s^{-1}$) |
|---------|--------------------------------------|
| M1F13   | $1.38 \pm 0.08$ |
| M1FE2   | $4.84 \pm 0.30$ |
| M1FE3   | $3.69 \pm 0.10$ |
| M1bFE4  | $4.04 \pm 0.22$ |

**Table 3.3: PEG-PFE Ostwald ripening rate derived from first 21 days of particle growth**.

*3.2.3 Electrostatic Potential Surfaces of Perfluorooligoethers*

The experimental studies based on the stabilization of fluorous nanoemulsions were supplemented with electrostatic potential surface (EPS) calculations to verify a difference in fluorophilicity between PFCs and PFEs. Figure 2 shows the EPSs of the fluorocarbon $C_{12}F_{26}$, the

perfluorooligo (ethylene glycol) $C_8F_{18}O_4$, and the polyether $C_8H_{18}O_4$ for comparison. A blue

color identifies an excess of positive potential, while a red color identifies an excess of negative

potential. Simple visual analysis of the three molecular electrostatic potential surfaces shows that

the perfluorocarbon **A** (Figure 3.3) is the least polar of the three molecules consistent with

fluorophilic behavior. Next is the perfluorooligo (ethylene glycol) **B**, which shows increased

polarity due to the presence of the oxygen atoms. It is this additional polarity that reduces the

fluorophilicity of the PFEs and makes impossible the stabilization of a purely fluorous

nanoemulsions. Finally, the polyether **C** shows the standard high polarity present in oligo

(ethylene glycol) molecules.
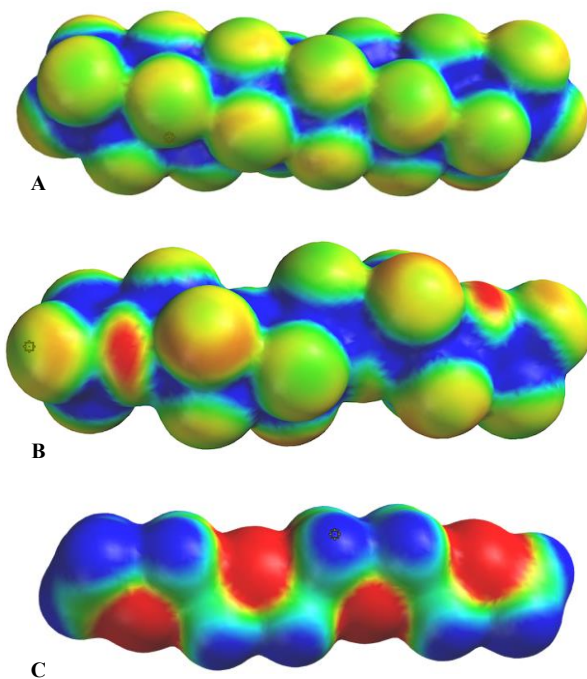


**Figure 3.3: Electrostatic potential surfaces of: A. The perfluorocarbon $C_{12}F_{26}$. B. The perfluorooligo (ethylene glycol) $C_8F_{18}O_4$. C. The oligo (ethylene glycol) $C_8H_{18}O_4$.** Red indicates an excess of negative potential while blue indicates an excess of positive potential. The ether oxygens in the perfluorooligo (ethylene glycol) **B**, contribute an increased molecular polarity as opposed to a pure perfluorocarbon (**A**) and this explains the decreased fluorophilicity of the PFEs. Electrostatic potential was mapped within the range -30/30 kJ/mol.

*3.2.4 Zebrafish Toxicity Studies*

The major reason for the transition in the chemical industry from pure perfluorocarbon surfactants to PFE surfactants is due to the bioaccumulation and toxicity of perfluoroalkyl derivatives. Previous toxicity studies on perfluorinated compounds have mostly focused on perfluorooctanoic acid (PFOA) and perfluorooctanesulfonic acid (PFOS), which were major byproducts emitted into the environment from industrial applications. However, the production of these perfluorocarbon derivatives has halted and alternative PFCs are taking their place. Therefore, it's important to also look into these compounds to see if they possess the same environmental effects. The zebrafish study focuses on the toxicity effect of heteroatom introduction as well as PEGylation of perfluorinated chains. The data suggests PEGylation of fluorinated alcohols imparts both water solubility and reduced toxicity.

From the zebrafish toxicity study, it can be seen that the all fluorinated acids have a toxic effect on developing zebrafish embryos. As previously seen, PFOA is toxic to zebrafish down to 333 μM. While some zebrafish at this concentration survived up until 96 hpf, there were observable developmental malformations, a second sign of toxicity. Common signs of toxicity (at 333 μM) were pericardial edema (pe) and altered axial curvatures (aac) (Figure 3.5a).

PFTDA, a longer chain perfluorinated acid showed decreased toxicity in relation to PFOA. However, it is important to note that PFTDA was not completely soluble at the highest exposure concentrations. Precipitate was observed in the exposure wells, indicating that the embryos were exposed to concentrations effectively lower than the target concentrations. Additionally, zebrafish embryos displayed a third sign of toxicity: delayed hatching down to 37 μM PFTDA.

The perfluoroether acids were also tested and showed zebrafish toxicity. Interestingly, FE3-COOH, the intermediate length perfluoroether acid, showed to be the most toxic, with fish mortality and malformations down to 12.3 μM. The IC50 value was calculated at 7.5 μM FE3-COOH. Next, the bFE4-COOH showed toxicity down to 111 μM, with an IC50 value of 133.5 μM. Finally, the shortest perfluoroether acid, FE2-COOH displayed limited toxicity, with mortality and malformations at the 1 mM concentration only. From this data, it can be concluded that introduction of an oxygen between perfluoroalkyl groups does not itself decrease the toxicity.

To rule out the acid's inherent low pH as the reason for toxicity, each perfluoroether acid was buffered to egg water's pH (7.2) with MOPS buffer and exposed to zebrafish embryos. Interestingly, the buffered acids showed relatively the same level of toxicity as the unbuffered solutions. One slight discrepancy observed was with the FE3-COOH, which killed 80% buffered versus 100% unbuffered at 12.3 μM. While the bFE4-COOH acid killed all developing zebrafish at the 111 μM, the buffered bFE4-COOH only killed 40% embryos as this concentration. The FE2-COOH buffered compound only killed 11.1% of the embryos at 1 mM, while it killed 87.5% unbuffered at 1 mM (Appendix 2).
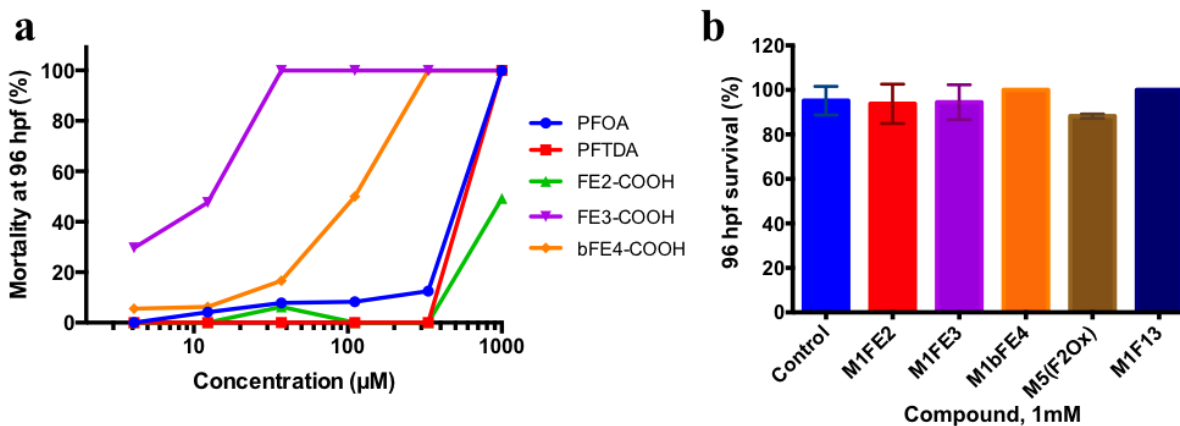
**Figure 3.4: Toxicity of fluorous acids and semifluorinated polymers to zebrafish**. **a**) Dose-response relationships for mortality at 96 hpf. Standard error removed for clarity (found in Appendix 2). **b**) 96 hpf mortality (%) of semifluorinated polymers at 1mM. Control column is egg water only.

Unlike PFOA, PFTDA and the three perfluoroether acids (FE2-COOH, FE3-COOH and bFE4-COOH), the PEG-PFE polymers showed no toxicity for this zebrafish model over the five day experiment. All polymers tested; M1F13, M1FE2, M1FE3, M1bFE4 and $M5(F2Ox)_n$ showed no mortality or malformations at 1 mM or below (Figure 3.4b). The absence of a toxic effect shows that PEGylation produces a stealth effect for these fluorinated molecules. While the absence of any toxic effect of the polymers shows promise for these alternative perfluorinated molecules, further studies are needed.

**Figure 3.5: Pictures of zebrafish exposed to fluorinated acids and PEGylated fluoropolymers at 96 hpf.** Morphological malformations at 96 hpf from fluorinated acids indicated by altered axial curvatures (aac), yolk sac malformations (ysm), and pericardial edema (pe). Control is zebrafish in egg water only.

### 3.3 Conclusions

Long perfluoroalkyl chain surfactants and derivatives are known to present a major environmental impact in terms of bioaccumulation and inherent toxicity. Due to these undesirable properties, these fluorous compounds have been replaced in the chemical industry with long perfluoropolyethers (PFPEs). PFPEs have highly desirable reduced bioaccumulation due to their quick elimination *in vivo* and degradation in the environment. Here we have characterized PFEs and their derivatives in terms of their physicochemical properties as well as

their toxicity. Colloidal assembly and studies of these colloids in the stabilization of fluorous nanoemulsions have shown that perfluorooligo (ethylene glycols) and similar molecules have a reduced fluorophilicity as compared to pure perfluorocarbons. These findings have been further supported and explained through electrostatic potential surface calculations, which showed an increased polarity in perfluorooligo (ethylene glycol) as opposed to a perfluorocarbon of the same size. This increase in polarity leads to a reduction of the PFE fluorophilicity and explains the fluorous nanoemulsions low stability. Furthermore, we have conducted extensive zebrafish studies to establish the toxicity potential of perfluorooligo (ethylene glycol) and their derivatives. We have found that PFE acids are as toxic to zebrafish as perfluorooctanoic acid and perfluorotetradecanoic acid. However, derivatives in which the PFE is conjugated to a standard poly(ethylene glycol) showed total absence of toxicity up to 1 mM concentrations. These concentrations are much higher than possible environmental contamination and imply that PFEs neutral derivatives may not have a significant environmental impact.

## 3.4 Experimental Section

### 3.4.1 Materials and Methods

Perfluorotetradecanoic acid, perfluoro-3,6-dioxadecanoic acid, perfluoro(2,5,8,11-tetramethyl-3,6,9,12-tetraoxapentadecanoic) acid,  1H,1H-perfluoro-3,6-dioxadecanol, 1H,1H-perfluoro-3,6,9-trioxatridecanol, 1H,1H-perfluoro(2,5,8,11-tetramethyl-3,6,9,12-tetraoxapentadecan-1-ol) and perfluorooctyl bromide are from Synquest Laboratories. Perfluoro-3,6,9-trioxatridecanoic acid was purchased from Matrix Scientific. All other chemicals were purchased from Sigma-Aldrich. All chemicals were used as purchased, unless otherwise specified. Polymers were purified by automated flash chromatography using a CombiFlash® Rf 4x system equipped with ELSD for compound visualization and a REDI-Sep Rf Gold C-18 silica

high-performance aqueous reverse phase cartridge. Products were eluted with a 10–100% methanol in water (0.1% formic acid) gradient. All zebrafish were monitored and imaged using a Nikon SMZ18, in combination with NIS Elements Imaging Software.

*3.4.2 Synthesis of Methoxy-PEG1000 methane sulfonate (M1-OMs) (3-1)*

To a dry round bottom flask, anhyd. $CH_2Cl_2$ and monomethoxy poly(ethylene glycol) (6.05 g, 6.05 mmol) were added. The mixture was cooled to 0°C before adding triethyl amine (2.11 mL, 12.1 mmol), which was then allowed to stir for 30 minutes before methanesulfonyl chloride (0.94 mL, 12.1 mmol) was added. The reaction was allowed to react for 24 hours and then diluted with $CH_2Cl_2$ and washed with aq. $NH_4Cl$, dried over $MgSO_4$ and volume reduced under pressure. The M1-OMs was then precipitated with cold ether and freeze dried to recover 5.47 g (79% yield). $^1$H-NMR (500 MHz, $CDCl_3$): δ 4.18 (m, 2 H), 3.57 (m, 2 H), 3.47 (m, 86 H), 3.36 (m, 2 H), 3.19 (s, 3 H), 2.91 (s, 3 H). $[M+Na]^+= 1145.63$.

*3.4.3 Synthesis of PEGylated perfluorooligoethers, M1FE2, M1FE3, M1bFE4*

PEGylated perfluorooligoethers were synthesized following the general procedure. The perfluorooligoether alcohol (2 eq.) was added to a dry round bottom flask and flushed with argon. M1-OMs (1 eq.) was added as a solution in THF and added to the flask. The mixture was flushed with argon and sodium hydride (5 eq.) added. The reaction was heated to reflux for 5 days, then cooled to room temperature and quenched with water. Layers were separated and organic layer reduced under vacuum. Polymers were then purified by an automated Combi*Flash*® system.

M1FE2: $^1$H NMR (400 MHz, $CDCl_3$) δ 3.91 (t, *J*= 9.8 Hz, 2H), 3.78 (m, 2H), 3.7-3.55 (m, ), 3.55 (m, 2H), 3.38 (s, 3H). $^{19}$F NMR (300 MHz, $CDCl_3$) δ -77.74 (dt, 2F), -80.89 (t, *J*= 8.4 Hz,

3F), -83.43 (dt, 2F), -88.56 (4F), -126. 45 (m, 4F). MALDI: Distribution centered on $[M+Na]^+=$ 1613.71.

M1FE3 (3-3): $^1$H NMR (400 MHz, CDCl$_3$) δ 3.90 (t, $J$= 10.0 Hz, 2H), 3.78 (m, 2H), 3.69-3.61 (m, 113 H), 3.55 (m, 2H), 3.38 (s, 3H). $^{19}$F NMR (300 MHz, CDCl$_3$) δ -78.40 (dt, $J$=26.5, 9.9 Hz, 2F), -81.59 (t, $J$=9.0 Hz, 3F), -84.08 (dt, $J$= 19.6, 8.8 Hz, 2F), -89.24 (m, 4F), -89.42 (m, 4F), -127.15 (m, 4F). MALDI: Distribution centered on $[M+Na]^+$= 1686.

M1bFE4 (3-4): $^1$H NMR (400 MHz, CDCl$_3$) δ 4.10 (d, $J$=12.4 Hz, 2H), 3.74 (m, 2H), 3.70-3.3.54 (m, 80 H), 3.55 (m, 2H), 3.38 (s, 3H). $^{19}$F-NMR (300 MHz, CDCl3) δ -80.09 (m, 4F), -81.36 (t, $J$=7.6 Hz, 4F), -82.50 (m, 3F), -82.64 (m, 8F), -129.63 (m, 8F), -145.04 (m, 2F).

### 3.4.4: Synthesis of other semifluorinated polymers

The synthesis of M1F13 has been previously described.[17] The synthesis of M5(F2Ox) has also been previously described.[18]

### 3.4.5 Particle size determination by dynamic light scattering (DLS)

Particle sizes of polymeric micelles were analyzed by dynamic light scattering (Zetasizer Nano-ZS, Malvern Instruments, Worcestershire, UK). The polymer solution was measured directly without dilution and analyzed. Each particle size analysis was run at room temperature and repeated in triplicate with the number of scans of each run determined automatically by the instrument according to the concentration of the solution. The data was analyzed using Malvern software analysis and reported as volume weighted average diameters. Particle sizes of emulsions were analyzed by dynamic light scattering (NICOMP 380ZLS, Particle Sizing Systems, Santa Barbara, CA). The emulsions were diluted at the intensity factor of 300 by adding 60mL of the emulsion to 2.940 mL of Millipore water. Each particle size analyzing was

run for 5 min at room temperature and repeated three times. The data was analyzed using

Gaussian analysis and reported as volume weighted average diameters.

*3.4.6 Critical micelle concentration (CMC) determination—surface tensiometry*

Polymer was dissolved in Millipore water to a concentration of 1 mM and concentrations

down to 1 nm were prepared by serial dilution and transferred to 20 mL disposable scintillation

vials. After solutions were made, the samples were vortexed and sonicated and then heated in a

water bath at 40°C for 2–3 h. Solutions were then allowed to equilibrate for 24 hours. Surface

tensions were measured on a KSV sigma 701 tensiometer (KSV Instruments, Helsinki, Finland)

equipped with a Julabo F12-MC circulator for constant temperature control. Custom round rod

made of platinum with a diameter of 1.034 nm with wetted length of 3.248 mm was used. First,

the rod was submerged into absolute alcohol and flame dried with a Bunsen burner for 4 s, then

repeated after 4 min and hung on instrument and allowed to cool to room temperature without

touching any surface. Before running the experimental samples, the surface tension of Millipore

water was measured as control to confirm vial and rod were fully cleaned and surface tension

was within 1 of 78.2 mN/m. The surface tension measurements began with the least concentrated

solution and proceed to successively more concentrated solutions. The surface tension at each

concentration was measured in quadruplet and average recorded. The critical micelle

concentration value was determined from crossover point of two lines: the baseline of minimal

surface tension and the slope where surface tension showed linear decline; error determined by

weighted least squares analysis.

*3.4.7 Fluorous Anesthetic Emulsion Formulation*

Polymer solution in normal saline solution (10 mM, 11.9 mL) was prepared freshly.

Normal saline is composed of 0.9% (w/w) of sodium chloride. Sevoflurane (3.4 mL) and

perfluorooctyl bromide (1.7 mL) were added to the polymer solution, for a total volume of 17 mL. The mixture is then homogenized with the high-speed homogenizer (Power Gen 500, Fisher Scientific, Hampton, NH) for 1 min at 21000 rpm at room temperature. The crude emulsion made with the high speed homogenizer was further homogenized with a Microfluidizer (model 110 S, Microfluidics Corp., Newton, MA) for 1 min under 5000 psi with the cooling bath kept at 15°C. The final emulsion was then filtered with a 0.45 μm nylon filter and stored in plastic centrifuge tubes (Corning Inc., Corning, NY) at 4°C.

*3.4.8 Particle Size Determination by Dynamic Light Scattering (DLS)*

Particle sizes of emulsions were analyzed by DLS (NICOMP 380ZLS, Particle Sizing Systems, Santa Barbara, CA). The emulsions were diluted at the intensity factor of 300 by adding 60 μL of the emulsion to 2.94 mL of Millipore water. Each particle size analysis was run for 5 min at room temperature and repeated three times. The data was evaluated using Gaussian analysis and reported as volume weighted average diameters.

*3.4.9 Electrostatic Potential Surface Calculations.*

All calculations were carried out using the SPARTAN 10 software package. All molecular geometries were optimized at the HF 6-31G* *ab initio* level. Electrostatic potential surfaces were HF 6-31G** single point calculations at the optimized geometries. Electrostatic potential was mapped within the range -30/30 kJ/mol.

*3.4.10 Zebrafish Husbandry*

All experiments were conducted using a wild-type zebrafish strain (AB). Zebrafish embryos and larvae, obtained through mating, were held in egg water (60 μL/mL of "Instant Ocean" sea salts added in distilled water). Zebrafish were maintained in the experimental facilities of about 28°C and 14 h-10 h light-dark cycles. All experiments were carried out with the approval of the Research Animal Resource Center of the University of Wisconsin-Madison.

*3.4.11 Zebrafish Exposure to Fluorinated Compounds*

Within 1-2 hours post-fertilization (hpf), zebrafish embryos were exposed to solutions ranging from 4.3 µM to 1 mM in egg water. Exposures were conducted in a 24-well plate format with an average of 8 embryos per well, and overall volume of 1.2 mL. Zebrafish embryos were monitored daily until 96 hpf for mortality and morphological signs of toxicity. These experiments were conducted in duplicate. Detailed experimental procedures can be found in the Supplementary Information (Appendix 2).

## 3.5 References

(1) Agency, U. S. E. P. Emerging Contaminants – Perfluorooctane Sulfonate (PFOS) and Perfluorooctanoic Acid (PFOA) At a Glance. **2012**.

(2) Zaggia, A.; Ameduri, B. Recent Advances on Synthesis of Potentially Non-Bioaccumulable Fluorinated Surfactants. *Curr. Opin. Colloid Interface Sci.* **2012**, *17*(4), 188–195.

(3) Buck, R. C.; Franklin, J.; Berger, U.; Conder, J.M.; Cousins, I. T.; de Voogt, P.; Jensen, A. A.; Kannan, K.; Mabury, S. A.; van Leeuwen, S. P. Perfluoroalkyl and polyfluoroalkyl substances in the environment: terminology, classification, and origins. *Integr. Environ. Assess. Manag.* **2011**, *7*(4), 513-541.

(4) Olsen, G. W.; Mair, D. C.; Church, T. R.; Ellefson, M. E.; Reagen, W. K.; Boyd, T. M.; Herron, R. M.; Medhdizadehkashi, Z.; Nobiletti, J. B.; Rios, J. A.; Butenhoff, J. L.; Zobel, L. R. Decline in Perfluorooctanesulfonate and Other Polyfluoroalkyl Chemicals in American Red Cross Adult Blood Donors, 2000-2006. *Environ. Sci. Technol.* **2008**, *42*(13) 4989-4995.

(5) Olsen, G.W.; Burris, J. M.; Burlew, M. M.; Mandel, J. H. Plasma Cholecystokinin and Hepatic Enzymes, Cholsterol and Lipoproteins in Ammonium Perfluorooctanoate Production Workers. *Drug Chem. Toxicol.* **2000**, *23,* 603-620.

(6) US EPA, United States Environmental Protection Agency. 2010/15 PFOA Stewardship program, http://www.epa.gov/oppt/pfoa/pubs.stewardship/, 2006.

(7) Kraft, M. P.; Riess, J. G.; Weers, J. G. The design and engineering of oxygen-delivering fluorocarbon emulsions in: S. Benita (Ed.), Submicronic Emulsion in Drug Targeting and Delivery, Harwood Academic Publishers, Amsterdam, 1998, 235-333.

(8) Wellen, B. A.; Lach, E. A.; Allen, H. C. Surface p$K_a$ of octanoic, nonanoic, and decanoic fatty acids at the air-water interface: applications to atmospheric aerosol chemistry. *Phys. Chem. Chem. Phys.* **2017**, *19*, 26551-26558.

(9) Goss, K. The pK$_a$ Values of PFOA and Other Highly Fluorinated Carboxylic Acids. *Environ. Sci. Technol,* **2008**. *42*(2). 456-458.

(10) Berthiaume, J.; Wallace, K.B. Perfluorooctanoate, perfluoroctanesulfonate, and N-ethyl perfluorooctanesulfonadmido ethanol; peroxisome proliferation and mitochondrial biogenesis. *Toxic. Lett.* **2002**, *129*, 23-32.

(11) Buck, R.C.; Franklin, J.; Berger, U.; Conder, J.M.; Cousins, I.T.; Voogt, P.; Jensen, A.A.; Kannan, K.; Mabury, S.A.; Leeuwen, S.PJ. Perfluoroalkyl and Polyfluoroalkyl Substances in the Environment: Terminology, Classification, and Origins. *Integr. Environ. Assess. Manag.* **2011**, *7(4),* 513-541.

(12) Wang, Z.; Cousins, I. T.; Scheringer, M.; Hungerbühler, K. Fluorinated alternatives to long-chain perfluoroalkyl carboxylic acids (PFCAs), perfluoroalkane sulfonic acids (PFSAs) and their potential precursors. *Environ. Int.* **2015**, *60*, 242–248.

(13) Krusic, P.; Lu, H.; Yang, Z.-Y.; Law, C.; Garner, J. (E I du Pont de Nemours and Co.) Compositions containing functionalized carbon materials. US Patent 20,060,093,885A1, May 4, 2006.

(14) Wei, J.; Fong, W.; Bogy, D. B.; Singh Bhatia, C. The decomposition mechanisms of a perfluoropolyether at the head/disk interface of hard disk drives. *Tribol. Lett*. **1998**, *5*, 203-209.

(15) Kirsch, P. Modern Fluoroorganic Chemistry, Synthesis, Reactivity, Applications, 1$^{st}$ ed.; Wiley-VCH: Weinhem, 2004; pp 205-211.

(16) Kissa, E. Fluorinated surfactants: Synthesis, properties, and applications; Marcel Dekker: New York, 1994.

(17) Fast J.P.; Perkins M.G.; Pearce R.A.; Mecozzi S. Fluoropolymer-based emulsions for the intravenous delivery of sevoflurane. *Anesthesiology*. **2008**, *109*, 651-656.

(18) Fleetwood, M. C.; McCoy, A. M.; Mecozzi, S. Synthesis and Characterization of Environmentally Benign, Semi-Fluorinated Polymers and Their Applications in Drug Delivery. *J. Fluor. Chem.* **2016**, *190*, 75–80.

(19) Chen, J.; Sun, H.; Wang, W.; Xu, W.; He, Q.; Shen, S.; Qian, J.; Gao, H. Polyethylene Glycol Modification Decreases the Cardiac Toxicity of Carbonaceous Dots in Mouse and Zebrafish Models. *Acta Pharmacol. Sin.* **2015**, *36*(11), 1349–1355.

(20) Chakraborty, C.; Sharma, A. R.; Sharma, G.; Lee, S. S. Zebrafish: A Complete Animal Model to Enumerate the Nanoparticle Toxicity. *J. Nanobiotechnology* **2016**, *14*(65), 1–13.

(21) Hill, A. J.; Teraoka, H.; Heideman, W.; Peterson, R. E. Zebrafish as a Model Vertebrate for Investigating Chemical Toxicity. *Toxicol. Sci.* **2005**, *86* (1), 6–19.

(22) Jee, J.-P.; Parlato, M. C.; Perkins, M. G.; Mecozzi, S.; Pearce, R. A. Exceptionally Stable Fluorous Emulsions for the Intravenous Delivery of Volatile General Anesthetics. Anesthesiology **2012**, *116*(3), 580-855.

(23) Ameduri, B.; Sawada, H. *Fluorinated Polymers,* 2nd ed.; The Royal Society of Chemistry: Cambridge, 2017; p 120.

(24) Hougham, G.; Cassidy, P.E.; Johns, K.; Davidson, T. *Fluoropolymers 1: Synthesis.* Kluwer Academic: New York, 2002; p 213.

(25) Hamada, T. Rotational isomeric state study of molecular dimensions and elasticity of perfluoropolyethers: Differences between Demnum-, Fomblin-, and Krytox type main chains. *Phys. Chem. Chem. Phys.,* **2000**, *2*, 115-122.

# Chapter 4: Aggregation Induced Emission to Elucidate Micelle Kinetic Stability

**Aggregation Induced Emission to Elucidate Micelle Kinetic Stability**

**Abstract**

Studying the *in vitro* stability of drug delivery systems is necessary for the translation of pharmaceutical research to clinical trials. However, current methods of studying micelle stability in serum have challenges. A new method was developed, in which the fluorescence of an aggregation induced emission (AIE) luminogen was used to monitor the dissociation of polymeric micelles when diluted in human serum. Commercially available methoxy poly(ethylene glycol)-*block*-poly(D,L-lactide) (mPEG-PLA) and methoxy poly(ethylene glycol)-*block*-distearoylphosphatidylethanolamine (mPEG-DSPE), along with the synthesized semifluorinated polymer, M2F8H18, were used to formulate polymeric materials. Five lipophilic dyes were subsequently encapsulated within these polymeric micelles, leading to aggregation and corresponding fluorescence of the luminogen. As the micelles dissociated within serum, the dye was released and fluorescence diminished. This method allows for quick quantification of polymeric micelle kinetic stability when in the presence of serum proteins.

**4.1 Introduction**

Polymeric micelles have been studied extensively for the delivery of poorly water soluble and amphiphilic drugs. Block copolymers that self-assemble into nanoparticles within water can effectively solubilize highly hydrophobic molecules and deliver them to target sites, mainly tumors, *via* the enhanced permeation and retention (EPR) effect.[1] This ability greatly reduces off-target toxicity seen with general intravenous injection of the active pharmaceutical.

In order for a micellar system to be considered for *in vivo* applications, the system must; i) be small enough (10-200 nm) to penetrate tissue, ii) be unrecognizable by the mononuclear phagocyte system (MPS); iii) be eliminated either after degradation or dissolution; iv) avoid premature release of cargo before it can accumulate at the target site; v) locate and interact with

the target cells; vi) improve the pharmacokinetic profile of the encapsulated drug; vii) possess

high drug loading capability and viii) be synthesized in a reproducible method which is

somewhat inexpensive.[2-4]

For a system to be stable *in vivo*, micelles must be stable upon dilution into the

bloodstream. Protein adsorption is a key factor in nanoparticle stability, as it may induce

premature release of the encapsulated drug.[5] Many characteristics of the polymeric nanoparticle

(NP) such as particle size,[6] hydrophobicity,[7, 8] surface charge,[9] and shape[10, 11] can affect their

ability to adsorb to serum proteins. This NP-protein interaction can influence the blood

circulation time of the delivery vehicles, by causing micelle dissociation and loss of encapsulated

payload. Due to the variety of factors influencing circulation time, it is important to study the

kinetic stability of polymeric micelles. The kinetic stability refers to the rate at which the

micelles disassemble upon dilution, once the polymer concentration falls below the critical

micelle concentration (CMC).[12] Many stability studies focus on purely water-based systems,

which do not adequately represent physiological environments. To get a better representation of

how adsorption to proteins affects dissociation, *in vitro* stability studies are done in serum

solutions.

Current methods to investigate the kinetic stability of micelles in serum include size

exclusion chromatography (SEC),[13] particle size determination through DLS,[13, 14] atomic force

microscopy,[15] combination DLS/ cryogenic transmission electron microscopy (cryo-TEM)[16] and

fluorescence using a Förster resonance energy transfer (FRET) dye pair.[17, 18] However, each of

these systems has its challenges. SEC techniques use UV-Vis to detect single polymer chains

from aggregated micelles. Detection, however, is non-specific and overlap between polymer

chains of the micelle and encapsulated molecules is a potential deterrent. Likewise, the large size

of micelles can have similar retention times as serum proteins, causing another unavoidable problem when experiments are done in physiological media. Particle size techniques, such as dynamic light scattering (DLS), suffer from a high minimum polymer concentration as well as size overlap between polymer and encapsulated molecules that also occurs in SEC. Atomic force microscopy has been used to study the force needed to disassemble micelles, however this technique was solvent dependent and has yet to be used with serum.[12]

The most common and most recently developed method to measure kinetic stability is FRET and it involves the encapsulation of two large hydrophobic dyes, donor DiO and acceptor DiI. When both FRET molecules are encapsulated inside one micelle and excited at the appropriate wavelength, energy transfer occurs due to the close proximity between the dyes. When micelles then disassemble, the FRET molecules were released and diffused apart, eliminating the energy transfer. Due to the steric constraints and small size of micelle cores for particular amphiphiles, this co-encapsulation can be difficult.[12] Still, fluorescence experiments show enhanced sensitivity relative to other techniques, and therefore a new method using one fluorophore was developed to measure the kinetic stability of micelles.

Since its inception in 2001 by Tang et al.,[19] aggregation induced emission (AIE) has been increasingly studied and applied to many fields such as optoelectronics,[20] bioimaging,[21] and chemosensing.[22, 23] Recently, AIE luminogens have been studied in the context of micelles—looking at critical micelle concentrations (CMC),[24] micelle transitions,[25] and imaging of intracellular delivery.[26] However, there have been no reports of using AIE in studying the kinetic stability of micelles in human serum.

AIE luminogens are non-emissive in dilute solutions, and fluorogenic when in an aggregated state.[27-30] The properties of these dyes are in contrast to typical luminogens, which

experience aggregation-caused quenching (ACQ), rendering them useless. The ACQ effect is generally considered detrimental to many practical applications, especially biological systems in which hydrophobic luminogens quench readily in physiological solutions. Instead of passively avoiding aggregation, AIE dyes allow for the exploitation of this phenomenon. Upon aggregation, emission of the AIE dye is induced through π-π stacking if the molecule is planar or by the restricted intramolecular rotation (RIR) of the phenyl rotors if the molecule is propeller-shaped and non-planar. In dilute solutions, these luminogens can freely rotate and thus emit almost no light. The molecular friction caused by the rotational or twisting motions against each other and with the solvent transforms the photonic energy to thermal energy, leading to non-radiative relaxation of the exciton energy (Figure 4.1).[27]
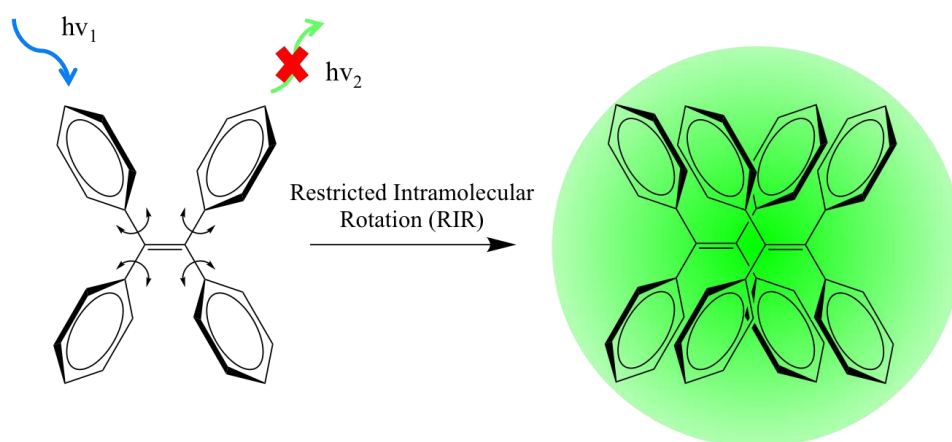


**Figure 4.1: Schematic representation of an AIE dye's mechanism of action.** Shown here, tetraphenylethylene (TPE), becomes emissive once phenyl groups experience restricted intramolecular rotation (RIR) in the aggregated state.

This study aims to use AIE fluorescent probes to study the dissociation of polymeric micelles over time in human serum. AIE luminogens were encapsulated by polymeric micelles, causing them to fluoresce within the lipophilic core. As time goes on and micelles dissociate, the loss of AIE encapsulation and aggregation causes a decrease in fluorescence. From the observed

micelle dissociation, a half-life was derived, which can be related to the nanoparticle's kinetic

stability. These *in vitro* tests are necessary in the development of drug delivery systems.

## 4.2 Results and Discussion

### 4.2.1 Synthesis of AIE fluorophores and general methods

Two classes of AIE fluorophores were studied that exhibit fluorescence upon aggregation

inside of polymeric micelles (Figure 4.2). The first class of AIE fluorophores investigated were

derivatives of the well-studied AIE dye tetraphenylethylene (TPE).[31] TPE itself was not

particularly soluble in physiological media, so commercially available 4,4′-(1,2-Diphenylethene-

1,2-diyl)diphenol (TPE-DOH) and 4,4′,4″,4‴-(Ethene-1,1,2,2-tetrayl)tetraphenol (TPE-TOH),

which both show increased hydrophilicity, were explored.
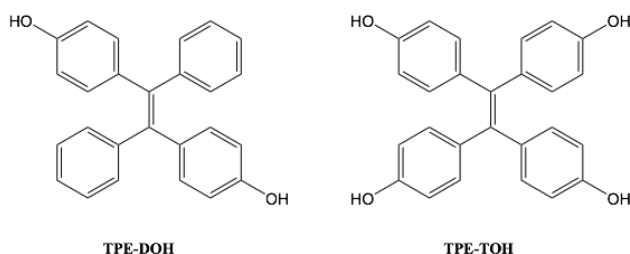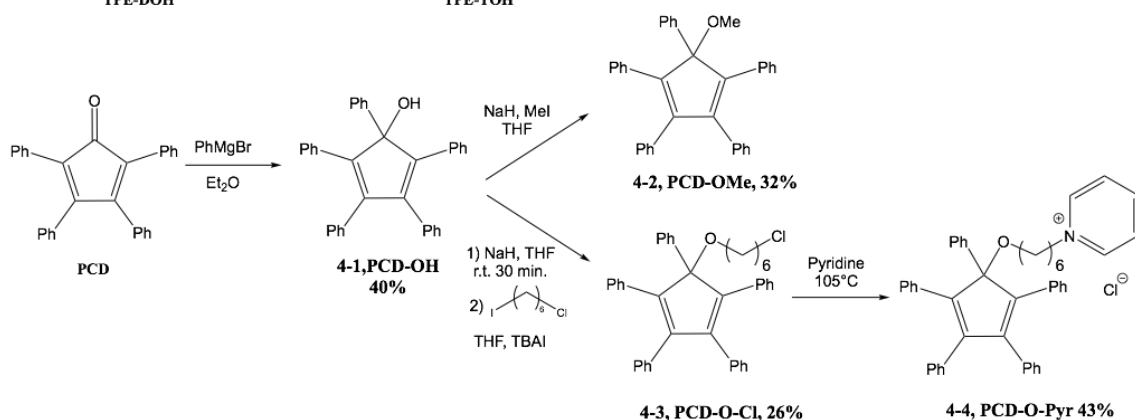


**Figure 4.2: Two classes of AIE fluorophores.** Tetraphenylethylene derivatives, TPE-DOH and TPE-TOH, showcased in Class 1. Synthesized derivatives of tetraphenylcyclopentadienone are designated in class 2.

The second class of AIE fluorophores studied were derived from the non-emissive

tetraphenylcyclopentadienone: 1,2,3,4,5-pentaphenyl-2,4-cyclopentadien-ol (PCD-OH, 4-1),

1,2,3,4,5-pentaphenyl-2,4-cyclopentadien-1-yl methyl ether (PCD-OMe, 4-2) and 1-(1-(6-pyridiniumhexyloxy)-2,3,4,5-tetraphenylcyclopenta-2,4-dienyl)benzene chloride (PCD-O-Pyr, 4-4), which also segregate into the hydrophobic core when encapsulated within a micelle. These luminogens include five phenyl rotors that become physically constrained and thus emissive in the aggregated state. More promising results were observed in this work with PCD-derived fluorophores because PCD-OH had a higher quantum yield than TPE, i.e. the fluorescence intensity was larger when in an aggregated state at the same concentration (Figure 4.3).
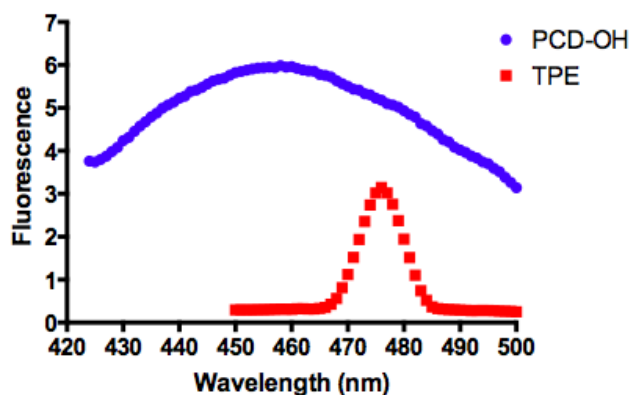


**Figure 4.3: Relative fluorescence emission from AIE dyes TPE and PCD-OH at 1.8 μM.**

Modification of tetraphenylcyclopentadienone (TCD) produced two dyes that fluoresce within the visible range. First, a Grignard reaction was performed to produce PCD-OH (4-1), adding a fifth phenyl ring to the cyclopentadienyl core, thus breaking conjugation around the ring. In the top pathway, the resulting alcohol was then converted to a methoxy-functionalized dye, PCD-OMe (4-2) via an SN2 reaction.[32] PCD-OH was also functionalized with a pyridinium via a carbon tether to yield PCD-O-Pyr (4-4).[33] The synthesis of PCD-O-Pyr was undertaken due to poor water solubility of PCD-OMe, which led to aggregation within human serum. Aggregation outside of the micelle increased the observed fluorescence baseline, so a more water-soluble dye was investigated. Absorbance and fluorescence studies were used to find the optimal excitation and emission wavelengths for each fluorophore.

Time-based fluorescence studies in human serum were conducted to measure *in vitro* stability. Polymeric micelles with and without encapsulated AIE dye were prepared by the lyophilization method, as the previously-studied thin-film preparation method led to less consistent encapsulation between triplicate vials.[34] After the polymer cakes were redispersed with 60°C PBS buffer and filtered, solutions were diluted in human serum (1:20).The fluorescence of serum solution aliquots was measured over two hours. The background micelle/serum absorbance was subtracted out to produce a corrected fluorescence spectrum of each dye. Other experimental variables were tested: i) the concentration of tested AIE dye (0.5, 1, 5 wt. %) ii) the ratio of water/tert-butanol during micelle lyophilization preparation and iii) the use of an orbital shaker in between time points to keep solutions well mixed. It was found that at 0.5 wt. % dye, the fluorescence was too low, that an emission decay was not always seen, whereas when 5 wt. % dye was too concentrated and the polymeric nanoparticles could not always encapsulate this amount (Appendix 2). The ratio of water/tert-butanol gave the most consistent results at a 50/50 ratio, when compared to 60/40, 40/60, 70/30 and 30/70 (Appendix 2).



**PEG-PLA**

**M2F8H18**

**M2DSPE**
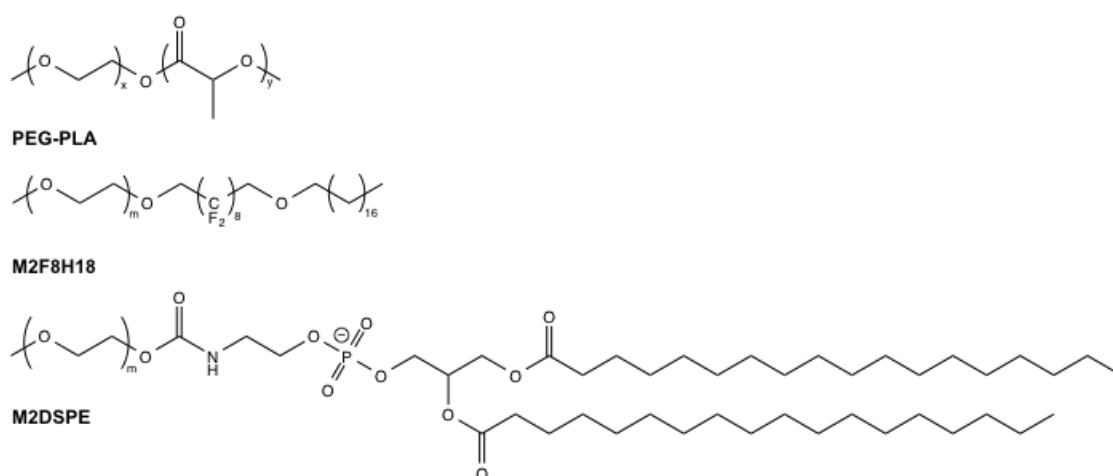
**Figure 4.4: Structures of amphiphilic polymers used to create micelles for *in vitro* dissociation studies.** mPEG-PLA (average MW=6,000, with PEG=4,000, PLA=2,000) and mPEG-DSPE (m=50) were commercially bought, while M2F8H18 (m=50) is synthesized in house.

Polymers used in this study are shown in Figure 4.4. Methoxy poly(ethylene glycol)-*b*-poly(L-lactide) (mPEG-PLA) and methoxy poly(ethylene glycol)-b-1,2-distearoyl-*sn*-glycero-3-phosphoethanolamine (mPEG-DSPE) both form spherical micelles in water and have been extensively studied for drug delivery applications.[35-37] Their physicochemical properties have been thoroughly examined, including their stability in serum. mPEG-PLA has shown to be relatively stable in serum, with a dissociation half-life of 28 minutes, whereas mPEG-DSPE micelles are not stable in serum, with dissociation occurring in just a few minutes.[17, 38] A third triphilic polymer, synthesized in the Mecozzi group, M2F8H18, was also studied as a non-standard amphiphilic polymer.[39] AIE fluorophores TPE-DOH, TPE-TOH, PCD-OH, PCD-OMe and PCD-O-Pyr were encapsulated within these polymers to investigate their dissolution kinetics and calculate *in vitro* half-lives.

### 4.2.2 Tracking micelle dissociation in serum using TPE fluorophores

Tetraphenylethylene is an archetypal AIE fluorophore, in which the RIR mechanism blocks the radiationless decay of excited molecules, causing these molecules to fluoresce.[31] Derivatives of this molecule were investigated for the determination of micelle kinetic stability, using mPEG-PLA.
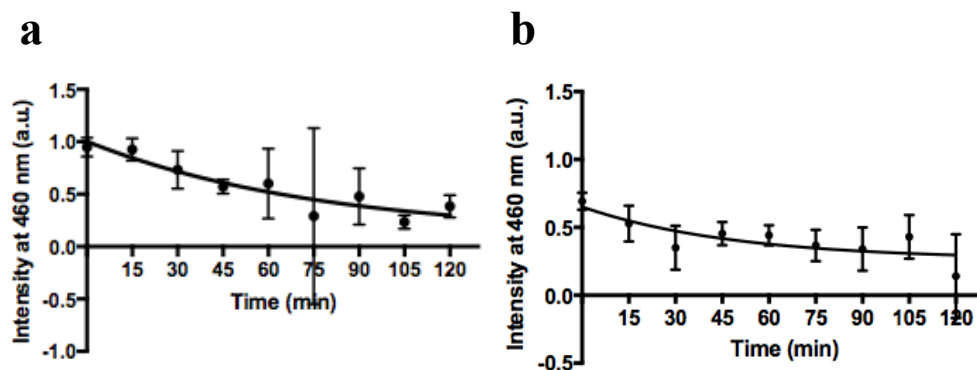


**Figure 4.5: Fluorescence studies of 1 wt. % a) TPE-DOH and b) TPE-TOH in mPEG-PLA micelles**.

Fitting a one-phase decay model to fluorescence vs. time curves produces half-lives of 53.6 and 34.0 minutes for TPE-DOH and TPE-TOH, respectively. It can be seen in Figure 4.5 both AIE luminogens TPE-DOH (a) and TPE-TOH (b) have inconsistent encapsulation within mPEG-PLA micelles. This is evident as the fluorescence between triplicate time points causes large error, as half-life standard deviations could not be calculated. These dyes were also encapsulated within mPEG-DSPE and M2F8H18 micelles, but results were even worse, and were unable to be fit with a trend line. This makes sense for mPEG-DSPE micelles, which are highly unstable in the presence of serum proteins.

*4.2.3 Tracking micelle dissociation in serum using TCD fluorophores*

Due to the large errors resulting from use of TPE-based dyes, another AIE luminogen class was studied. Tetraphenylcyclopentadienone (TCD) alone is non-emissive due to conjugation around the cyclic core, however derivatives of this molecule that break conjugation are highly emissive with multiple rotors being restricted in the aggregated state. The modified dye, PCD-OH, was found to have AIE properties when encapsulated within micelles, and was further studied for *in vitro* kinetic experiments. This AIE dye produced much more consistent fluorescence readings between triplicate vials (Figure 4.6). Half-lives were calculated to be 13.1 $\pm$ 5.4 min. for mPEG-PLA and 9.5 $\pm$ 14.1 min. for mPEG-DSPE. The large error seen for mPEG-DSPE micelle dissociation is due to the fact that these micelles are unstable in the presence of serum proteins, and a half-life can be difficult to calculate. One unexpected observation was the substantial drop in fluorescence between time zero and after fifteen minutes for mPEG-PLA micelles. This event could be explained by adsorbed AIE dye on the surface of the polymeric micelles, which fluoresces at time zero, but easily dissociates and becomes non-emissive in solution.
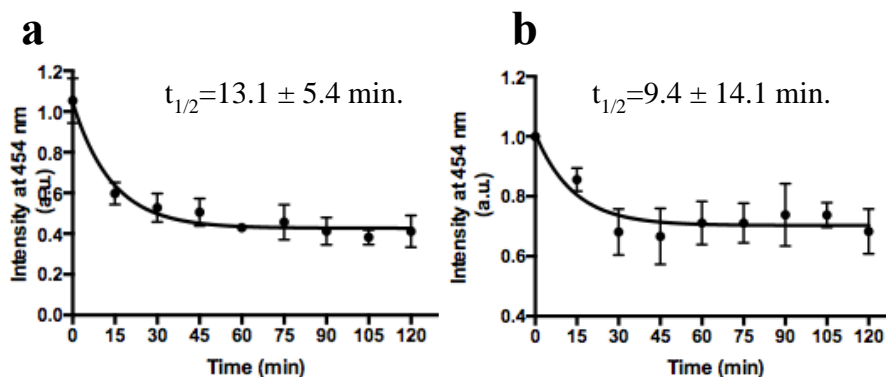
**Figure 4.6: Fluorescence studies of 1 wt. % PCD-OH in a) mPEG-PLA and b) mPEG-DSPE micelles.**

In an attempt to adsorb less dye to the polymer's PEG tail, an even more hydrophobic dye was synthesized which would associate only in the micelle's lipophilic core. This AIE luminogen, PCD-OMe, showed promise when encapsulated in mPEG-PLA micelles, as there is no drastic drop in fluorescence between time zero and fifteen minutes. The calculated half-life for mPEG-PLA was 13.9 ± 7.1 min. (Figure 4.7a), which is similar to past results with PCD-OH. However, these encouraging results could not be extended to micelles formed with mPEG-DSPE (Figure 4.7b) or M2F8H18 (Figure 4.7c), which did not allow for a half-life to be calculated. One reason for inconsistent fluorescence measurements between trials (mPEG-DSPE) or increasing fluorescence over time (M2F8H18) is the hydrophobicity of the dye. With five phenyl rotors and a methoxy group, it is possible the dye could aggregate outside of the micelle with serum proteins, causing a high level of background fluorescence, observed especially with M2F8H18 micelles. Additionally, in some studies a precipitate was seen overtime, which further indicates the poor water solubility of this dye.
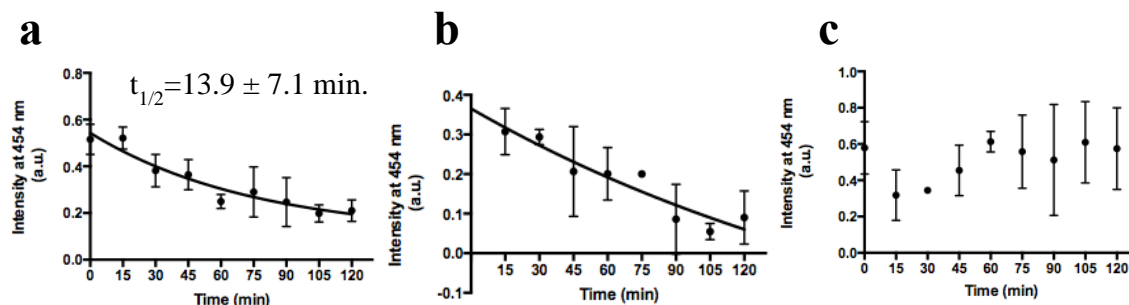
**Figure 4.7: Fluorescence studies of 1 wt. % PCD-OME in a) mPEG-PLA, b) mPEG-DSPE and c) M2F8H18 micelles.**

To mitigate these issues, while still using the PCD core, another dye was synthesized, PCD-O-Pyr. By functionalizing the oxygen with a pyridinium hexyl group, the dye becomes less likely to aggregate in solution, and potentially less association with the micelle hydrophilic shell. This dye was then encapsulated within tested polymers and the half-life derived from decreasing fluorescence over time. The half-life of mPEG-PLA micelles in human serum was calculated to be 12.8 ± 7.1 minutes using PCD-O-Pyr as the AIE luminogen (Figure 4.8a). This value compares well to the reported value (about 28 min.) using FRET techniques by Chen et al.[17] Our findings are similar, with a half-life of Previous FRET studies with mPEG-DSPE show these micelles are not stable under physiological conditions, and the kinetic stability can be hard to measure due to rapid dissociation. Some sources report a half-life at physiological conditions to be 4 minutes.[38] It can be seen in Figure 4.8b, the AIE study confirms that mPEG-DSPE micelles are unstable in human serum, with a half-life of 7.0 ± 3.7 min. using PCD-O-Pyr. The synthesized polymer M2F8H18, had a half-life of 3.5 min. (Figure 4.8c), however a standard error could not be derived. The inefficient encapsulation of PCD-O-Pyr can be attributed to this specific polymer. In other physicochemical studies, M2F8H18 micelles were also unable to encapsulate the chemotherapeutic paclitaxel or the FRET dyes DiO and DiI to an appreciable amount.[39]
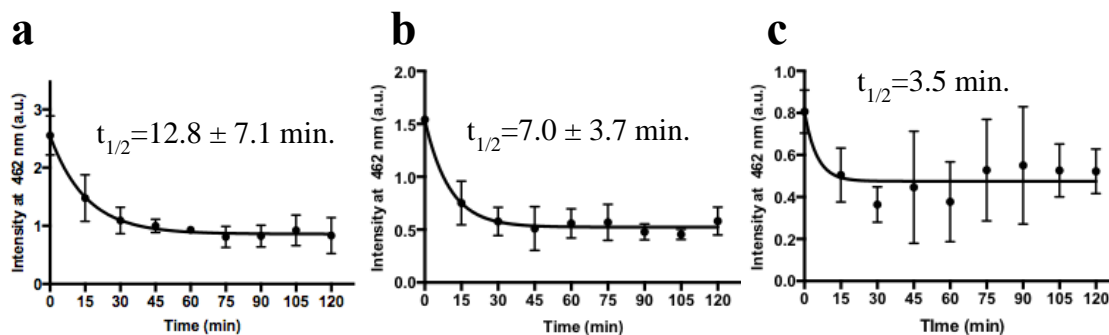
**Figure 4.8: Fluorescence studies of 1 wt. % PCD-O-Pyr in a) mPEG-PLA, b) mPEG-DSPE, and c) M2F8H18 micelles.**

Encapsulation of aggregation induced emission dyes within polymeric micelles leads to restriction of the phenyl rotors and sequential emission. As the micelle dissociates due to interactions with blood serum proteins, the dye is released into solution and its fluorescence greatly decreased. This technique was used to quantify kinetic stability of the micellar system. In contrast to previous FRET methods, this technique requires the encapsulation of only one hydrophobic dye within the polymeric aggregate, allowing for use within small lipophilic micellar cores.

**4.3 Conclusions**

Micelle integrity, including their ability to resist premature disassembly and drug loss, is the foundation of their success in drug delivery. Polymeric carriers suffer this requirement because they have to withstand challenges to their strength through contacts with biological fluids, cells, and macromolecules. Investigating the micelle kinetic stability is therefore essential to understanding the mechanisms of their dissociation and the controlled delivery of the encapsulated drugs. This work showed for the first time that the aggregation induced emission (AIE) phenomenon can be exploited for studying micelle stability in serum over time. The major advantage over the commonly used FRET system is the use of a singular fluorescent probe. Especially for micelles with a small lipophilic core, encapsulating two molecules can be a

challenge. This work explored two classes of AIE dyes for the use in probing micellar kinetic stability. It was found that tetraphenylcyclopentadienone (TCD) derivatives worked better than tetraphenylethylene (TPE) fluorophores. The success of the AIE luminogen depended heavily on its water solubility–with those that were less water soluble showing aggregation, and thus emission, outside of the micelle. The most hydrophilic dye, PCD-O-Pyr was lipophilic enough to be encapsulated within each polymeric micelle studied, while also be hydrophilic enough to be soluble in the serum environment.

## 4.4 Experimental Section

### 4.4.1 Materials

All materials were used as received without further purification. Pooled normal human serum was purchased from Innovative Research, Inc. mPEG-PLA was purchased from Advanced Polymer Materials Inc. mPEG-DSPE was purchased from NOF Corporations. All other chemicals were obtained from Sigma-Aldrich

### 4.4.2 Synthesis of 1,2,3,4,5-Pentaphenyl-2,4-cyclopentadien-1-ol (4-1)

To a dry 250-mL round bottom flask was added anhyd. THF (100 mL) and magnesium turnings (300 mg, 12.5 mmol). Under argon, bromobenzene (1.0 mL, 9.55 mmol) was added followed by one iodine crystal. The solution turned yellow and after 1 hour of slight heating, the Grignard started to initiate. This reagent was then added to a solution of tetraphenylcyclopentadienone (2 g, 5.2 mmol) in anhyd. THF (60 mL). The reaction was allowed to react for an additional hour at reflux. The reaction was then quenched with ammonium chloride and diluted with $H_2O$ and $CH_2Cl_2$. Layers were separated and organic solvent was then removed under reduced pressure to a minimum amount. Petroleum ether (50 mL) was then added and solution put in refrigerator to aid in crystallization. Solvent was then filtered off and solid

dried under high vacuum. The recovered crystals were recrystallized with petroleum ether to yield 960 mg of the yellow solid (2.075 mmol, 40% yield). $^1$H NMR (400 MHz, CDCl$_3$): δ 7.57 (d, $J$ = 7.7 Hz, 2 H), 7.29-7.25 (m, 2 H), 7.2-7.1 (m, 7 H), 7.1-6.97 (m, 14 H), 2.45 (s, 1 H). ESI: [M+Na]$^+$ = 485.19, 2[M+Na]$^+$ = 947.38.

*4.4.3 Synthesis of 1,2,3,4,5-pentaphenyl-2,4-cyclopentadien-1-yl methyl ether (4-2)*

1,2,3,4,5-Pentaphenyl-2,4-cylopentadien-1-ol (103 mg, 0.22 mmol) was dissolved in anhyd. THF (100 mL) and stirred under argon. The solution was cooled in an ice bath and sodium hydride (39 mg, 1.08 mmol) was added. After 1 h, methyl iodide (27 µL, 0.43 mmol) was added. The solution initially turned deep purple and then to yellow after 24 h of stirring. The reaction was quenched with water and diluted with ether. Organic layer was separated, dried over MgSO$_4$ and concentrated under reduced pressure. Purification was achieved using flash silica gel chromatography (17:3 petroleum ether/CH$_2$Cl$_2$) to afford a white solid (40 mg, 32% yield). $^1$H NMR (400 MHz, CDCl$_3$): δ 7.61 (d, $J$ = 7.3 Hz, 2 H), 7.24 (t, $J$ = 7.3 Hz, 2 H), 7.19-7.13 (m, 7 H), 7.05-6.90 (m, 1 4H), 3.47 (s, 3 H). ESI: [M+Na]$^+$ = 499.20.

*4.4.4 Synthesis of 1-(1-(6-chlorohexyloxy)-2,3,4,5-tetraphenylcyclopenta-2,4-dienyl)benzene (4-3)*

Under argon, a solution of PCD-OH (934.7 mg, 2.02 mmol) in anhyd. THF (10 mL) was added to a suspension of sodium hydride (99 mg, 4.12 mmol) in THF (25 mL) dropwise at room temperature. The yellow suspension was stirred for thirty minutes. Next, 1-chloro-6-iodohexane (338 µL, 2.22 mmol) was added dropwise and mixture stirred at room temperature for seven hours. Tetrabutylammonium iodide (79 mg, 0.214 mmol) was added and reaction allowed to stir for a further seventeen hours. After this time, the solvent from the suspension was removed by rotary evaporation. Saturated aq. NaCl (15 mL) was added and product extracted with CH$_2$Cl$_2$

(4x15 mL). The combined organic layers were dried over $MgSO_4$ and removed by rotary evaporation. The yellow solid was purified by flash silica gel column (eluent: 1:1 $CH_2Cl_2$/hexanes). The product was the first fraction off of the column with an $R_f$ value of 0.73. ^{1}H-NMR showed residual 1-chloro-6-iodohexane present in product, which was removed by drying under high vacuum. Recovered 310 mg yellow solid (0.533 mmol, 26.4% yield). ^{1}H NMR (400 MHz, $CDCl_3$): δ 7.62 (d, $J$=7.7 Hz, 2 H), 7.26-7.10 (m, 9 H), 7.03-6.95 (m, 14 H), 3.66 (t, $J$ = 6.1 Hz, 2 H), 3.41 (t, $J$ = 6.8 Hz, 2 H), 1.67-1.55 (m, 4 H), 1.25-1.19 (m, 4 H). ESI: $[M+Na]^+$= 603.24.

*4.4.5 1-(1-(6-pyridiniumhexyloxy)-2,3,4,5-tetraphenylcyclopenta-2,4-dienyl)benzene chloride (4-4)*

Under argon, 1-(1-(6-chlorohexyloxy)-2,3,4,5-tetraphenylcyclopenta-2,4-dienyl)benzene (300 mg, 0.52 mmol) and anhyd. pyridine (5 mL, 62 mmol) were heated at 105°C for 26 hours. Excess solvent was removed under reduced pressure, and the crude residue was purified using flash silica gel column (eluent: $CH_2Cl_2$ to 9:1 $CH_2Cl_2$/MeOH to 1:1 $CH_2Cl_2$/MeOH) to give 183 mg (0.28 mmol, 54% yield). ^{1}H NMR (400 MHz, $CDCl_3$): δ 9.36 (d, $J$ = 5.9 Hz, 2 H), 8.41 (t, $J$ = 7.8 Hz, 1 H), 8.05 (t, $J$ = 6.9 Hz, 2 H), 7.60 (d, $J$ = 7.6 Hz, 2 H), 7.27-7.10 (m, 9 H), 7.04-6.90 (m, 14 H), 4.84 (t, $J$ = 7.4 Hz, 2 H), 3.64 (t, $J$ = 5.9 Hz, 2 H), 1.92-1.83 (m, 2 H), 1.58-1.52 (m, 2 H), 1.28-1.12 (m, 4 H).  ESI: $[M-Cl]^-$ = 624.32.

*4.4.6 Micelle Preparation-Lyophilization method*

A 1 mM solution of polymer and 1 wt. % solution of AIE dye were separately prepared in tert-butanol, and heated to 60°C. To a 20-mL vial, polymer solution (1 mL) and dye solution (1 mL) were added, followed by 60°C DI water (2 mL). Different ratios of tert-butanol and water (70:30, 60:40, 40:60, and 30:70) were studied, but the 50:50 mixture gave the most consistent

results. Mixed solutions were added to a dry ice bath (-78°C). After 2 h, the micelles were transferred to a lyophilizer for 3 days. The polymer cakes were then redispersed with 60°C PBS solution and filtered through a 0.45 μm nylon filter to remove large aggregates.

*4.4.7 Fluorescence Studies*

All fluorescence spectra measured on an Aminco-Bowman Series 2 spectrophotometer (Thermo Fisher, Madison, WI). The detector high voltage was adjusted for 50% of a maximum output signal before the start of the experiment. Analytical samples were mixed just before analysis and repeated in triplicate. First, 50 μL empty micelles and 950 μL human serum used to set background. Then, 150 μL AIE dye loaded micelles and 2.85 mL human serum mixed gently before first measurement and set on shaker for the rest of experiment and the fluorescence measured every 15 min. for 2 h. Excitation and emission values of the AIE fluorophores are shown in Table 4.1. The fluorescence emission was measured in increments of 1 nm and spectra were collected from 400-500 nm. The micelle half-lives were calculated using a one-phase decay fit on GraphPad Prism 6.0 Software (equation below).

**Table 4.1: Excitation and emission wavelengths for AIE dyes studied.**

| AIE dye | Excitation (nm) | Emission (nm) |
|---------|-----------------|---------------|
| TPE-DOH | 330 | 460 |
| TPE-TOH | 320 | 460 |
| PCD-OH | 412 | 454 |
| PCD-OMe | 412 | 454 |
| PCD-O-Pyr | 360 | 462 |

One phase decay: $Y = (Y_0 - Plateau)(e^{-kx}) + Plateau$

Where: $Y_0$ is the Y value when X(time) is zero.

Plateau is the Y value at infinite times.

k is the rate constant, expressed in reciprocal minutes.

Half-life can then be calculated: $t_{1/2} = \frac{\ln(2)}{k}$

## 4.5 References

(1) Maeda, H.; Greish, K.; Fang, J. The EPR Effect and Polymeric Drugs: A Paradigm Shift for Cancer Chemotherapy in the 21st Century. *Adv. Polym. Sci.* **2006**, *193*(1), 103–121.

(2) He, C.; Hu, Y.; Yin, L.; Tang, C.; Yin, C. Effects of particle size and surface charge on cellular uptake and biodistribution of polymeric nanoparticles. *Biomaterials* **2010**, *31*, 3657–3666.

(3) Torchilin, V. P. Nanoparticulates as Drug Carriers, Imperial College Press: London, 2006.

(4) Kabanov, A. V.; Batrakova, E. V.; Meliknubarov, N. S.; Fedoseev, N. A.; Dorodnich, T. Y.; Alakhov, V. Y.; Chekhonin, V. P.; Nazarova, I. R.; Kabanov, V. A. A new class of drug carriers: micelles of poly(oxyethylene)-poly(oxypropylene) block copolymers as microcontainers for drug targeting from blood in brain. *J. Control. Release* **1992**, *22*, 141-157.

(5) Patel, H. M.; Moghimi, S. M. Serum-mediated recognition of liposomes by phagocytic cells of the reticuloendothelial system - The concept of tissue specificity. *Adv. Drug Deliv. Rev.* **1998**, *8*(32), 45-60.

(6) Lundqvist, M.; Stigler, J.; Elia, G.; Lynch, I.; Cedervall, T.; Dawson, K. A. Nanoparticle size and surface properties determine the protein corona with possible implications for biological impacts. *Proc. Natl. Acad. Sci. U.S.A.* **2008**, *105*(38), 14265-14270.

(7) Malmsten, M. Ellipsometry studies of the effects of surface hydrophobicity on protein adsorption. *Colloids Surf. B* **1995**, *3*, 297-308.

(8) Gessner, A.; Waicz, R.; Lieske, A.; Paulke, B. R.; Mader, K.; Muller, R. H. Nanoparticles with decreasing surface hydrophobicities: influence on plasma protein adsorption. *Int. J. Pharm.* **2000**, *196*(2), 245-249.

(9) Garret, Q.; Laycock, B.; Garret, R. W. Hydrogel Lens Monomer Constituents Modulate Protein Sorption. *Invest. Opthal. Vis. Sci.* **2000**, *47*, 1687-1695.

(10) Sharma, G.; Valenta, D. T.; Altman, Y.; Harvey, S.; Xie, H.; Mitragotri, S.; Smith, J. W. Polymer particle shape independently influences binding and internalization by macrophages. *J. Control. Release* **2010**, *147*, 408-412.

(11) Decuzzi, P.; Godin, B.; Tanaka, T.; Lee, S.-Y.; Chiappini, C.; Liu, X.; Ferrari, M. Size and shape effects in the biodistribution of intravascularly injected particles. *J. Control. Release* **2010**, *141*, 320–327.

(12) Owen, S. C.; Chan, D. P. Y.; Shoichet, M. S. Polymeric Micelle Stability. *Nano Today* **2012**, *7*(1)*,* 53–65.

(13) Zhao, X.; Poon, Z.; Engler, A. C.; Bonner, D. K.; Hammond, P. T. Enhanced Stability of Polymeric Micelles Based on Postfunctionalized Poly(ethylene glycol)-b-Poly(γ-propargyl-L-glutamate): the Substituent Effect. Biomacromolecules **2012**, *13*(5), 1315-1322.

(14) Lin, W. J.; Juang, L. W.; Lin, C. C. Stability and Release Performance of a Series of Pegylated Copolymeric Micelles. *Pharm. Res*. **2003**, *20*, 668-673.

(15) Yu, Y.; Wu, G.; Liu, K.; Zhang, X. Force Required to Disassemble Block Copolymer Micelles in Water. *Langmuir* **2010**, *26*(12), 9183–9186.

(16) Yin, L.; Dalsin, M. C.; Sizovs, A.; Reineke, T. M.; Hillmyer, M. A. Glucose-Functionalized, Serum-Stable Polymeric Micelles from the Combination of Anionic and RAFT Polymerizations. Macromolecules **2012**, *45*(10), 4322–4332.

(17) Chen, H.; Kim, S.; He, W.; Wang, H.; Low, P. S.; Park, K.; Cheng, J. X. Fast Release of Lipophilic Agents from Circulating PEG-PDLLA Micelles Revealed by in Vivo Förster Resonance Energy Transfer Imaging. *Langmuir* **2008**, *24*(10), 5213–5217.

(18) Jiwpanich, S.; Ryu, J.-H.; Bickerton, S.; Thayumanavan, S. Non-covalent Encapsulation Stabilities in Supramolecular Nanoassemblies. *J Am Chem Soc.* **2010**, *132*(31), 10683-10685.

(19) Luo, J.; Xie, Z.; Lam, J. W. Y.; Cheng, L.; Chen, H.; Qiu, C.; Kwok, H. S.; Zhan*, X.; Liu, Y.; Zhu, D.; Tang, B. Z. Aggregation-induced emission of 1-methyl-1,2,3,4,5-pentaphenylsilole. *Chem. Commun.* **2001**, *18,* 1740-1741.

(20) Sun, Y.; Wang, Y.-X.; Wu, M.; Yuan, W.; Chen, Y. p-Quaterphenylene as an Aggregation-Induced Emission Fluorogen in Supramolecular Organogels and Fluorescent Sensors. *Chem. Asian J*. **2017**, *12*, 52-59.

(21) Wu, W.-C.; Chen, C.-Y.; Tian, Y.; Jang, S.-H.; Hong, Y.; Liu, Y.; Hu, R.; Tang, B. T.; Lee, Y.-T.; Chen, C.-T.; Chen, W.-C.; Jen, A. K.-Y. Enhancement of Aggregation-Induced Emission in Dye-Encapsulating Polymeric Micelles for Bioimaging. *Adv. Funct. Mater.* **2010**, *20*, 1413-1423.

(22) Liu, Y.; Tang, Y.; Barashkov, N. N.; Irgibaeva. I. S.; Lam, J. W.Y.; Hu, R.; Birimzhanova, D.; Yu, Y.; Tang, B. Z. Fluorescent Chemosensor for Detection and Quantitation of Carbon Dioxide Gas. J. Am. Chem. Soc. **2010**, *132*(40), 13951-13953.

(23) Liu, Y.; Deng, C.; Tang, L.; Qin, A.; Hu, R.; Sun, J. Z.; Tang, B. Z. Specific Detection of d-Glucose by a Tetraphenylethene-Based Fluorescent Sensor. J. Am. Chem. Soc. **2011**, *133*(4), 660-663.

(24) Tang, L.; Jin, J.; Zhang, S.; Mao, Y.; Sun, J.; Yuan, W. Z.; Zhao, H.; Xu, H.; Qin, A.; Tang, B. Z. Detection of the critical micelle concentration of cationic and anionic surfactants based on aggregation-induced emission property of hexaphenylsilole derivatives. *Sci. China Ser. B-Chem.* **2009**, *52*(6), 755-759.

(25) Guan, W.; Zhou, W.; Lu, C.; Tang, B. T. Synthesis and Design of Aggregation-Induced Emission Surfactants: Direct Observation of Micelle Transitions and Microemulsion Droplets. *Angew. Chem. Int. Ed.* **2015**, *54*, 15160-15164.

(26) Zhang, C.; Jin, S.; Li, S.; Xue, X.; Liu, J.; Huang, Y.; Jiang, Y.; Chen, W.-Q.; Zou, G.; Liang, X.-J. Imaging Intracellular Anticancer Drug Delivery by Self-Assembly Micelles with Aggregation-Induced Emission. *ACS Appl. Mater. Interfaces* **2014**, *6*(7), 5212-5220.

(27) Hong, Y.; Lam, W. Y.; Zhong, B. Aggregation-Induced Emission. *Chem. Soc. Rev.* **2011**, *40*, 5361-5388.

(28) Xie, Z.; Yang, B.; Xie, W.; Liu, L.; Shen, F.; Wang, H.; Yang, X.; Wang, Z.; Li, Y.; Hanif, M.; Yang, G.; Ye, L.; Ma, Y. A Class of Nonplanar Conjugated Compounds with Aggregation-Induced Emission: Structural and Optical Properties of 2,5-Diphenyl-1,4-Distyrylbenzene Derivatives with All Cis Double Bonds. *J. Phys. Chem. B* **2006**, *110*(42), 20993-21000.

(29) Zhang, G.; Hu, F.; Zhang, D. Manipulation of the Aggregation and Deaggregation of Tetraphenylethylene and Silole Fluorophores by Amphiphiles: Emission Modulation and Sensing Applications. *Langmuir* **2014**, *31*(16), 4593-4604.

(30) Chambers, J. W.; Baskar, A. J.; Bott, S. G.; Atwood, J. L.; Rausch, M. D. Formation and Molecular Structures of Pentabenzylcyclopentadienyl and Pentaphenylcyclopentadienyl Dicarbonyl Derivatives of Cobalt and Rhodium. *Organometallics* **1986**, *5*(8), 1635-1641.

(31) Yang, Z.; Qin, W.; Leung, N.L.C.; Arseneault, M.; Lam, J.W.Y.; Liang, G.; Sung, H.H.Y.; Williams, I.D.; Tang, B.Z. A mechanistic study of AIE processes of TPE luimnogens: intramolecular rotation vs. configurational isomerization. *J. Mater. Chem. C*, **2016**, *4*, 99-107.

(32) Anariba, F.; Chng, L.L.; Abdullah, N.S.; Tay, F.E.H. Syntheses, optical properties, and bioapplications of the aggregation-induced emission of 2,3,4,5-tetraphenylcyclopenta-2,4-dienyl benzene derivatives. *J. Mater. Chem.* **2012**, *22*, 19303-19310.

(33) Anariba, F.; Leng Chng, L.L.; Abdullah, N.S.; Tay, F.E.H. Syntheses, optical properties, and bioapplications of the aggregation-induced emission of 2,3,4,5-tetraphenylcyclopenta-2,4-dienyl benzene derivatives. *J. Mater. Chem.*, **2012**, *22*, 19303-19310.

(34) Fournier, E.; Dufresne, M. H.; Smith, D. C.; Ranger, M.; Leroux, J. C. A Novel One-Step Drug-Loading Procedure for Water-Soluble Amphiphilic Nanocarriers. *Pharm. Res.* **2004**, *21*(6), 962-968.

(35) Simone, E. A.; Dziubla, T. D.; Arguiri, E. Loading PEG-catalase into filamentous and spherical polymer nanocarriers. *Pharm Res.* **2009**, *26*(1), 250-260.

(36) Kataoka, K.; Harada, A.; Nagasaki, Y. Block copolymer micelles for drug delivery: design, characterization and biological significance. *Adv. Drug Deliv. Rev.* **2001**, *47*, 113-131.

(37) Wang, R.; Xiao, R.; Zeng, Z.; Xu, L.; Wang, J. Application of poly(ethylene glycol)–distearoylphosphatidylethanolamine (PEG-DSPE) block copolymers and their derivatives as nanomaterials in drug delivery. *Int. J. Nanomedicine* **2012**, *7*, 4185-4198.

(38) Kastantin, M.; Missirlis, D.; Black, M.; Ananthanarayanan, B.; Peters, D.; Tirrell, M. Thermodynamic and Kinetic Stability of DSPE-PEG(2000) Micelles in the Presence of Bovine Serum Albumin. *J. Phys. Chem. B* **2010**, *114*, 12632-12640.

(39) Barres A. R.; Wimmer M. R.; Mecozzi S. Multicompartment Theranostic Nanoemulsions Stabilized by a Triphilic Semifluorinated Block Copolymer. *Mol. Pharm.* **2017**, *14*, 3916-3926.

# Appendix 1: Synthesis of poly(2-oxazoline)s as triphilic polymers for potential drug delivery

**Synthesis of poly(2-oxazoline)s as triphilic polymers for drug delivery applications**

**Abstract**

Numerous studies over the last ten years have demonstrated that PEGylation can actually cause decreased delivery of active pharmaceuticals, which includes enhanced protein binding in serum, reduced uptake into cells and an elicited immune response which causes rapid blood clearance. In response, many research groups have looked at poly(2-methyl-2-oxazoline) as an alternative hydrophilic block in polymeric drug delivery systems. In this appendix, poly(2-methyl-2-oxazoline) and poly(2-butyl-2-oxazoline) blocks were synthesized as the hydrophilic and lipophilic blocks, respectively. Additionally, attempts at synthesizing a semifluorinated 2-oxazoline monomer were undertaken, in hopes to create a triphilic polymer for applications in the delivery of hydrophobic pharmaceuticals.

**A1.1 Introduction**

Polyethylene glycol, commonly denoted as PEG, has been used for decades as the benchmark hydrophilic portion in polymeric nanoparticles for injectable drug delivery systems and polymer therapeutics.[1] PEG provides water-solubility for many pharmaceuticals, that otherwise cannot be administered due to precipitation and resulting toxicity.[2] This hydrophilic polymer can either be directly conjugated to drugs and proteins or attached to hydrophobic blocks in amphiphilic nanoparticles for delivery.[3-6] In addition to water-solubility, PEG has the advantage of being a stealth polymer--in that it is not readily recognized by the immune system. This characteristic leads PEG-conjugated drugs or PEG-nanoparticles to circulate in the blood stream for longer amounts of time without being eliminated.[2] Recent studies have argued however that PEG is not as bioinert as commonly believed, with several papers in the last decade showing that an intravenous (IV) injection of PEG-conjugates causes a second dose to lose its

long-circulating characteristics, when injected a few days later.[7] It has been found that around

25% of a healthy blood-donor population have pre-existing anti-PEG antibodies prior to

treatment, which could be from all of the PEG used in everyday products from shampoo to food

additives.[8] One study showed that 45% of patients developed anti-PEG antibodies when treated

with a PEG-asparaginase. As a result of these PEG-antibodies, drugs containing this hydrophilic

polymer have accelerated blood clearance (ABC), making them less effective as the increased

clearance lessens the area under the curve.[9] The identification of the biological activity of

PEGylated drugs exhibits a massive hurdle for the development of stealth drug delivery systems.

Although the PEG-antibody discovery is alarming for those studying PEG-conjugates and

PEG-based nanoparticles, there are those who still don't completely agree with some findings.

Many assays for PEG-antibodies are flawed and lack specificity. In addition, some studies have

inconsistent results-one of which shows increased PEG-antibodies, but a decreased ABC.[10] If

there are antibodies being produced for PEG, then these particles should be cleared from the

blood at an accelerated rate, which is not being seen. These inconsistencies need further

evaluation before there is a complete overhaul of PEG therapeutics.

However, due to the potential for PEG-based delivery systems being inefficient, the

search for a new standard hydrophilic polymer is under way. A specific class of polymers, called

Poly(2-oxazoline)s, have garnered increased attention for drug delivery and other biomedical

applications. Poly(2-oxazoline)s are nonionic, stable, and highly soluble in water and organic

solvents.[11] Additionally, these polymers can be produced with high quality, of different

architectures, and with varying functional groups.[12] They possess the main beneficial properties

of PEG, while also having characteristics that are unique for different drug delivery applications.

Interestingly, the hydrophobicity of poly(2-oxazoline)s can be tuned over a broad range by

alteration of the side chain.[13] Figure A1.1 shows the series of poly(2-alkyl-2-oxazoline)s that share the amide motif backbone, with decreasing water solubility as the 2-alkyl side chain becomes larger. Hydrophilic poly(2-methyl-2-oxazoline) and poly(2-ethyl-2-oxazoline) are considered homologues of PEG, due to their water solubility and rapid renal clearance.[13]
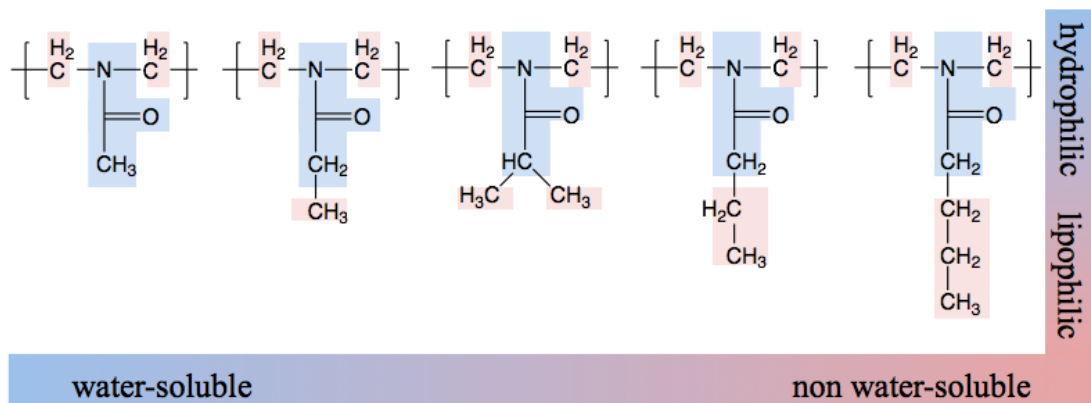


**Figure A1.1: A series of POx derivatives with increasing degree of hydrophobicity.** Adapted from reference 13.

In addition to tunable solubility, poly(2-oxazoline)s exhibit stealth and protein repellent effects.[11, 12] As these polymers are non-biodegradable, assessing their biocompatibility is of the utmost importance. Appropriate cytocompatibility has been found *in vitro* for these polymers of varying nanostructures.[14, 15] The toxicity profile of these polymers shows promise, as one *in vivo* study found that 10 and 20 kDa PEtOx showed no adverse effects in the range of concentrations studied (from 500 to 2,000 mg/kg), when injected intravenously in rats.[16] Biodistribution studies with radiolabeled PMeOx and PEtOx showed rapid blood clearance and low uptake into organs of the reticuloendothelial system.[17, 18]

The polyamide backbone of poly(2-oxazoline)s allows for versatile syntheses to create many different polymer architectures; linear,[19] star,[20] bow-tie,[21] and molecular brush.[22] Synthetic variety of these polymers can also allow for the development of many drug delivery systems,

such as protein-polymer conjugates,[23] polyplexes,[24] drug-polymer conjugates,[25] polymeric micelles,[26, 27] and hydrogels.[28]

**A1.2 Results and Discussion**

*A1.2.1 Hydrophilic oxazoline*

One of the most common hydrophilic oxazoline block studied for drug delivery applications is poly(2-methyl-2-oxazoline). The monomer, 2-methyl-2-oxazoline, is commercially available, and relatively inexpensive. As a test of synthetic polymerization methods, the synthesis of poly(2-methyl-2-oxazoline) was undertaken. Poly(2-oxazoline) polymers are prepared by the living cationic polymerization method. The most common experimental procedure involves the stoichiometric addition of an electrophile initiator such as an alkyl tosylate or alkyl triflate to the oxazoline monomer that is dissolved in a dry organic solvent, and in an inert atmosphere. The propagation stage is conducted at 80°C for approximately 1 to 3 days. The living polymeric cation is then terminated by the introduction of a nucleophile, commonly aqueous sodium carbonate in water to give a hydroxy-terminated polymer, as seen in Figure A1.2.[29] It is also common to keep the propagation stage going by adding a second, more lipophilic oxazoline monomer, making a biphilic polymer.



A1-1, 13%
Average MW=1,200
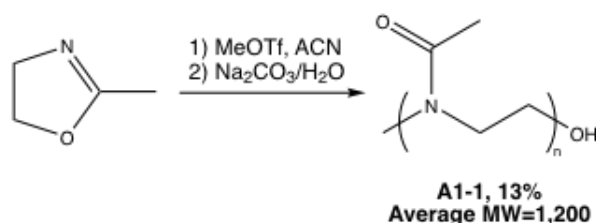
**Figure A1.2: Synthesis of hydrophilic portion, poly(2-methyl-2-oxazoline), i.e. PMOXA.**

*A1.2.2 Lipophilic oxazoline*

The Mecozzi group often uses triphilic polymers for encapsulating hydrophobic pharmaceuticals. Historically, a straight chain hydrocarbon has been used as the lipophilic block,

ranging from 8-18 carbons long.[30] We believe incorporating a lipophilic polyoxazoline block would be an interesting addition to this study. The typical hydrophobic poly(2-oxazoline) used as a lipophilic block is poly(2-butyl-2-oxazoline). However, the commercially available starting material, 2-butyl-2-oxazoline was quite expensive, so the synthesis of monomer was also undertaken.

One synthetic route to prepare 2-oxazolines starts with nitriles containing the R group of the desired oxazoline side chain. The nitrile is directly reacted with ethanolamine, along with the metal catalyst cadmium acetate dihydrate to form the five-membered ring. The lipophilic monomer, 2-butyl-2-oxazoline was synthesized as shown below in Figure A1.3.[31]
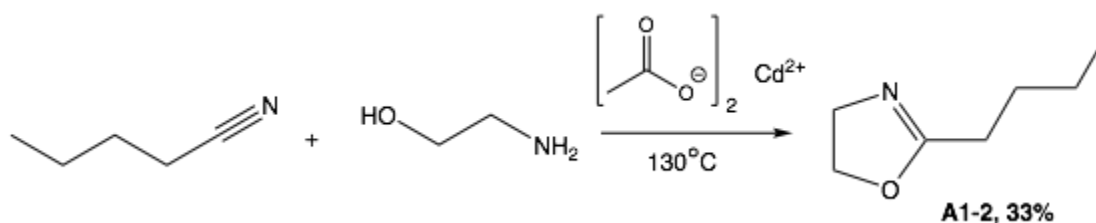


**Figure A1.3*: Synthesis of lipophilic monomer, 2-butyl-2-oxazoline.**

An amphiphilic polymer was next synthesized, by polymerizing this lipophilic monomer off of an already polymerized poly(2-methyl-2-oxazoline) block. The second polymerization of the lipophilic block was terminated by addition of piperidine (Figure A1.4).[32]
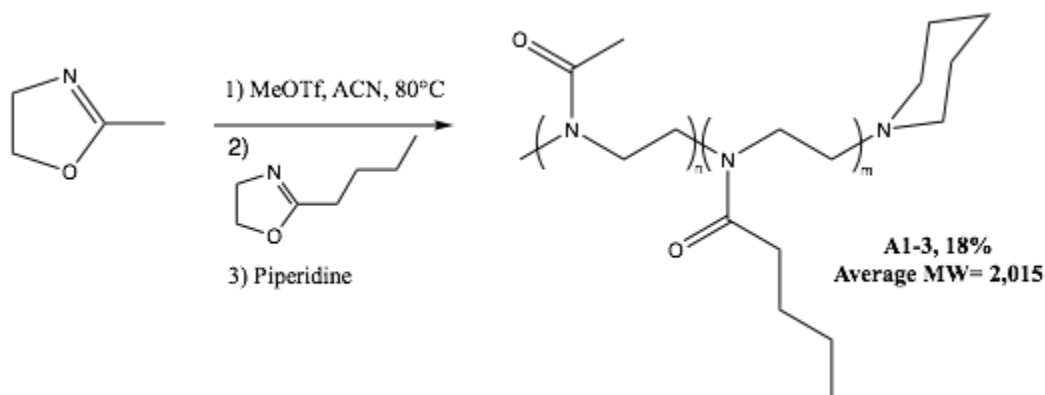


**Figure A1.4: Synthesis of biphilic polymer, poly(2-methyl-2-oxazoline)-b-poly(2-butyl-2-oxazoline) i.e. P(MOXA-b-BOXA).**

To create a triphilic polymer, in which a fluorophilic segment is incorporated (hydrophilic-*b*-lipophilic-*b*-fluorophilic), this polymerization would instead be followed by polymerizing a fluorous oxazoline monomer, and then subsequent termination. The synthesis of a fluorous monomer is discussed in section A1.2.3.

*A1.2.3 Fluorophilic oxazoline*

As the synthesis of both hydrophilic and lipophilic poly(2-oxazoline) blocks proceeded with relative ease, the synthesis of a fluorous poly(2-oxazoline) block was studied. The first synthetic route for oxazoline, described above in the hydrophilic oxazoline segment, reacts ethanolamine with the nitrile corresponding to the desired polymer side chain. This route was not chosen because short-chain fluorinated nitriles have extreme flammability and low boiling points. Another synthetic route towards 2-oxazolines begins with a carboxylic acid containing the R group of the desired side chain, which is then converted to the acid chloride with thionyl chloride.  The acid chloride product is then reacted with ethanolamine, to form the intermediate amide (Figure A1.5). This can then undergo a ring-closing reaction similar to Robinson-Gabriel synthesis in which the carbonyl oxygen acts as the nucleophile.[33] This route was attempted below, with two different starting acids, perfluoropropionyl acid and perfluorobutyryl acid.

Due to the low boiling point of each fluorous acid chloride, they were distilled and directly added to the following reaction in a separate flask.
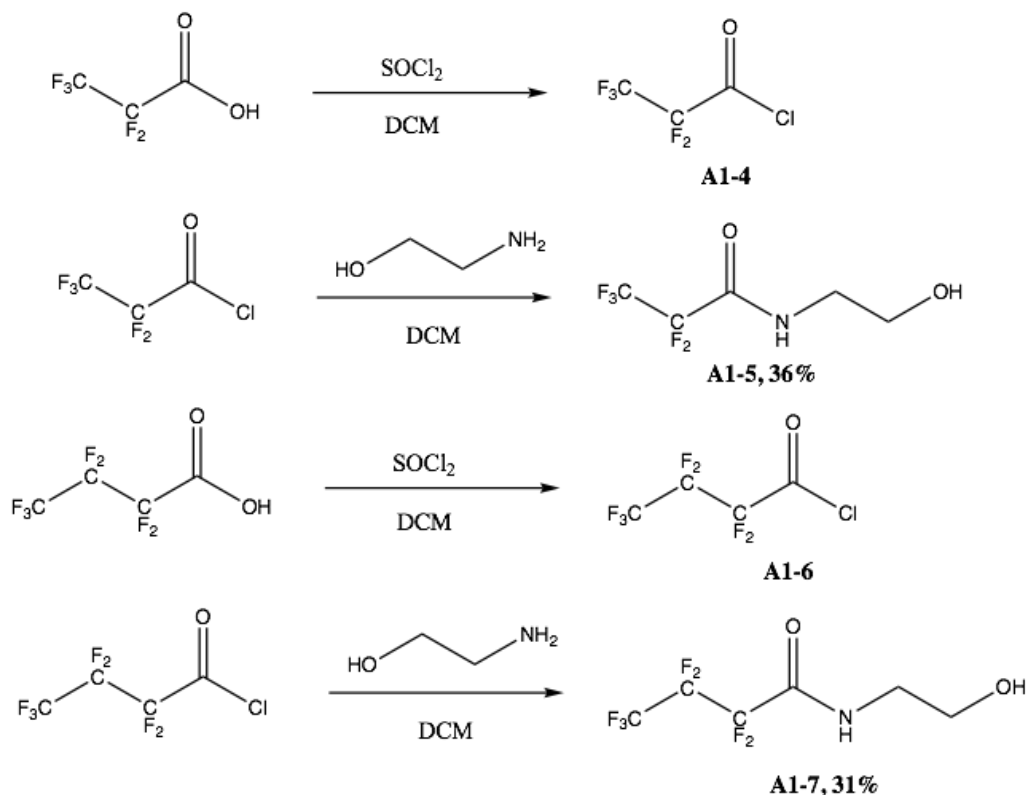
**Figure A1.5: Syntheses of starting materials for a fluorous 2-oxazoline.**

These reactions had somewhat low yields, and it was found the purifications of the amides were unsuccessful. Published methods for purification were attempted, but they did not separate the desired product from ethanolamine.[33] Other solvent combinations were also tested for separation, but also proved unsuccessful. One reason for these results is that the fluorous acid chlorides had very low boiling points, making it difficult to capture for the following reaction. Additionally, having fluorous groups off these molecules made them somewhat unreactive, leading to low yields.

Due to the unsuccessful purification of the above amides, a different synthetic route towards oxazolines was attempted. In this case, the perfluoropropionyl chloride was reacted directly with 2-chloroethylamine hydrochloride to form an amide with better leaving group for the subsequent ring closure (Figure A1.6).[34, 35]
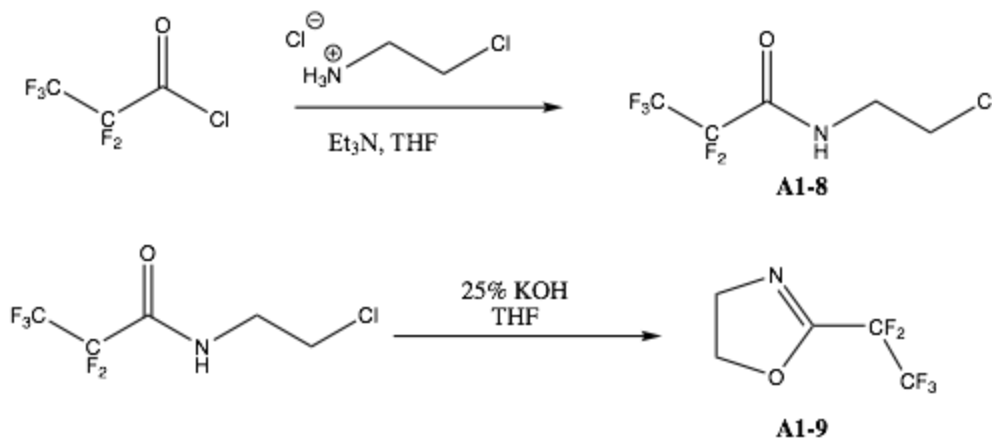
**Figure A1.6: Synthesis of N-(2-chloroethyl)-2,2,3,3,3-pentafluoropropanamide and 2-pentafluoroethyl-2-oxazoline.**

Although the NMR spectra show oxazoline product was formed through this method, purification was unsuccessful. Additionally, the reagent 2-chloroethylamine hydrochloride is extremely hygroscopic and second attempts in using it for synthesis proved to be difficult as the reaction proceeds under anhydrous conditions.

## A1.3 Conclusions and Future Works

After perusing the literature, one study discussed the attempts at polymerizing the fluorinated oxazoline, 2-pentafluoroethyl-2-oxazoline. It was found that little polymer was formed as the reactivity of fluorous oxazoline to ring-opening and subsequent polymerization is very slow. The solubility of these oxazoline is also low in many solvents. To form any polymer, elevated temperatures were used and the solvent of choice was nitromethane.[36] Due to this decreased reactivity, many groups that want to incorporate a fluorous polyoxazoline block instead synthesize monomers where the R group is a perfluorobenzyl group. By doing so, the reactivity of the monomer is not as affected by the electronegative fluorines.[37]

Although the fluorous block was not readily synthesized, the use of poly(2-methyl-2-oxazoline) as the hydrophilic portion of amphiphilic polymers will be a continued area of research. As polyethylene glycol receives more criticism for its apparent immunogenicity, many

research groups will have to switch to alternative hydrophilic polymers. This preliminary work serves as a starting step towards this goal for the Mecozzi group.

**A1.4 Experimental Section**

*A1.4.1 Materials and Methods*

All solvents and other reagetns were of ACS grade or higher and were purchased from Sigma-Aldrich Inc. or Fischer Scientific. Perfluoropropionyl acid and perfluorobutyryl acid were purchased from Synquest Labs, Inc. All reagents were used as received, unless otherwise mentioned. Regular phase chromatographic separations were performed using Silicycle 60 Å silica. Reverse phase chromatographic separations were performed using C18 Gold Column. $^1$H, $^{13}$C, and $^{19}$F NMR spectra were obtained on a Varian UI-400 or a Bruker AV-400 spectrometer using the indicated deuterated solvent and TMS as internal reference.

*A1.4.2 Synthesis of poly(2-methyl-2-oxazoline) i.e. PMOXA, (A1-1)*

2-methyl-2-oxazoline (8 mL, 94.48 mmol) was dissolved in anhyd. ACN (17 mL) under argon. Methyl trifluoromethanesulfonate (214 µL, 1.9 mmol) was added at 0°C under argon. The mixture was then heated to 70°C for 22 h. After that time, the reaction was cooled and subsequently quenched by addition of $H_2O$ (1.1 mL) and solid $Na_2CO_3$ (2.1 g, 19.8 mmol). The mixture was then heated to 80°C for 19 h. The polymer was purified by reverse phase chromatography on CombiFlash system to obtain 916 mg white solid (13% yield). $^1$H-NMR (CDCl$_3$, 400 MHz): δ 3.49 (m, 64 H), 3.10 (m, 3H), 2.17 (m, 49H).

*A1.4.3 Synthesis of 2-butyl-2-oxazoline (A1-2)*

To a dry 100 mL round bottom flask was added valeronitrile (143 mmol), aminoethanol (172 mmol) and cadmium acetate dihydrate (35 mmol). The mixture was stirred and heated to 130°C for 16 h. The reaction was then cooled to room temperature and purified by vacuum

distillation, with product distilling around 46°C. Recovered 6.05 g colorless liquid (33% yield).

$^1$H-NMR (CDCl$_3$, 400 MHz): δ 4.18 (t, *J*=9.5 Hz, 2H), 3.78, (t, *J*=9.5 Hz, 2H), 2.23 (t, *J*=7.6 Hz, 2H), 1.58 (p, *J*=7.5 Hz, 2H), 1.33 (sextet, *J*=7.5 Hz, 2H), 0.89 (t, *J*=7.3 Hz, 3H). $^{13}$C-NMR (CDCl$_3$, 100 MHz): δ 168.63, 67.05, 54.26, 27.99, 27.59, 22.27, 13.64.

*A1.4.4 Synthesis of poly(2-methyl-2-oxazoline)-b-poly(2-butyl-2-oxazoline) i.e. P(MOXA-b-BOXA) (A1-3)*

Under argon, methyl triflate (2.6 mmol) and 2-methyl-2-oxazoline (64.9 mmol) were dissolved in anhyd. ACN (15 mL). The mixture was heated to 75°C for 22 h. After cooling to room temperature, 2-butyl-2-oxazoline (26 mmol) was added and the mixture was heated to 75°C for 22 h. The reaction mixture was then cooled to room temperature and polymerization terminated by addition of piperidine (13 mmol) and stirred overnight. Next, potassium carbonate (excess) was added and mixture allowed to stir for several hours. The solution was then filtered and solvent removed in vacuo. Attempted purification on the CombiFlash, but polymer did not dissolve from the solvent combinations (H$_2$O/MeOH or CH$_2$Cl$_2$/MeOH). Removed silicon wafer from cartridge, redissolved polymer in MeOH, and filtered off Celite and silica. Once again removed solvent and added 10 mL chloroform to polymer residue. Precipitated in dry ice bath with 100 mL cyclohexane/diethyl ether. Finally, dissolved polymer in water and lyophilized to give a white solid. NMR shows a substantial amount of water remains after lyophilization. MALDI centered around [M+Na]$^+$=2015.19.

*A1.4.5 Synthesis of perfluoropropionyl chloride (A1-4)*

Thionyl chloride (47.5 mmol) and pentafluoropropionic acid (9.5 mmol) were added to a 250-mL round bottom flask and flushed with argon. A stir bar was added and reagents heated to

reflux, while distilling off product into a cooled reaction flask containing components for the next reaction. The clear oil was distilled at 9°C, and added directly to the subsequent reaction.

*A1.4.6 Synthesis of 2,2,3,3,3-pentafluoro-N-(2-hydroxyethyl) propanamide (A1-5)*

To an iced, stirring solution of ethanolamine (9.5 mmol) in $CH_2Cl_2$, pentafluoropropionyl chloride was added dropwise from the previous reaction. The reaction was allowed to proceed overnight and cool to room temperature. Next, the mixture was quenched with water and additional $CH_2Cl_2$. The solution was washed with water three times, dried over magnesium sulfate and solvent removed to yield 792 mg (37% yield). ^{1}H-NMR ($D_2O$, 400 MHz): δ 3.75 (t, *J*=5.45 Hz, 2H), 2.27 (t, *J*= 5.45 Hz, 2H). ^{19}F-NMR ($D_2O$, 376 MHz): δ -83.15 (3F), -120.80 (2F).

*A1.4.7 Synthesis of perfluorobutyryl chloride (A1-6)*

Thionyl chloride (115 mmol) and heptafluorobutyric acid (23 mmol) were added to a 250-mL round bottom flask and flushed with argon. A stir bar was added and reagents heated to reflux, while distilling off product into a cooled reaction flask containing components for the next reaction. The product was distilled at 39°C and added directly to the subsequent reaction.

*A1.4.8 Synthesis of 2,2,3,3,4,4,4-heptafluoro-N-(2-hydroxyethyl)-butanamide (A1-7)*

To an iced, stirring solution of ethanolamine (1.2 g, 20 mmol) in $CH_2Cl_2$, heptafluorobutyryl chloride was added dropwise from the previous reaction. This reaction was allowed to stir overnight and was then cooled to room temperature. The mixture was quenched with water and washed with $CH_2Cl_2$ and solvents removed under reduced pressure. Purified with a flash column, eluting with 10% MeOH/$CH_2Cl_2$ to yield 903 mg (33% yield). ^{1}H-NMR ($D_2O$, 400 MHz): δ 3.74 (t), 3.64 (t), 3.43 (t), 3.07 (t). ^{19}F-NMR ($D_2O$, 376 MHz): δ -80.86 (t, *J*= 8.37 Hz, 3F), -121.31 (q, *J*= 8.54 Hz, 2F), -127.55 (b, 2F).

*A1.4.9 N-(2-chloroethyl)-2,2,3,3,3-pentafluoropropanamide (A1-8)*

To an iced, stirring solution of Triethylamine (12.18 mmol) and 2-chloroethylamine hydrochloride (6.36 mmol) in anhyd. THF, pentafluoropropionyl chloride was added dropwise from the previous solution. The reaction was allowed to proceed overnight and cool to room temperature. The mixture was then diluted with water (100 mL) and organic product extracted with $CH_2Cl_2$ (2 x 75 mL). Combined organic layers washed with aq. $NH_4Cl$ (100 mL), dried over $MgSO_4$ and solvent evaporated to give 2.552 crude oil. Due to instability of this product, did not purify before next step.

*A1.4.10 Synthesis of 2-pentafluoroethyl-2-oxazoline (A1-9)*

A solution of 2,2,3,3,3-pentafluoro-N-(2-hydroxyethyl) propanamide (2.55 g) in 8 mL of THF was added dropwise to a stirred aq. KOH (25%). After stirring the reaction mixture for 16 h at room temperature, the mixture was extracted with acetone and isolation of product was attempted with distillation. $^1$H-NMR (500 MHz, $CDCl_3$): δ 3.75 (t, *J*= 5.45 Hz, 2H), 2.27 (t, *J*=5.45 Hz, 2H). $^{19}$F-NMR (376 MHz, $CDCl_3$: δ -83.12 (s, 3H), -120.8 (s, 2F).

**A1.5 References**

(1) Pasut, G.; Veronese, F. M. Polymer–drug conjugation, recent achievements and general strategies. *Prog. Polym. Sci.* **2007**, *32*, 933–961.

(2) Knop, K.; Hoogenboom, R.; Fischer, D.; Schubert, U. S. Poly(ethylene glycol) in Drug Delivery: Pros and Cons as Well as Potential Alternatives. *Angew. Chem. Int. Ed.* **2010**, *49*, 6288-6308.

(3) Veronese, F. M.; Schiavon, O.; Pasut, G.; Mendichi, R.; Andersson, L.; Tsirk, A.; Ford, J.; Wu, G.; Kneller, S.; Davies, J.; Duncan, R. PEG−Doxorubicin Conjugates: Influence of Polymer Structure on Drug Release, in Vitro Cytotoxicity, Biodistribution, and Antitumor Activity. *Bioconjug. Chem.* **2005**, *16*(4), 775-84.

(4) Hemley, I. W. PEG−Peptide Conjugates. *Biomacromolecules* **2014**, *15*, 1543-1559.

(5) Torchilin, V. P. Recent advances with liposomes as pharmaceutical carriers. *Nat. Rev. Drug. Discov*. **2005**, *4*(2), 145-160.

(6) Zhang, Y.; Huang, Y.; Li, S. Polymeric Micelles: Nanocarriers for Cancer-Targeted Drug Delivery. *AAPS PharmSciTech*. **2014**, *15*(4), 862-871.

(7) Verhoef, J. J. F.; Anchordoquy, T. J. Questioning the use of PEGylation for drug delivery. *Drug Deliv. and Transl. Res*. **2013** *3*, 99–503.

(8) Tagami, T.; Nakamura, K.; Shimizu, T.; Yamazaki, N.; Ishida, T.; Kiwada, H. CpG motifs in pDNA-sequences increase anti-PEG IgM production induced by PEG-coated pDNA-lipoplexes. J. Control. Release **2010**, *142*, 160-166.

(9) Armstrong, J. K.; Hempel, G.; Koling, S.; Chan, L. S.; Fisher, T.; Meiselman, H. J.; Garratty, G. Antibody against poly(ethylene glycol) adversely affects PEG-asparaginase therapy in acute lymphoblastic leukemia patients. Cancer **2007**, *110*(1), 103-111.

(10) Scheliekens, H.; Hennink, W.E.; Brinks, V. The Immunogenicity of Polyethylene Glycol: Facts and Fiction. *Pharm. Res*. **2013**, *30*, 1729-1734.

(11) Luxenhofer, R.; Han, Y.; Schulz, A.; Tong, J.; Heb, Z.; Kabanov, A. X.; Jordan, R. Poly(2-oxazoline)s as Polymer Therapeutics. *Macromol. Rapid Commun.* **2012**, *33*(19), 1613-1631.

(12) Hoogenboom, R. Poly(2-oxazoline)s: A polymer class with numerous potential applications. Angew. Chem. Int. Ed. **2009**, *48*(43), 7978-7994.

(13) de la Rosa, V. R. Poly(2-oxazoline)s as materials for biomedical applications. *J. Mater. Sci. Mater. Med.* **2014**, *25*, 1211-1225.

(14) Bauer, M.; Lautenschlaeger, C.; Kempe, K.; Tauhardt, L.; Schubert, U. S.; Fischer, D. Poly(2-ethyl-2-oxazoline) as alternative for the stealth polymer poly(ethylene glycol): comparison of in vitro cytotoxicity and hemocompatibility. *Macromol. Biosci*. **2012**, *12*(7), 986-998.

(15) Luxenhofer, R.; Sahay, G.; Schulz, A.; Alakhova, D.; Bronich, T. K.; Jordan, R. Structure-property relationship in cytotoxicity and cell uptake of poly(2-oxazoline) amphiphiles. *J. Control. Release* **2011**, *153*(1), 73-82.

(16) Viegas, T. X.; Bentley, M. D.; Harris, J. M.; Fang, Z.; Yoon, K.; Dizman, B. Polyoxazoline: chemistry, properties, and applications in drug delivery. *Bioconjug. Chem.* **2011**, *22*(5), 976-86.

(17) Gaertner, F. C.; Luxenhofer, R.; Blechert, B.; Jordan, R.; Essler, M. Synthesis, biodistribution and excretion of radiolabeled poly(2-alkyl-2-oxazoline)s. *J. Control. Release* **2007**, *119*(3), 291-300.

(18) Goddard, P.; Hutchinson, L. E.; Brown, J.; Brookman, L. J. Soluble polymeric carriers for drug delivery. Part 2. Preparation and in vivo behavior of N-acylethylenimine copolymers. *J. Control. Release* **1989**, *10*(1), 5-16.

(19) Reif, M.; Jordan, R. α,ω-Functionalized Poly(2-Oxazoline)s Bearing Hydroxyl and Amino Functions. *Macromol. Chem. Phys.* **2011**, *212*, 1815-1824.

(20) Luxenhofer, R.; Bezen, M.; Jordan, R. Kinetic Investigations on the Polymerization of 2-Oxazolines Using Pluritriflate Initiators. *Macromol. Rapid Commun.* **2008**, *29*, 1509-1513.

(21) Kowalczuk, A.; Kronek, J.; Bosowska, K.; Trzebicka, B.; Dworak, A. Star poly(2-ethyl-2-oxazoline)s—synthesis and thermosensitivity. *Polym Int.* **2011**, *60*, 1001-1009.

(22) Zhang, N.; Luxenhofer ,R.; Jordan, R. Thermoresponsive Poly(2-oxazoline) Molecular Brushes by Living Ionic Polymerization: Kinetic Investigations of Pendant Chain Grafting and Cloud Point Modulation by Backbone and Side Chain Length Variation. *Macromol. Chem. Phys*. **2012**, *213*, 973-981.

(23) Luxenhofer, R.; Lopez-Garcia, M.; Frank, A.; Kessler, H.; Jordan, R. First poly(2-oxazoline)-peptide conjugate for targeted radionuclide cancer therapy. *PMSE Prepr*. **2006**, *95*, 283-284.

(24) Jeong, J. H.; Song, S. H.; Lim, D. W.; Lee, H.; Park, T. *G.*DNA transfection using linear poly(ethylenimine) prepared by controlled acid hydrolysis of poly(2-ethyl-2-oxazoline). *J. Control. Release.* **2001**, *73*(2-3), 391-399.

(25) Moreadith, R. W.; Viegas, T. X.; Bentley, M. D.; Harris, J. M.; Fang, Z.; Yoon, K.; Dizman, B.; Weimer, R.; Rae, B. P.; Li, X.; Rader, C.; Standaert, D.; Olanow, W. Clinical development of a poly(2-oxazoline) (POZ) polymer therapeutic for the treatment of Parkinson's disease – Proof of concept of POZ as a versatile polymer platform for drug development in multiple therapeutic indications. *Eur. Polym. J.* **2017**, *88*, 524-552.

(26) Wang, C. H.; Wang, W. T.; Hsiue, G. H. Development of polyion complex micelles for encapsulating and delivering amphotericin B. *Biomaterials* **2009**, *30*(19), 3352-3358.

(27) Lee S. C.; Kim, C.; Kwon, I. C.; Chung, H.; Jeong S. Y. Polymeric micelles of poly(2-ethyl-2-oxazoline)-block-poly(epsilon-caprolactone) copolymer as a carrier for paclitaxel. *J. Control. Release* **2003**, *89*(3):437-446.

(28) Wang, C. H.; Hwang, Y. S.; Chiang, P. R.; Shen, C. R.; Hong, W. H.; Hsiue, G. H. Extended release of bevacizumab by thermosensitive biodegradable and biocompatible hydrogel. *Biomacromolecules* **2012**, *13*(1), 40-48.

(29) Konradi, R.; Pidhatika, B.; Mühlebach, A.; Textor, M. Poly-2-methyl-2-oxazoline: A Peptide-like Polymer for Protein-Repellent Surfaces. *Langmuir* 2008, *24*(3), 613-616.

(30) Tucker, W.; McCoy, A.; Fix, S.; Stagg, M.; Murphy, M.;, Mecozzi, S. Synthesis, physicochemical characterization, and self-assembly of linear, dibranched, and miktoarm semifluorinated triphilic polymers. *J. Polym. Sci. A* **2014**, 1-13.

(31) Schulze, H.; Kmiecik, J. (Texaco Inc., USA) Metal catalyzed cyclization of organic nitriles and amino alcohols oramino thiols. US Patent 3,741,961A, June 26, 1973.

(32) Luxenhofer, R.; Schulz, A.; Roques, C.; Li, S.; Bronich, T. K.; Batrakova, E. V.; Jordan, R.; Kabanov, A. V. Doubly-Amphiphilic Poly(2-oxazoline)s as High-Capacity Delivery Systems for Hydrophobic Drugs. *Biomaterials* **2010**, *31*(18), 4972-4979.

(33) L.V. Saloutina, A.Ya. Zapevalov, M.I. Kodess, Saloutin, V. I. Synthesis of polyfluoroalkylated 1,4-diazinols and 1,4-oxazinols using polyfluoro-2,3-epoxyalkanes32 + 13. J. Fluorine Chem. **1998**, *87*(1), 49-55.

(34) Miyamoto, M.; Aoi, K.; Saegusa, T. Novel Covalent-Type Electrophilic Polymerization of 2-(Perfluoroalkyl)-2-oxazolines Initiated by Sulfonates. Macromolecules **1991**, *24*, 11-16.

(35) Ivanova, R.; Komenda, T.; Bonne, T. B.; Ludtke, K.; Mortensen, K.; Pranzas, P. K.; Jordan, R.; Papadakis, C. M. Micellar Structures of Hydrophilic/Lipophilic and Hydrophilic/Fluorophilic Poly(2-oxazoline) Diblock Copolymers in Water. *Macromol. Chem. Phys*. **2008**, *209*, 2248–2258.

(36) Miyamoto, M.; Kaoi, K.; Saegusa, T. Mechanisms of Ring-Opening Polymerization of 2-(Perfluoroalkyl)-2-oxazolines Initiated by Sulfonates: A Novel Covalent-Type Electrophilic Polymerization. *Macromolecules* **1988**, *21*(6), 1880-1883.

(37) Lobert, M.; Kohn, U.; Hoogenboom, R.; Schubert, U. S. Synthesis and microwave assisted polymerization of fluorinated 2-phenyl-2-oxazolines: the fastest 2-oxazoline monomer to date. *Chem. Commun.* **2008**, *12*, 1458–1460.

# Appendix 2: Supplementary Data

**Appendix 2: Supplementary Data**

## A2.1 Electrospray Ionization Mass Spectra (ESI-MS)

## PCD-OH (4-1)

**PCD-OMe (4-2)**



20170531_Fleetwood_PCD_Ome.d: +MS, 0.02-2.00min #1-120

411.13533

[M+Na]⁺
515.17585

637.19810

815.27484

905.32145

[M+Na]⁺
499.20268

500.20598

501.18181

502.18509

503.18854

Ion of interest isotopic
distribution overlaps
with another ion.

**PCD-O-Cl (4-3)**



20170427_MCF_230.d: +MS, 0.05-1.19min #3-71

[M+Na]⁺ 603.24315

360.33088

408.31376

[M+Na]⁺ 603.24315

619.21706

685.43521

780.56728

907.52264

1201.46748

20170427_MCF_230.d: +MS, 0.05-1.19min #3-71

[M+Na]⁺ 603.24315

604.24641

605.24213

606.24421

607.24716

**PCD-O-Pyr (4-4)**



Intens.
x10⁶

[M]⁺
624.32614

2017053_Mecozzi_MCF_II_223.d: +MS, 0.09-1.03min #5-62

Intens.
x10⁶

[M]⁺
624.32614

625.32934

626.33235

2017053_Mecozzi_MCF_II_223.d: +MS, 0.09-1.03min #5-62

## A2.2 Matrix Assisted Laser Desorption/Ionization (MALDI)

### M1(F2Ox)$_{3-4}$
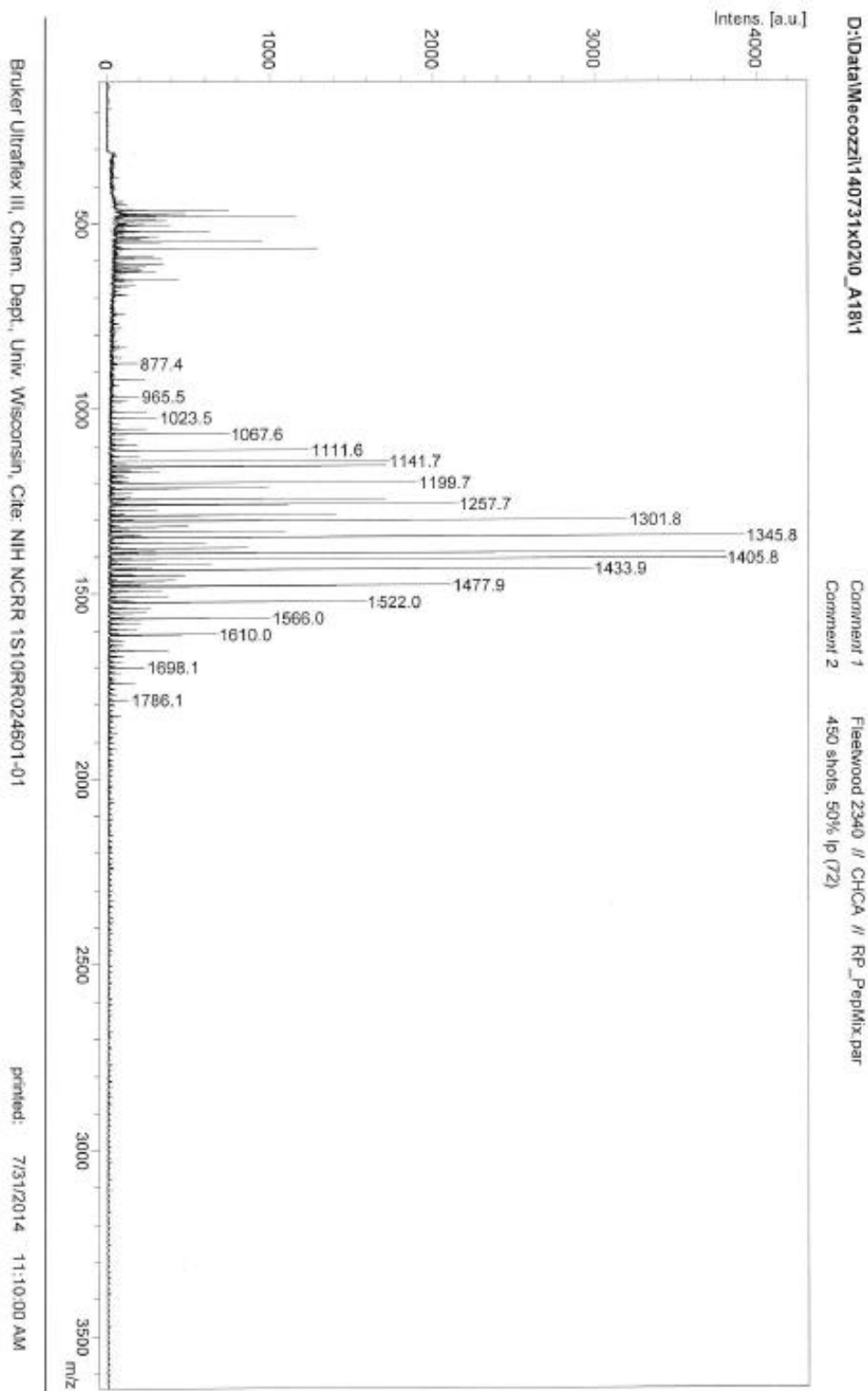
**M1(F2Ox)4-5**
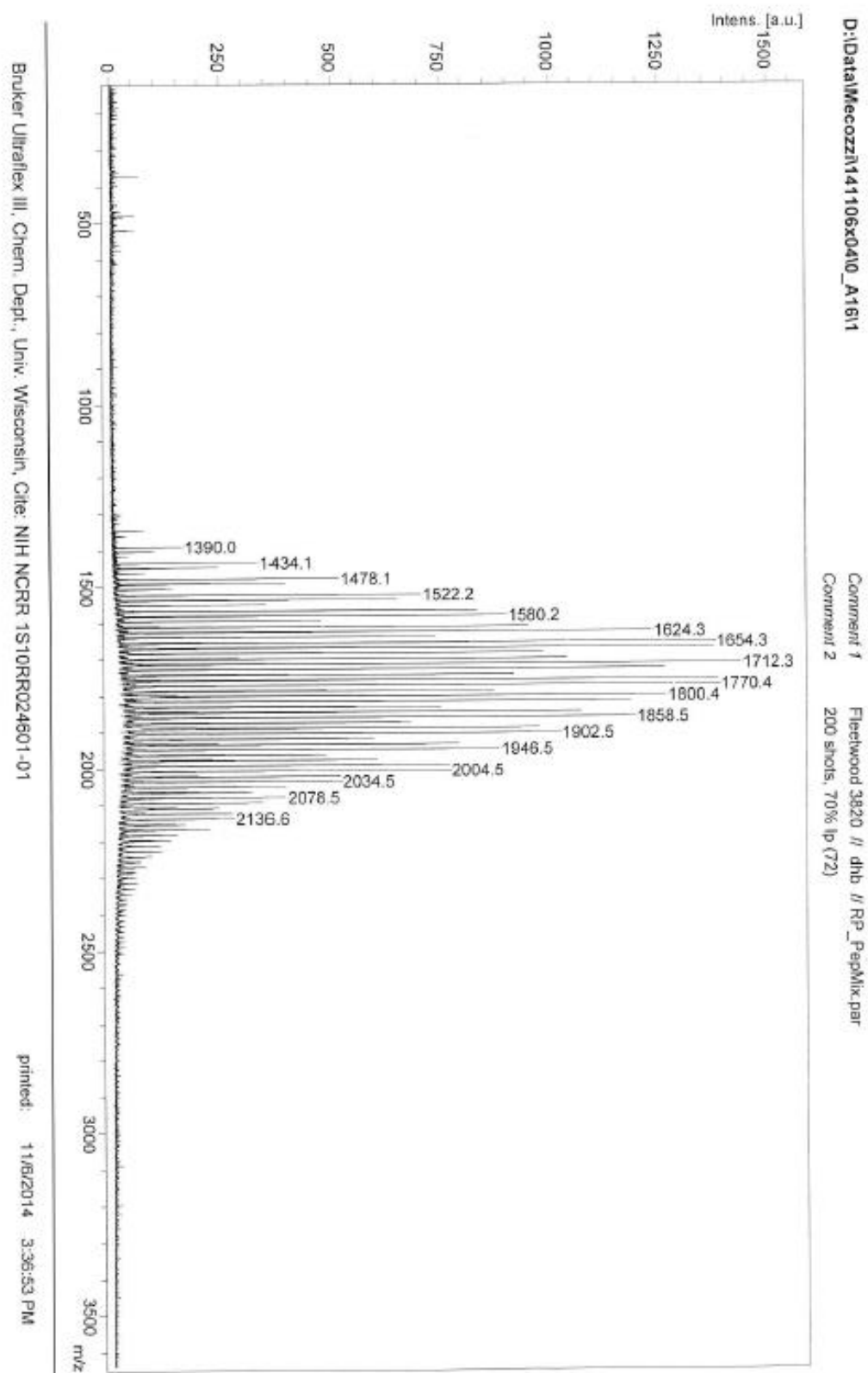
**M5(F2Ox)3-5**
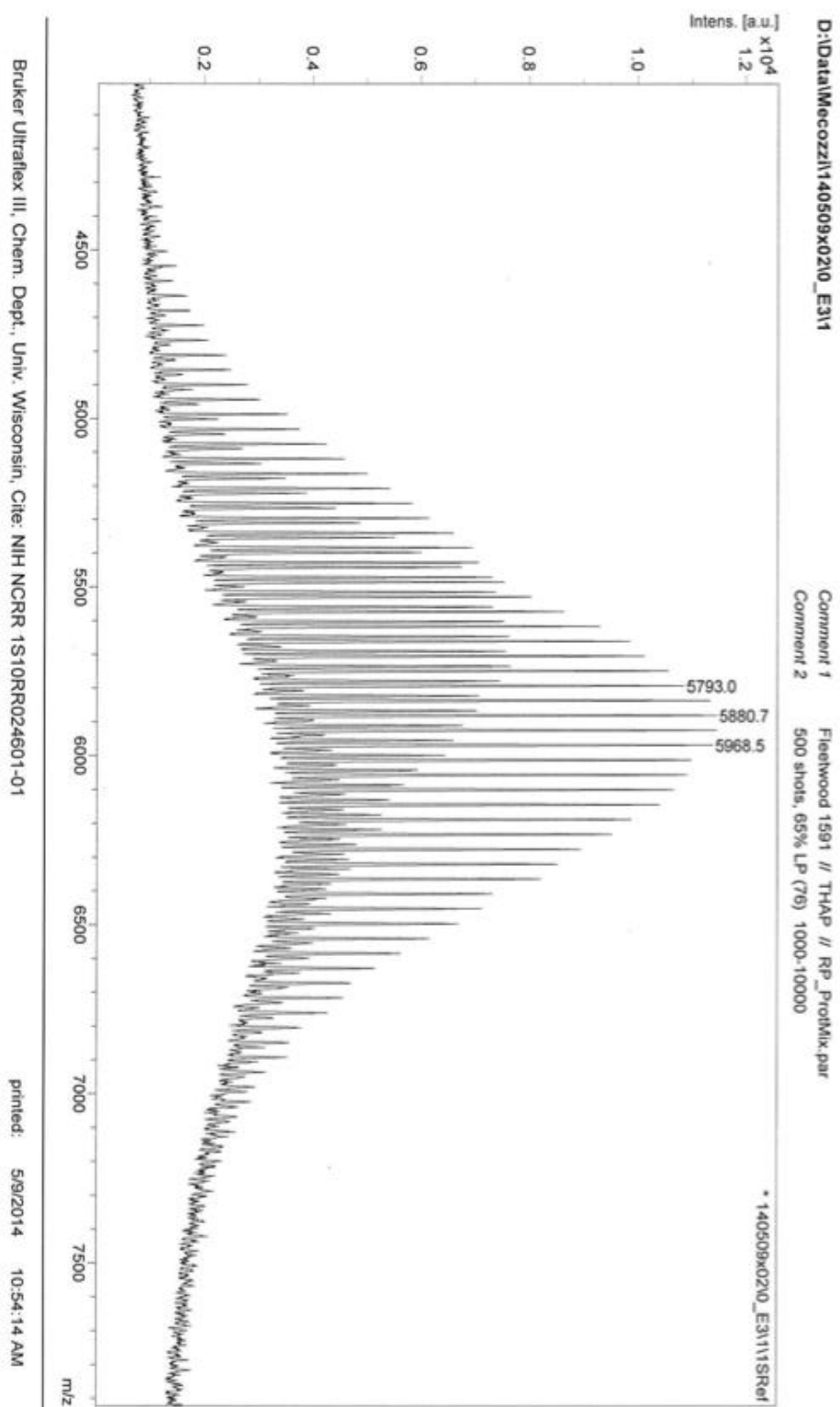
**M5(F2Ox)<sub>6-7</sub>**

**M5(F2Ox)<sub>7-9</sub>**

**H10(F2Ox)₂-8 (2-7)**



D:\Data\Mecozzi\140825x02\0_A141\1

Comment 1    Fleetwood 3043  // CHCA  // RP_PepMix.par
Comment 2    300 shots, 20% lp (72)

**M1-Oms (3-1)**



MCF-II-80

Intens. [a.u.] x10⁴

675.990
749.385
793.414
837.444
881.474
925.496
969.526
1013.551
1057.579
1145.633
1233.686
1321.739
1365.766
1409.793
1453.820
1497.847
1541.876
1585.902
1629.931
1717.986
1947.289 2096.351
2266.429

**M1FE2 (3-2)**



Peaks labeled: 672.037, 935.548, 1085.372, 1129.401, 1173.427, 1217.452, 1261.480, 1305.511, 1349.539, 1393.567, 1437.595, 1481.624, 1525.652, 1613.708, 1701.762, 1745.791, 1789.818, 1833.844, 1877.870, 1921.898, 1965.925, 2009.951, 2053.975, 2097.975, 2186.049, 2409.889, 2585.963, 2762.046, 2938.102, 3114.144, 3290.173

**M1FE3 (3-3)**

Intens. [a.u.]
×10⁴

666.050
715.453 847.545
935.610
1023.667
1199.781
1333.515
1377.544
1421.569
1465.598
1509.627
1553.653
1597.681
1685.738
1817.820
1861.849
1905.879
1949.908
1993.935
2037.964
2081.988
2126.019
2170.049
2214.074
2302.130
2862.125
3082.259

m/z

**M1bFE4 (3-4)**

Intens. [a.u.]
×10⁴

666.079
803.525
935.609
1067.693
1243.804
1511.449
1555.483
1599.512
1643.539
1687.572
1731.601
1775.631
1819.663
1951.750
2083.838
2127.869
2171.896
2215.924
2244.828
2259.953
2303.980
2348.009
2392.031
2436.054
2480.044

m/z

**P(MOXA-b-BOXA) (A1-3)**

*A2.3 Gel Permeation Chromatography (GPC)*

**Methoxypolyethylene glycol (mPEG, MW=5000):**
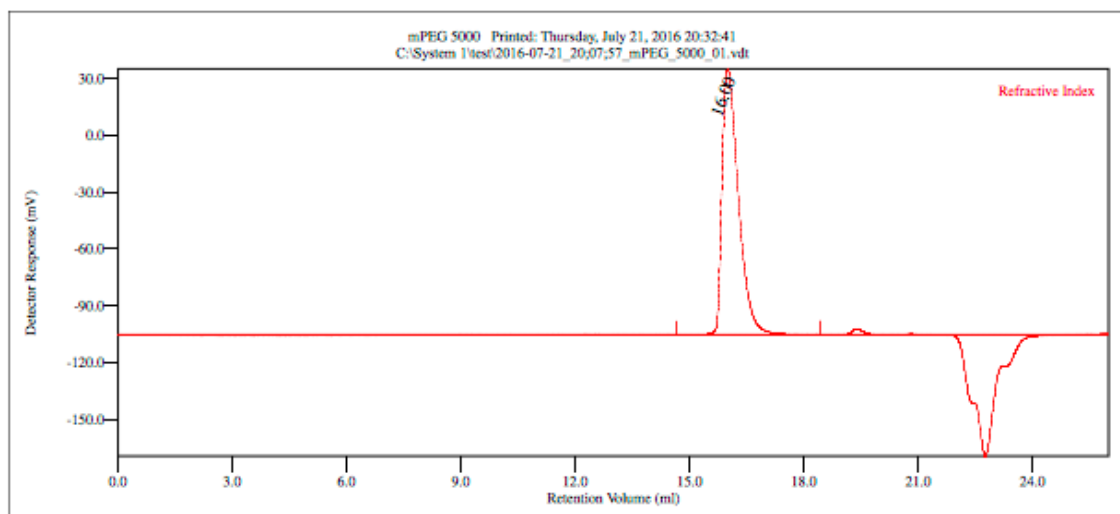


| Peak RV - (ml) | | 15.997 |
|---|---|---|
| Mn - (Daltons) | | 4,600 |
| Mw - (Daltons) | | 4,904 |
| Mz - (Daltons) | | 5,145 |
| Mp - (Daltons) | | 5,416 |
| Mw / Mn | | 1.066 |
| Percent Above Mw: | 0 | 0.000 |
| Percent Below Mw: | 0 | 0.000 |
| Mw 10.0% Low | | 2,879 |
| Mw 10.0% High | | 6,533 |
| RI Area - (mvml) | | 70.05 |
| UV Area - (mvml) | | 0.00 |

**M5(F2Ox)₃-₅:**
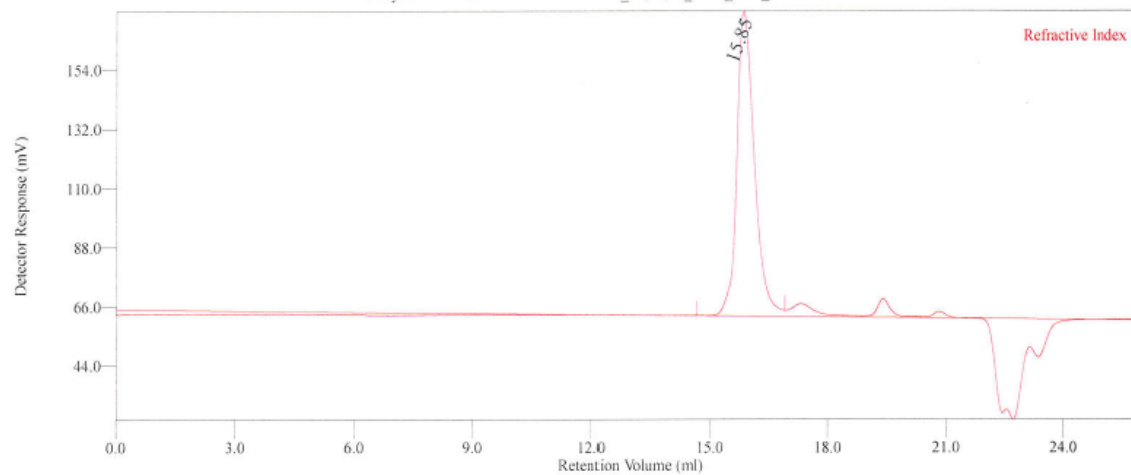
| Peak RV - (ml) | | 15,850 |
|---|---|---|
| Mn - (Daltons) | | 5,976 |
| Mw - (Daltons) | | 6,377 |
| Mz - (Daltons) | | 6,758 |
| Mp - (Daltons) | | 6,712 |
| Mw / Mn | | 1.067 |
| Percent Above Mw: | 0 | 0.000 |
| Percent Below Mw: | 0 | 0.007 |
| Mw 10.0% Low | | 3,759 |
| Mw 10.0% High | | 9,347 |
| RI Area - (mvml) | | 58.01 |
| UV Area - (mvml) | | 0.00 |

*A2.4 ¹H-NMR*

**3-bromo-2-bromomethyl-2-methylpropyl acetate (2-2)**
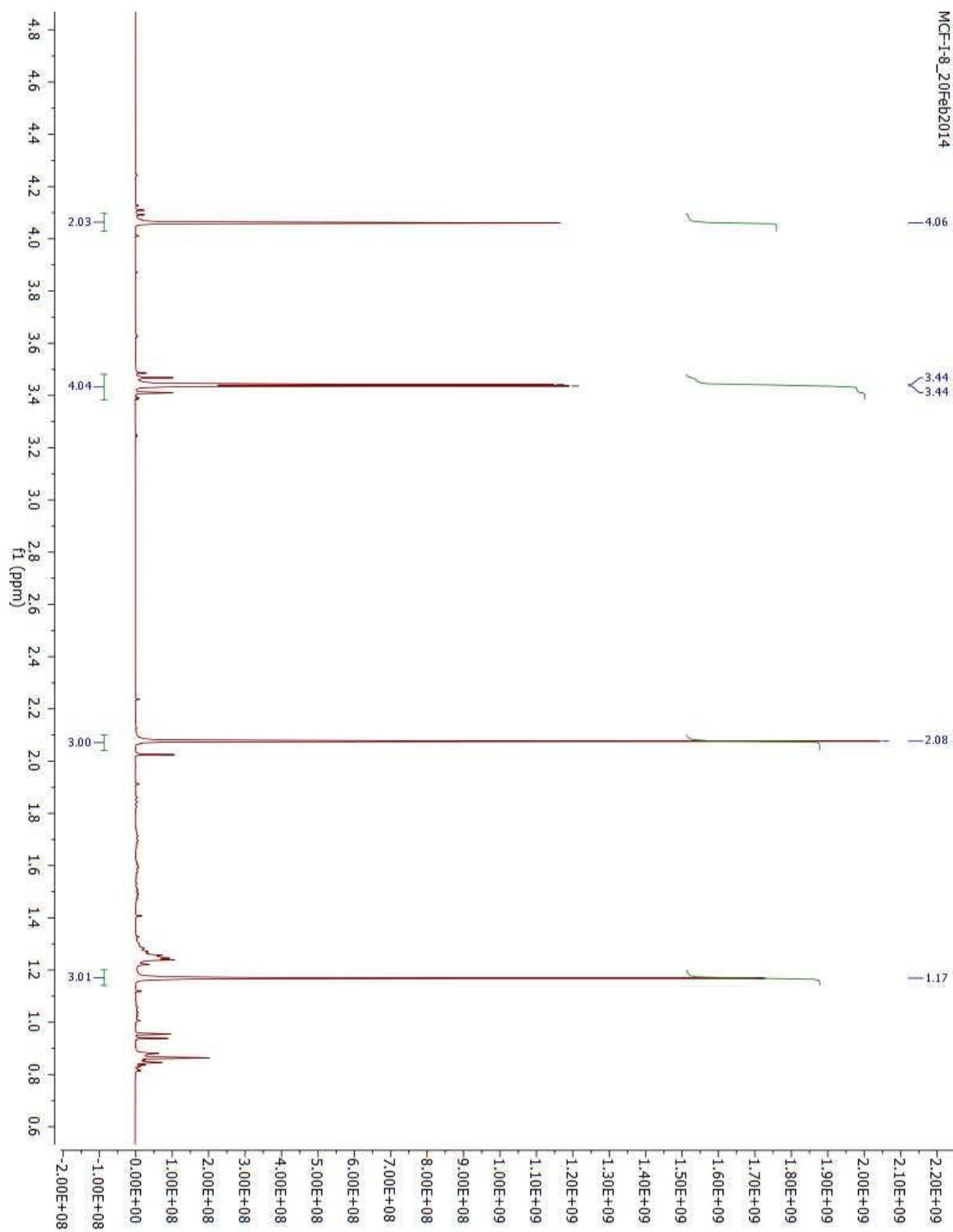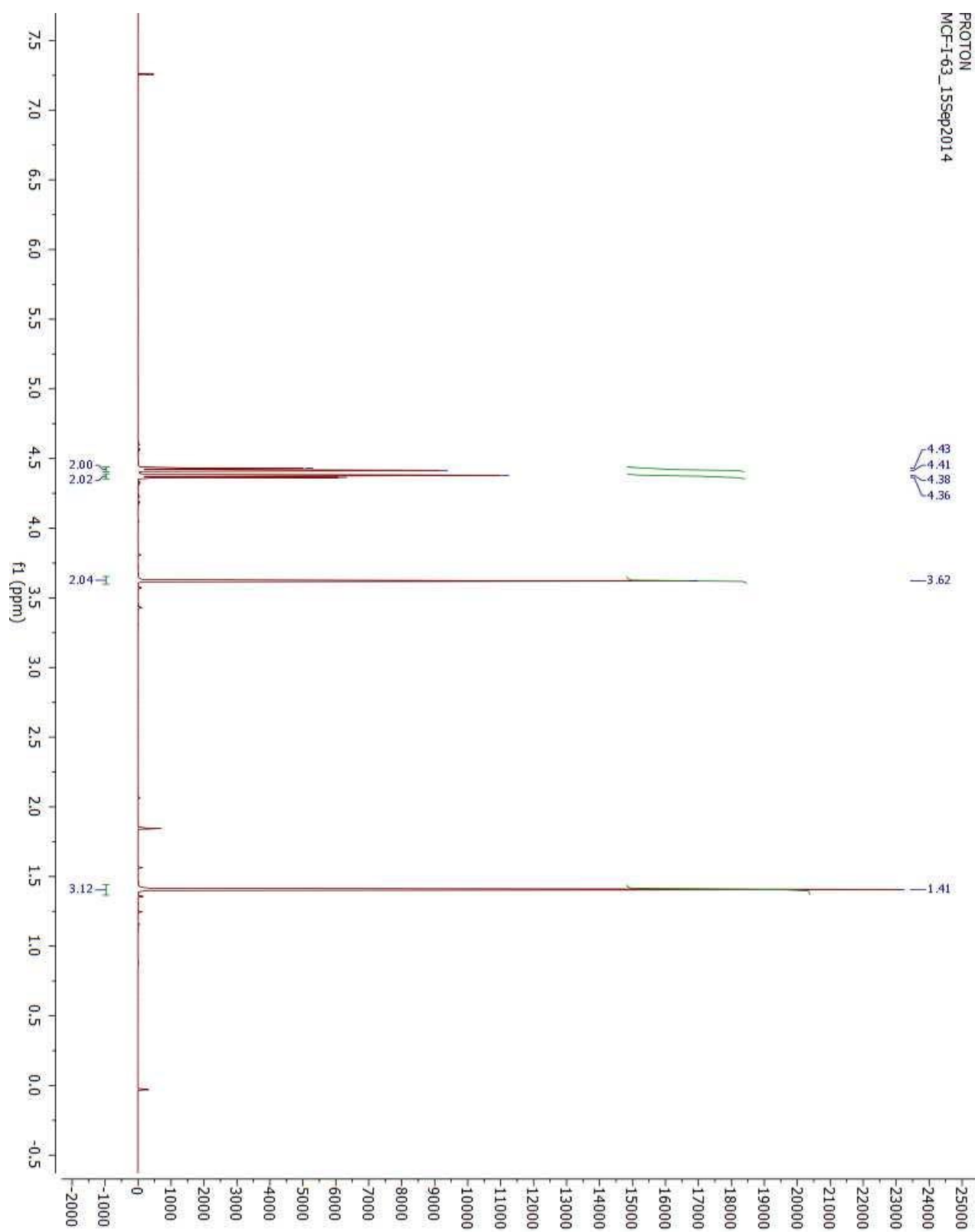
# 3-(bromomethyl)-3-methyloxetane (2-3)

**3-(1H,1H-perfluoropropan-1-oxymethyl)-3- methyloxetane (2-4)**
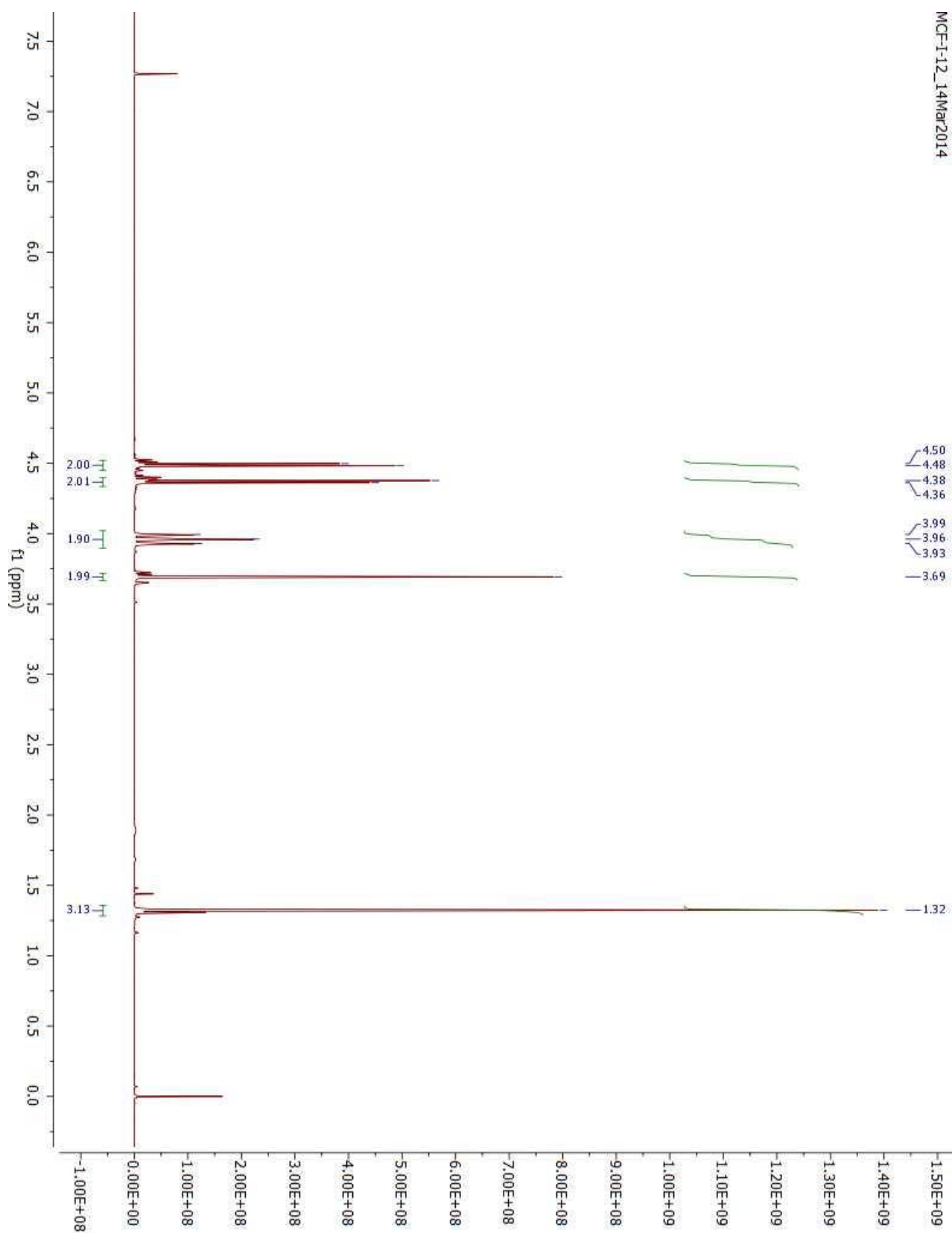
# M1(F2Ox)n (2-5)
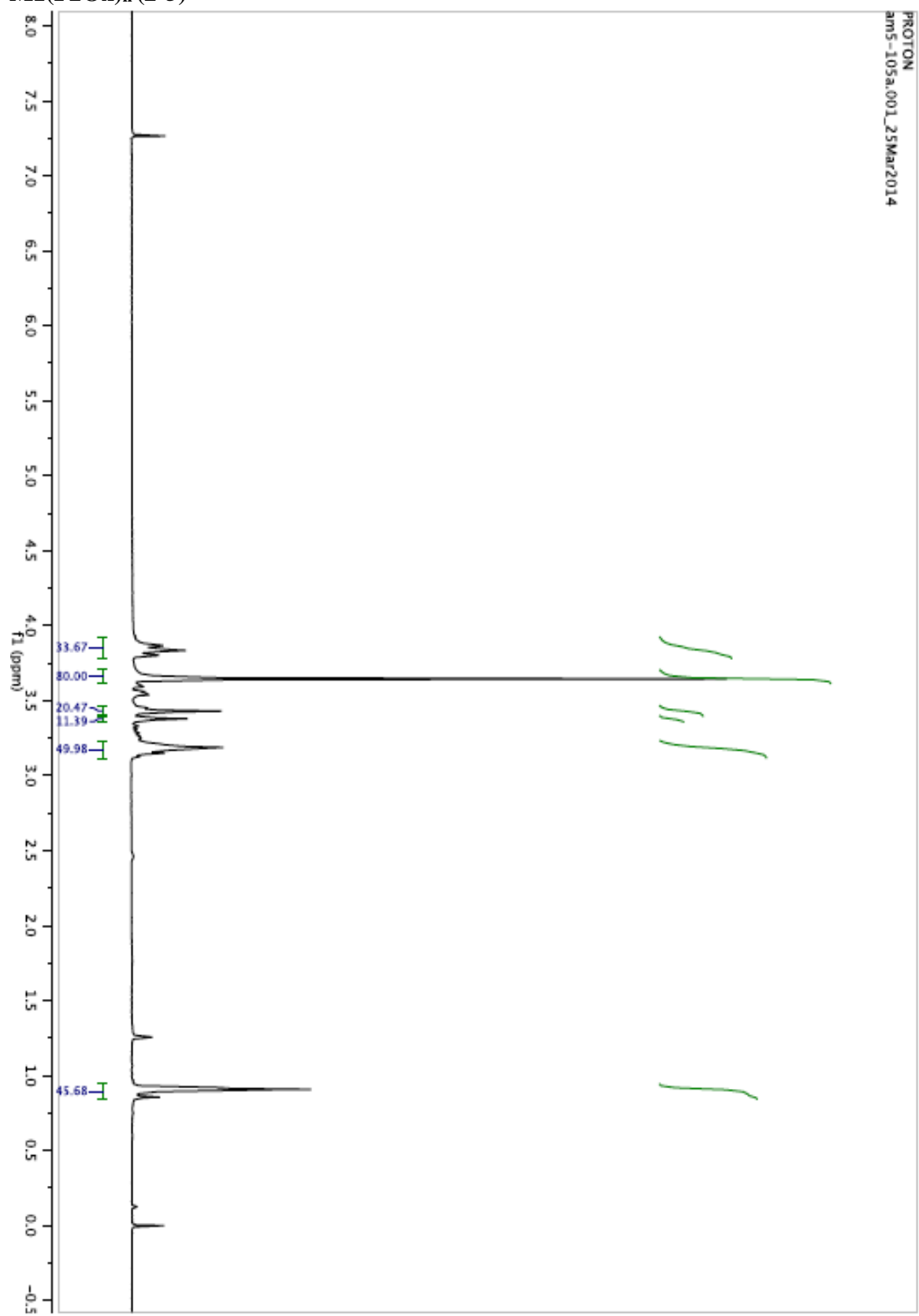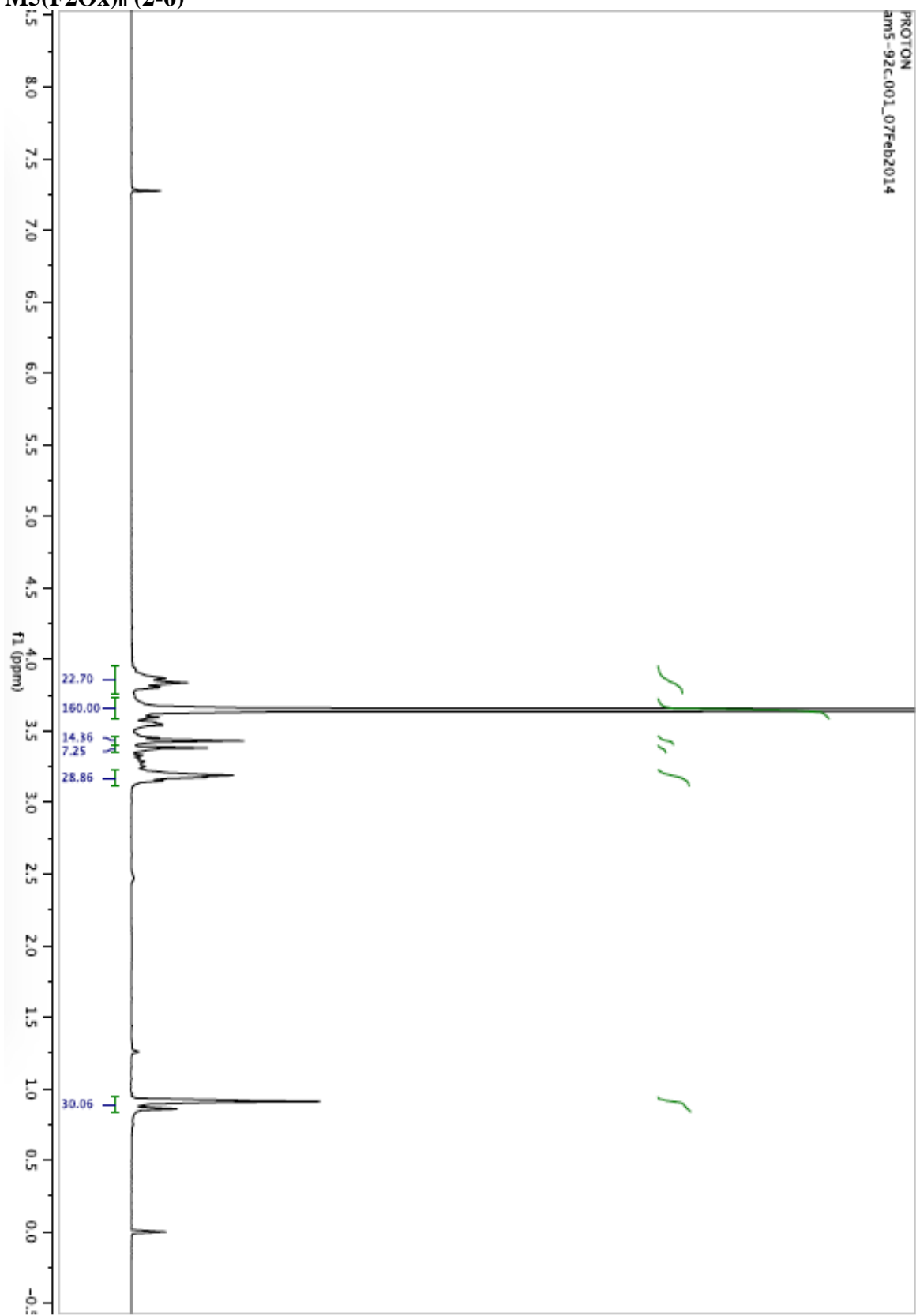
**M5(F2Ox)ₙ (2-6)**

**M1-Oms (3-1)**
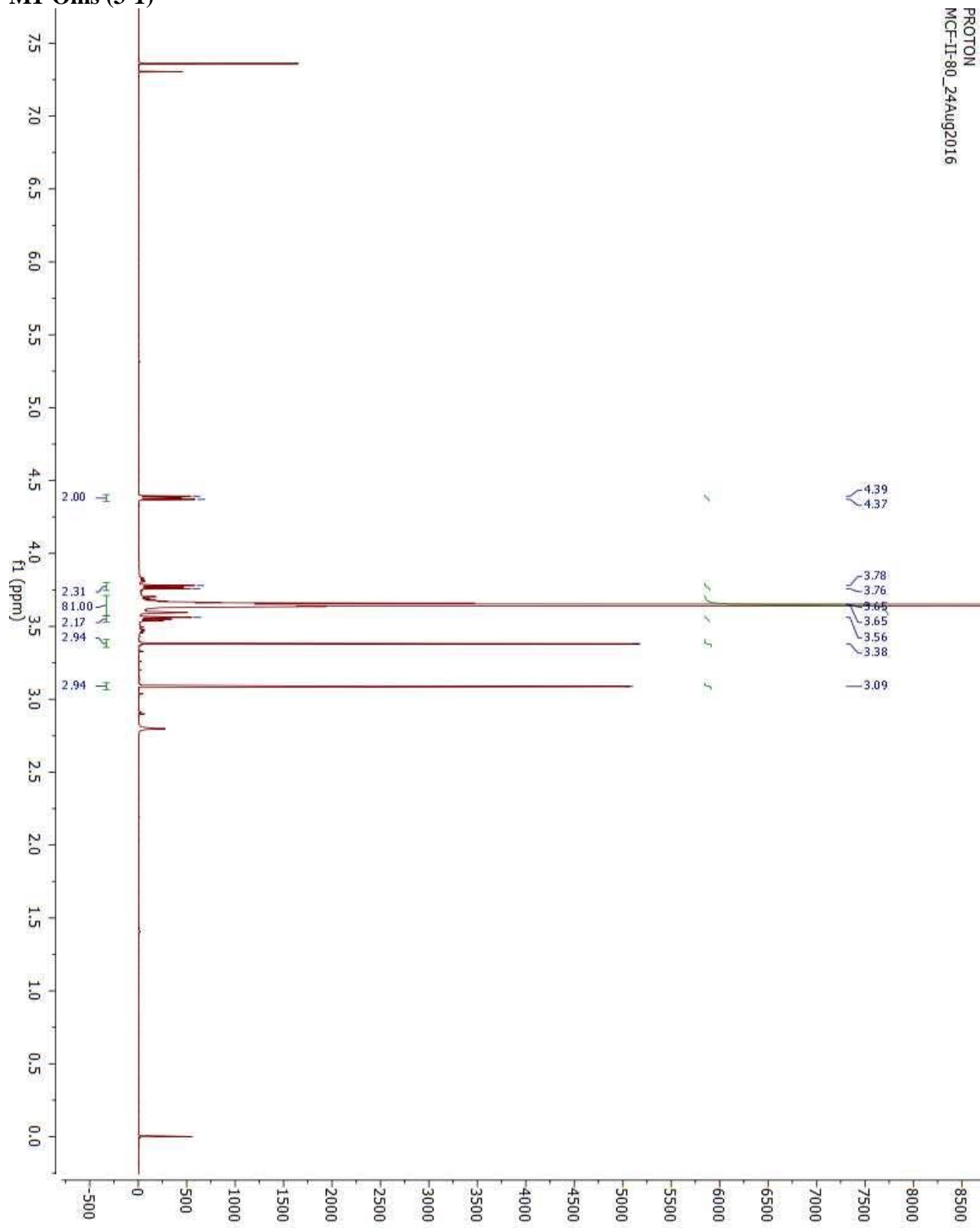
**M1FE2 (3-2)**
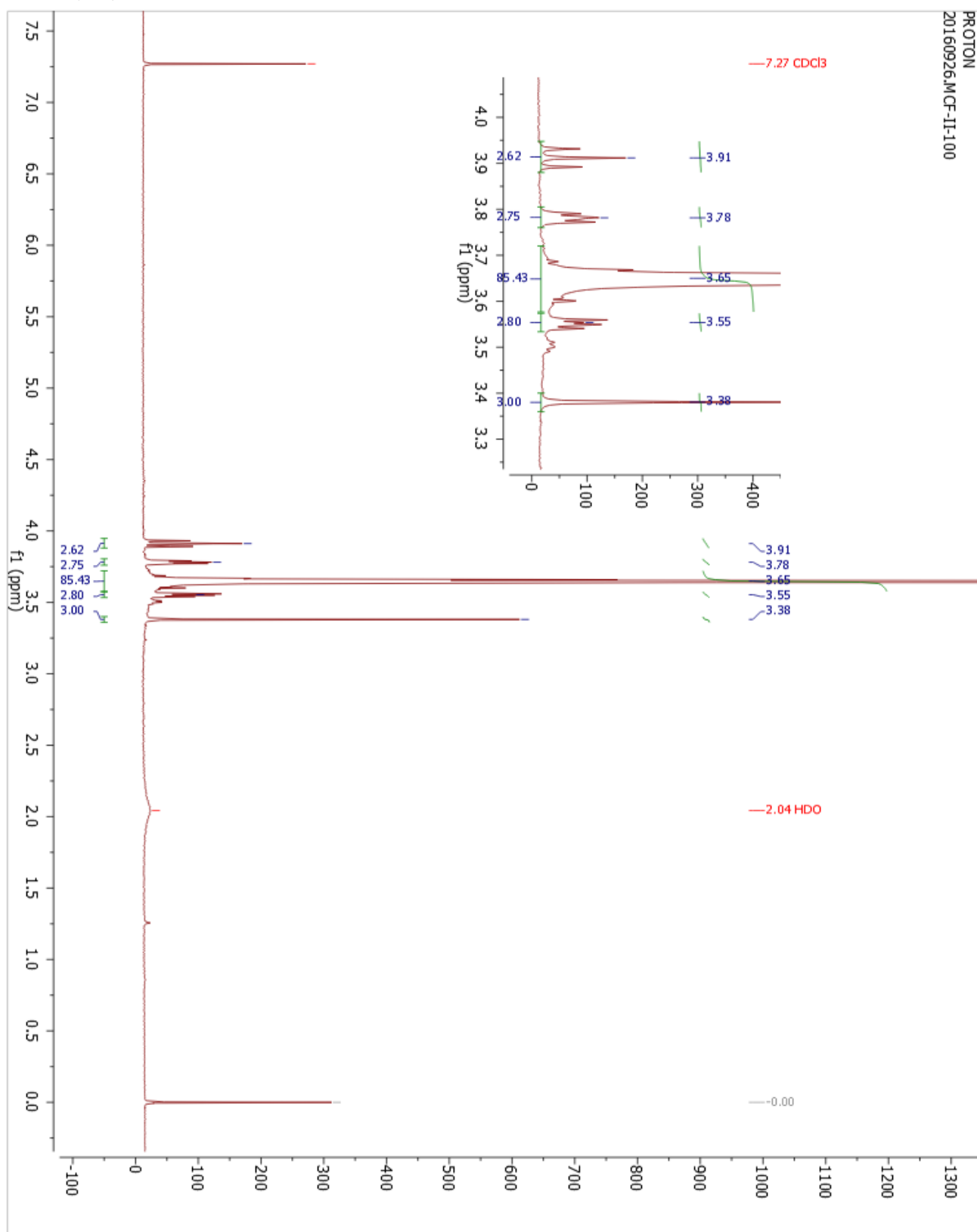
**M1FE3 (3-3)**
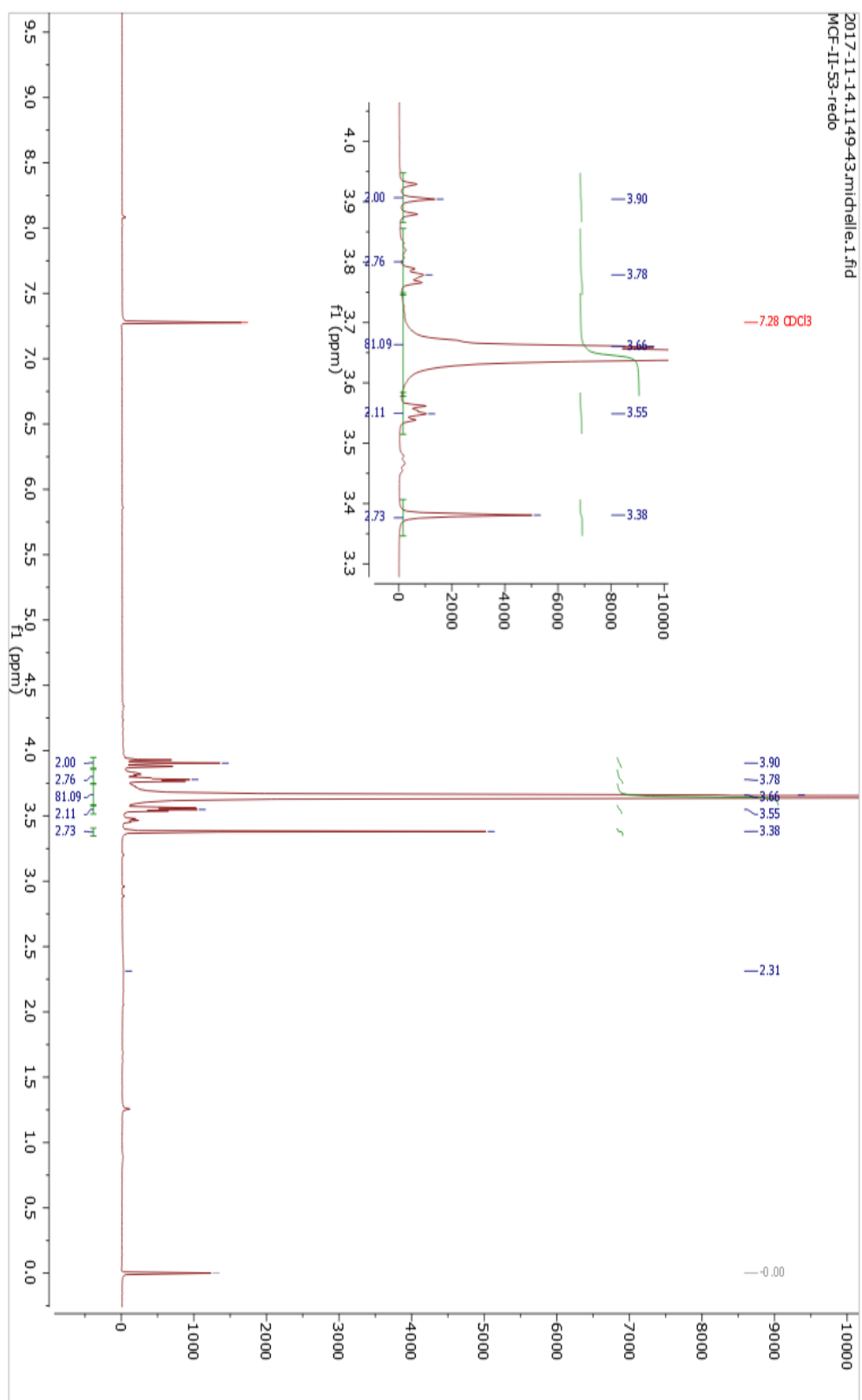
**M1bFE4 (3-4)**
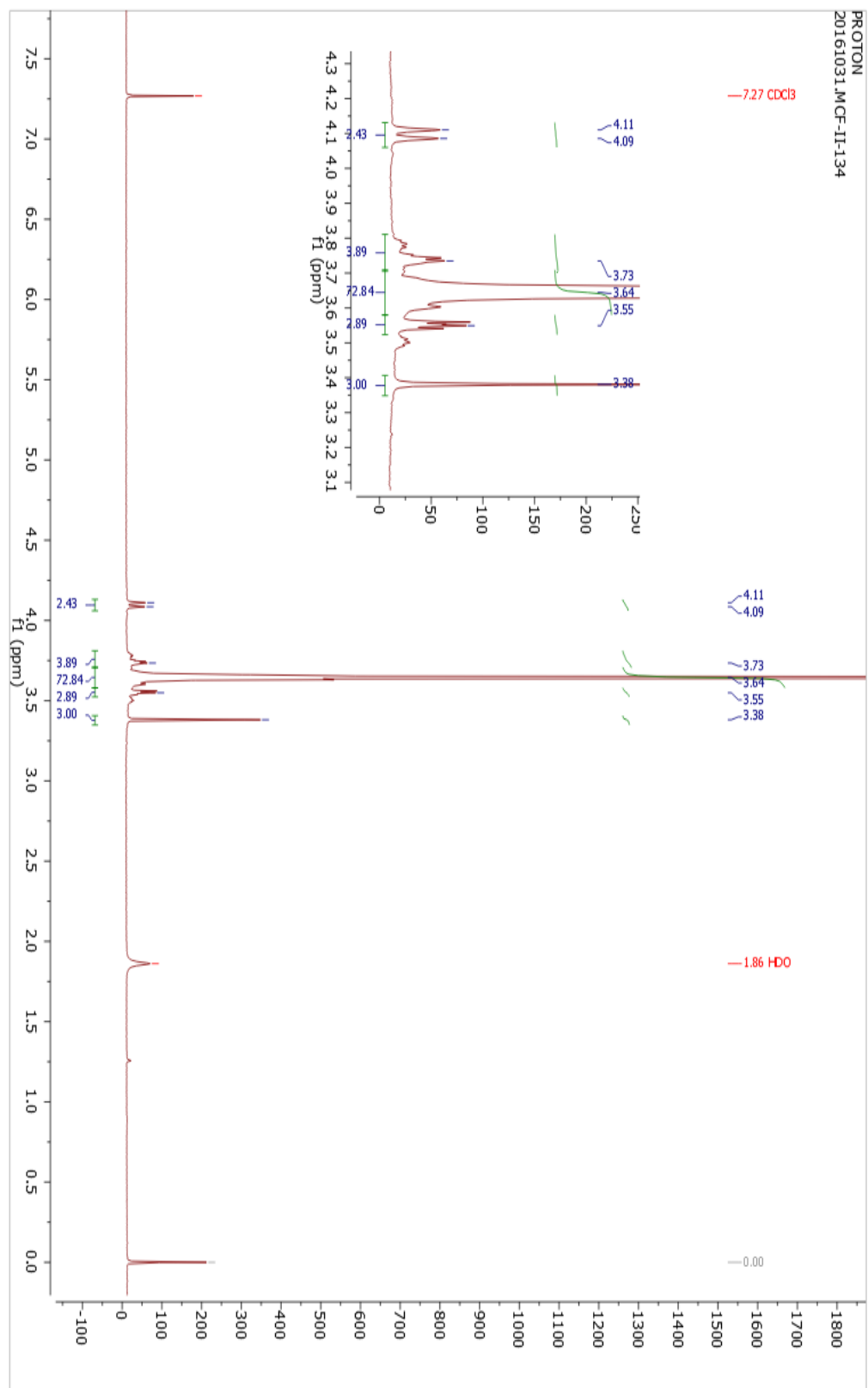
**PCD-OH (4-1)**
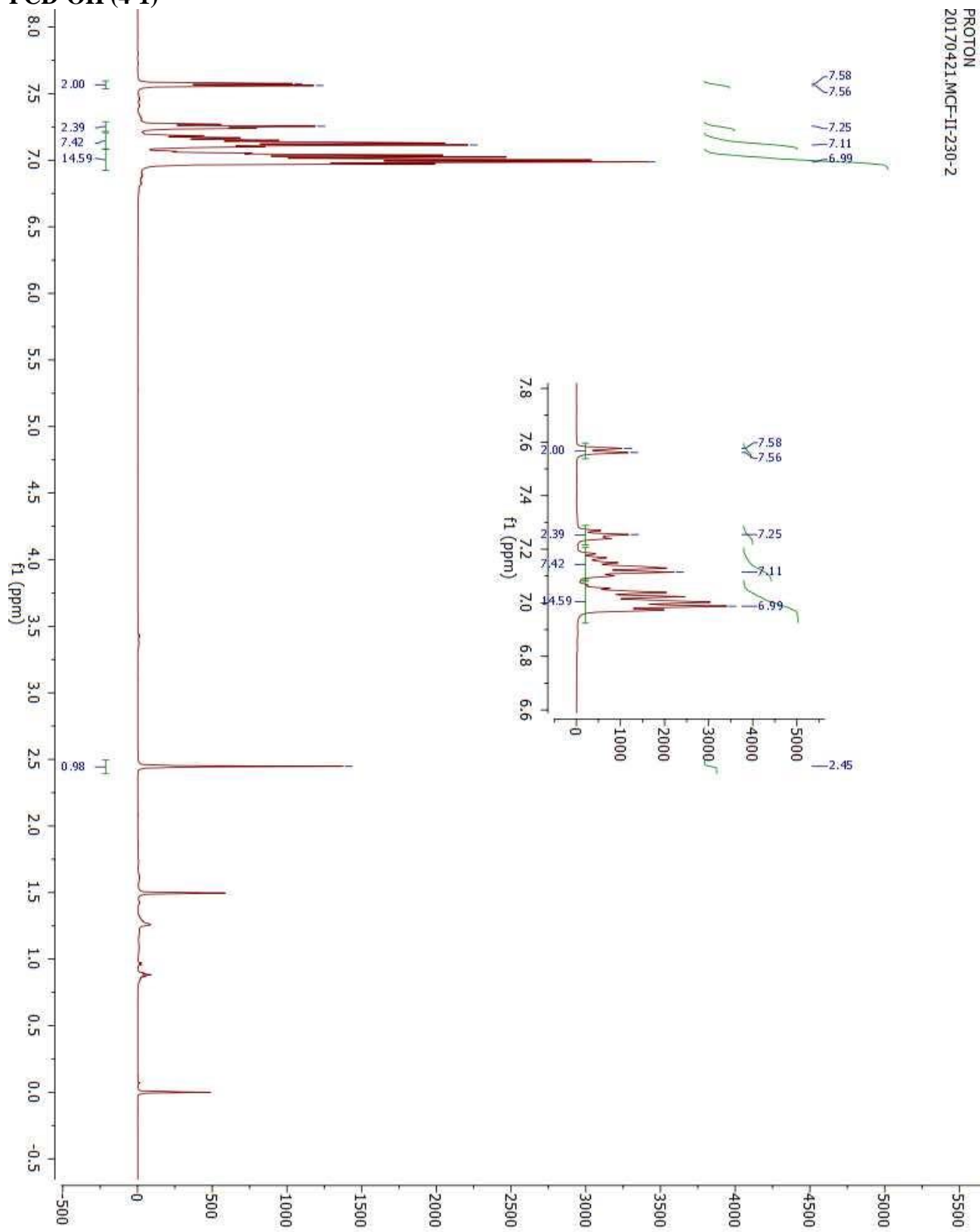
**PCD-OMe (4-2)**
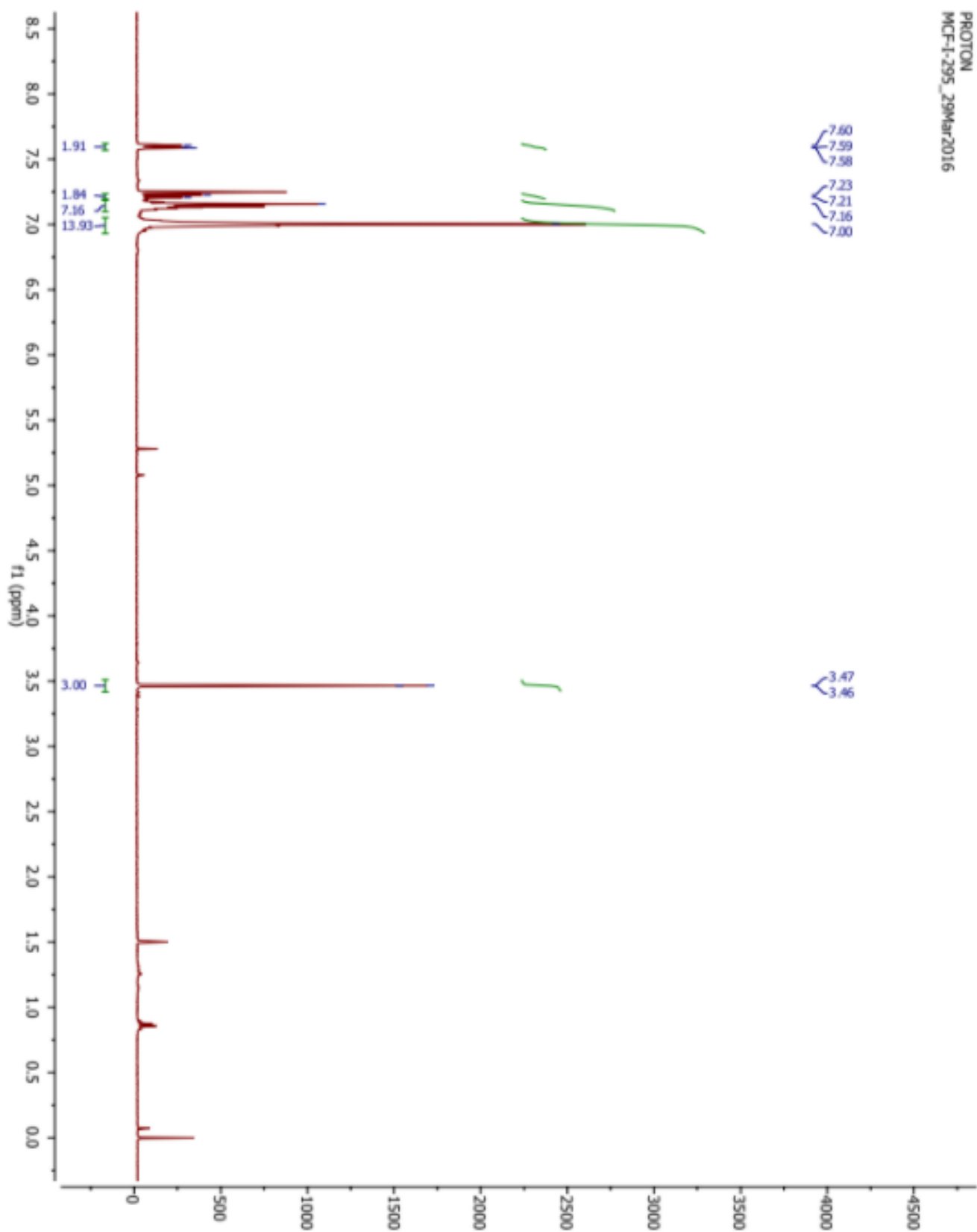
**PCD-O-Cl (4-3)**
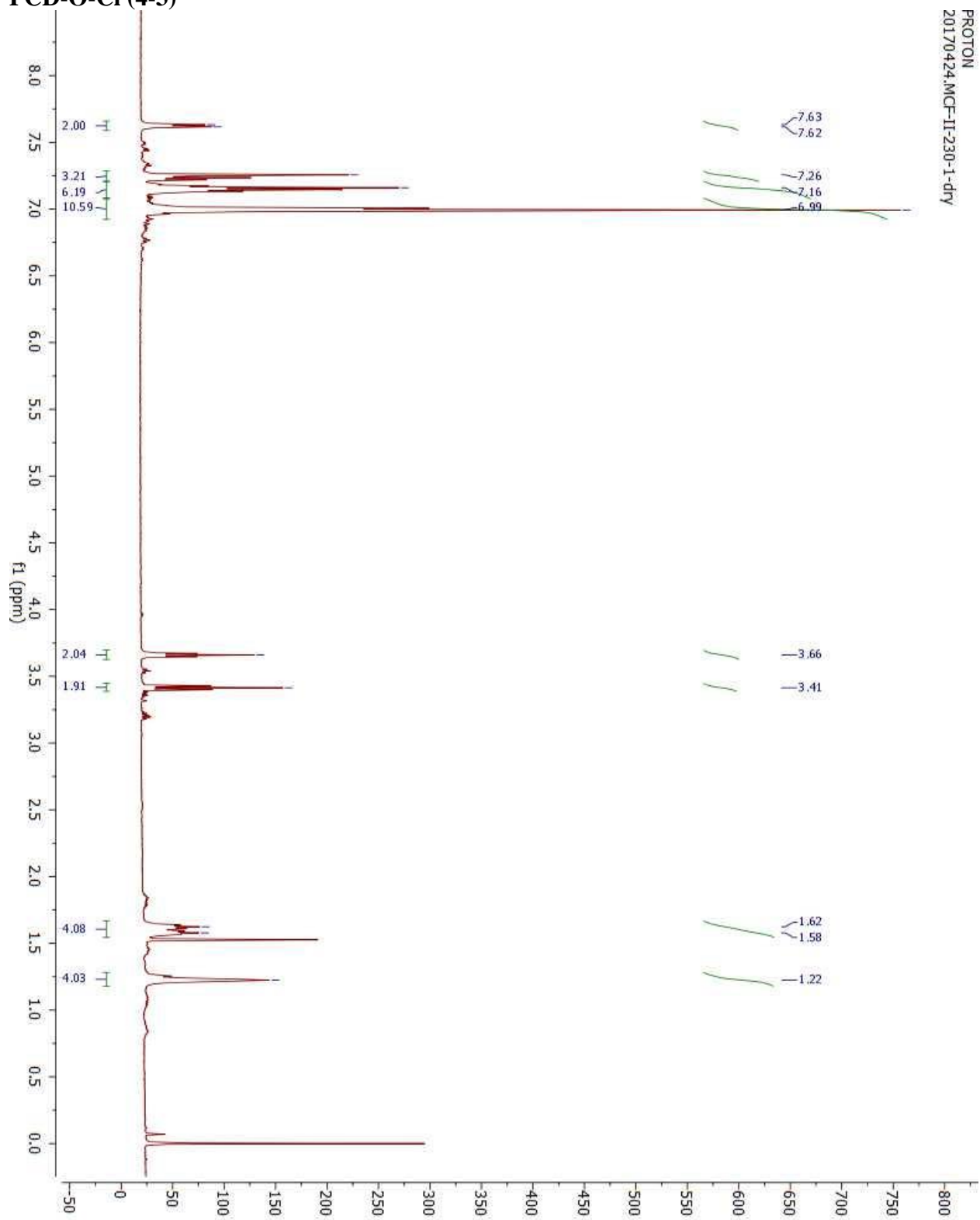
**PCD-O-Pyr (4-4)**
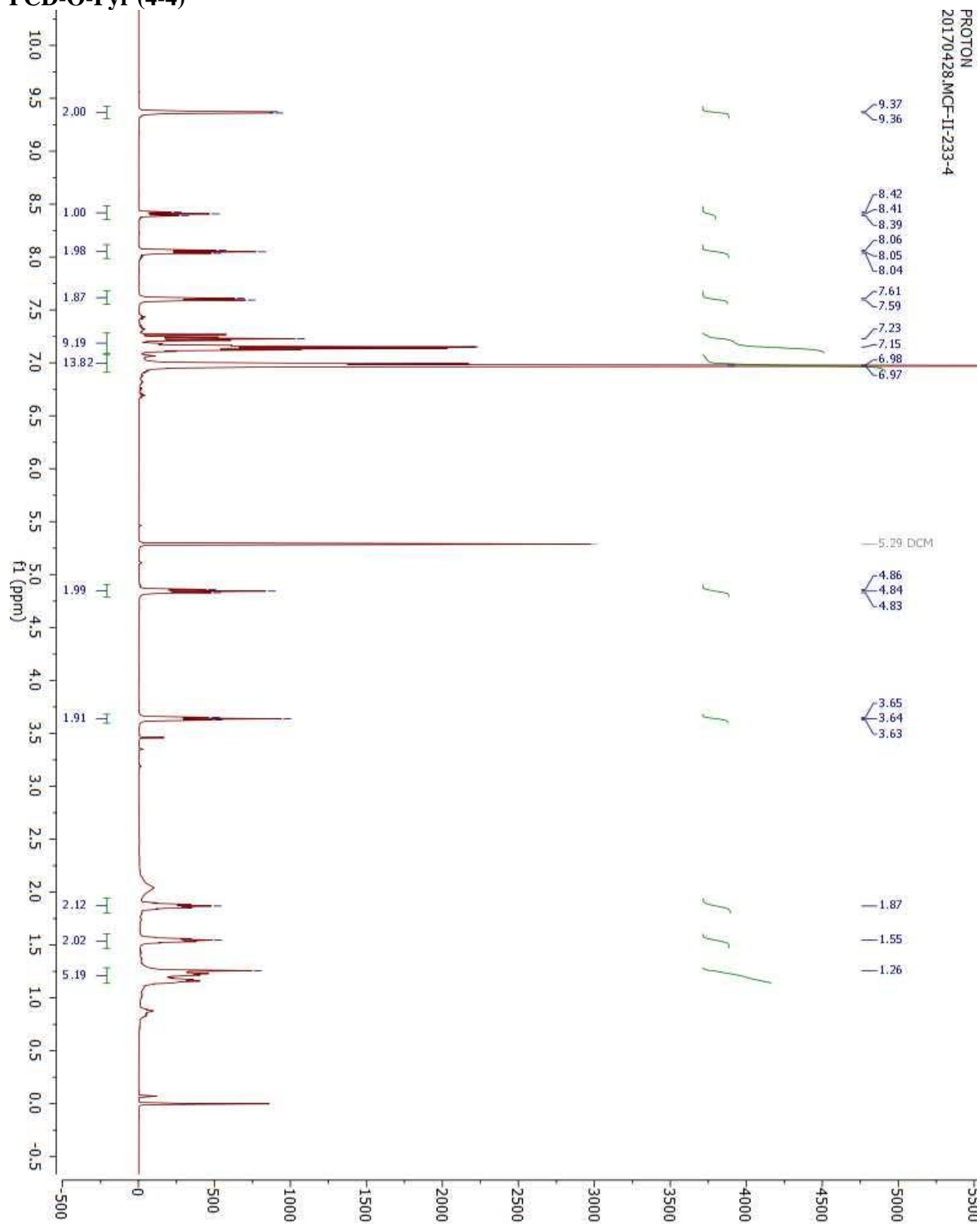
**PMOXA (A1-1)**
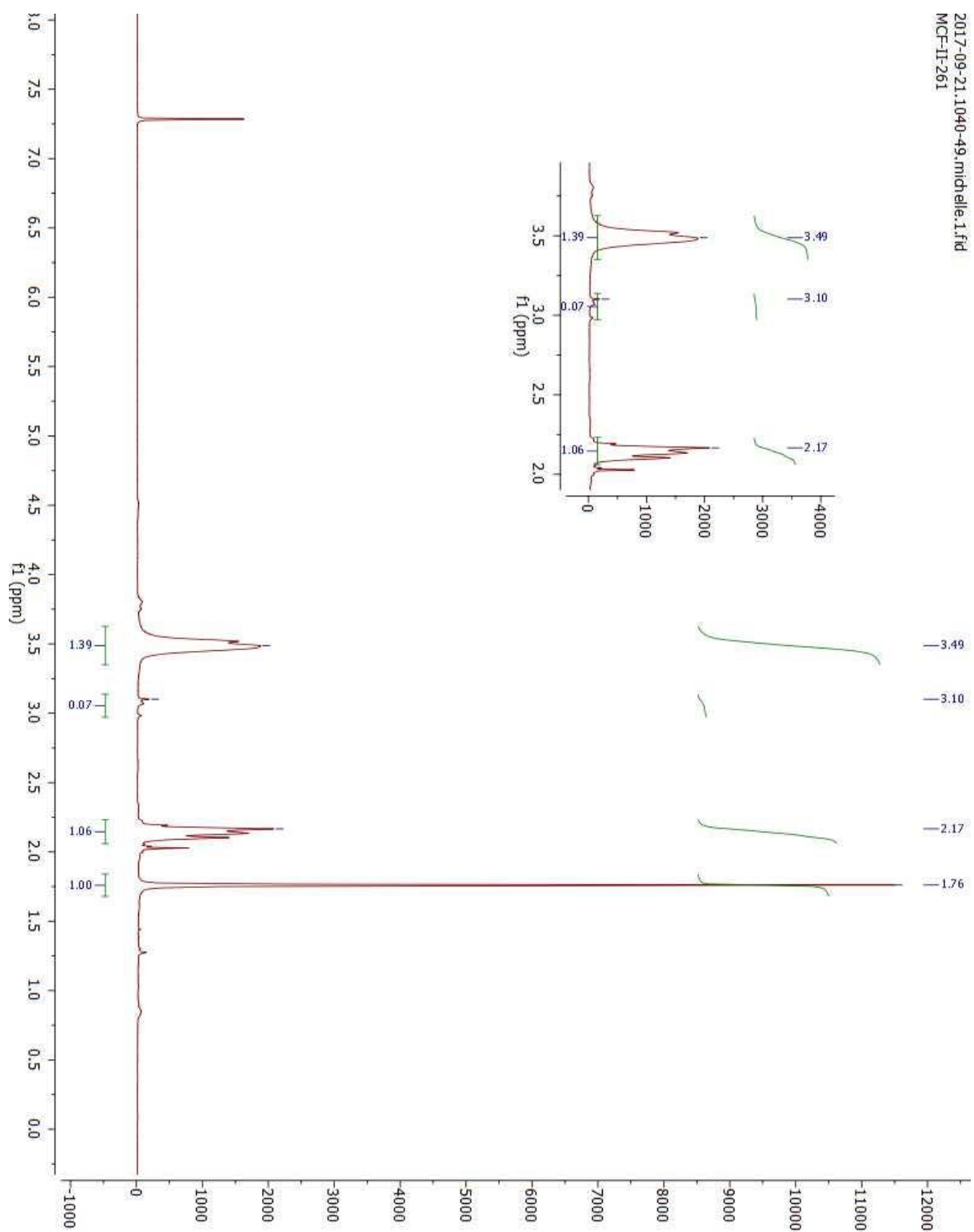
**2-butyl-2-oxazoline (A1-2)**
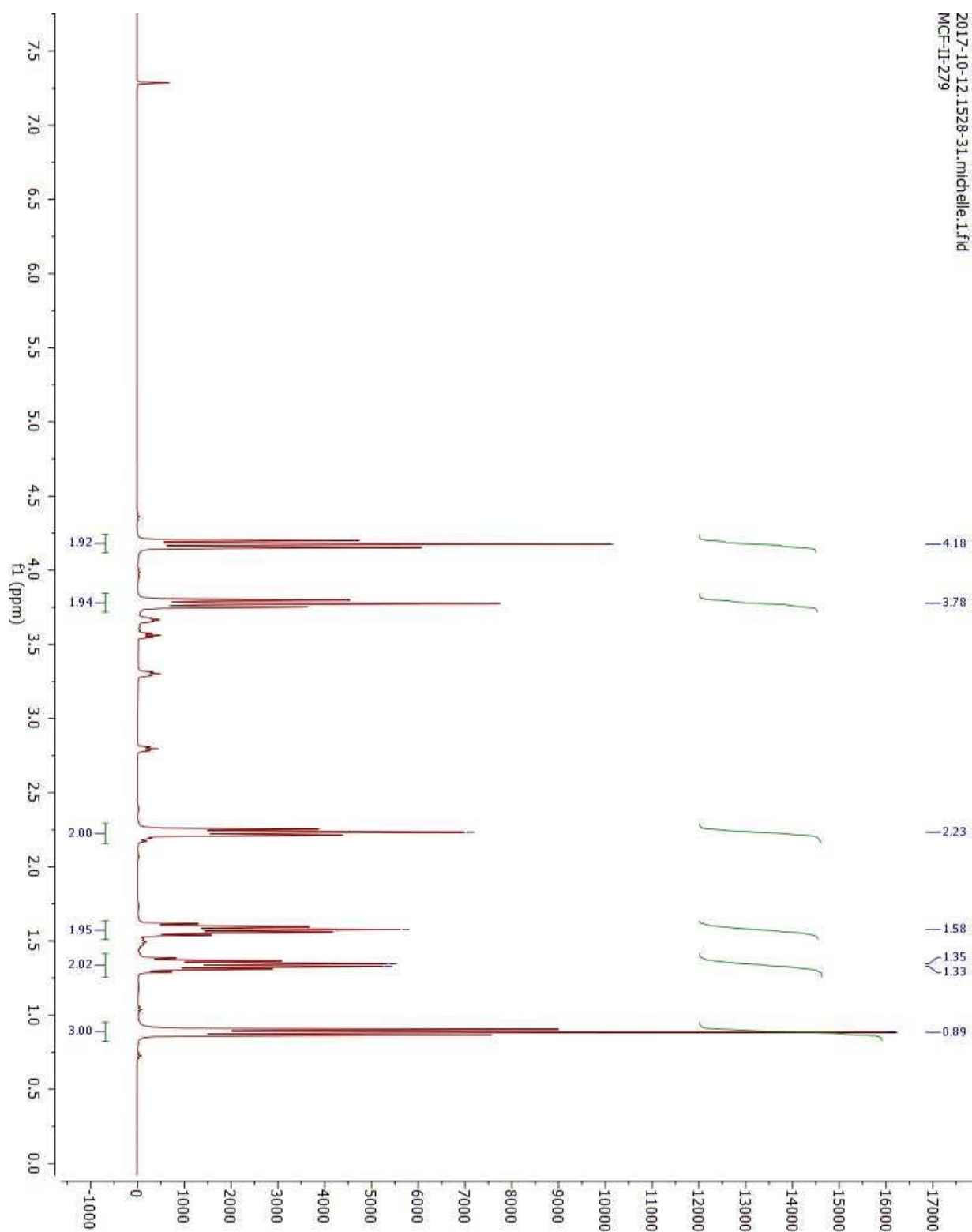
**N-(2-Hydroxyethyl)-2-perfluoroethane acidamide (A1-5)**



2017-11-06.1250-4.michelle.1.fid
MCF-II-287-water
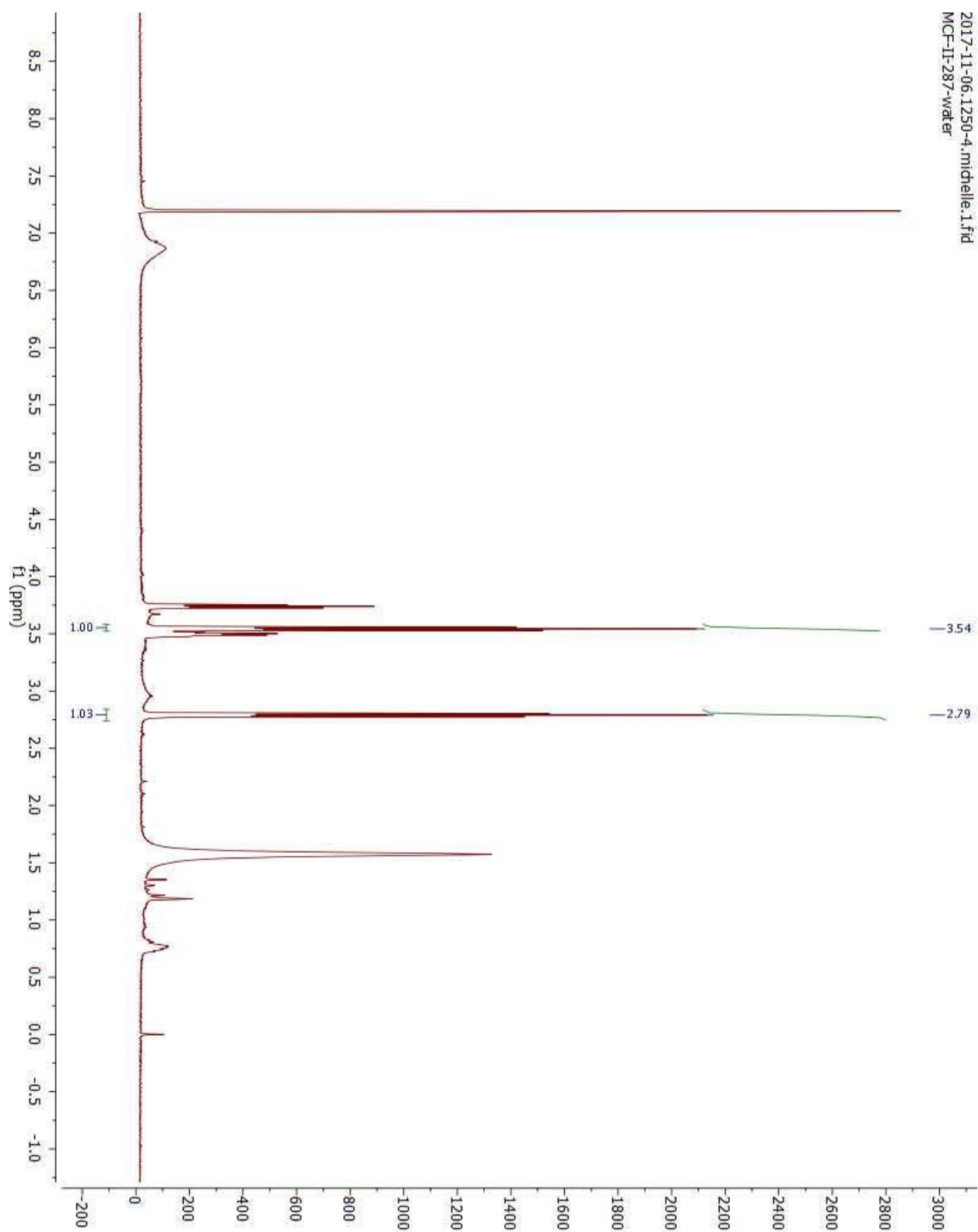
**2-perfluoroethyl-2-oxazoline (A1-9)**
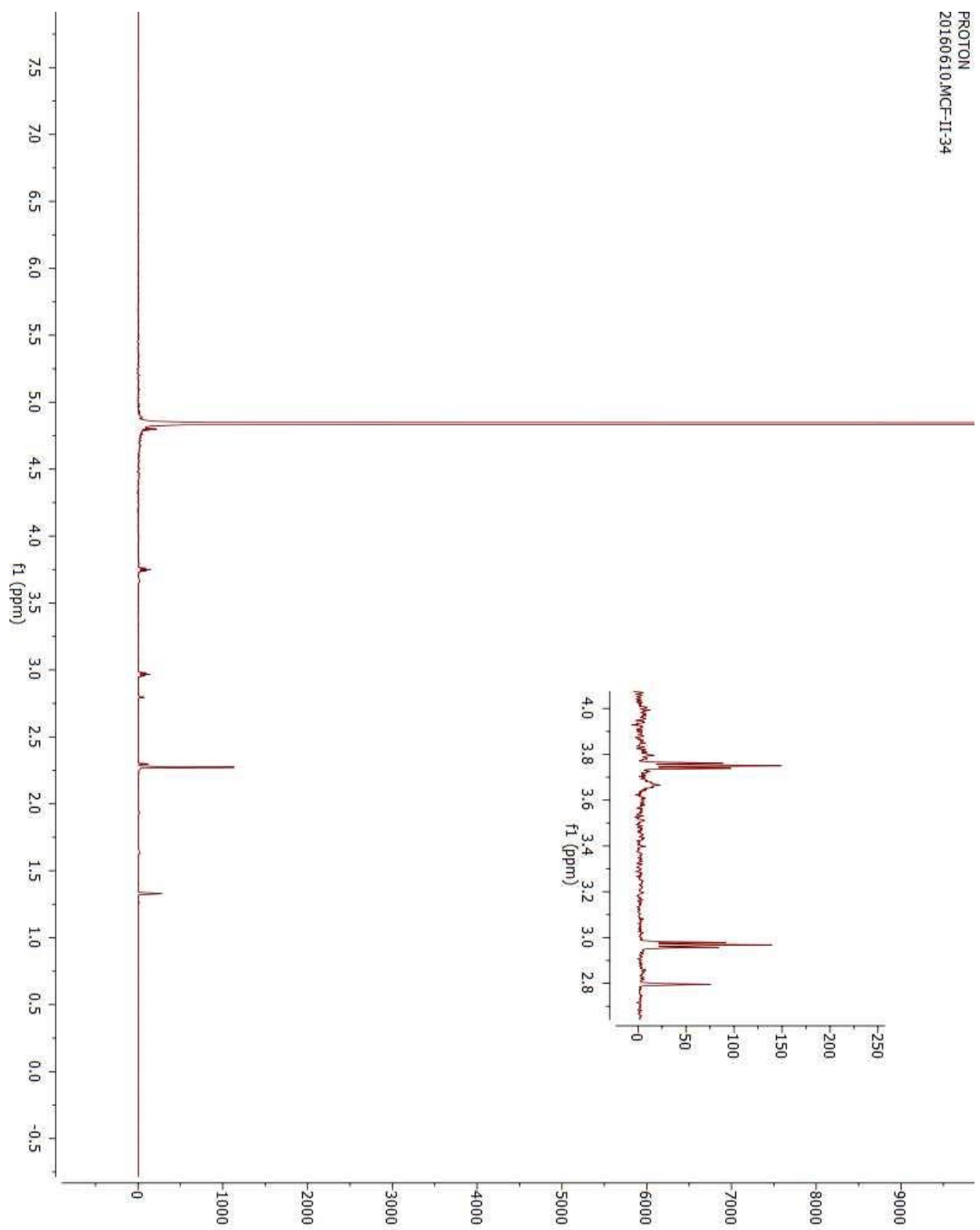
*A2.5 <sup>13</sup>C-NMR*

**3-bromo-2-bromomethyl-2-methylpropyl acetate (2-2)**
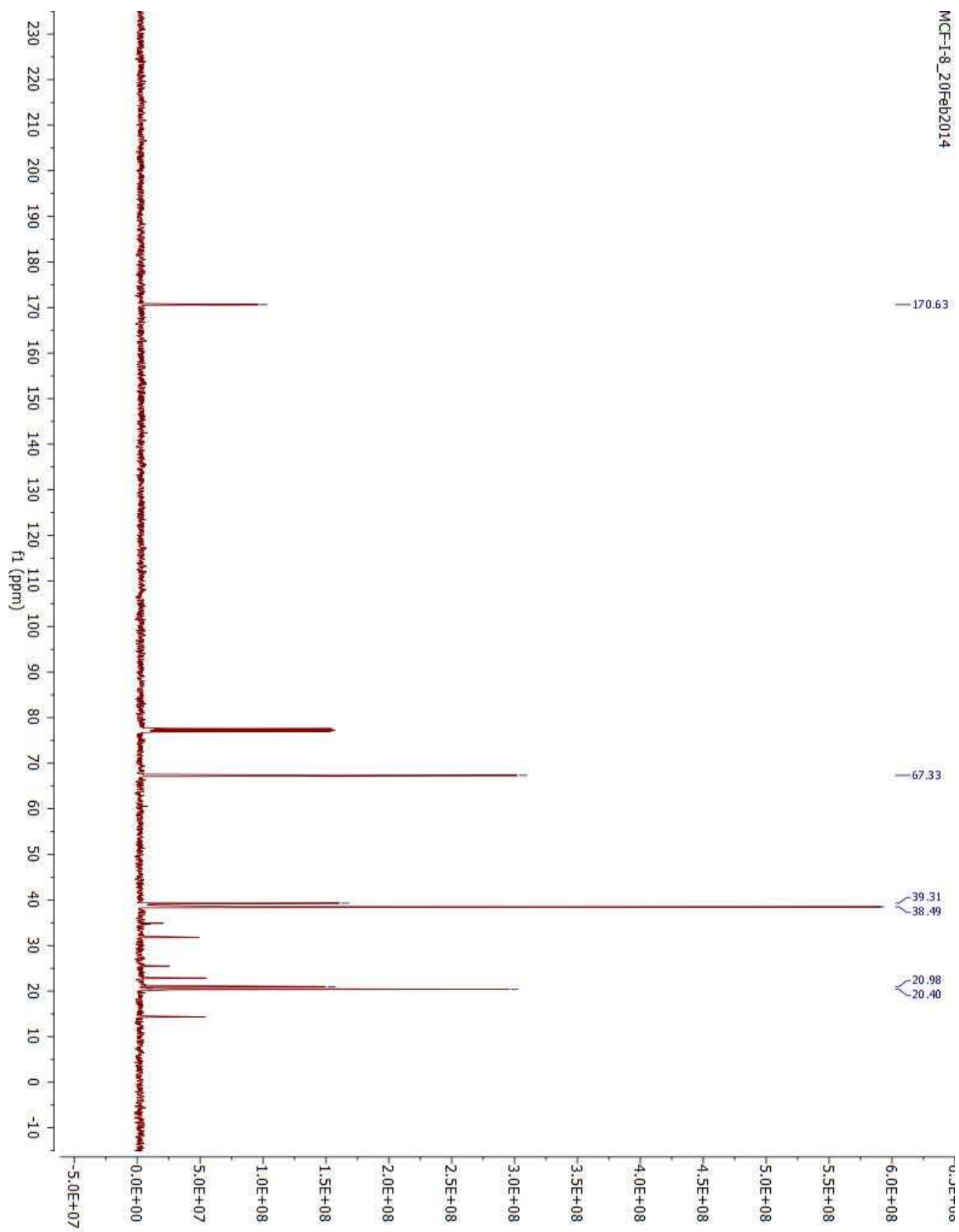
**3-(bromomethyl)-3-methyloxetane (2-3)**
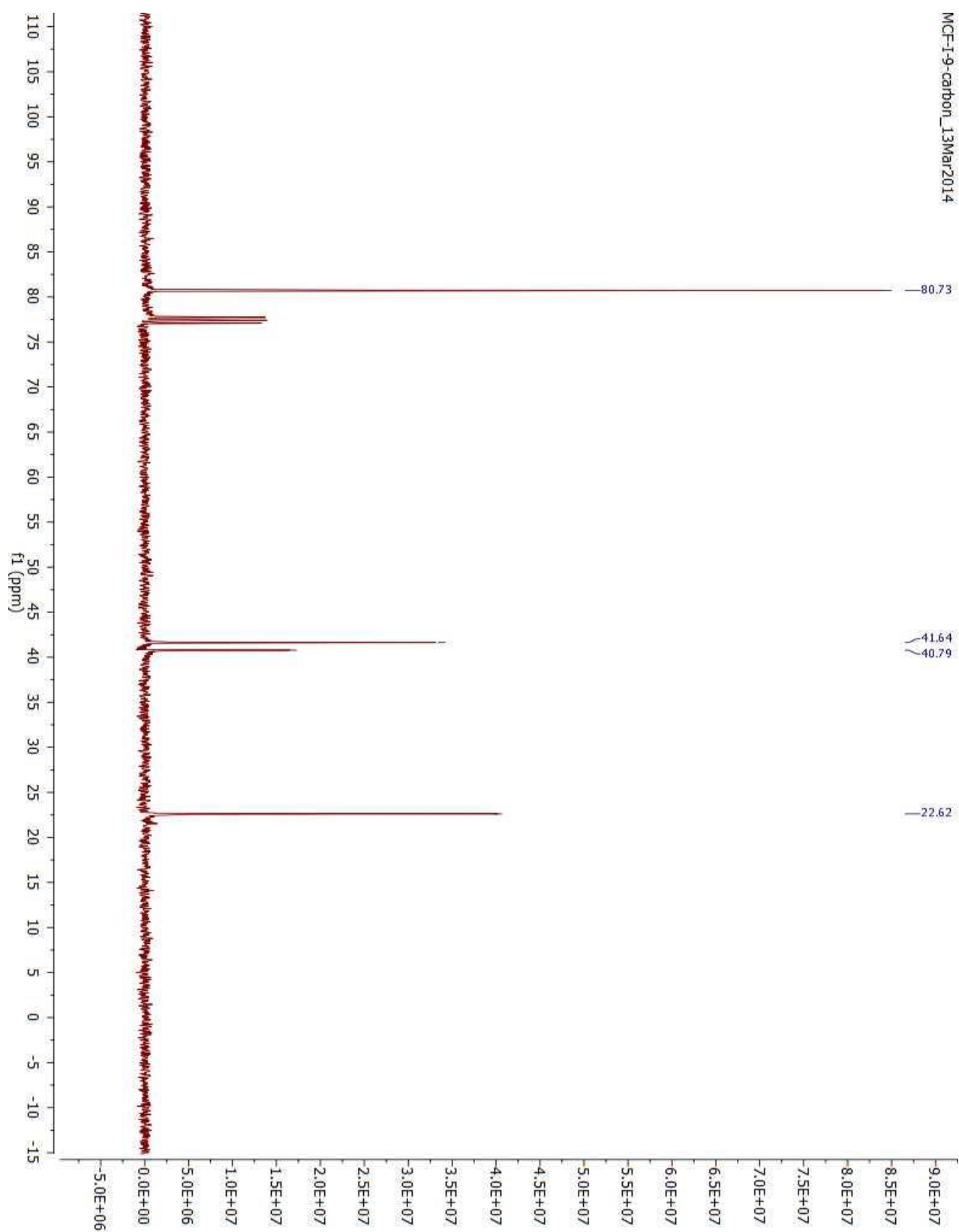
**3-(1H,1H-perfluoropropan-1-oxymethyl)-3- methyloxetane (2-4)**
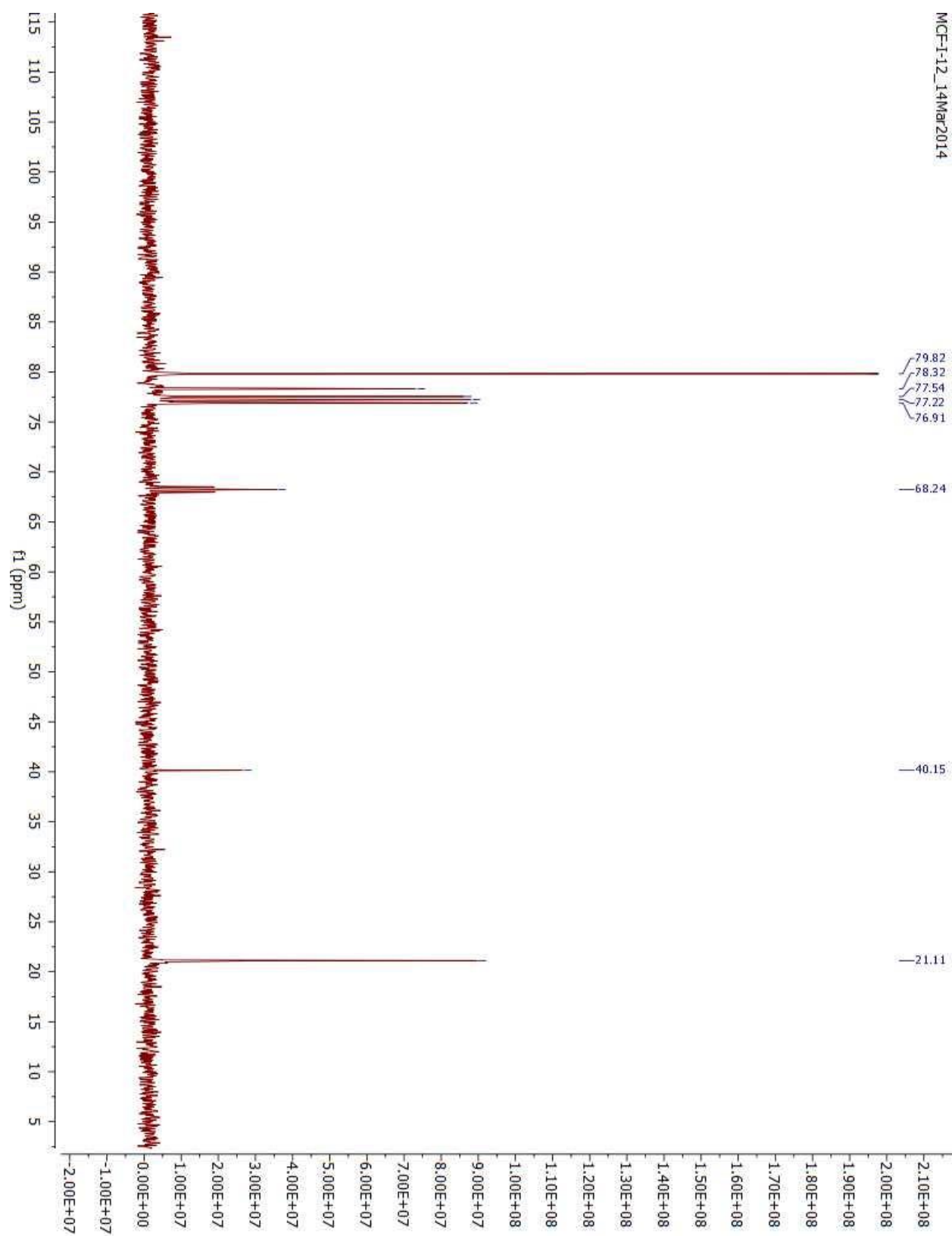
**2-butyl-2-oxazoline (A1-2)**
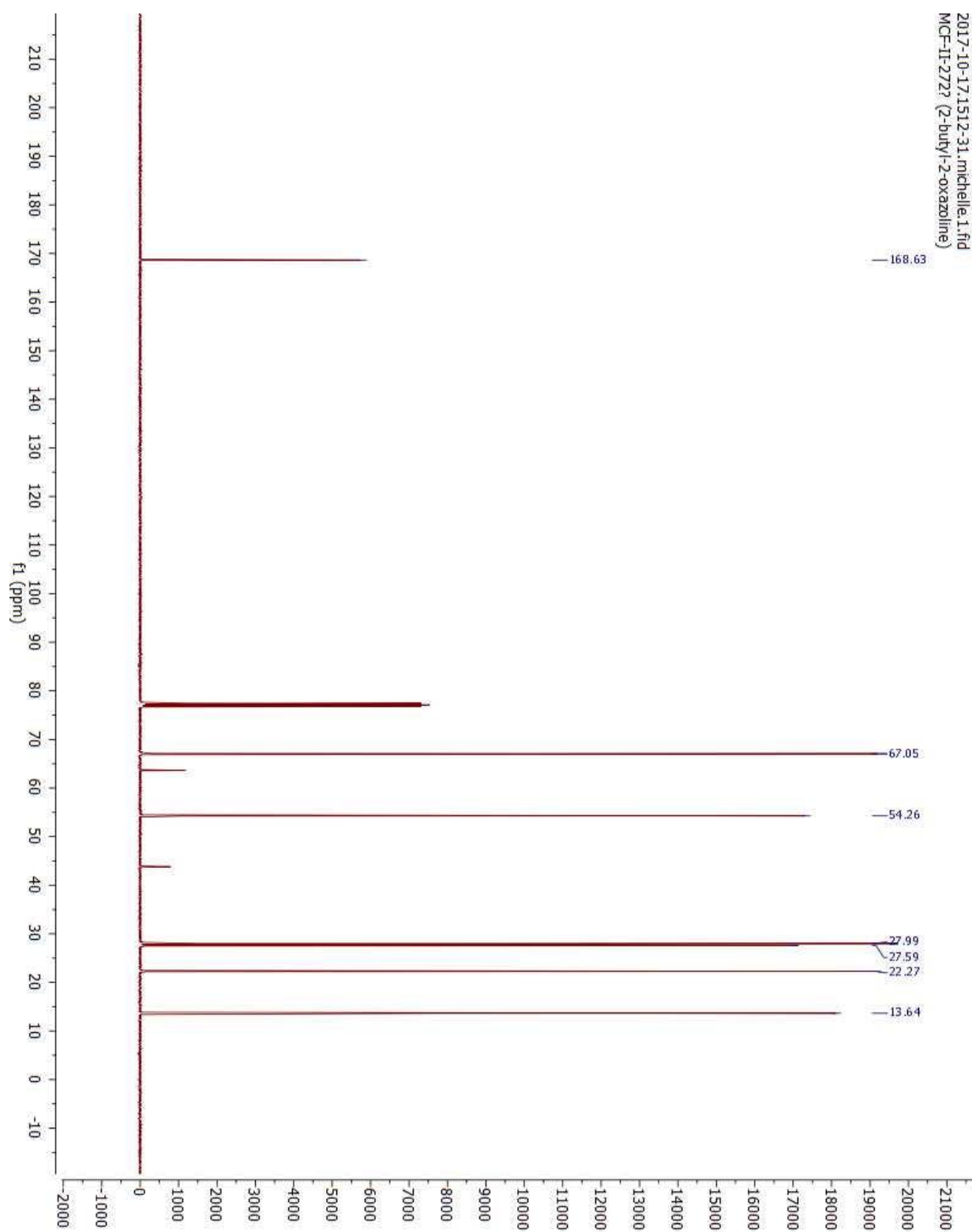
## A2.6 $^{19}$F-NMR

## 3-(1H,1H-perfluoropropan-1-oxymethyl)-3- methyloxetane (2-4)
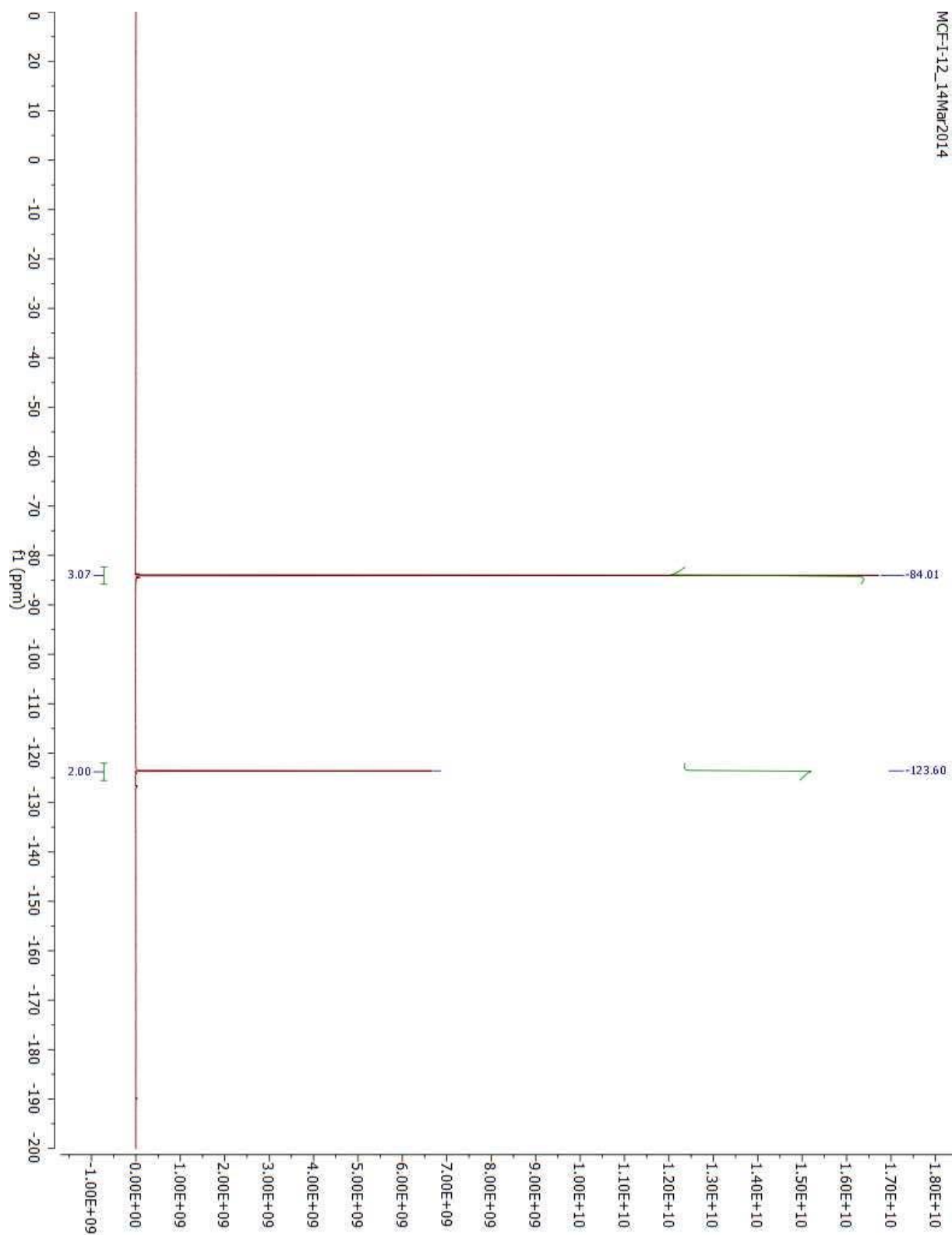
**M1(F2Ox)n (2-5)**

# M5(F2Ox)ₙ (2-6)

**M1FE2 (3-2)**



FLUORINE
20160926.MCF-II-100

-77.69
-77.71
-77.73
-77.74
-77.75
-77.77
-77.79
-80.88
-80.89
-80.91
-83.43

-88.56
-88.57

-126.45

2.08
3.23
2.00
4.92

2.73

88.45  -88.50  -88.55  -88.60  -88.65  -88.70
f1 (ppm)

-41611.49
-41619.70
-41624.50
-41629.48
-41637.59
-41643.66
-41656.55
-41669.22

4.92

77.60  -77.65  -77.70  -77.75  -77.80  -77.85
f1 (ppm)

2.08

-36528.35
-36538.25
-36547.55
-36551.14
-36555.00
-36564.27
-36574.09

f1 (ppm)
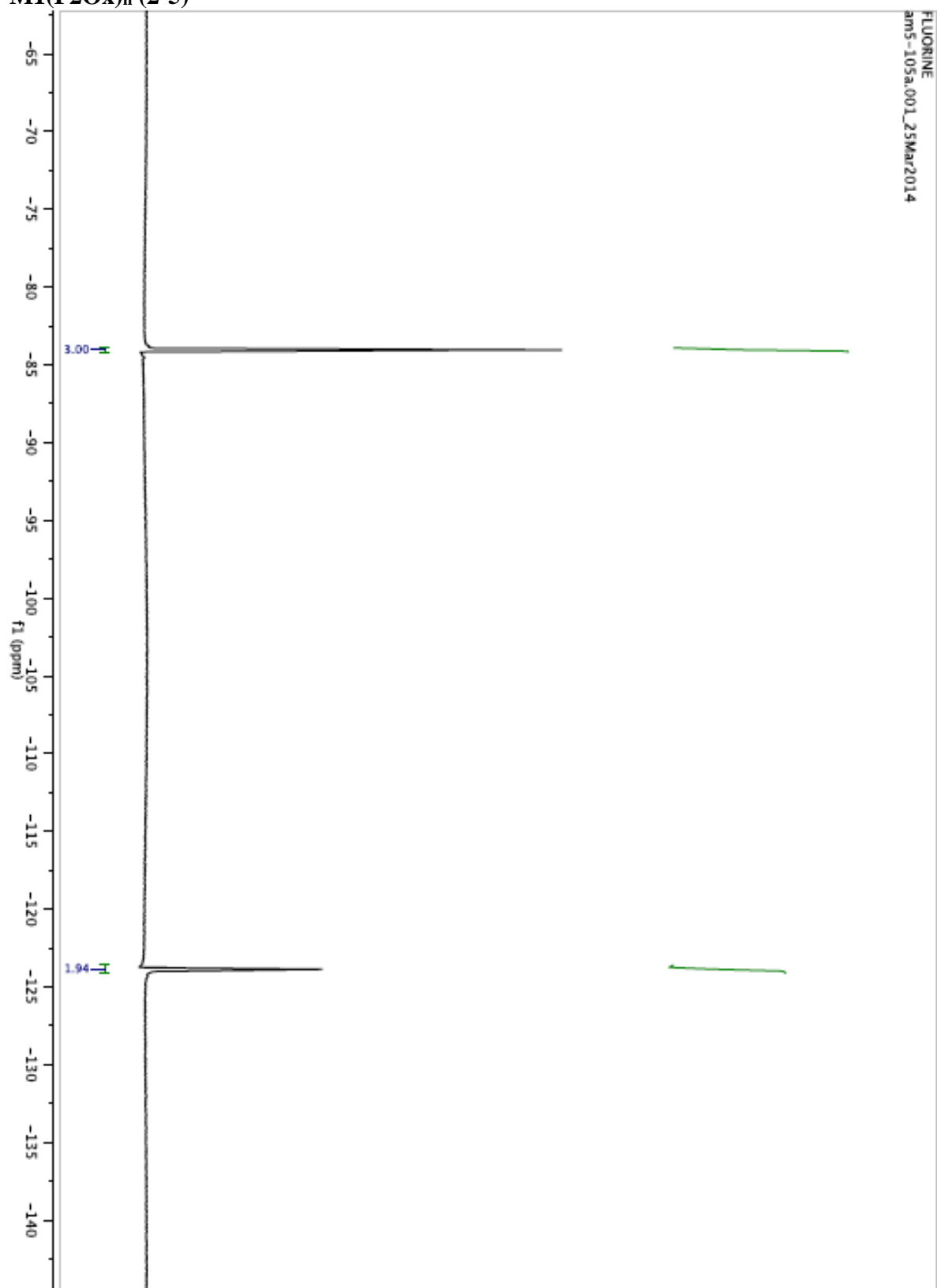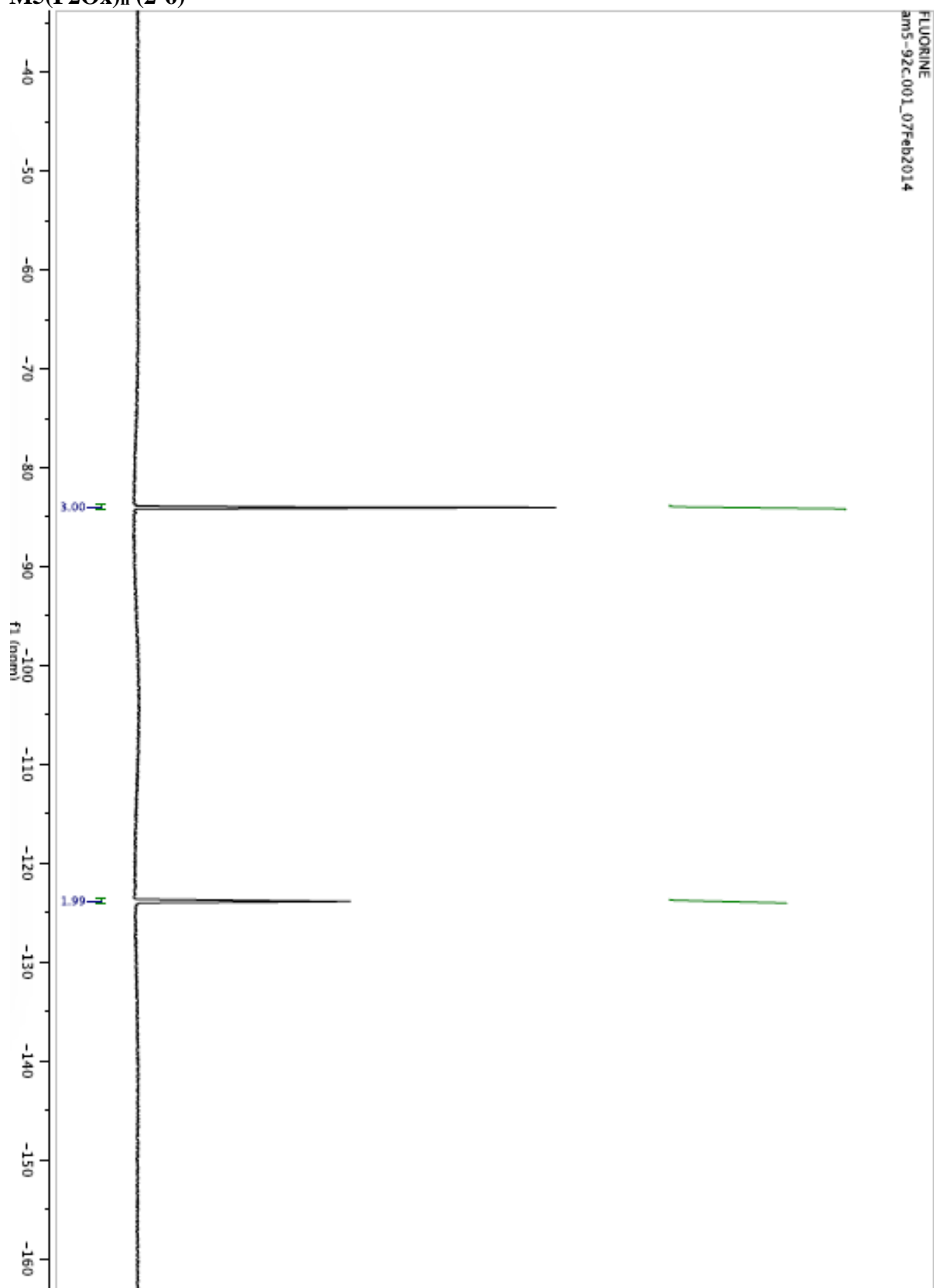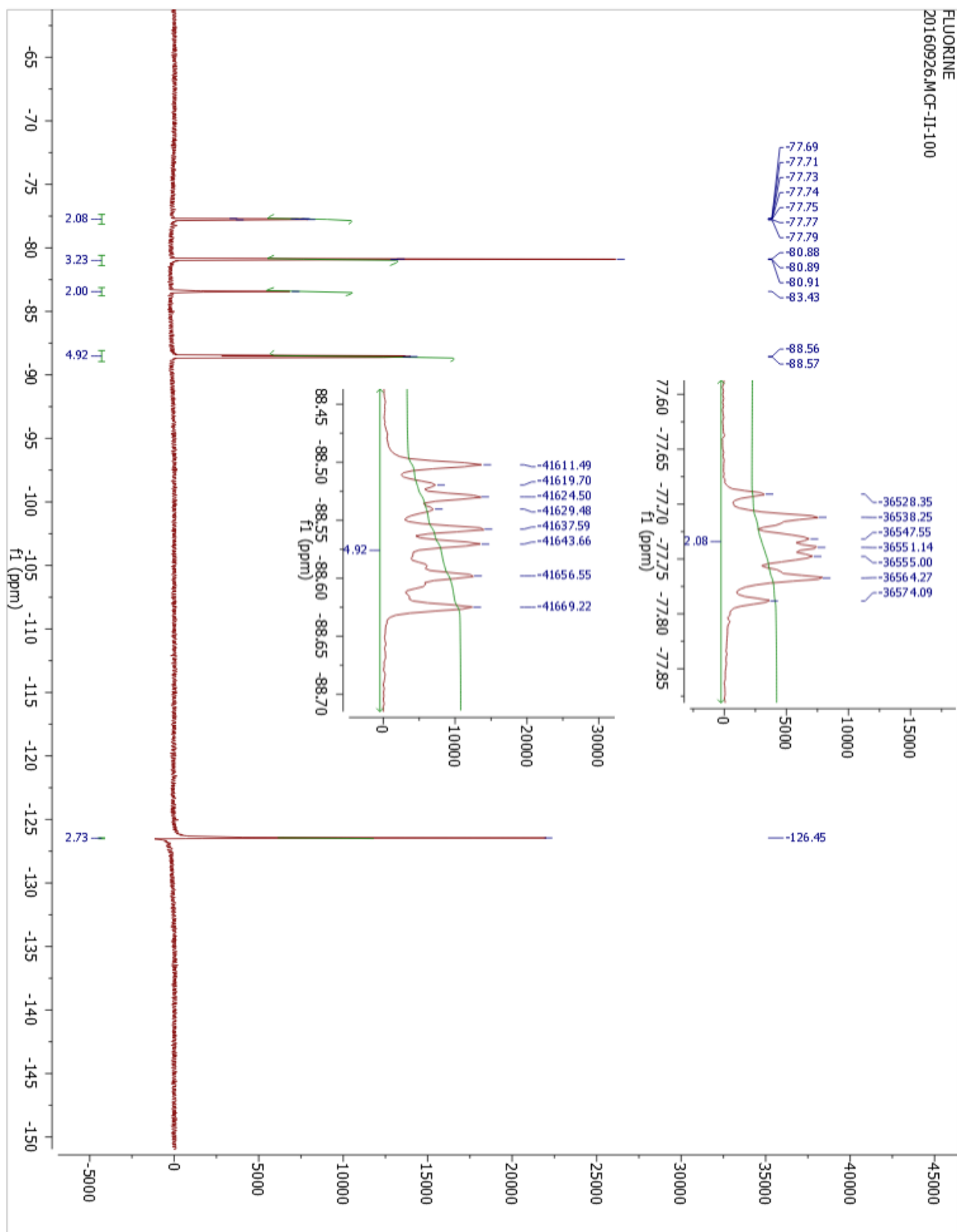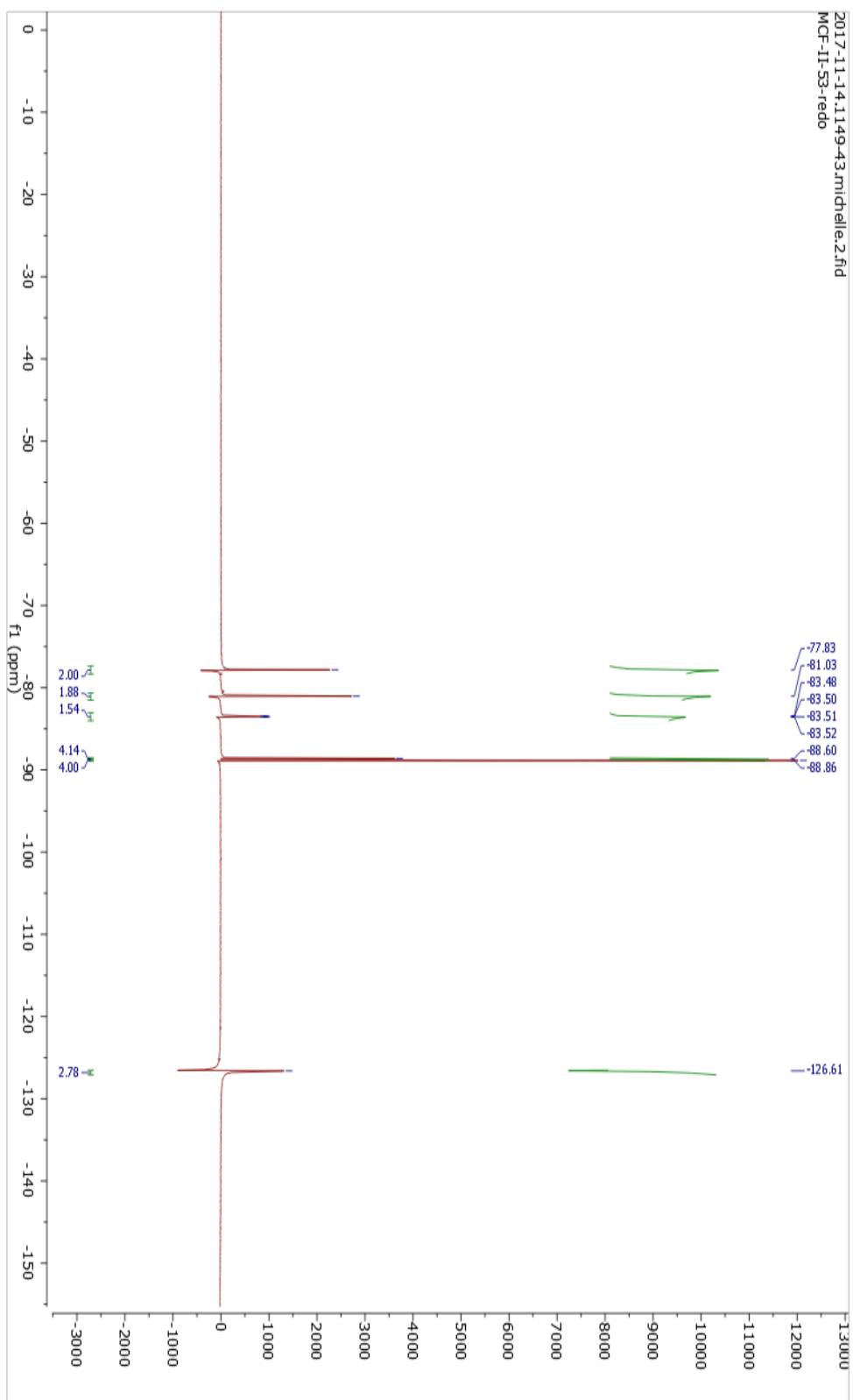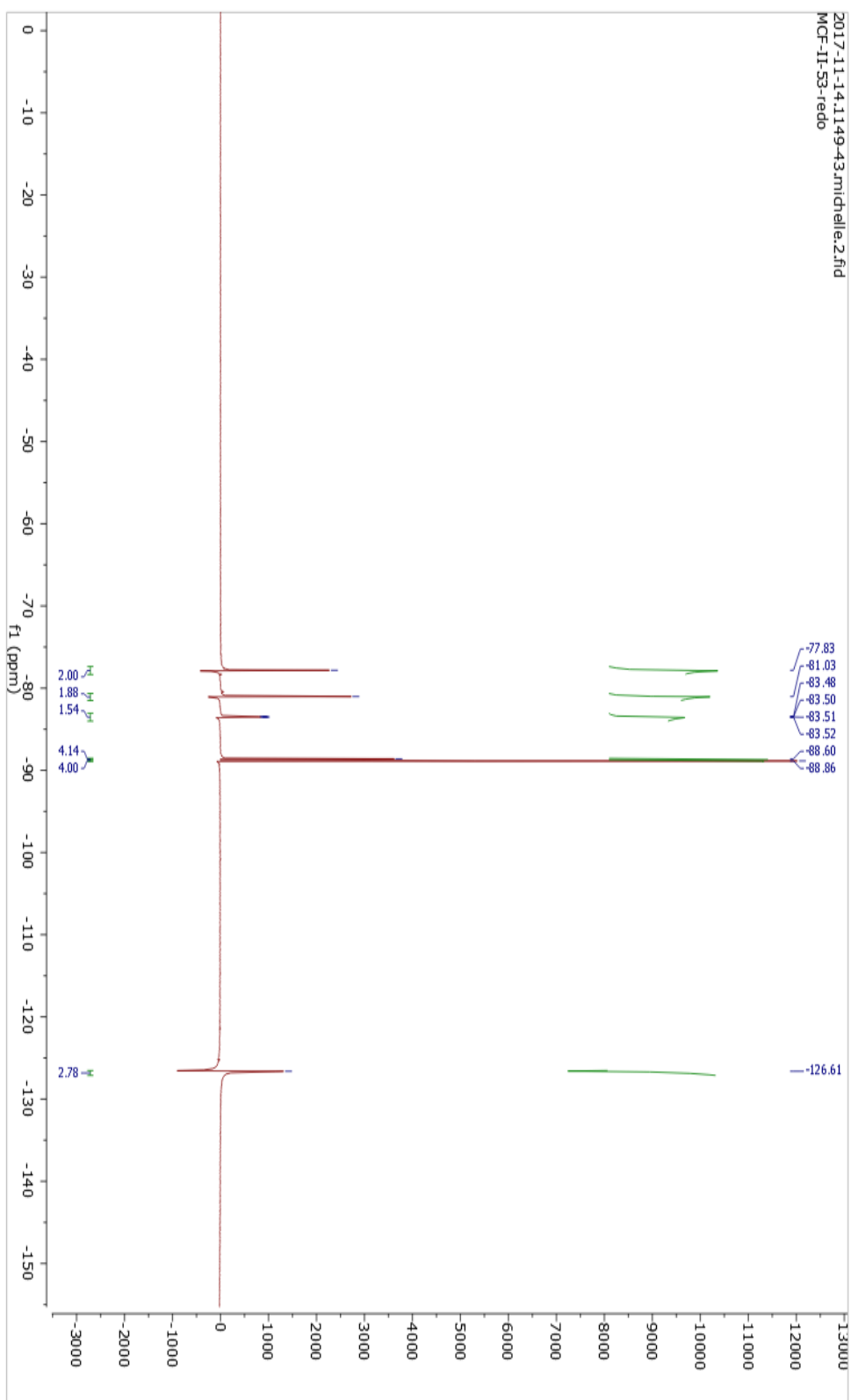
**M1FE3 (3-3)**

**M1bFE4 (3-4)**

**2-perfluoroethyl-2-oxazoline (A1-9)**
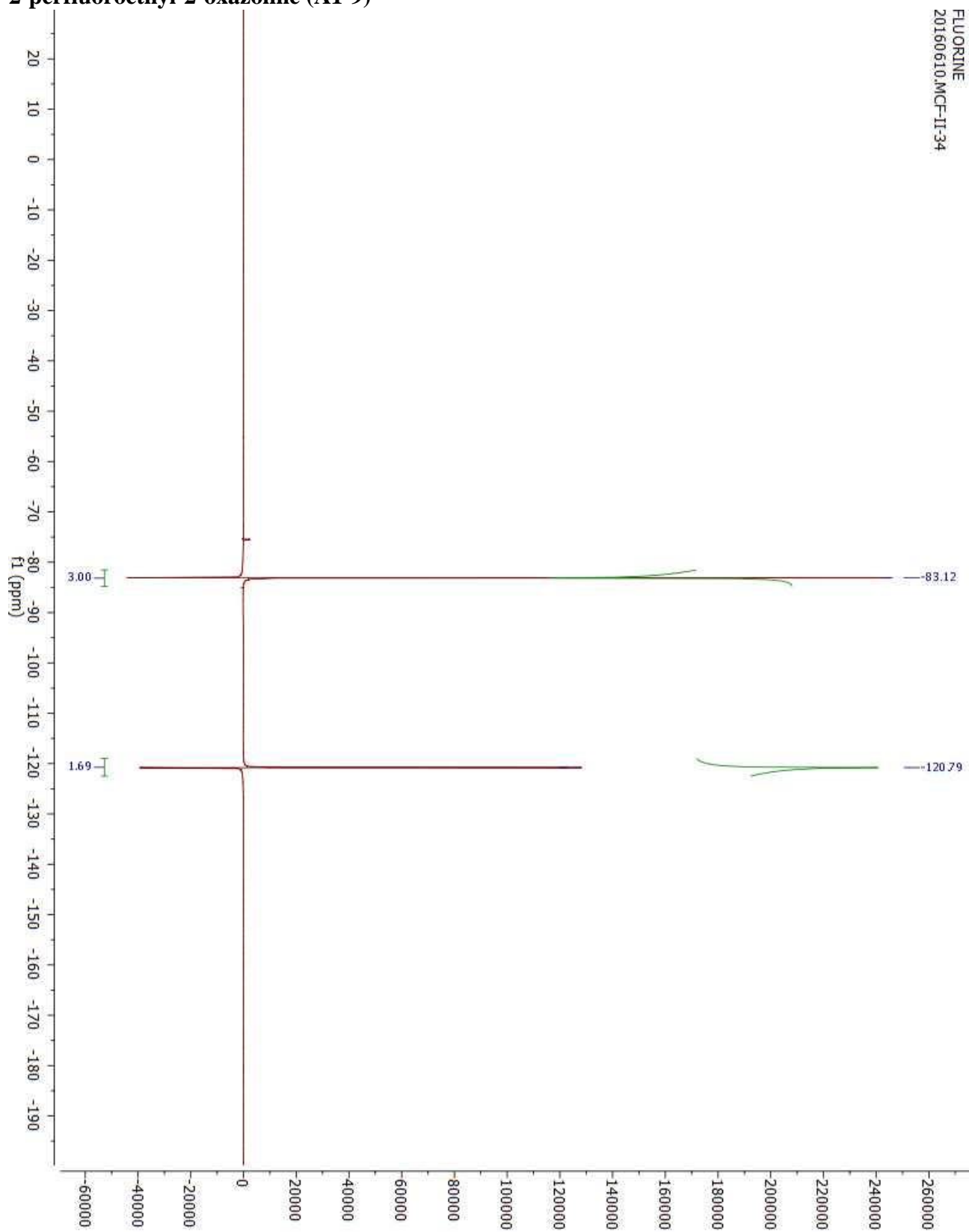
*A2.7 HPLC*

**M1(F2Ox)ₙ**
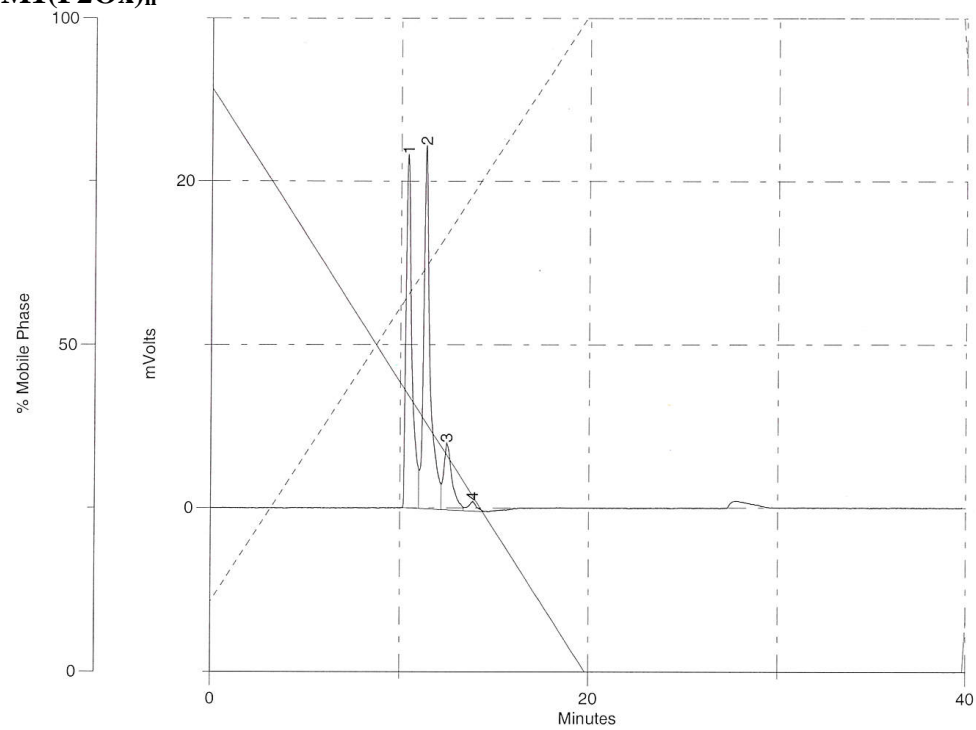


**M5(F2Ox)ₙ**
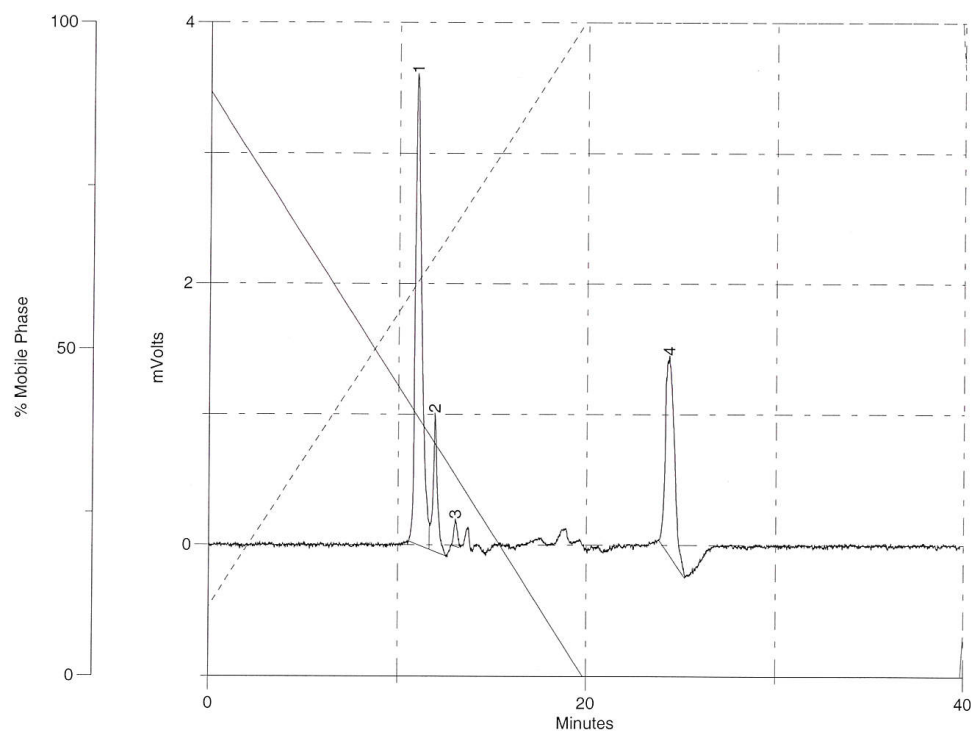
**M1FE2 (3-2)**
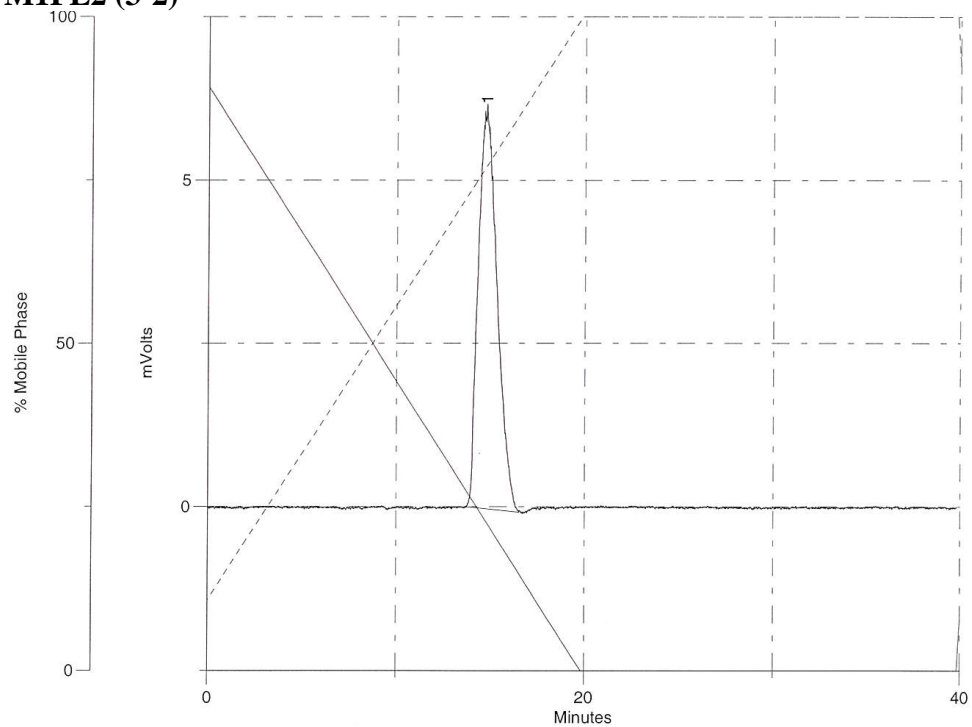


**M1FE3 (3-3)**
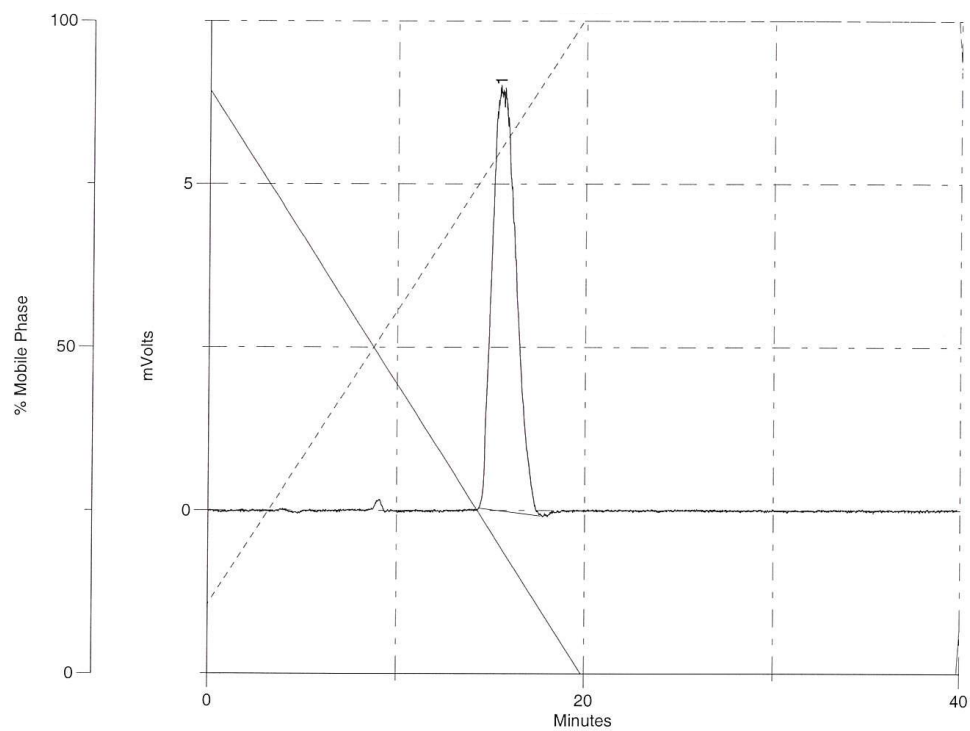
**M1bFE4 (3-4)**
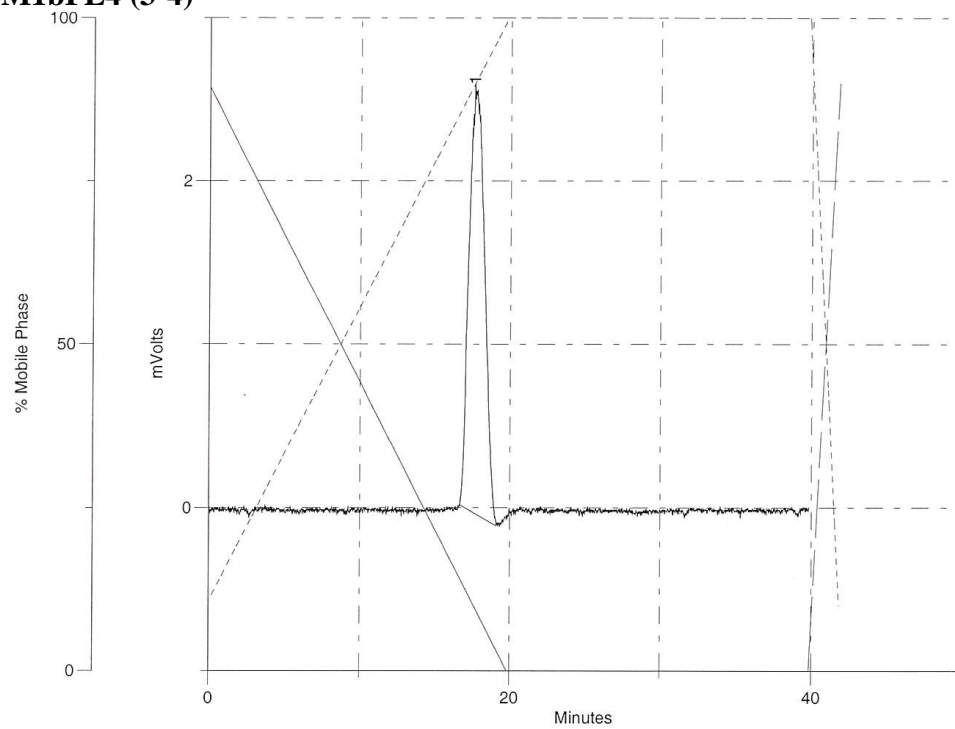
## *A2.8 DLS: Micelle Particle Size*

### M1(F2Ox)$_{3-4}$
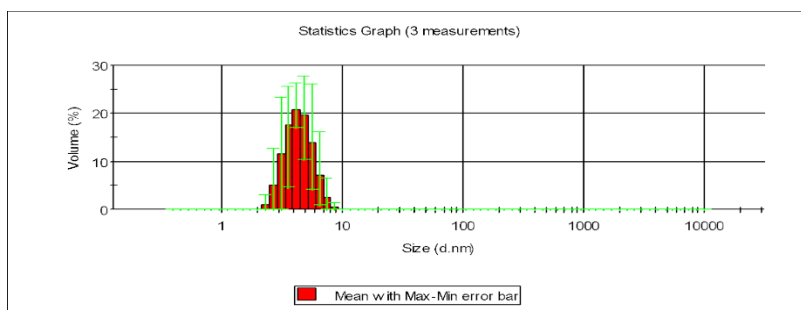


### M1(F2Ox)$_{4-5}$
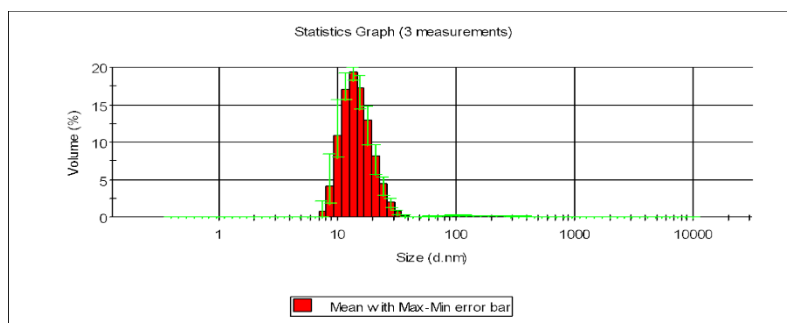


### M1(F2Ox)$_{7-9}$
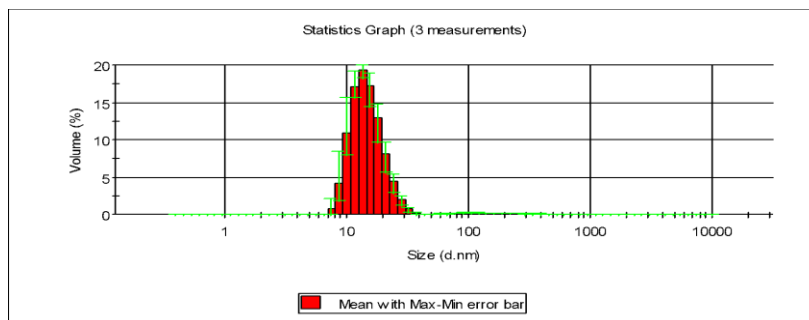


### M5(F2Ox)$_{3-5}$
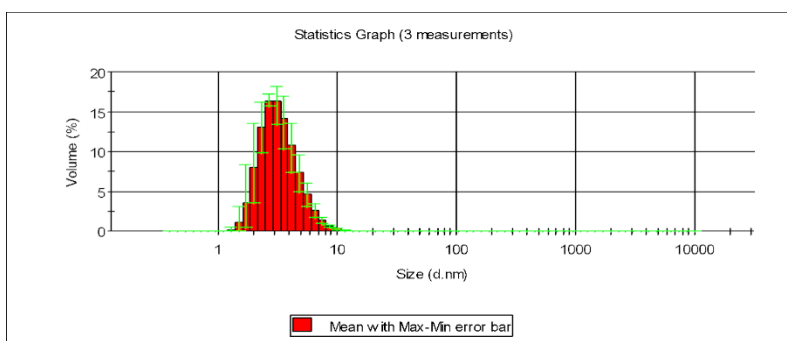
**M5(F2Ox)<sub>6-7</sub>**
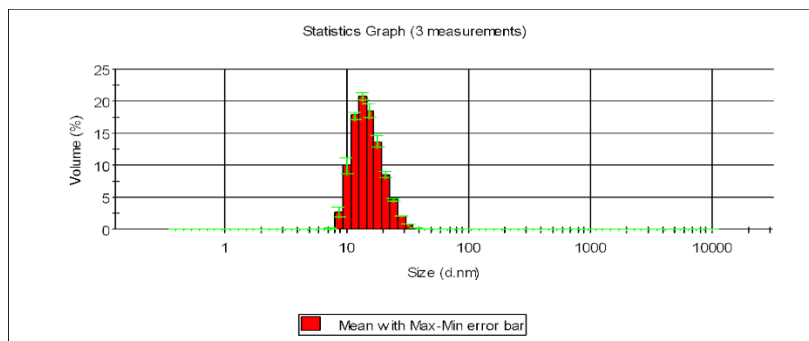


**M5(F2Ox)<sub>8-10</sub>**
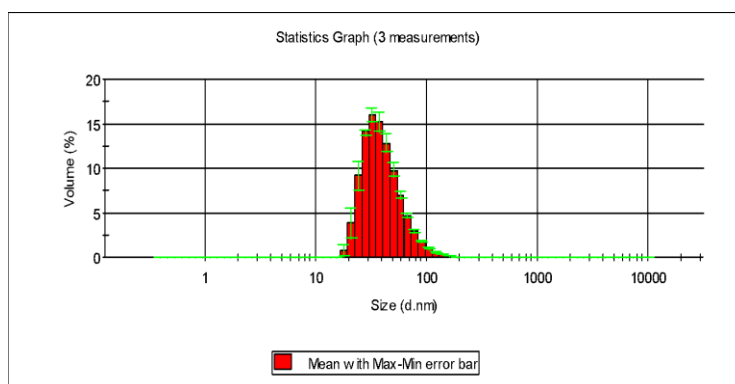


**M1FE2 (3-2)**
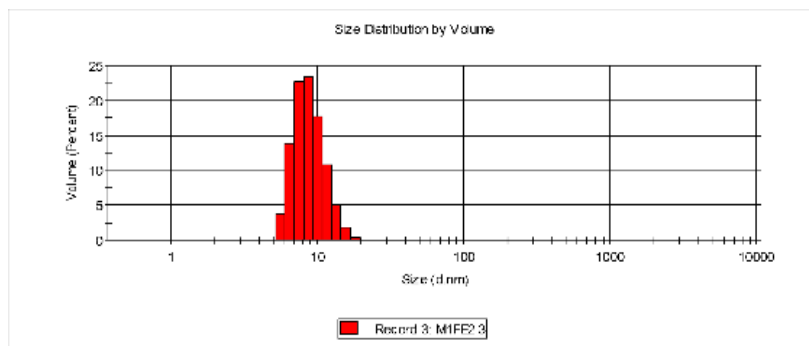
**M1FE3 (3-3)**
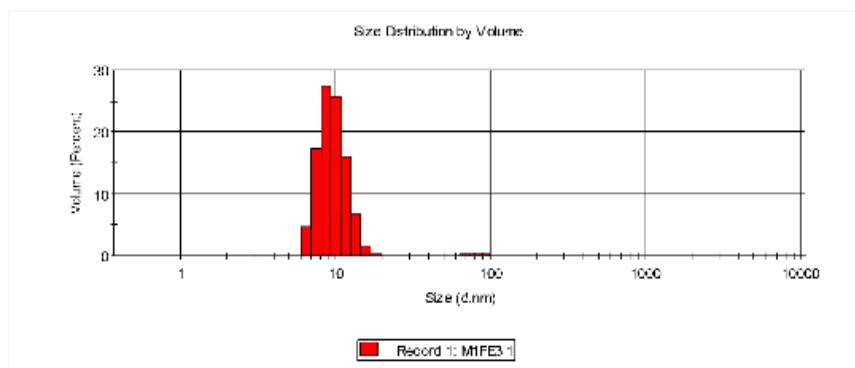


**M1bFE4 (3-4)**
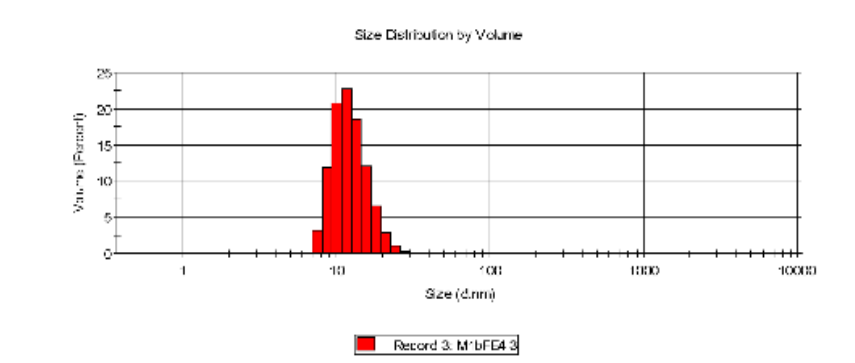
*A2.9 CMC data*

**M1(F2Ox)₃₋₄**

| Log(M) | Ave. Surface Tension (mN/m) | Std. Dev. |
|---|---|---|
| -3.00 | 26.59 | 0.02 |
| -3.50 | 27.11 | 0.10 |
| -4.00 | 27.72 | 0.10 |
| -4.50 | 28.77 | 0.20 |
| -5.00 | 38.23 | 0.39 |
| -5.50 | 41.33 | 0.08 |
| -6.00 | 60.95 | 0.09 |
| -6.50 | 72.43 | 0.02 |
| -7.00 | 72.80 | 0.03 |
| -7.50 | 72.53 | 0.08 |
| -8.00 | 72.62 | 0.04 |
| -8.50 | 72.92 | 0.04 |
| -9.00 | 72.75 | 0.09 |
| -10.00 | 72.84 | 0.10 |
| -11.00 | 72.76 | 0.11 |
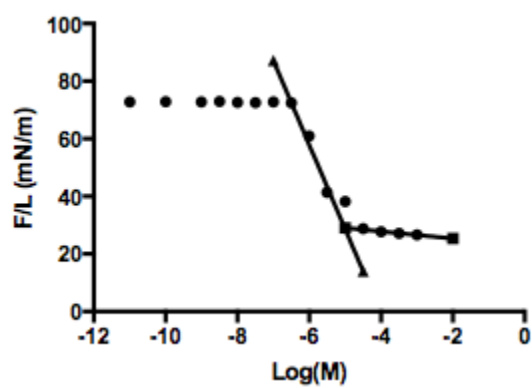


CMC (log(M))=-5.01 ± 0.03

**M1(F2Ox)₄₋₅**

| Log(M) | Ave. Surface Tension (mN/m) | Std. Dev. |
|--------|------------------------------|-----------|
| -3.00  | 23.56 | 0.10 |
| -3.50  | 23.43 | 0.12 |
| -4.00  | 23.96 | 0.24 |
| -4.50  | 25.64 | 0.15 |
| -5.00  | 32.00 | 0.30 |
| -5.50  | 41.81 | 0.13 |
| -6.00  | 53.08 | 0.61 |
| -6.50  | 65.75 | 0.34 |
| -7.00  | 72.52 | 0.18 |
| -7.50  | 73.48 | 0.19 |
| -8.00  | 73.16 | 0.04 |
| -8.50  | 72.78 | 0.17 |
| -9.00  | 73.61 | 0.22 |
| -10.00 | 73.18 | 0.27 |
| -11.00 | 73.29 | 0.18 |
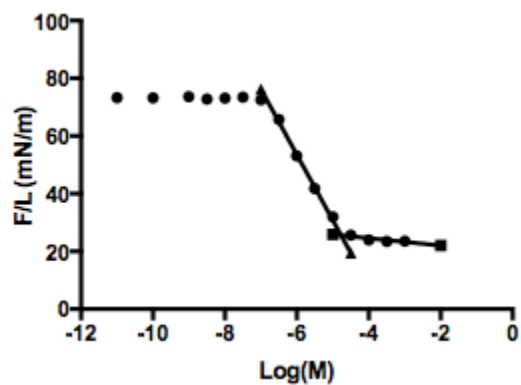


CMC (log(M))= -4.77 ± 0.03

**M5(F2Ox)<sub>3-5</sub>**

| Log(M) | Ave. Surface Tension (mN/m) | Std. Dev. |
|--------|------------------------------|-----------|
| -3.00 | 29.43 | 0.08 |
| -3.50 | 29.95 | 0.21 |
| -4.00 | 30.71 | 0.17 |
| -4.50 | 33.28 | 0.38 |
| -5.00 | 36.49 | 0.36 |
| -5.50 | 40.34 | 0.15 |
| -6.00 | 48.30 | 0.13 |
| -6.50 | 55.09 | 0.11 |
| -7.00 | 67.78 | 0.09 |
| -7.50 | 72.49 | 0.14 |
| -8.00 | 72.43 | 0.07 |
| -8.50 | 72.51 | 0.10 |
| -9.00 | 72.58 | 0.08 |
| -10.00 | 72.54 | 0.06 |
| -11.00 | 72.65 | 0.12 |
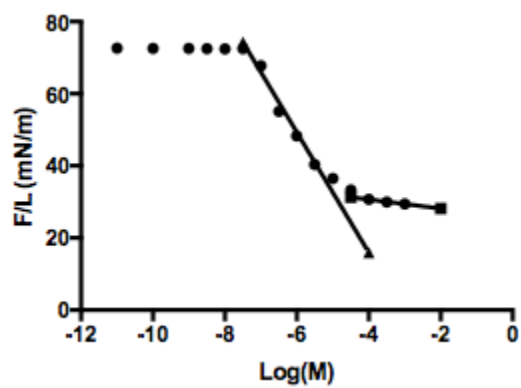


CMC (log(M))= -4.99 ± 0.08

**M1FE2**

| Log(M) | Ave. Surface Tension (mN/m) | Std. Dev. |
|--------|------------------------------|-----------|
| -3.00 | 26.75 | 0.19 |
| -3.50 | 28.72 | 0.12 |
| -4.00 | 27.57 | 0.07 |
| -4.50 | 33.24 | 0.22 |
| -5.00 | 40.09 | 0.19 |
| -5.50 | 46.25 | 0.03 |
| -6.00 | 58.19 | 0.15 |
| -6.50 | 69.71 | 0.18 |
| -7.00 | 72.89 | 0.15 |
| -7.50 | 72.91 | 0.04 |
| -8.00 | 72.62 | 0.11 |
| -8.50 | 73.14 | 0.10 |
| -9.00 | 72.94 | 0.11 |
| -10.00 | 73.14 | 0.08 |
| -11.00 | 73.16 | 0.11 |
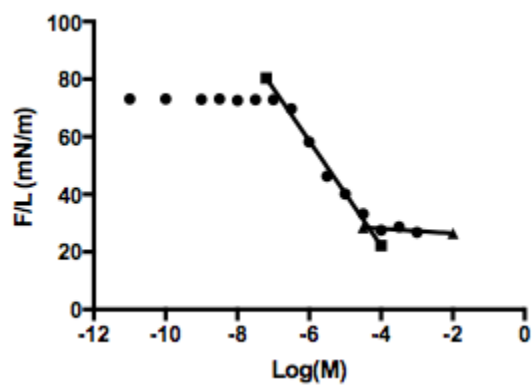


CMC (log(M))= -4.34 ± 0.07

**M1FE3**

| Log(M) | Ave. Surface Tension (mN/m) | Std. Dev. |
|--------|------------------------------|-----------|
| -3.00 | 26.86 | 0.26 |
| -4.00 | 27.18 | 0.07 |
| -5.00 | 27.98 | 0.10 |
| -6.00 | 29.89 | 0.17 |
| -7.00 | 47.85 | 0.16 |
| -8.00 | 71.61 | 0.13 |
| -9.00 | 72.06 | 0.06 |
| -10.00 | 71.76 | 0.11 |
| -11.00 | 72.00 | 0.08 |
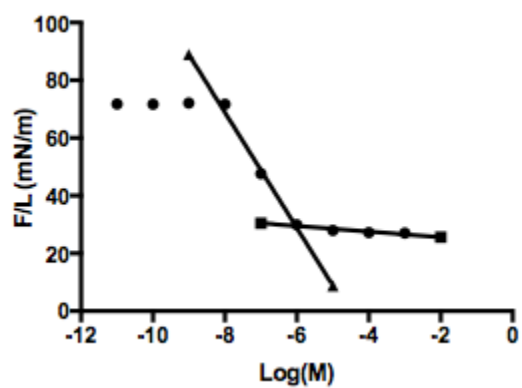


CMC (log(M))= -6.03 ± 0.

**M1bFE4**

| Log(M) | Ave. Surface Tension (mN/m) | Std. Dev. |
|--------|------------------------------|-----------|
| -3.00 | 23.59 | 0.53 |
| -3.50 | 24.50 | 0.61 |
| -4.00 | 25.77 | 0.48 |
| -4.50 | 31.91 | 1.43 |
| -5.00 | 40.53 | 1.32 |
| -5.50 | 43.03 | 1.22 |
| -6.00 | 55.57 | 0.12 |
| -6.50 | 72.63 | 0.06 |
| -7.00 | 72.65 | 0.40 |
| -7.50 | 73.05 | 0.13 |
| -8.00 | 72.86 | 0.16 |
| -8.50 | 73.16 | 0.11 |
| -9.00 | 73.15 | 0.11 |
| -10.00 | 73.06 | 0.16 |
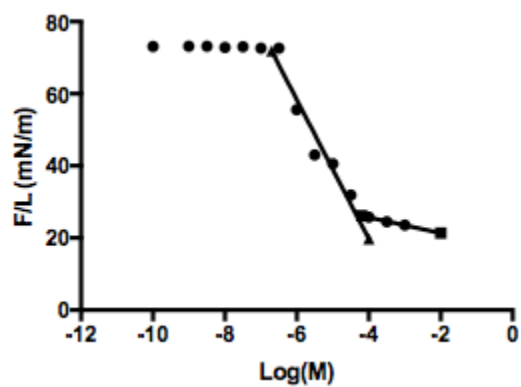


CMC (log(M))= -4.35 ± 0.14

*A2.10 Microviscosity data*

| M1(F2Ox)4-5 | | | |
|---|---|---|---|
| *376* | *480* | $I_M/I_E$ ratio | |
| 1.86 | 0.82 | 2.28 | |
| 1.84 | 0.74 | 2.50 | |
| 1.44 | 0.61 | 2.37 | |
| | | 2.38 | Ave |
| | | 0.11 | Std. Dev. |

| M1(F2Ox)7-9 | | | |
|---|---|---|---|
| *376* | *480* | $I_M/I_E$ ratio | |
| 2.44 | 0.34 | 7.23 | |
| 2.49 | 0.36 | 6.84 | |
| 2.66 | 0.34 | 7.84 | |
| | | 7.30 | Ave |
| | | 0.51 | Std. Dev. |

**M5(F2Ox)3-5**

| *376* | *480* | $I_M/I_E$ *ratio* | |
|-------|-------|--------------------|-----------|
| 3.06 | 1.01 | 3.04 | |
| 3.21 | 0.84 | 3.81 | |
| 3.10 | 0.93 | 3.32 | |
| | | 3.40 | Ave |
| | | 0.40 | Std. Dev. |

**M5(F2Ox)6*7**

| *376* | *480* | $I_M/I_E$ *ratio* | |
|-------|-------|--------------------|-----------|
| 1.50 | 0.27 | 5.64 | |
| 1.29 | 0.25 | 5.26 | |
| 1.34 | 0.25 | 5.39 | |
| | | 5.43 | Ave |
| | | 0.19 | Std. Dev. |

| M5(F2Ox)$_{8\text{-}10}$ | | | |
|---|---|---|---|
| *376* | *480* | $I_M/I_E$ *ratio* | |
| 2.27 | 0.13 | 18.01 | |
| 2.34 | 0.13 | 18.00 | |
| 2.35 | 0.13 | 18.22 | |
| | | 18.08 | Ave |
| | | 0.12 | Std. Dev. |

## A2.11 FRET data

FRET Ratio: $I_{565}/(I_{501}+I_{565})$ where $I_{501}$ =emission of donor dye and $I_{565}$ = emission of acceptor dye

M1(F2Ox)$_5$
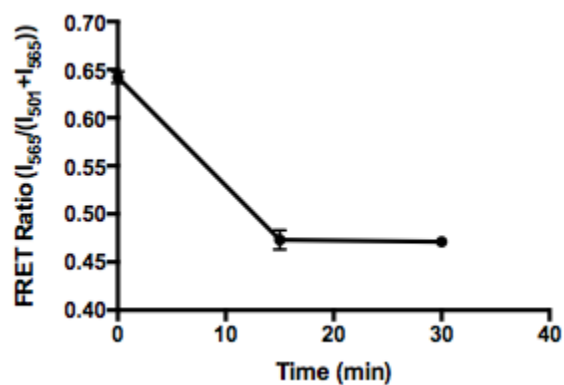


| Time (min) | Ave. FRET Ratio | Std. Dev. |
|:---:|:---:|:---:|
| **0** | 0.642 | 0.006 |
| **15** | 0.473 | 0.010 |
| **30** | 0.471 | 0.005 |

*A2.12 DLS: Emulsion Particle Size*

| | M5(F2Ox)$_3$ iso | | M5(F2Ox)$_4$ iso | | M5(F2Ox)$_3$ sevo | | M5(F2Ox)$_7$ sevo | |
|---|---|---|---|---|---|---|---|---|
| Day | Mean | Std. Dev. | Mean | Std. Dev. | Mean | Std. Dev. | Mean | Std. Dev. |
| 0 | 224.8 | 55.984 | 180.7 | 79.344 | 143.9 | 39.418 | 191.6 | 54.985 |
| 1 | 245.5 | 52.784 | 214.4 | 74.81 | 214.8 | 47.041 | 230.5 | 63.844 |
| 2 | 257.2 | 72.518 | 236.2 | 63.29 | 235.9 | 53.077 | 260.8 | 88.421 |
| 3 | 266.7 | 66.143 | 247.2 | 69.963 | 260.2 | 59.059 | 287.9 | 88.648 |
| 5 | 257.8 | 65.473 | 268.8 | 83.05 | 290.7 | 65.990 | 331.4 | 105.391 |
| 7 | 279.6 | 74.657 | 277.4 | 79.614 | 305.4 | 33.594 | 370.4 | 138.516 |
| 14 | 315.1 | 76.26 | 304.2 | 52.01 | 371.1 | 105.751 | 480.8 | 233.670 |
| 21 | 327.4 | 101.826 | 333.1 | 76.946 | 450.4 | 166.191 | 604.5 | 350.614 |
| 28 | 338.7 | 124.974 | 344.9 | 95.886 | 496.4 | 216.919 | 709.4 | 455.409 |
| 35 | 344.3 | 104.664 | 380.7 | 140.493 | 550.1 | 213.987 | 780.2 | 490.721 |
| 42 | 359.7 | 108.642 | 380.0 | 129.955 | 647.7 | 292.740 | 965.9 | 488.724 |
| 49 | 369.2 | 146.949 | 406.3 | 169.815 | 590.0 | 267.262 | 975.3 | 527.635 |
| 56 | 368.8 | 167.85 | 406.4 | 121.115 | 751.5 | 381.778 | 947.4 | 553.304 |
| 63 | 381.4 | 164.016 | 414.3 | 149.961 | 786.0 | 411.838 | 1133.9 | 638.387 |
| 70 | 383.7 | 162.68 | 399.3 | 39.929 | 830.2 | 457.429 | | |
| 77 | 400.6 | 189.507 | 414.5 | 139.267 | 923.5 | 434.972 | | |
| 84 | 402.4 | 206.814 | | | 914.7 | 434.490 | | |
| 91 | 418.3 | 212.069 | | | | | | |
| 98 | 429.6 | 220.372 | | | | | | |
| 105 | 428.5 | 227.958 | | | | | | |
| 113 | 421.2 | 244.28 | | | | | | |
| 119 | 429.7 | 241.473 | | | | | | |
| 126 | 431.8 | 245.716 | | | | | | |

| | | | | | | | | |
|---|---|---|---|---|---|---|---|---|
| 133 | 411.8 | 232.675 | | | | | | |
| 140 | 435.2 | 246.775 | | | | | | |
| 147 | 463.5 | 265.609 | | | | | | |
| 154 | 429.6 | 251.317 | | | | | | |
| 161 | 411.1 | 244.582 | | | | | | |
| 168 | 415.7 | 245.702 | | | | | | |
| 175 | 412.8 | 238.183 | | | | | | |
| 182 | 404.1 | 228.329 | | | | | | |
| 189 | 407.7 | 229.057 | | | | | | |
| 199 | 396.4 | 225.57 | | | | | | |
| 203 | 399.0 | 223.828 | | | | | | |
| 210 | 392.4 | 226.73 | | | | | | |
| 217 | 363.7 | 218.223 | | | | | | |
| 224 | 379.4 | 222.718 | | | | | | |
| 231 | 356.9 | 196.986 | | | | | | |
| 238 | 363.8 | 202.975 | | | | | | |
| 252 | 369.8 | 212.993 | | | | | | |
| 259 | 364.0 | 196.192 | | | | | | |
| 266 | 399.1 | 231.868 | | | | | | |
| 273 | 380.3 | 213.71 | | | | | | |
| 280 | 364.0 | 205.279 | | | | | | |
| 287 | 369.1 | 208.546 | | | | | | |
| 294 | 340.3 | 196.011 | | | | | | |
| 301 | 362.4 | 208.746 | | | | | | |
| 308 | 384.2 | 231.697 | | | | | | |
| 315 | 372.6 | 209.016 | | | | | | |

| 322 | 371.7 | 211.495 | | | | | | |
|-----|-------|---------|---|---|---|---|---|---|
| 329 | 376.1 | 217.921 | | | | | | |
| 336 | 384.1 | 227.031 | | | | | | |
| 343 | 373.4 | 226.271 | | | | | | |
| 350 | 360.7 | 232.286 | | | | | | |
| 357 | 368.1 | 218.662 | | | | | | |
| 364 | 359.0 | 239.78 | | | | | | |

| | 20% sevoflurane, 10% PFOB | | | | | |
|-----|-------|-----------|-------|-----------|-------|-----------|
| | M1FE2 | | M1FE3 | | M1bFE4 | |
| Day | Mean | Std. Dev. | Mean | Std. Dev. | Mean | Std. Dev. |
| 0 | 177.4 | 60.7 | 197.2 | 63.7 | 190.0 | 64.8 |
| 1 | 210.9 | 78.7 | 223.1 | 71.2 | 212.7 | 73.4 |
| 2 | 235.3 | 80.0 | 244.4 | 99.0 | 231.0 | 80.2 |
| 3 | 251.7 | 88.3 | 259.6 | 100.5 | 243.7 | 92.6 |
| 5 | 273.0 | 91.7 | 282.1 | 113.9 | 268.6 | 89.7 |
| 7 | 295.5 | 100.8 | 297.8 | 99.6 | 288.6 | 99.9 |
| 14 | 353.8 | 137.3 | 348.4 | 126.1 | 340.1 | 125.5 |
| 21 | 431.4 | 223.7 | 399.0 | 136.4 | 409.3 | 190.3 |
| 28 | All emulsions phase separated | | | | | |

*A2.13 Aggregation Induced Emission (AIE) data*

**Representative decrease in fluorescence spectrum over time for PEG-PLA micelles, with PCD-OH AIE dye:**
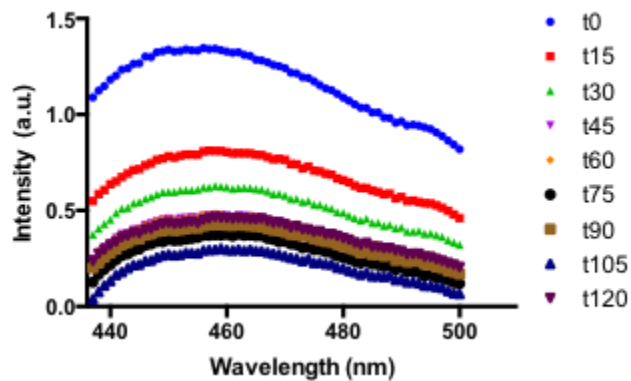


**PEG-PLA micelles with varying amounts of PCD-OH encapsulated. Note: 1 wt. % was chosen for dye concentration, and is reported in Chapter 4.**

**0.5 wt. % PCD-OH**
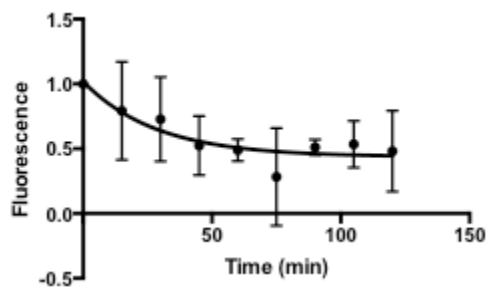


Standard error bars larger than comparison for the experiment with 1 wt. % dye.

**2 wt. % PCD-OH**
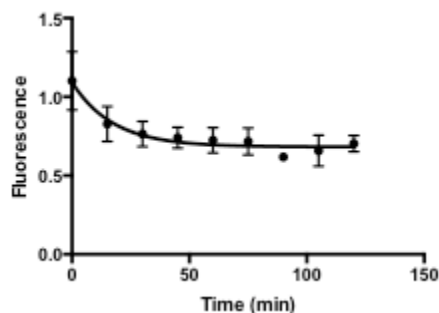


Error bars were small, but baseline was very large for higher dye concentrations.

**5 wt. % PCD-OH**
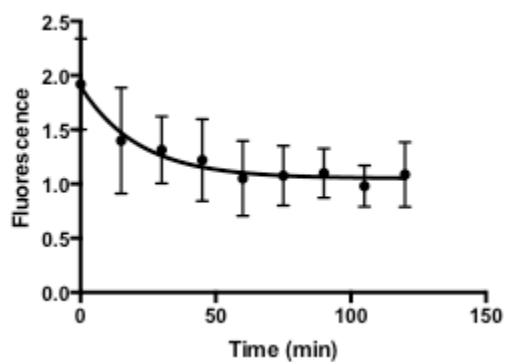


Error bars were small, but baseline was very large for higher dye concentrations.

**PEG-PLA micelles with varying ratios of TBA:$H_2O$ used in their lyophilization preparation. Note: 50:50 ratio for solvent ratio, and is reported in Chapter 4.**
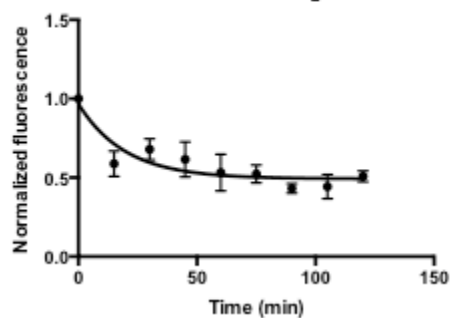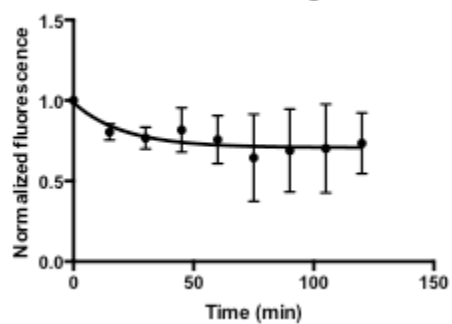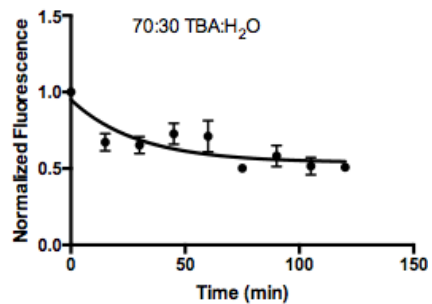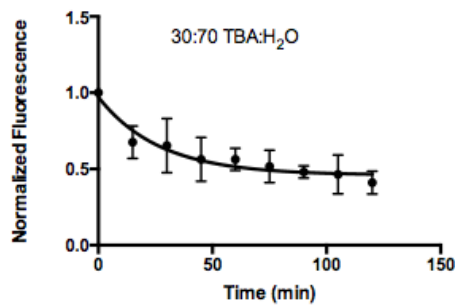
*A2.14 Zebrafish Toxicity procedures and data*

**Standard experimental procedure:**

<u>Day 0</u>
- Basket cross (~2 female, ~2male) per container.
- Birthdays on fish tanks must be the same to cross.
- Use fish after 1 week ideally, 4 days minimum.
- Allow stagnant water to drain from hose, fill container to 1 inch from top, and add the fish and cover.

<u>Day 1 (0 hpf)</u>
- Lights on at 9 AM, check eggs at 9:30, collect within 2 hours.
- Pour cross containers through strainer, collecting embryos and rinse with egg water to remove debris.
- Transfer to petri dishes for analysis.
- Embryos are observed using stereoscope. Obtained embryos between 4-16 cell stages.
- A 24-well plate used, and added ~8 eggs per cell, along with 600 μL egg water.
- 180 μL compounds added, using a 10 mM stock solution.
- Final solution diluted to 1.2 mL.
- The 24-well plate was then kept in an incubator at 28.5°C.

<u>Day 2-5 (24-96 hpf)</u>
- Recorded number of embryos, whether they are dead/hatched.
- Observed embryos for malformations for hatched fish.

<u>Day 5 (96 hpf)</u>
- Anesthetize fish for imaging by exposing to a 0.4% tricaine solution
    - Prep: 200 mg tricaine + 50 mL Milli-Q water + 1 mL TRIS base
    - Dilute 1:20 (9.5 mL egg $H_2O$, 0.5 mL tricaine solution)
    - Can be found in Taylor dark room
- Fill medium size petri dish with 10 mL diluted tricaine solution; add fish one at a time until they stop moving (1-2 min).
- Transfer fish to agarose, position for imaging and wait ~1 min. for gel to harden.
- A stereoscope with a Nikon camera was used to image fish.
- Euthanized all fish: add ample ice, and splash of Clorox bleach.

**Perfluorooligo ether acids survival graph:**
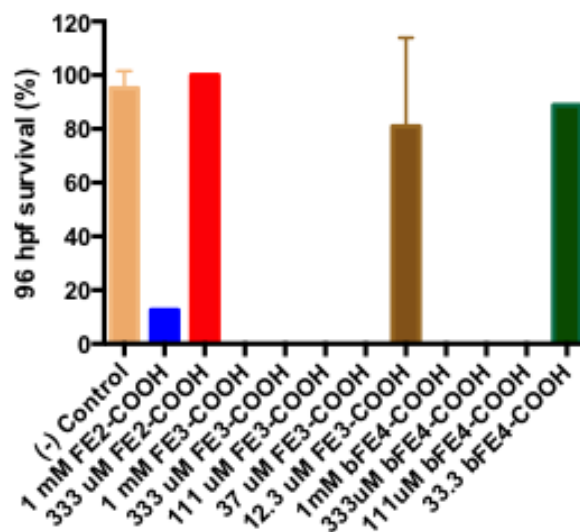


**Buffered Perfluorooligo ether acids survival graph:**
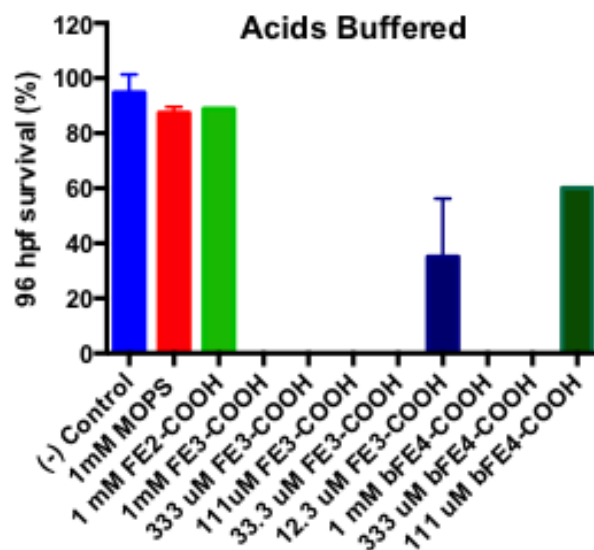
**Dose-response curve for fluorinated acids:**
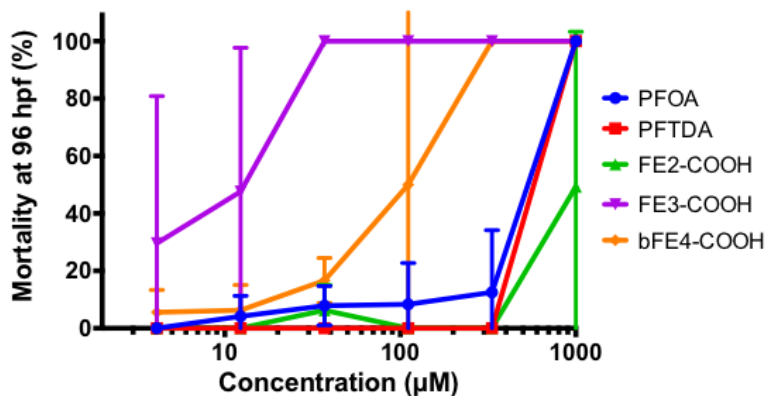


**Transform of dose-response graph:**
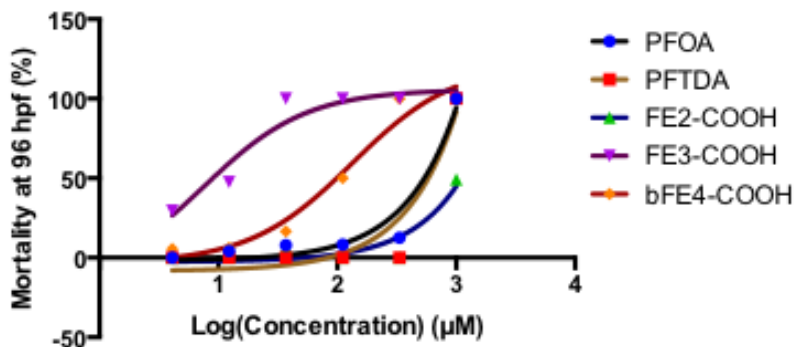


IC50 calculations for fluorinated acids were completed with the GraphPad Prism® (version 6.0, La Jolla, CA) software program. In the GraphPad Prism® equation, log-transformed concentration values and the effect data were fitted to a four-parameter logistic equation. The original, %control, or % inhibition data are represented by Y along with their minimal (min) and maximal (max) values. The inhibitor concentration is represented by X, IC50 is the concentration at 50% maximal value, and HillSlope is the slope factor.

$$Y = \frac{(\text{max} - \text{min})}{(1 + 10^{((X - logIC_{50})(Hill\ slope))})}$$